The characterization of DNAJC3: Elucidating the function of the TPR domains

A thesis submitted in fulfilment of the requirement for the degree of

Doctor of Philosophy (Biochemistry)

Of

Rhodes University

By

Lorraine Zvichapera Mutsvunguma

April 2014

Declaration

I declare that this dissertation is my own unaided work, except where acknowledged, submitted for the degree of Doctor of Philosophy in Biochemistry of Rhodes University in the Faculty of Science. It has not been submitted for any degree for examination in any other university.

……

Ms Lorraine Mutsvunguma, April 2014

Abstract

DNAJC3 is a novel member of the DNAJ family with two domains linked to co-chaperone functions, namely the tetratricopeptide repeat (TPR) and J domain. Out of the two domains, the TPR domains are the least characterized. Therefore, the aim of this study was to characterize and elucidate additional functions of DNAJC3 TPR domains through *in silico*, *in vitro* and *ex vivo* approaches. Through multiple sequence and structural alignment as well as electrostatic potential analysis, DNAJC3 TPR domain were found to be most similar to TPR-containing proteins with Hsp90 or Hsp70 independent functions. *In vitro* pull down assays illustrated that DNAJC3 TPR domains did not interact with either cytosolic Hsp90 and Hsp70 or Grp78 and Grp94 directly, however a potential indirect interaction with Grp94 and Hsp90 was observed in mammalian lysates, via pull down assays; suggesting the formation of a complex between the proteins mediated by a specific substrate. DNAJC3 TPR domains were found to bind indiscriminately to both native and heat denatured substrates in a dose dependent manner. DNAJC3 TPR domains bound to β-galactosidase with greater affinity than malate dehydrogenase (MDH), suggesting that DNAJC3 TPR domains might exhibit substrate specificity that has not been reported before. Preliminary *ex vivo* analysis of DNAJC3 in mammalian cells showed that induced stress conditions did not alter the cytosolic or endoplasmic reticulum (ER) localization, or levels of DNAJC3 protein, suggesting that the protein is not stress inducible. However, protein levels of DNAJC3 were dramatically reduced by Hsp90 inhibitor novobiocin at 500 µM. Transient knockdown DNAJC3 did not change the protein levels of either Grp78 or Grp94, but decreased the protein levels of Hsp70/Hsp90 organizing protein HOP. On the other hand, protein levels of DNAJC3 were increased in HOP depleted cells. In conclusion, this study was the first to experimentally demonstrate that DNAJC3 TPR domains do not interact directly with Hsp90, Hsp70, Grp78 or Grp94, and therefore DNAJC3 is unlikely to participate in traditional co-chaperone interactions with those proteins via its TPR domain. However, the J domain is known to interact with Grp78. The discovery that DNAJC3 TPR domains resemble that of TPR-containing proteins with functions independent of Hsp90 or Hsp70 suggests that DNAJC3 might link the Hsp70/Grp78 chaperone machinery to non co-chaperone related functions, which requires further analysis.

Dedication

This thesis is dedicated to my mother and sister, Miriam and Ronah Mutsvunguma

Thank you for keeping the promise you made to me 10 years ago on the night of my High school graduation. I will always be eternally grateful for the sacrifices you have made for me.

Table of Contents

List of Figures

List of Tables

List of Abbreviations

17-AAG	17-*N*-Allylamino-17-Demethoxygeldanamycin
AD	DNA Activation Domain
ADP	Adenosine Diphosphate
Aha1	Activator of the Hsp90 ATPase
ATF	Activating Transcription Factor
ATP	Adenosine Triphosphate
BAG1/5	Bcl-2-Associated Athanogene 1/5
BD	DNA Binding Domain
BIC	Bayesian Information Criterion
BiP	Binding Immunoglobulin Protein
BLAST	Basic Local Sequence Alignment Tool
BSA	*Bovine Serum Albumin*
Cdc37	Cell Division Cycle 37
cDNA	Complementary Deoxyribonucleic Acid
CHIP	E3 Ubiquitin Ligase C-Terminus Hsc70 Interacting Protein
CHOP	CCAAT-Enhancer-Binding *Protein* Homologous *Protein*
CVB3	Coxsackie virus B3
Cyp40	Cyclophilin 40
DMEM	Dulbecco's Modified Eagle Medium
DMSO	Dimethyl Sulfoxide
DNA	Deoxyribonucleic Acid
dsRNA	Double Stranded RNA
DTT	Dithiothreitol
EDTA	Ethylenediaminetetraacetic Acid
EGFP	Enhanced Green Fluorescent Protein
eIF2α	Eukaryotic Translation Initiation Factor 2 A Subunit
ELISA	Enzyme-Linked Immunosorbent Assay
ELM	Eukaryotic Linear Motifs
ER	Endoplasmic Reticulum
ERAD	ER Mediated Degradation
FCS	Fetal Calf Serum
FKBP	FK506-Binding Family of Immunophilins
FLAR	Firefly Luciferase Assay Reagent
GA	Geldenamycin
GAPDH	Glyceraldehyde 3-Phosphate Dehydrogenase
Grp78	Glucose-Regulated Protein with Molecular Mass of 78 kDa
Grp94	Glucose-Regulated Protein with Molecular Mass of 94 kDa
GST	Glutathione S-Transferase
GTP	Guanosine Triphosphate
HA	Human Influenza Hemagglutinin
HIP	Hsp70 Interaction Protein

HOP	Hsp70/Hsp90 Organizing Protein
Hsc70	Heat-Shock Cognate 70
Hsp100	Heat Shock Protein 100
Hsp40	Heat Shock Protein 40
Hsp60	Heat Shock Protein 60
Hsp70	Heat Shock Protein 70
Hsp90	Heat Shock Protein 90
IGF	Insulin-Like Growth Factors
IPTG	Isopropyl B-D-1-Thiogalactopyranoside
IRE1	Inositol-Requiring Enzyme 1
ITRAQ	Isobaric Tags for Relative and Absolute Quantitation
JNK	c-Jun N-Terminal Kinase
JTT	Jones-Taylor-Thornton
M2/3	Matrix Protein
MAPK	Mitogen-Activated Protein Kinase
MAPKAPK	MAPK-Activated Protein Kinases
MDH	Malate Dehydrogenase
MEGA	Molecular Evolutionary Genetics Analysis
MEME	Multiple Em for Motif Elucidation
MG132	Z-Leu-Leu-Leu-Al
mtHsp70	Mitochondria Hsp70
NCBI	National Centre of Biotechnology Information
NEF	Nucleotide Exchange Factor
NOVO	Novobiocin
NP40	Nonidet-P 40
P52^{ripk}	52 kDa Repressor of the Inhibitor of the Protein Kinase
P58^{IP}^{K}	58 kDa Inhibitor of Protein Kinase
P88^{ripk}	88 kDa Repressor of the Inhibitor of the Protein Kinase
PBS	Phosphate Buffered Saline
PDB	Protein Data Bank
PDI	Protein Disulfide Isomerase
PERK	PKR-Like ER Kinase
PEX5	Peroxin 5
PI3K	Phosphatidylinositide-3-Kinase
PKR	dsRNA-Activated Protein Kinase
PMA	Phorbol 12-Myristate 13-Acetate
PMSF	Phenylmethylsulfonyl Fluoride
PP5	Protein Phosphatase
PSA	Penicillin-Streptomycin-Amphotericin
Psi-BLAST	Position-Specific Iterative BLAST
RIPA	Radioimmunoprecipitation Assay
RMSD	Root Mean Square Deviation
RNA	Ribonucleic Acid

ROS	Reactive Oxygen Species
RT-PCR	Reverse Transcription Polymerase Chain Reaction
S**DS**	Sodium Dodecyl Sulphate
SDS-PAGE	SDS- Polyacrylamide Gel Electrophoresis
SGT	Small Glutamine-Rich Tetratricopeptide Repeat-Containing
shRNA	Short Hairpin RNA
siRNA	Small Interfering RNA
SMART	Simple Modular Architecture Research Tool
TAE	Tris-Acetate-EDTA
TBS	Tris Buffered Saline
TEV	Tobacco Etch Virus
TMB	3,3',5,5'-Tetramethylbenzidine
TMV	Tobacco Mosaic Virus
TNF	Tumor Necrosis Factor
TOM20	Mitochondrial Preprotein Translocases of the Outer Membrane 20
TOM34	Mitochondrial Preprotein Translocases of the Outer Membrane 34
TOM70	Mitochondrial Preprotein Translocases of the Outer Membrane 70
TPR	Tetratricopeptide Repeat
TRAP1	Mitochondrial Tumour Necrosis Factor Receptor-Associated Protein 1
Tun	Tunicamycin
UPR	Unfolded Protein Response
UV	Ultraviolet
YT	Yeast Tryptone

Acknowledgements

I would like to take this moment to acknowledge the following people for their contributions:

- To my supervisor and mentor, Dr Adrienne Edkins. Words can never express how grateful I am for the support and encouragement you gave me throughout the past 3 years. Your passion for science is very contagious and has reignited my love for the subject.
- To my co-supervisors, Dr Tastan Bishop and Prof Blatch. Thank you for all the support, guidance and input you gave me during my studies.
- To my friends, Bu, Fiki, Tumi, Jo, Lara, Jackie, Phumeza, Christine, Mpho, Fouch and Pru. Without you guys I don't think I would have been able to handle the pressures of this degree. Your friendship both in and out the lab helped me enjoy the ups and downs of Rhodes and life. To my fellow lab mates in Biobru, thank you for making the lab feel like home.
- To my parents, Daniel and Miriam Mutsvunguma, without you I wouldn't have gotten this far, thank you for believing in me. Especially my mommy, for being the best cheerleader, friend and counsellor a girl could ask for. To my siblings, especially my sister Ronah, thank you guys for being there for me.
- I would also like to thank Rhodes University and NRF, for financial assistance.
- Lastly, I would like to thank God; with Him all things are possible.

Research Output

Publications

de la Mare J, Contu L, Hunter MC, Moyo B, Sterrenberg JN, **Mutsvunguma LZ**, Dhanani KCH and Edkins AL. (2013) Breast cancer: Current developments in molecular approaches to diagnosis and treatment. *Recent Patents on Anti-Cancer Drug Discovery Journal*

Conferences

Mutsvunguma LZ, Tastan Bishop Ö, Blatch GL, Edkins AL. Bioinformatic analysis of DNAJC3, a type 3 DNAJ protein. VI International Conference on Stress Proteins in Biology and Medicine 2013, Sheffield, UK 18-22 August. **Oral Presentation**

Chapter 1: Literature review

1.1 The chaperoning function

The folding and assembly of proteins into their functional form was thought to be a spontaneous process that required no assistance, a hypothesis heavily supported by Anfinsen's observation of reversible denaturation and renaturation of ribonuclease *in vitro* (Anfinsen, 1973). It was not until the mid-1970s that the concept of the molecular chaperone was introduced by Fohlman *et al* (1976). They found that the active neurotoxic subunit of the Taipan snake venom proteins was surrounded by two other protein subunits that not only increased the toxin's specificity, but also protected the neurotoxin subunit from degradation, acting almost as chaperones (Fohlman *et al*., 1976). During the same period, Laskey and colleagues discovered the chaperoning activity of nucleoplasmin on histones, were it helped the histones assemble into functional nucleosomes (Laskey *et al*., 1978). This was the first time that the term "molecular chaperones" was used. Although both groups had illustrated the existence of chaperoning molecules, it was not until 30 years ago that the concept of the chaperoning function was clarified. It was noted that the over expression of a special type of protein, heat shock protein 70 (Hsp70), was induced by heat shock and was able to disrupt complexes of unfolded protein that had formed due to the changes in the cellular environment caused by the heat (Pelham, 1984, Lewis and Pelham, 1984). Although Pelham conducted various experiments with the Hsp70 family (Munro and Pelham, 1986, Bienz and Pelham, 1986), the molecular chaperoning concept was made famous by John Ellis (Ellis, 1987). This was based on his observations on the assembly of Rubisco assisted or chaperoned by a Rubisco binding protein (Ellis *et al*., 1987, Ellis and van der Vies, 1988). Nowadays, the term "molecular chaperones" is used to describe a group of structurally unrelated proteins that are able to help correctly fold or refold nascent proteins that are newly synthesised, misfolded, denatured or aggregated into their functional conformations (Ellis, 1987, Young *et al*., 2004), hence the chaperoning function and molecular chaperones are essential to maintaining cell homeostasis.

1.2 Heat Shock Proteins (HSP)

The detection of "puffs" on the chromosomes of heat shocked *Drosophila* chromosomes by Ferruccio Ritossa represented one of the greatest discoveries in the understanding of cellular

survival mechanisms and escalated the study of an important group of cellular genes (Ritossa, 1962). The protein products of these genes were identified a few years later through the work of Alfred Tissières (Tissières *et al*., 1974). These proteins have been termed Heat Shock Proteins (Hsps) due to the fact that they were first observed to be induced after heat shock treatment of cells. However, the expression of Hsps can be induced by various stresses such as hypoxia, oxidative stress, free radical damage, UV damage, various mutation and even diseases. Since the expression of Hsps can be triggered by a variety of stress conditions, it has been suggested that these proteins be called "stress proteins" instead of heat shock proteins (Bagatell and Whitesell, 2004).

1.3 Heat shock proteins functioning as molecular chaperones

Although Hsps are over expressed during stress conditions, they are also known to be constitutively expressed within the cells during homeostasis. The biological functions of Hsps are numerous and vary, from the modulation of folding, degradation and translocation of protein, to buffering of cell mutations and regulation of cell survival and apoptosis (Ellis, 1987; Feldman and Frydman, 2000; Frydman, 2001, Tutar and Tutar, 2010, Tkáčavá and Angelovičova, 2012). The ability of Hsps to perform such diverse functions within the cell by assisting the function of other proteins without becoming part of the final protein product, has resulted in some Hsps being grouped as molecular chaperones (Hartl, 1995, Rutherford, 2003 and Young *et al*., 2004). The protein folding process is the primary function of chaperones. Chaperones are able to distinguish between unfolded and native proteins based on segments of hydrophobic residues exposed by unfolded proteins (Fink, 1999, Yim *et al*., 2013). Hsps are a highly abundant and conserved group of proteins that is mainly classified based on their molecular sizes in kilodaltons (kDa). Currently, there are six Hsp families which are localized in various cell compartments and have varying functions (Table 1.1). These include the Hsp100, Hsp90, Hsp70, Hsp60, Hsp40 and small Hsps families. Although most Hsp chaperones are involved primarily in ensuring proper protein folding conformations, it has been noted that some proteins can only be chaperoned by a single class of Hsps, suggesting that there might be a process that directs specific substrates to specific Hsps for folding. In addition, molecular chaperone activity has been shown to require the cooperation of different classes of Hsps to fulfil their role (Fink, 1999, Deuerling and Bukau, 2004, Yim *et al*., 2013).

Table 1.1: Sub-cellular localization and function of the six known Heat shock protein families

Family	Molecular weight (kDa)	Example members	Localization	Function	References
Small Hsps/HSPB	18–40	Hsp10, Hsp17, Hsp22-23, Hsp27-28	Mitochondria, cytoplasm, perinuclear, nucleus	ATP independent substrate aggregation suppression. Apoptosis inhibition. Protection of cells from heat and oxidative stress	Van Montfer *et al*., 2001, Haslbeck *et al*., 2005, Arrigo, 2005
Hsp40/DNAJ		DNAJA1, DNAJB4, DNAJC3, DNAJC7, DBAJC21	Endoplasmic reticulum, nucleus, mitochondria, cytosol, ribosomes	Stimulation of Hsp70 ATPase activity, substrate binding, suppression of protein aggregation	Tsai *et al*., 1996, Cheetham and Caplan, 1998, Qiu *et al*., 2006; Rosser and Cyr, 2007
Hsp60/HSPD	58-65	Hsp58, Hsp60, Hsp65	Mitochondria	Protein folding and assembly of translocated proteins. Maintenance of mitochondrial functions and biogenesis	Cheng *et al*., 1990, Bukau and Horwich, 1998, Shan *et al*., 2003
Hsp70/HSPA	67-76	Hsp68, Hsc70, Hsp70, Hsp72-73, Hsp75, Grp78	Cytoplasm, nucleus, mitochondria, endoplasmic reticulum, lysosomes	ATP-dependent protein folding and degradation. Translocation of proteins across membranes	Mayer and Bukau, 1998; 2005; Fink, 1999; Pratt and Toft, 2003
Hsp90/HSPC	82-96	Hsp90α, Hsp90β, Grp94, TRAP1, Hsp90N	Cytoplasm, nucleus, mitochondria, endoplasmic reticulum, plasma membrane	ATP-dependent chaperone activity. Involved in protein folding, degradation, controlling cell proliferation, differentiation and apoptosis	Sreedhar *et al*., 2004, Sreedhar and Csermely, 2004, Chiosis *et al*., 2004
Hsp110/HSPH	80-110	Hsp100, Hsp104	Cytoplasm, nucleus, mitochondria, plasma membrane	ATP-dependent protein renaturation or degradation, Reactivation of stress denatured proteins from aggregates with Hsp70	Sanchez and Lindquist, 1990, Kruger *et al*., 1994, Schirmer *et al*., 1996, Lee *et al*., 2004, Miot *et al*., 2011

1.4 Heat shock protein 90 (Hsp90)

Hsp90 (HSPC) is the most abundant molecular chaperone and soluble protein in eukaryotic cells, comprising about 1-2 % of total soluble protein under homeostatic conditions and these levels have been shown to increase up to 10-fold during stress conditions (Lai *et al.*, 1984, Borkovish *et al*., 1989, Buchner, 1999, Whitesell and Lindquist, 2005). Similar to other chaperones, Hsp90 is involved in the folding, transportation, maturation and degradation of proteins, however unlike other chaperones such as Hsp70 which bind to unfolded proteins; Hsp90 interacts with specialized client proteins such as kinases (Xu and Lindquist, 1993), steroid hormone receptors (Picard *et al*., 1990) and transcription factors (Minet *et al*., 1999). At present over 300 client proteins whose maturation, folding and activity is depended on Hsp90 have been discovered (for a comprehensive list see http://www.picard.ch/downloads/Hsp90interactors.pdf). Hsp90 client proteins are involved in a range of biological roles within the cells such as controlling cell cycle progression, cell growth and cell death by influencing cellular signalling from kinases and steroid receptors (Picard *et al*., 1990, Pratt and Toft, 2003, Picard, 2002, Jackson, 2013). Due to the specialized functions of Hsp90 client proteins, Hsp90 has been associated with the regulation of several factors involved in buffering cell mutations (Rutherford and Lindquist, 1998, Sangster *et al*., 2008, Rohner *et al*., 2013), cell survival promotion/ anti-apoptosis (Schulte *et al*., 1995, Sato *et al*., 2000, Fortugno *et al*., 2003 Zhao and Wang, 2004) and the preservation of the transformation state of several cell types (Chiosis *et al.*, 2004). Additionally, Hsp90 has been shown to be essential for cell viability and survival, since inhibition of Hsp90 by various drugs lead to the degradation of client proteins via the ubiquitin proteasome system resulting in arrested cell growth (Schulte *et al*., 1998, Marcu *et al*., 2000a).

Hsp90 structure and function

Hsp90 has three conserved domains, an N-terminal ATP-binding domain, a C-terminal domain which is responsible for dimerization, and a middle domain that connects the N and C terminal domains (Figure 1.1) (Didenko *et al*., 2012, Jackson, 2013). Currently five isoforms of Hsp90 have been identified (Figure 1.1). These include two cytosolic isoforms, Hsp90α (HSPC2) and Hsp90β (HSPC3), which differ in their expression pattern within the cell. While the β form is constitutively expressed, the α form is inducible by stress conditions (Csermely *et al*., 1998). Hsp90β is an essential gene for development of the mouse, while the main phenotype in knockout mice for Hsp90α is a defect in spermatogenesis (Voss *et al*., 2000, Grad *et al*., 2010). The two isoforms

share a nucleotide identity of about 76 % (Moore *et al*., 1986, Csermely *et al*., 1998, Sreedhar *et al*., 2004a) and amino acid identity of 86 % and 93 % similarity (Chen *et al*., 2005). The third isoform of Hsp90, HSPC5, also known as TRAP1 (mitochondrial tumour necrosis factor receptor-associated protein 1) or Hsp75 localizes to the mitochondrial matrix, where it is found in lower levels suggesting a specialized function in the cell (Song *et al*., 1995, Chen *et al*., 1996). TRAP1 shares 35 % sequence identify to the cytosolic isoforms (Picard, 2002). The fourth isoform, Grp94 (glucose-regulated protein with molecular mass of 94 kDa) or HSPC4, localizes and is retained in the ER lumen. Grp94 is the most abundant protein in the ER and shares 50 % identity with the cytosolic Hsp90 isoforms (Gupta, 1995). The last isoform of Hsp90, Hsp90N, was identified as being membrane associated (Grammatikakis *et al*., 2002). Hsp90N is roughly 70 kDa in size and shares high sequence similarity with Hsp90α although it has a shortened N-terminal domain which consists of only 30 amino acids. Functionally, Hsp90N has been shown to bind to the Ras protein with a higher affinity than other Hsp90 isoforms (Powers and Workman, 2006). This isoform is controversial in that some authors do not believe there is sufficient evidence to support the presence of Hsp90N as a separate gene (Zurawska *et al*., 2008).

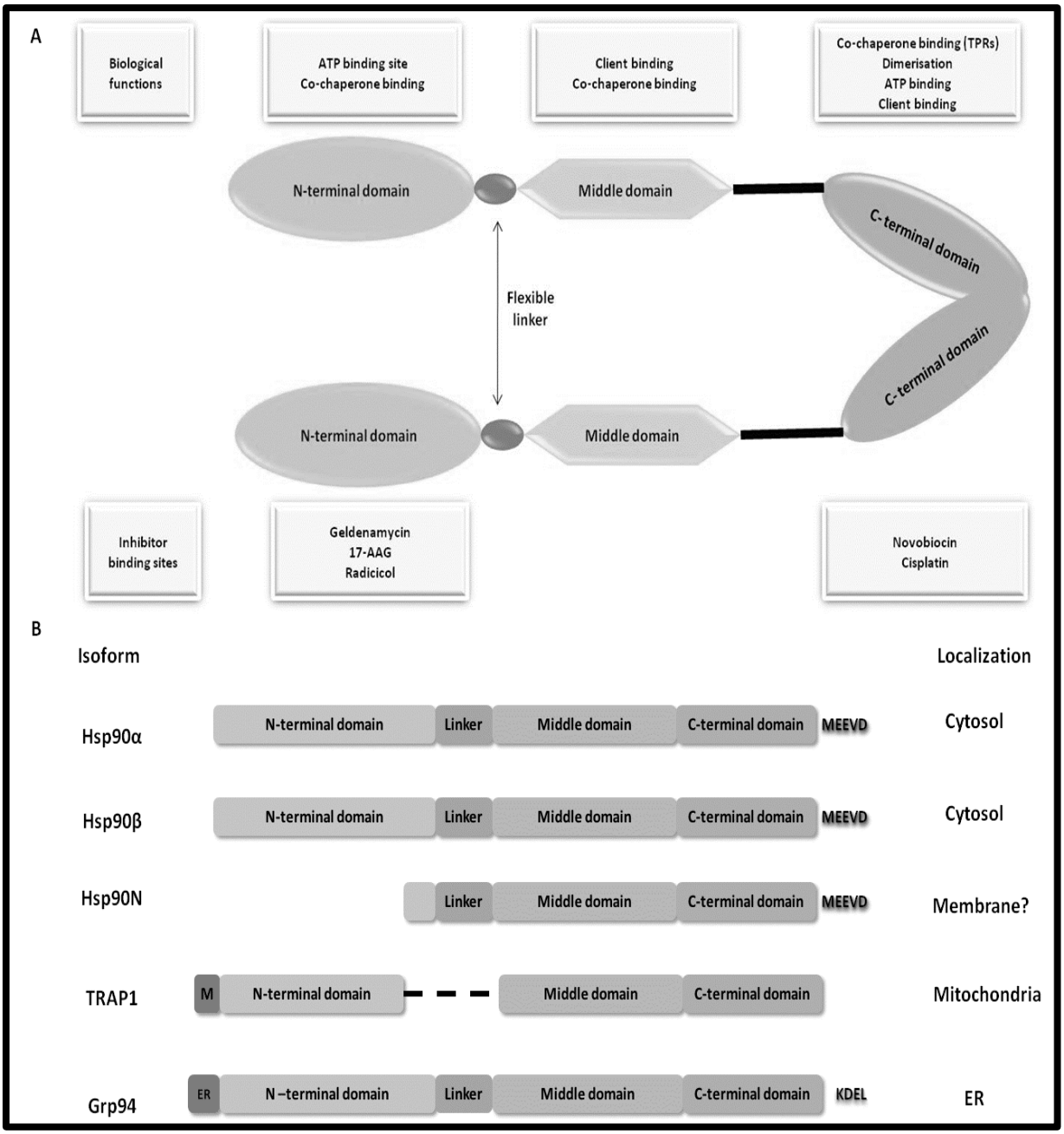

Figure 1.1: Schematic diagram of the three highly conserved functional domains of Hsp90 isoforms. (A) Hsp90 exists as a dimer within the cell. Located at the N-terminus domain is the ATP binding domain. A flexible linker region connects the N-terminus and Middle domain. The Middle domain is responsible for the binding of Hsp90 clients and certain co-chaperones. While the C-terminus binds TPR-containing co-chaperones and is also thought to have a client binding site. The N- terminus is also the binding site of Hsp90 inhibitors geldanamycin (GA), 17-AAG and radicicol, while the C- terminus is the binding site of novobiocin (NOVO) and cisplatin (B) The domain organisation of the five isoforms of Hsp90, highlighting the differences found between the proteins. Although all isoforms have the three domains indicated in A, the N-terminus is slightly varied, with Hsp90N missing the majority of this domain. TRAP1 is missing the linker charged region and both TRAP1 and Grp94 are missing the highly conserved MEEVD motif located at the end of the C-terminus. In Grp94, this motif is replaced by the ER retention KDEL motif. (Adapted from Buchner, 1999, Sreedhar *et al*., 2004a, Whitesell and Lindquist, 2005).

The N-terminal domain of Hsp90 is the most highly conserved and most intensively studied domain of the three Hsp90 domains. The domain is comprised of approximately 220 amino acids and has been shown to bind both ATP and ADP (Prodromou *et al*., 1997a, Grenert *et al*., 1997). Hsp90 is classified as a member of the GHLK ATPase family, along with bacterial DNA gyrase, the DNA repair protein MutL and several bacterial histidine kinases because of the structurally unique ATP binding site (Dutta and Inouye, 2000). Hsp90 chaperone activity is known to be ATP dependent and ATP hydrolysis causes a conformational change within the protein that allows it to bind and release client proteins (Figure 1.2) (Prodromou *et al*., 1997a; 1997b; 2000). The N-terminal ATP-binding site is also the binding site of several Hsp90 inhibitors such as geldanamycin (GA) and its analogues 17-*N*-allylamino-17-demethoxygeldanamycin (17-AAG) and radicicol (Grenert *et al*., 1997; Stebbins *et al*., 1997; Roe *et al*., 1999), and is also involved in the binding of Hsp90 client proteins (Prodromou *et al*., 1997a). Connecting the N- terminus and Middle domain of Hsp90 is a flexible charged linker region that can vary in size and is only present in eukaryotic cells. This region is completely missing in mammalian TRAP1 (Figure 1.1) (Gupta, 1995). The linker region has been show to participate in the interaction of Hsp90 with steroid receptors (Cadepond *et al*., 1993, Dittmar *et al*., 1997, Kosano *et al*., 1998) and kinases (Miyata and Yahara, 1995). However through mutational studies, it was found that the absence of the linker region did not affect the essential functions of Hsp90 (Louvion *et al*., 1996). The Middle domain, which is also similar to that of GHKL proteins (Meyer *et al*., 2003, 2004, Pearl and Prodromou, 2006), is known as the binding site for most Hsp90 client proteins and some of the Hsp90 co-chaperones (Ali *et al*., 2006). The last domain is the C-terminal domain which is responsible for the constitutive dimerization ability of Hsp90, which is essential for functionality (Minami *et al*., 1994, Nemoto *et al*., 1995, Meng *et al*., 1996, Chadli *et al*., 2000). Also located at the C-terminus is another less characterized ATP-binding site. It is believed that this site opens up when the N-terminal ATP-binding site is occupied and has also been shown to have weak but detectable binding affinity for both ADP and GTP (Söti *et al*., 2002). Hsp90 inhibitors novobiocin (NOVO), cisplatin and taxol are known to bind the C-terminal ATP-binding site (Marcu *et al*., 2000a, 2000b, Donnelly and Blagg, 2008). The highly conserved MEEVD motif is located at the extreme end of the C-terminus in the cytosolic isoforms (Figure 1.1). This motif has been shown to be vital for the interaction of Hsp90 with a specialized group of co-chaperones that contain a tetratricopeptide repeat (TPR) motif, which will be discussed in depth in section 1.4.1 below.

The mitochondria and ER isoforms of Hsp90, TRAP1 and Grp94 both lack the MEEVD motif (Figure 1.1) that is required for the interaction with TPR-containing co-chaperones. For Grp94, the MEEVD motif is replaced by a KDEL motif, an ER retention signal, resulting in Grp94 being predominately an ER lumen residential protein (Munro and Pelham, 1987, Argon and Simen, 1999, Marzec *et al*., 2012). However, Grp94 has shown to be secreted by pancreatic acinar cells (Bruneau *et al*., 1998) and a subpopulation has been found on the cell surface (Altmeyer *et al*., 1996, Frasson *et al*., 2009, Koo and Apte, 2010). Secreted and cell surface Grp94 has been shown to lack the N-terminal ER targeting signal peptide and C-terminal retention motif (Eletto *et al*., 2010, Marzec *et al*., 2012). Similar to cytosolic Hsp90, Grp94 has three domains, an N-terminal domain linked to the Middle domain by a charged linker region and a C-terminal domain (Figure 1.1). The N-terminal domain is the site of ATP binding, together with the charged linker region as well as a number of residues from the Middle domain which make up the catalytic loop are required to assist in ATP hydrolysis (Dollins *et al*., 2007, Frey *et al*., 2007). The N-terminal domain is also the binding site of client proteins such as dendritic cell receptors (Biswas *et al*., 2002, Berwin *et al*., 2003) and inhibitors such as GA, radicicol or their derivatives (Chavany *et al*., 1996, Schulte *et al*., 1998, 1999). *In vitro* competitive binding assays and co-crystallization studies illustrated that ATP/ADP and Grp94 inhibitors bind the same pocket located opposite the substrate binding site (Schulte *et al*., 1998, 1999, Soldano *et al*., 2003, Dollins *et al*., 2007). By binding to the nucleotide binding site, GA and radicicol are able to affect the ATP dependent activity of Grp94 towards substrates (Wearsch and Nicchitta, 1997, Vogen *et al*., 2002). Interestingly, a nucleotide analogue N-ethylcarboxamidoadenosine (NECA) has been shown to bind specifically to Grp94 due to the unique nature of the entry site to the nucleotide binding site, suggesting that Grp94 specific compounds can be designed or discovered and used in Grp94 specific inhibition (Rosser and Nicchitta, 2000). Besides assisting the hydrolysis of ATP through the catalytic loop, no additional functions have been linked to the Middle domain, which is known to bind substrates and co-chaperones in cytosolic Hsp90 (Ali *et al*., 2006). Unlike in cytosolic Hsp90s, the charged linker region that connects the N-terminal and Middle domain is essential in Grp94, because it assists and mediates conformational changes required for ATP hydrolysis which affects the binding between Grp94 and its substrates (Hainzl *et al*., 2009). Similar to other Hsp90s, the C-terminal domain is the domain responsible for constitutive homodimerization of Grp94, which is mediated by a stretch of 44 hydrophobic amino acids (Nemoto *et al*., 1996, Wearsch and Nicchitta, 1996).

In cytosolic Hsp90s, the C-terminal domain is the binding site of the inhibitor NOVO (Marcu *et al*., 2000a, 2000b). The binding site for NOVO centers around the $K^{559}KQEEKK^{564}$ sequence (Matts *et al*., 2011), however this site is not accessible while the protein is in the closed conformation, suggesting that binding to this site by various substrates is linked to the conformational equilibrium of the whole protein (Dollins *et al*., 2007). Interestingly, this site is not conserved in Grp94 proteins. On the other hand, the SPC sequence adjacent to the NOVO binding site found in cytosolic Hsp90s, which is a part of the conformational control point affecting the dimerization of the protein (Ratzke *et al*., 2010), is conserved in the Grp94 protein (Dollins *et al*., 2007, Marzec *et al*., 2012). Overall, this observation suggests that NOVO might still be able to bind to the C-terminal domain of Grp94 as the binding of the inhibitor could be linked to the conformation state of the proteins as opposed to the sequence itself. At present the client binding site on Grp94 has yet to be identified or defined, however it is thought to be located along the Middle and C-terminal domain of the protein (Marzec *et al*., 2012).

Similar to other Hsp90 proteins, the most important function of Grp94 is linked to its chaperoning activities, where it assists in folding, assembly or degradation of secreted and membrane proteins (Eletto *et al*., 2010, Marzec *et al*., 2012). However, unlike other ER chaperones such as Grp78 and refolding enzymes such as protein disulfide isomerase (PDI) and the calreticulins, Grp94 is highly selective of its client proteins. This is illustrated by its ability to chaperone specify members within a protein family while excluding others as well as by the many secretory and membrane proteins that do not require the chaperone for proper folding (Randow and Seed, 2001, Yang *et al*., 2007, Morales *et al*., 2009). However in special cases, entire protein families such as insulin-like growth factors (IGF)-I and -II require the chaperoning activity of Grp94 for maturation and in the absence of the Grp94, precursor IGF proteins accumulate in the ER and are targeted for ER mediated degradation (ERAD) (Ostrovsky *et al*., 2009, 2010). Like other ER protein folding components such as Grp78, Grp94 expression is upregulated in response to ER stress in an attempt to increase protein folding or degradation efficiency in order to restore ER homeostasis (Chang *et al*., 1989, Eletto *et al*., 2010, Marzec *et al*., 2012). A complex made up of various ER proteins including Grp78 and Grp94 was identified and proposed to permanently exist as stable multichaperone complex within the ER rather than being formed in response to the folding needs of specific client protein (Meunier *et al*., 2002). However this was later disproved based on the measurement of the mobility of tagged- Grp94 and Grp78 (Snapp *et al*., 2006). An alternative explanation to the

formation of the complex could be linked to the requirements of the type of client protein requiring folding or maturation assistance. Certain proteins require both Grp78 and Grp94 at the same time, while others require assistance from the two chaperones at different stages of their maturation or folding (Eletto *et al*., 2010). In other cases, certain proteins require Grp78 but not Grp94 activity and vice versa as seen in the case of IGF proteins, which associate with Grp94 and not Grp78, suggesting that Grp78 is not always required during the Grp94 cycle (Ostrovsky *et al*., 2009, 2010).

1.4.1 Hsp90 co-chaperones

Whereas client proteins are defined as proteins that require chaperones such as Hsp90 for maturation and activity, co-chaperones are described as non-client binding proteins that participate or facilitate the function of chaperones. Examples include proteins like p23 and the Hsp70/Hsp90 organizing protein (HOP) (Caplan, 2003). Some co-chaperones may have chaperone activity themselves and can bind both the client and chaperone, while others are unable to bind clients and are mainly regulators of chaperone activity or function (Caplan, 2003). Hsp90 interacts with several co-chaperones which assist its chaperoning functions or cycle (Figure 1.2). The co-chaperones form multichaperone complexes with Hsp90 and its substrates during the Hsp90 cycle. Hsp90 co-chaperones are diverse and it has been suggested that the type and combination of the co-chaperones within the complexes can determine the type of client protein with which Hsp90 interacts. Hsp90 co-chaperones can be categorized into two groups, namely non-TPR-containing and TPR-containing co-chaperones (Caplan, 2003, summarized in Table 1.2).

Non-TPR co-chaperones of Hsp90 include p23, cell division cycle 37 (Cdc37) and activator of the Hsp90 ATPase (Aha1). These three proteins are structurally diverse and have different functions within the Hsp90 cycle. The co-chaperone p23 is known to bind and stabilize Hsp90 in its closed conformation or ATP bound state by inhibiting its ATPase activity, prolonging the interaction of Hsp90 with client proteins. It has also been shown to be involved in stimulating the release of the client proteins when ATP is hydrolyzed (Young and Hartl, 2000, Sullivan *et al*., 2002, McLaughlin *et al*., 2006). Aha1 binds the Middle domain of Hsp90, activating ATP hydrolysis and this is thought to lead to the release of client protein (Mayer *et al*., 2002, Meyer *et al*., 2004, Retzalaff *et al*., 2010). Cdc37 is known to interact specifically with kinase client proteins, binding to the N-terminal domain, where it competes for the ATP binding site, thus inhibiting ATPase activity (Grammatikakis *et al*., 1999, Matts and Caplan, 2007).

The majority of Hsp90 co-chaperones contain the TPR domain, which binds to the highly conserved MEEVD motif that is located at the C-terminal domain of Hsp90α and Hsp90β (Scheufler *et al*., 2000, Young *et al*., 2003). TPR-containing co-chaperones are structurally conserved but functionally diverse, binding and acting at different points in the Hsp90 cycle. The first TPR co-chaperone to have a role in the Hsp90 cycle is HOP which acts as an adaptor protein between Hsp90 and Hsp70, enabling the transfer of client proteins from Hsp70 to Hsp90. HOP is thought to stabilize the open conformation of Hsp90 (ADP bound state) and also inhibit ATP hydrolysis (Young *et al*., 2001, Schmid *et al*., 2012). Other TPR co-chaperones of Hsp90 include the protein phosphatase PP5, cyclophilin 40 (Cyp40), FK506-binding family of immunophilins (FKBP51/52) and the E3 ubiquitin ligase C-terminus Hsc70 interacting protein (CHIP), which have distinct functions during the cycle, from changing the phosphorylation state of Hsp90 and client proteins, transportation of Hsp90-client complexes or facilitating proteosome-targeted degradation (Cyr *et al*., 2002, Davies and Sanchez, 2005, Cox and Johnson, 2011, Mollapour and Neckers, 2012).

At present no isoforms of the cytosolic Hsp90 co-chaperones, both non-TPR and TPR-containing, have been identified in the ER or the mitochondria (Caplan, 2003). Thus there are currently no known equivalent of Hsp90 co-chaperones for TRAP1 and Grp94. Both chaperones lack the EEVD motif that is essential for the interaction with TPR-containing co-chaperones. The possibility that ER/mitochondrial co-chaperones that perform similar functions to cytosolic co-chaperones might exist is feasible, although they are yet to be discovered (Caplan, 2003). Another plausible scenario is that ER equivalents of cytosolic co-chaperones are structurally different and interact via novel mechanisms in the organelles. For example the ER resident protein cyclophilin B is an ER isoform that lacks the TPR domains contained in its cytosolic relative Cyp40. Cyclophilin B has been shown to interact with a multichaperone complex that also contained Grp94, although whether this interaction is direct or indirect is yet to be determined (Meunier *et al*., 2002).

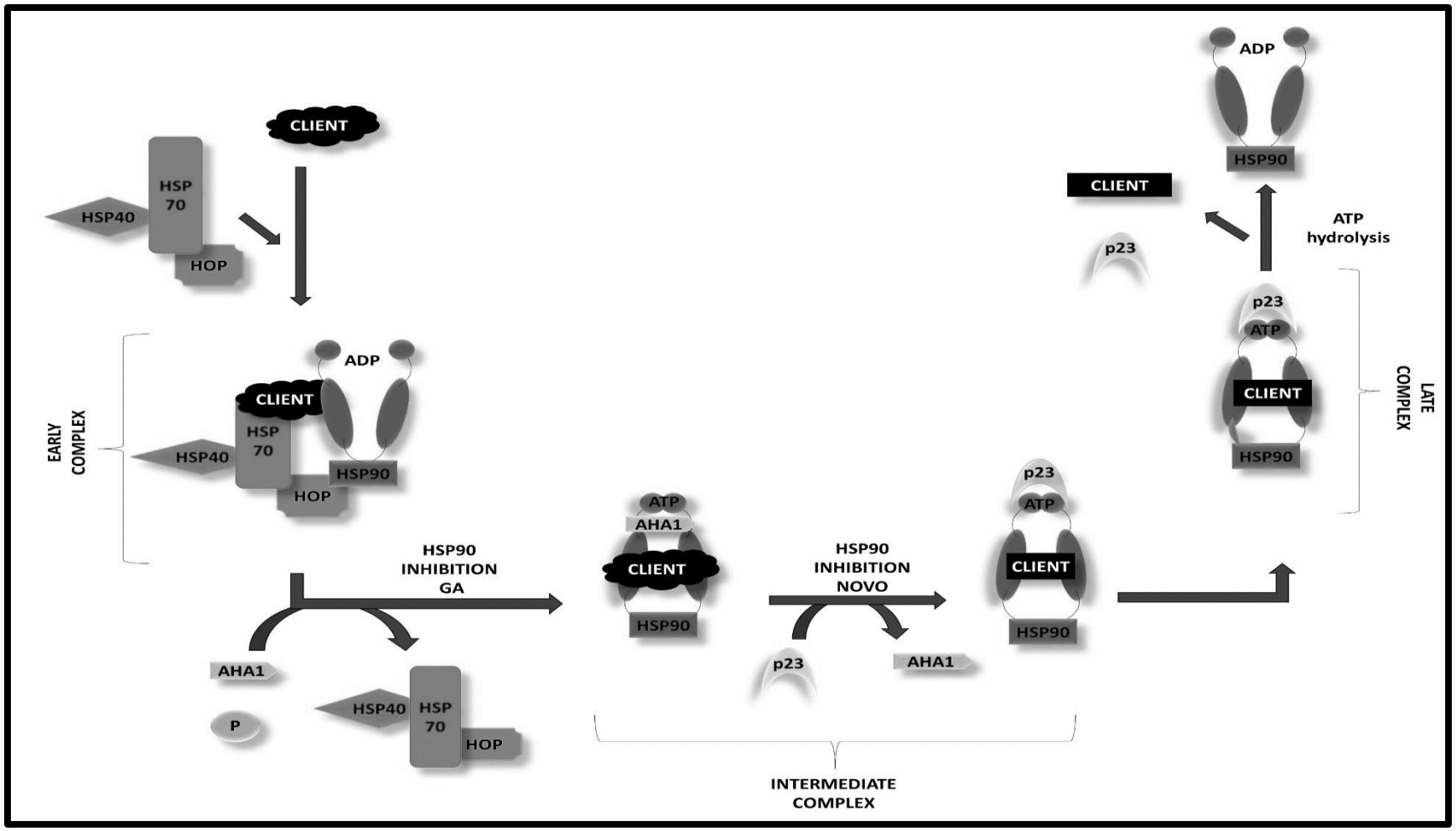

Figure 1.2: Schematic diagram illustrating the Hsp90 pathway. The pathway begins with the binding of the unfolded client protein by Hsp70 and its co-chaperones Hsp40 and HOP (early complex). HOP acts as a linker protein between Hsp70 and Hsp90 by binding to the C-terminus of both chaperones using distinct TPR domains. Aha1, a co-factor of Hsp90 disassociates HOP/Hsp70/Hsp40 interaction to Hsp90 and promotes the conformational change of Hsp90. An ATPase dependent interaction occurs between Hsp90 and its co-factor, p23 (intermediate complex), displacing Aha1 and this interaction stabilizes the closed conformation of Hsp90. After the maturation of the client protein, ATP hydrolysis occurs, causing Hsp90 to undergo a conformational change back to an ADP bound state, followed by the dissociation of the late complex and the release of the client protein (adapted from Mahalingam *et al*., 2009, Li *et al*., 2013)..

1.5 Heat shock protein 70 (Hsp70)

The Hsp70 (HSPA) family is the most studied and highly conserved class of molecular chaperones. Hsp70 proteins are often regarded as the housekeeping chaperones as they are a crucial component in the maintenance of cellular homeostasis. Hsp70 proteins are also known to be involved in various functions such as protein folding and degradation (Hartl and Hayer-Hartl, 2002), protein translocation (Ryan and Pfanner, 2001), complex assembly and disassembly (Chromy *et al*., 2003) and protein aggregation suppression (Mayer and Bukau, 1998, 2005, Fink, 1999; Pratt and Toft, 2003). Currently there are thirteen known human isoforms of Hsp70 which are localized in various organelles (Kampinga and Craig, 2010). Heat-shock cognate 70 (Hsc70) or HSPA8 is the cytosolic constitutive form, while Hsp72 (HSPA1A) is stress inducible. During stress conditions, Hsp72 has greater affinity for unfolded proteins and is known to promote the refolding of aggregated proteins and targeting of irreversibly damaged proteins for degradation via the lysosomal or ubiquitination pathway (Mayer and Bukau, 1998, 2005, Agarraberes and Dice, 2001, Höhfeld *et al*., 2001, Callaham *et al*., 2002). Glucose-regulated protein with molecular mass of 78 kDa (Grp78), also known as binding immunoglobulin protein (BiP) or HSPA5, and mitochondrial Hsp70 (mtHsp70), are the ER and mitochondrial Hsp70 isoforms, respectively (Munro and Pelham, 1986, Ting and Lee, 1988, Domanico *et al*., 1993, Wadhwa *et al*., 2002). Hsp70 proteins have three conserved domains, namely an N-terminal ATPase domain, a substrate binding domain and a C-terminal lid, which has the GPTIEEVD motif at the extreme end of the domain (Figure 1.3) (Flaherty *et al.*, 1990; Zhu *et al.*, 1996; Fink, 1999, Daugaard *et al*., 2007).

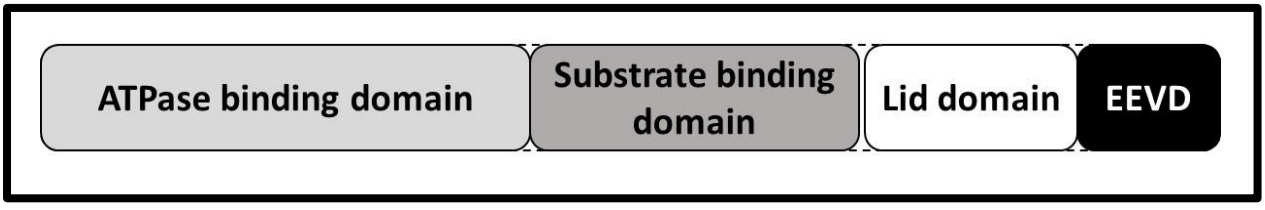

Figure 1.3: Schematic representation of Hsp70 structural domains. An ATPase binding domain of about 44 kDa is located on the N-terminus of the protein and is the binding site of ATP and ADP. The substrate binding domain of about 15kDa is located in the middle of the protein and is the binding site of Hsp70 client proteins/substrates. The lid domain is located on the C-terminus of the protein and is the binding site of the majority of Hsp70 co-chaperones through interactions with the EEVD motif (adapted from Fan *et al*., 2003).

Hsp70 proteins are known to have ATP dependent activity with the ATPase domain on the N-terminus as the site of ATP hydrolysis. This hydrolysis of ATP results in a conformational change which regulates the binding capabilities of the substrate binding domain. In the ATP bound form, Hsp70 has low affinity for substrate binding, while ATP hydrolysis to ADP stimulated by the Hsp70 co-chaperone, Hsp40/DNAJ, results in a conformational change which increases the binding affinity for substrates (Mayer and Bukau, 1998; 2005, Kampinga and Craig, 2010). The substrate binding domain of Hsp70 is highly conserved amongst the different isoforms, although subtle differences have been observed. The mechanism by which these differences infer isoform specific function is however unknown (Mayer and Bukau, 2005). Binding and releasing of substrates by the substrate domain is dependent on the ATP-ADP cycle (Mayer and Bukau, 2005). The GPTIEEVD motif (different from Hsp90 MEEVD motif) is located on the extreme end of the C-terminus of some Hsp70 isoforms and is responsible for the interaction of the chaperone with TPR-containing co-chaperones such as HOP (Scheufler *et al*., 2000; Odunuga *et al*., 2003).

Grp78, the ER homologue of Hsp70 and mtHsp70, the mitochondria resident protein, are two of the Hsp70 isoforms that lack the EEVD motif essential for the interaction with TPR-containing co-chaperones. Grp78 resides in the lumen of the ER; secretion out of the ER is prevented by the presence of the KDEL ER retention motif at the C terminus of the protein (Munro and Pelham, 1987, Takemoto *et al*., 1992, Zhang *et al*., 2010a). Grp78 is involved in protein translocation into the ER, protein folding, targeting of misfolded proteins for ER-associated degradation (ERAD) and sensing ER stress (Hendershot, 2004, Roller and Maddalo, 2013). As an ER stress sensor, Grp78 is able to regulate ER stress caused by the accumulation of unfolded proteins resulting in the unfolded protein response (UPR) (Lee, 2005). Grp78 regulates ER stress by activating various components of the UPR signalling pathway. In brief, upon ER stress, Grp78 releases three ER transmembrane signal transducers; PKR-like ER kinase (PERK), inositol-requiring enzyme 1 (IRE1) and activating transcription factor 6 (ATF6) (Rutkowski and Kaufman, 2004). The release of PERK causes attenuation of protein synthesis through the phosphorylation of the eukaryotic translation initiation factor 2 α subunit (eIF2α), thereby halting protein synthesis and alleviating the protein load in the ER (Shi *et al*., 1998). The release of ATF6 and IRE1 results in the upregulation of ER proteins involved in protein folding and degradation such as chaperones (Grp78, Grp94), folding enzymes (PDI) and co-chaperones (DNAJ) (Ye *et al*., 2000, Yoshida *et al*., 2000, Calfon *et al*., 2002). To further relieve ER stress caused by the accumulation of unfolded

proteins, Grp78 works in conjunction with ER resident DNAJ co-chaperones to refold aggregated proteins or target misfolded proteins for degradation, until ER homeostasis is restored (Feldheim *et al*., 1992, Brightman *et al*., 1995, Shen *et al*., 2002, Hosoda *et al*., 2003, Shen and Hendershot, 2005, Oyadomari *et al*., 2006, Rutkowski *et al*., 2007).

1.5.1 Hsp70 co-chaperones

Similar to Hsp90, Hsp70 has co-chaperones that facilitate its chaperoning function. Hsp70 chaperones can also be divided into two groups, namely DNAJ and non-DNAJ co-chaperones. DNAJ proteins regulate the chaperone functions of Hsp70 by passing substrates to Hsp70 and controlling the ATPase cycle of the chaperone (Fan *et al*., 2003). The DNAJ proteins will be discussed in depth in the following section.

The C-terminal domain of Hsp70, similar to Hsp90 also contains the conserved EEVD motif that allows TPR-containing co-chaperones to interact with that domain. HOP acts as an adaptor protein between Hsp70 and Hsp90, allowing the exchange of client proteins between the two chaperones (Chen *et al*., 1996). CHIP can negatively regulate the refolding activity of Hsp70 by affecting its ATPase activity, while at the same time assisting in chaperone mediated protein degradation (Connell *et al*., 2001). While co-chaperones like CHIP and HOP bind both Hsp70 and Hsp90, there are also Hsp70 specific non-DNAJ co-chaperones. Hsp70 interacting protein (HIP) stabilizes the ADP bound state of Hsp70, which in turn enhances its chaperoning activity (Höhfeld *et al*., 1995). Bcl-2-associated athanogene isoforms 1-5 (BAG1-5) are non-TPR nucleotide exchange factor co-chaperones that negatively regulate Hsp70 chaperone function by causing the disassociation of ADP or competing with the co-chaperone HIP, therefore destabilizing the protein (Nollen *et al*., 2001). BAG5 has also been shown to bind to CHIP, affecting its ability to target proteins for degradation (Kalia *et al*., 2011).

It is interesting to note that some of the TPR co-chaperones such as HOP and CHIP act as co-chaperones for both Hsp90 and Hsp70 (Table 1.2). HOP has three functional TPR domains; TPR-1, TPR-2A and TPR-2B. TPR-1 is known to bind selectively to Hsp70, while TPR-2A selectively binds Hsp90 (Chen *et al*., 1996, Lässle *et al*., 1997, Southworth and Agard, 2011, Lee *et al*., 2012). In the case of CHIP, only one TPR domain is present and this domain can bind indiscriminately to both Hsp90 and Hsp70 (Smith, 2004). TPR domain specificity between Hsp90 and Hsp70 has been linked to unique amino acid residues upstream of the EEVD motif (Scheufler *et al*., 2000), and

mutation studies have shown that TPR-1 can be mutated to interact with Hsp90 and vice versa for TPR-2A (Odunuga *et al*., 2003).

Table 1.2: Partial list of co-chaperones of Hsp90 and Hsp70

Co-chaperone	Binding partner	Binding site	TPR/ Non-TPR	Function	Reference
Aha1	Hsp90	Middle domain	Non-TPR	Effective stimulator of Hsp90; ATPase activity and triggers the release of client proteins from the Hsp90 complex	Mayer *et al*., 2002
BAG1-5	Hsp70	Middle domain	Non-TPR	Nucleotide exchange factor and modulator of Hsp70 activity	Nollen *et al*., 2000, Mayer *et al*., 2005
Cdc37	Hsp90	N-terminal	Non-TPR	Kinase binding co-chaperone; Slows down the ATPase cycle of Hsp90, extending the holding time of clients	Mandal *et al*., 2007, Gary *et al*., 2008
CHIP	Hsp90/ Hsp70	C-terminal of Hsp90 and Hsp70	TPR	Proteosome-targeted degradation facilitator; Inhibits Hsp70 protein refolding activity	Ballinger *et al*., 1999, Meacham *et al*., 2001
Cyp40	Hsp90	C-terminal	TPR	Co-chaperone activity unknown	Ratajczak *et al*., 1996, Duina *et al*., 1996, 1998, Carrello *et al*., 2004
HIP	Hsp70	N-terminal	TPR	Stabilizes Hsp70 in its ADP bound state	Nollen *et al*., 2001, Li *et al*., 2013
HOP	Hsp90/ Hsp70	C-terminal	TPR	Adaptor protein of Hsp90 and Hsp70; Mediates substrate transfer between Hsp70 and Hsp90	Southworth and Agard, 2011, Lee *et al*., 2012
Hsp40/DNAJ	Hsp70	N-terminal	Non-TPR*	Targets unfolded proteins to Hsp70 and stimulates the ATPase activity of Hsp70.	Tsai *et al*., 1996, Greene *et al*., 1998, Fan *et al*., 2003, Kampinga and Craig, 2010
p23	Hsp90	N-terminal	Non-TPR	Stabilizes the interaction of Hsp90 and client proteins in ATP bound state (closed conformation) by inhibiting the ATPase function of Hsp90	Freeman *et al*., 2000, McLaughlin *et al*., 2006
PP5	Hsp90	C-terminal	TPR	Changes phosphorylation state of Hsp90, co-chaperones and client proteins	Das *et al*., 1998, Vaughat *et al*., 2008

*** Exception is DNAJC7 and DNAJC3 which contain TPR domains**

1.6 Heat shock protein 40 (Hsp40)

The most abundant and diverse group of molecular chaperones is the Hsp40 or DNAJ family members, defined by the presence of the canonical J domain (Cheetham and Caplan, 1998). Currently there are forty-nine known DNAJ members expressed in humans and localized in

various compartments such as the cytoplasm, nucleus, mitochondria and ER (Walsh *et al*., 2004, Qui *et al*., 2006). Homologues of DNAJ proteins have been identified in different organisms such as *Saccharomyces cerevisiae* and *Escherichia coli* (*E. coli*), where twenty-two and six members have been identified, respectively (Walsh *et al*., 2004). DNAJ proteins are divided into different types based on their structural domains (Figure 1.4). DNAJA (Type 1) which has four members of four domains, namely consists of a J domain, a glycine/ phenylalanine (Gly/Phe) rich domain, a cysteine (Cys) repeat region and a C-terminal domain. DNAJB (Type 2) which has thirteen members, lacks the Cys repeat region found in DNAJA proteins, but has the J domain, Gly/Phe rich domain. DNAJC (Type 3) is the largest DNAJ group with thirty-two members and only has the J domain conserved, and unlike DNAJA and DNAJB groups, this domain can be located at any position along the protein (Cheetham and Caplan, 1998, Vos *et al*., 2008, Kampinga and Craig, 2010). DNAJC proteins are considered to have more specialized functions compared to DNAJA and DNAJB members, due to the presence of unique domains which are not normally linked to DNAJ functions (Sterrenberg *et al*., 2011). The existence of a fourth DNAJ group has been proposed (Botha *et al*., 2007). The so-called Type 4 DNAJ proteins have a compromised histidine, proline, and aspartic acid (HPD) motif, (Figure 1.4) (Botha *et al*., 2007). This motif is located within the J domain and is essential for stimulation of the ATPase DNAJ co-chaperoning activity towards Hsp70 proteins. The majority of proposed Type 4 DNAJ proteins are found in parasitic organisms such as *Plasmodium falciparum* (Botha *et al*., 2007). At present a putative Type 4 DNAJ protein, DNAJB13 has been identified in humans, mice and zebrafish and is thought to have J domain independent functions (Guan and Yuan, 2008, Yang *et al*., 2008). Interestingly, the coelacanth homologue has an intact HPD motif (Tastan Bishop *et al*., 2013).

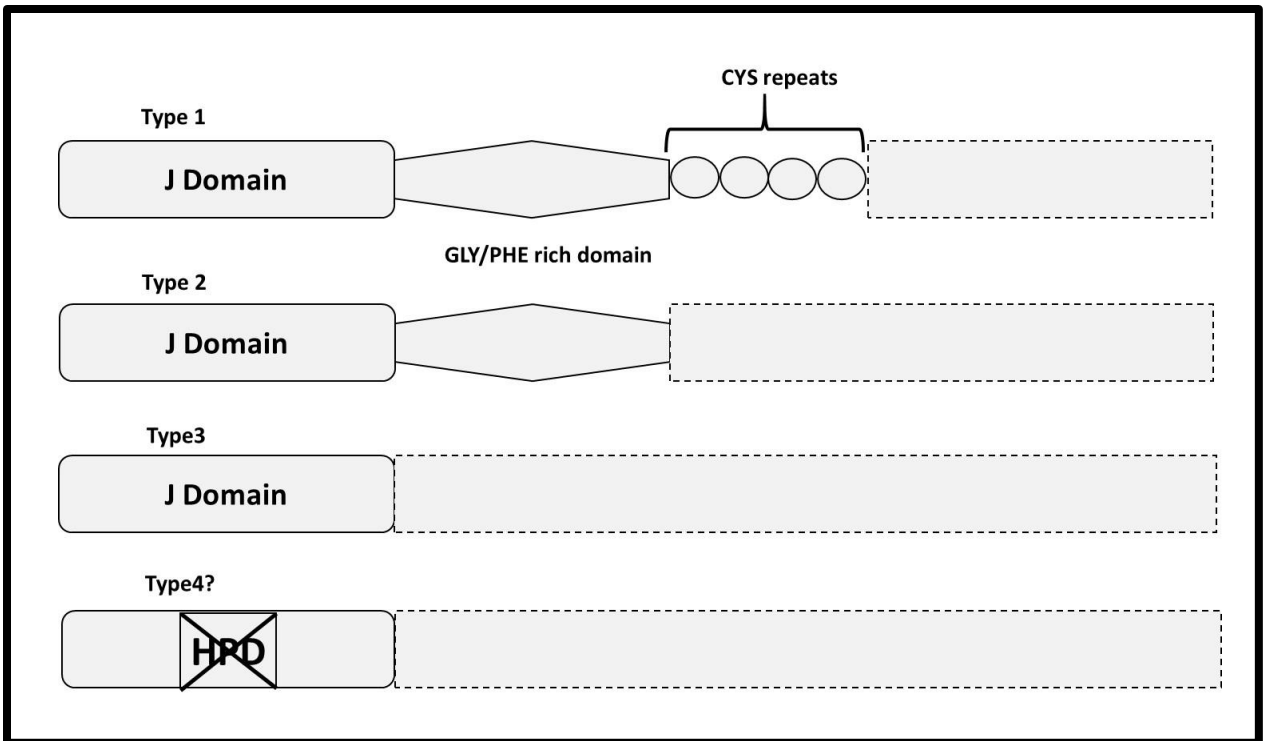

Figure 1.4: Schematic diagram of the different families of DNAJ protein. Classification of DNAJ proteins is based on the presence of the different domains. The J domain is present in all DNAJ and is involved in facilitating the interaction between DNAJ and Hsp70. The Gly/Phe rich domain is found in DNAJA and DNAJB members and the zinc domain which consists of 4 CysXXCysXGlyXGly repeats, where X indicates any amino acid, is only present in DNAJA proteins. Type 4 is a newer group of DNAJ proteins with a corrupted HPD motif (adapted from Qiu *et al*., 2006; Botha *et al*., 2007, Rosser and Cyr, 2007).

The signature domain of all DNAJ proteins is the J domain which is made up of approximately 70 amino acids and is highly conserved across all organisms. Structurally, the J domain is made up of four alpha helices, with a loop region between helix II and III that contains the highly conserved and functionally important HPD motif (Cheetham and Caplan, 1998). DNAJ proteins are known to stimulate the ATPase activity of Hsp70 proteins through the J domain, and the HPD motif is essential for this interaction, as mutation studies targeted at the motif lead to the loss of ATPase stimulation of Hsp70 (Feldheim *et al.,* 1992; Wall *et al.,* 1994; Tsai and Douglas, 1996). The Gly/Phe domain found in DNAJA and DNAJB members is thought to also interact with Hsp70 proteins and assists J domain interaction with the ATPase domain of Hsp70 by stabilizing the complex. Although the Gly/Phe domain assists in the stimulation of Hsp70 ATPase activity, the presence of the domain is not essential as the J domain has been shown to be able to interact and stimulate Hsp70 ATPase activity in the absence of this domain in numerous DNAJC members, (Wall *et al*., 1994), as well as isolated J domains from *E. coli* (Greene *et al*., 1998, Wittung-

Stafshede *et al*., 2003, Horne *et al*., 2010). The zinc finger domain, also referred to as the Cys-repeat region found only in DNAJA members, has a Cys rich region that has a CysXXCysXGlyXGly motif repeated four times where the X can represent any amino acid (Figure 1.4). Proteins with similar repeats have been found to be involved in DNA binding (Song *et al*., 1995). The Cys-rich domain is thought to be involved in the presentation of substrates to Hsp70, as well as the stabilization of Hsp70-substrate complexes (Szabo *et al.*, 1994; Banecki *et al.*, 1996). The C-terminal region of DNAJ protein remains largely uncharacterized, however in DNAJA and DNAJB members, this domain is thought to contain the substrate binding domain and is essential for their co-chaperoning function (Lu and Cyr, 1998a, 1998b, Sha *et al*., 2000). However, with DNAJC members, this domain usually contains varied domains that are not classically linked to DNAJ proteins, and the diversity of these domains is thought to be crucial for functionality and substrate specificity observed in various DNAJC members (Cheetham and Caplan, 1998, Fliss *et al*., 1999, Kampinga and Craig, 2010).

The most recognised functions of DNAJ proteins is their ability to act as co-chaperones to Hsp70 proteins, where they assist the protein during its chaperoning functions by recruiting Hsp70 towards client proteins, presenting client substrates to Hsp70 and stimulating the ATPase activity required for Hsp70 ATP dependent chaperone functions (Liberek *et al*., 1991, Cheetham and Caplan, 1998, Qiu *et al*., 2006, Kampinga and Craig, 2010). Hsp70 chaperone activity is ATP dependent; the chaperone binding affinity for client substrates is regulated by the phosphorylation state of the nucleotide (Cheetham and Caplan, 1998, Qiu *et al*., 2006, Kampinga and Craig, 2010). Bound to ATP through the ATPase domain, Hsp70 has low binding affinity for client substrates. Interaction with the J domain of DNAJ proteins via the HPD motif stimulates Hsp70 ATPase activity which results in the hydrolysis of ATP to ADP (Wall *et al*., 1994, Tsai and Douglas, 1996). The change in the phosphorylation state of the nucleotide causes a conformational change in Hsp70 which increases the chaperones binding affinity towards client proteins (Wall *et al*., 1994, Tsai and Douglas, 1996, Qui *et al*., 2006). Overall, Hsp70 chaperone activity is ATP dependent and cyclic in nature as it requires repeat cycles of ATP hydrolysis (stimulated by DNAJ proteins) and nucleotide exchange (catalysed by nucleotide exchange factors), enabling it to bind and release client substrates (Figure 1.5) (Fink, 1999; Mayer and Bukau, 2005; Qiu *et al.*, 2006; Rosser and Cyr, 2007, Kampinga and Craig, 2010, Sterrenberg *et al*., 2011).

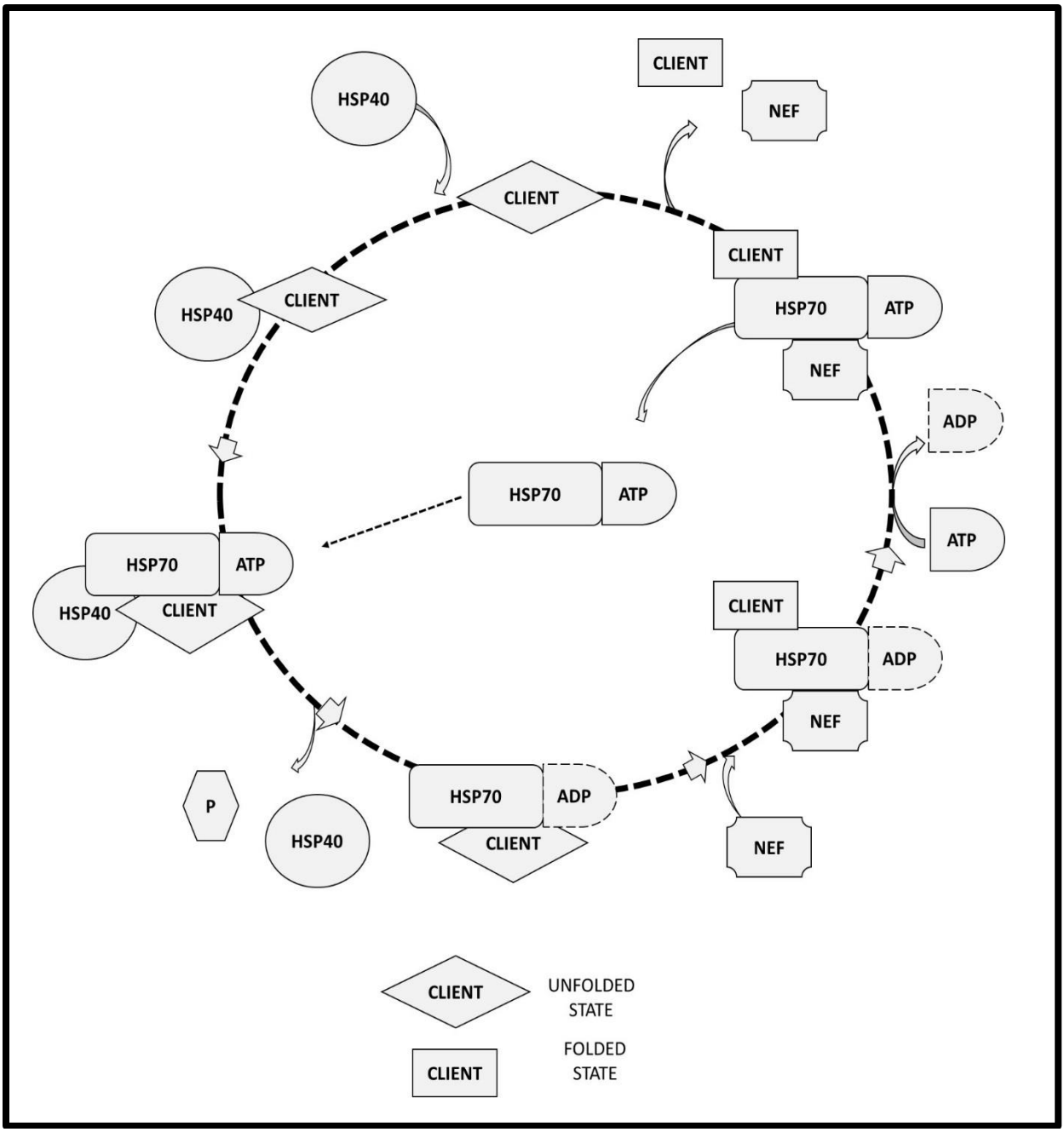

Figure 1.5: Systematic diagram illustrating the functions of DNAJ as a co-chaperone to Hsp70. The cycle begins with the binding of the client by DNAJ. This is followed by the recruitment of Hsp70 in its ATP bound form by its co-chaperone DNAJ. ATP hydrolysis is stimulated by DNAJ, which results in the increase of the affinity of Hsp70 for substrate binding, as well as the release of DNAJ from the complex. The next step is the binding of the NEF (nucleotide exchange factor) which has a higher binding affinity for Hsp70-ADP than Hsp70-ATP. ADP dissociates from Hsp70 allowing the re-binding of ATP, returning Hsp70 to a state where it has low binding affinity for the substrate. This is followed by the release of NEF and the substrate (adapted from Kampinga and Craig, 2010).

1.7 DNAJC3

DNAJC3 also known as ERdj6 or $p58^{IPK}$ (58 kDa inhibitor of protein kinase), is a novel DNAJC protein that contains two functional co-chaperone domains, namely the TPR and the J domain (Oyadomari *et al*., 2006, Rutkowski *et al*., Petrova *et al*., 2008, Tao *et al*., 2010, Svärd *et al*., 2011). DNAJC3 was first discovered in influenza virus infected cells where it was shown to act as an inhibitor of double stranded (dsRNA)-activated protein kinase (PKR) (Lee *et al*., 1990, 1992, 1994). DNAJC3 has also been identified as a co-chaperone of Grp78 and an inhibitor of PKR-like ER kinase (PERK) during ER stress (Yan *et al*., 2002, van Huizen *et al*., 2003, Rutkowski *et al*., 2007). The following sections will discuss the existing data on DNAJC3 in depth, from its functions, roles in diseases and structural organization.

1.7.1 Functions of DNAJC3

1.7.1.1 DNAJC3 functions during viral infection

DNAJC3 was first identified in influenza virus infected cells as an inhibitor of the interferon and dsRNA induced protein kinase PKR, an important component of the cellular antiviral response (Lee *et al*., 1990, 1992, 1994). In the presence of dsRNA or polyanions, PKR undergoes dimerization and autophosphorylation (Galabru and Hovanessian, 1987, Langland and Jacobs, 1992, Thomis and Samuel, 1993, Langland *et al*., 1995) which in turn causes the phosphorylation of the alpha subunit of *e*ukaryotic Initiation factor 2 (eIF2) on serine 51 (Merrick, 1992). The phosphorylation of the alpha subunit of eIF2 results in the attenuation, or in some cases the inhibition, of protein synthesis. Viruses due to their RNA genome with essential secondary structures have been shown to activate PKR activity (Katze, 1995). During viral infections, the presence of viral dsRNA triggers the autophosphorylation of PKR, which triggers a domino effect that ultimately results in the decrease of protein synthesis or the shutdown of protein synthesis machinery within the cell (Gale and Katze, 1998). Although this action prevents the formation of host proteins, the process also ensures that no viral proteins are produced, preventing the replication of viral particles and stopping the life cycle of the virus. However, some viruses such as the influenza virus have found ways to evade this defence system by using the host's own regulatory systems against it, in this case a natural inhibitor of PKR, DNAJC3 (Katze *et al*., 1988, Lee *et al*., 1990, 1992, 1994, Korth *et al*., 1996, Goodman *et al*., 2007, 2009, 2011). Under homeostatic conditions, DNAJC3 is normally inactive due to its association with its own inhibitors

such as p52^{rIPK} (Gale *et al*., 1998, 2002), recently renamed as p88^{rIPK} due to its 88 kDa size (Luig *et al*., 2010). Inhibition of DNAJC3 by p88^{rIPK} occurs through direct interaction although the mechanism of regulation is still unknown (Melville *et al*., 1997, 2000, Gale *et al*., 2002, Luig *et al*., 2010),

In influenza viral infection, the presence of viral dsRNA does not trigger the autophosphorylation of PKR that would result in the shutdown of protein synthesis. Instead when the virus infects the cells, it recruits or activates DNAJC3, which will in turn bind to PKR using its TPR motif 6, which has been shown to have limited homology to the eIF2α subunit, the natural substrate of PKR (Polyak *et al*., 1996, Tang *et al*., 1996, Gale *et al*., 1996). By binding to PKR, DNAJC3 blocks its autophosphorylation preventing the phosphorylation of the alpha subunit of eIF2 and allowing protein synthesis to occur normally, which will result in viral protein being produced (Figure 1.6) (Gale *et al*., 1996, Tan *et al*., 1998). The matrix protein (M2) of both influenza A and B virus is the viral protein that binds to DNAJC3, enhancing the autophosphorylation of PKR which affects the infected cell's life cycle and virus replication (Guan *et al*., 2010). Recently, Luig *et al*., (2010) have shown that influenza virus stimulated mitogen-activated protein kinase (MAPK)-activated protein kinases (MAPKAPKs) MK2 and MK3. This study demonstrated that active MKs recruit and bind directly to p88^{rIPK} which is in complex with DNAJC3 and the complex recruits and binds PKR. This binding results in the inhibition of PKR activity (Luig *et al*., 2010). In addition, the nucleoprotein in influenza a virus was also found to interact with DNAJC3 with an unidentified DNAJ protein, referred to as Hsp40, which is thought to be another inhibitor of DNAJC3 (Melville *et al*., 1997). The interaction between the nucleoprotein and Hsp40 results in the release of DNAJC3, allowing it to bind to PKR, preventing the kinase from phosphorylating eIF2α (Sharma *et al*., 2011).

DNAJC3 has also been shown to be downregulated in Coxsackie virus B3 (CVB3) infected cells, which leads to mitochondrial mediated apoptosis (Chau *et al*., 2007), suggesting that unlike influenza infected cells, the upregulation of DNAJC3 promotes cell survival and counteracts apoptosis induced by CVB3 (Zhang *et al*., 2010b). In CVB3-infected cells, inhibition of CVB3 induced apoptosis is accomplished by the activation of the PI3K/Akt pathway which requires the activation of activating transcription factor 6a (ATF6a) a protein responsible for the expression of chaperones in response to ER stress (Haze *et al*., 1999) and the upregulation of a mitochondrial membrane protein mitofusin 2 (Zhang *et al*., 2010b).

A plant orthologue of DNAJC3 has been identified in *Nicotiana benthamiana* and *Arabidopsis thialiana* (Bilgin *et al*., 2003). Bilgin *et al*., showed that DNAJC3 interacts with the helicase proteins of tobacco mosaic virus (TMV) and tobacco etch virus (TEV), were it is thought to assist in virus replication and pathogenicity. The knockdown of DNAJC3 in virus infected plants lead to the reduction of virus titre and ultimately death of the host cell. Cell death in DNAJC3 depleted cells was attributed to the phosphorylation of eIF2α by PKR in response to the presence of viral dsRNA (Bilgin *et al*., 2003).

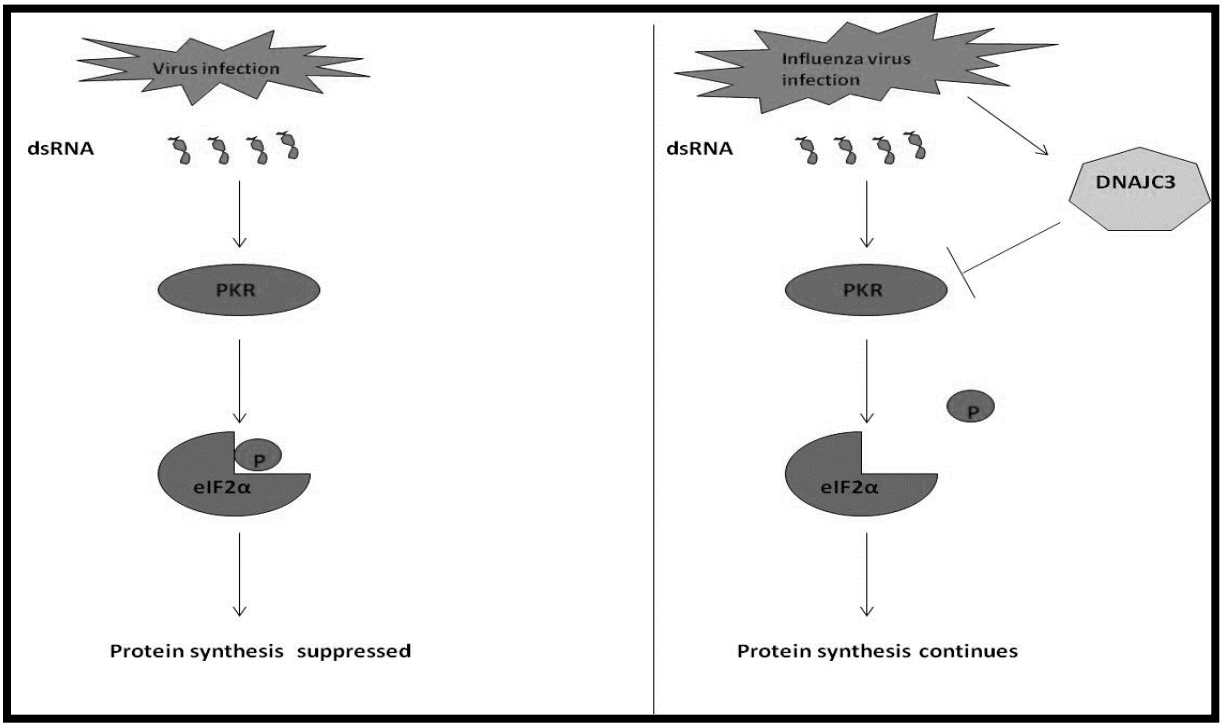

Figure 1.6: Schematic diagram illustrating the inhibitory activity of DNAJC3 on PKR during Influenza viral infection. In the presence of dsRNA, PKR undergoes autophosphorylation which leads to the phosphorylation the α subunit of eIF2, resulting in protein synthesis being suppressed. During influenza virus infection, the virus synthesises dsRNA which would normally activate PKR. However, the virus has evolved a mechanism that activates PKR's cellular inhibitor, DNAJC3 upon infection. The binding of DNAJC3 and PKR prevents the autophosphorylation of the kinase which blocks its activation and ability to phosphorylate eIF2. The consequence of PKR inactivation permits the synthesis of viral proteins along with host protein (Lee *et al*., 1990; 1994).

1.7.1.2 DNAJC3: Dual functions during the unfolded protein response (UPR)

Initially, DNAJC3 was thought to be an ER membrane-bound protein facing the cytosol, where it interacted with Hsp70 (Yan *et al*., 2002, Oyadomari *et al*., 2006). However, the discovery of the cleavable ER signal peptide at the N-terminus of DNAJC3 identified the protein as an ER

residential lumen protein (Rutkowski *et al*., 2007). The same group also illustrated that DNAJC3 that functions in the cytosol as PKR inhibitor represents a subpopulation that likely arose as a result of inefficiency in the translocation of the protein or, that under certain conditions, sufficient amounts of DNAJC3 can accumulate in the cytosol (Rutkowski *et al*., 2007).

In the ER, DNAJC3 has been shown to play an important role during the unfolded protein response (UPR), which is a response to ER stress resulting in the accumulation of unfolded proteins in the ER (Schröder and Kaufman, 2005, Walter and Ron, 2011). UPR ultimately results in the attenuation of protein synthesis alleviating the protein load in the ER as well as the upregulation of genes that code for ER chaperones such as Grp78 and components of the ER associated degradation pathway (Kaufman, 1999, Zhang and Kaufman, 2006, Ron and Walter, 2007, Wiseman *et al*., 2010, Patil and Walter, 2011). Activation of UPR has been observed in numerous diseases such as cancer, diabetes, obesity, autoimmune conditions and neurodegenerative disorders, resulting in the UPR pathway becoming a therapeutic target to treat these diseases (Wang and Kaufman, 2012, Cornejo and Hetz, 2013, Hetz *et al*., 2013, Lee and Ozcan, 2014).

DNAJC3 has been shown to act as a co-chaperone to Grp78 during the early stages of UPR, where it aids in the processing of unfolded proteins that accumulate in the ER by binding to the proteins and transferring them to Grp78, as well as stimulating the ATPase activity of the protein (Figure 1.7) (Oyadomari *et al*., 2006, Rutkowski *et al*., Petrova *et al*., 2008, Tao *et al*., 2010, Svärd *et al*., 2011). At the later stages of UPR, DNAJC3 has been found to have a role in downregulating or inhibiting the activity of ER-like PKR (PERK) (Yan *et al*., 2002, van Huizen *et al*., 2003). PERK acts in a similar way as cytosolic PKR, where it attenuates protein synthesis by phosphorylating eIF2α during UPR, preventing the synthesis of protein which would normally be translocated to the ER for processing, alleviating the burden to the ER (Harding *et al*., 1999, 2000). However, at the later stages when homeostasis has been restored to the ER, DNAJC3 inhibits PERK, resulting in the recovery of protein synthesis suppressed during UPR (Harding *et al*., 2000, 2002) (Figure 1.7).

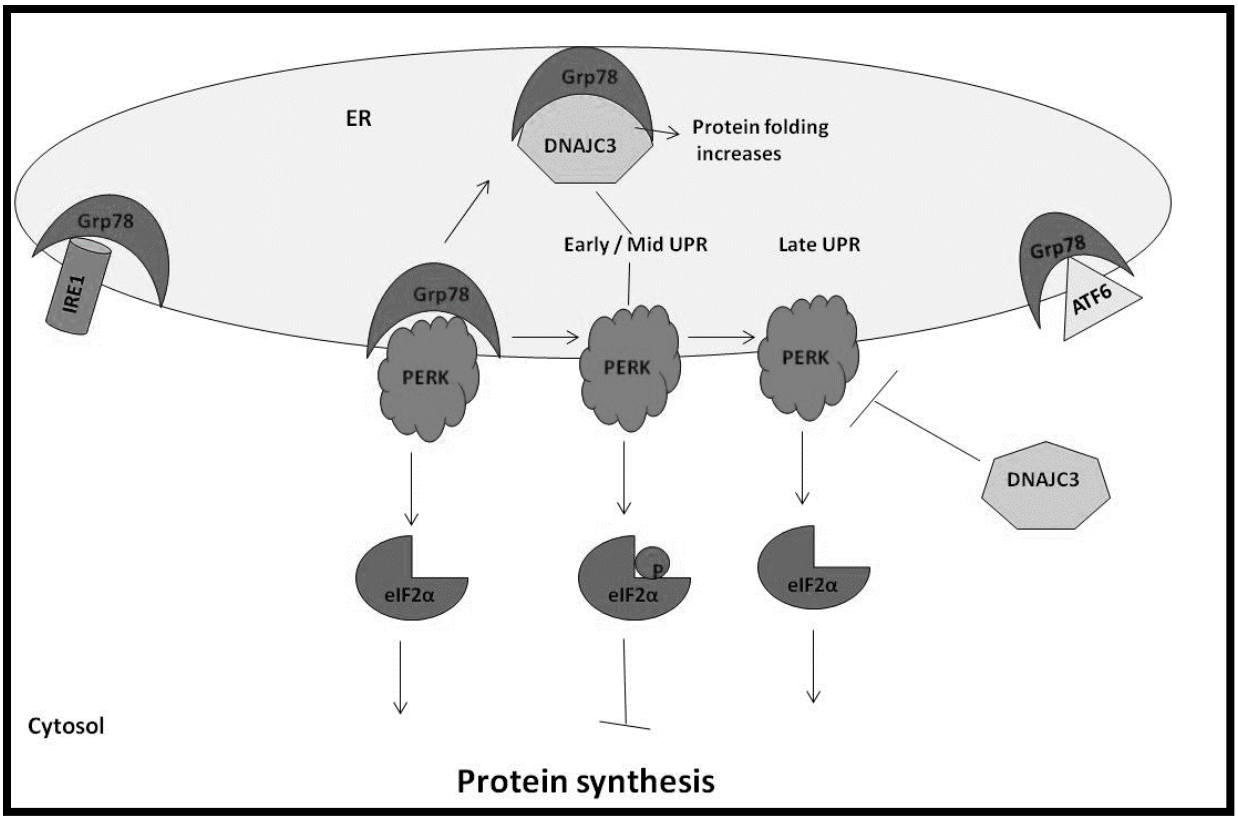

Figure 1.7: Schematic diagram illustrating the dual function of DNAJC3 during UPR. Under homeostasis, Grp78 is bound to ER-like PKR (PERK), inhibiting its kinase activity on eIF2α, allowing protein synthesis to occur. Upon ER stress, UPR is activated and at the early and mid-stages, Grp78 releases PERK and assumes its role as a chaperone, with DNAJC3 acting as 1 of the 7 ER DNAJ co-chaperones helping to reduce the load of unfolded proteins within the ER. Simultaneously, released PERK phosphorylates eIF2α resulting in the attenuation of protein synthesis, reducing the load of unfolded protein translocated in the ER. At the late stages of UPR when ER homeostasis has been restored, DNAJC3 resumes its functions as an inhibitor of PERK, preventing its phosphorylation of eIF2α, allowing protein synthesis to resume.

1.7.2 Role of DNAJC3 in disease

Similar to other molecular chaperones and DNAJ proteins, DNAJC3 has been implicated in disease. This section will review the role of DNAJC3 in cancer and diabetes.

Cancer

DNAJC3, like other DNAJ proteins has been found to play a role in cancer biology (Mitra *et al*., 2007, Sterrenberg *et al*., 2011). Studies have shown that DNAJC3 has anti-apoptotic functions, where it protects cells against TNF-α and dsRNA induced cell death (Tang *et al*., 1999). In NIH3T3 cells, over expression of DNAJC3 has been shown to lead to malignant cell formations which, when injected into nude mice, caused tumours (Barber *et al*., 1994, Korth *et al*., 1996). Another example of the role of DNAJC3 as an oncoprotein is related to its function as the inhibitor of PKR,

which plays an important role as an effector of apoptotic cell death (Tan and Katze, 1999), meaning that by inhibiting PKR, DNAJC3 can suppress apoptosis. Through the use of isobaric tags for relative and absolute quantitation (iTRAQ) quantitative proteomics profiling, expression of DNAJC3 was found to be upregulated in metastatic SW620 colon carcinoma compared to the paired primary SW480 colon carcinoma, although the implications of this observation is still unknown (Ghosh *et al*., 2011).

In breast cancer cells, overexpression of endoplasmic reticulum protein 29 (ERp29) an ER luminal residential protein involved in protein unfolding and secretion, delays the initiation of tumourigenesis in MBA-MB-231 breast cancer cells (Bambang *et al*., 2009). Overexpression of ERp29 promotes the activation (phosphorylation) of p38 which negatively regulates the expression of eIF2α and promotes G0/G1 arrest resulting in the attenuation of cell proliferating (Aguirre-Ghiso *et al*., 2001, 2003). At the same time, the overexpression of ERp29 upregulates the expression of DNAJC3 which in turn inhibits the phosphorylation of eIF2α by PERK, affecting the downstream pro-apoptotic ATF4/CHOP/caspase-3 signalling pathway (Gao *et al*., 2012). This demonstrates a link between the activation of p38 and upregulation of DNAJC3 in cell growth arrest and survival caused by ERp29.

DNAJC3 has also been implicated in circumventing UPR promoted apoptosis in response to glucose shortages associated with malignant tumour expansion or growth (Huber *et al*., 2013). Glucose shortages associated with tumour expansion are known to trigger UPR and this results in the promotion of apoptosis through the PERK-CHOP pathway. However, the expression of DNAJC3, a known PERK inhibitor (Harding *et al*., 2000, 2002, Yan *et al*., van Huizen *et al*., 2003), has been shown to attenuate the PERK/CHOP pathway, negating the protective apoptotic response triggered by UPR (Huber *et al*., 2013).

Diabetes

Maintenance of ER homeostasis is crucial for the survival of a cell as it is the site of protein folding, modification, and trafficking of secretory and membrane proteins (Kaufman, 1999, 2002, Rutkowski and Kaufman, 2004). Disruption of ER homeostasis caused by ER stress triggers UPR, which attempts to restore balance to the ER and if this is not possible, will trigger ER-stress mediated apoptosis (Harding *et al*., 1999, Ferri & Kroemer, 2001, Marciniak *et al*., 2004, Li *et al*., 2006, Szegezdi *et al*., 2006). Pancreatic β cells which are responsible for the secretion of insulin, are highly dependent on the ER as this is the site of synthesis of proinsulin, the precursor of insulin

(Alarcón *et al*., 2002, Lipson *et al*., 2006, Zhuo *et al*., 2013). Therefore if UPR triggers ER-stress mediated apoptosis due to its inability to restore ER homeostasis after ER stress, pancreatic β cell numbers are depleted resulting in the onset of diabetes (Harding *et al*., 2001, Oyadomari *et al*., 2002a, 2000b, Zhang *et al*., 2006). DNAJC3 is known to be upregulated during ER stress and acts as a co-chaperone to Grp78 where it assists in the folding and degradation of proteins in an attempt to restore ER homeostasis and inhibits PERK activity once homeostasis is reached allowing protein synthesis to resume (Yan *et al*., 2002, van Huizen *et al*., 2003, Oyadomari *et al*., 2006, Rutkowski *et al*., 2007). Knockdown of DNAJC3 is known to increase the expression of ER stress induced genes such as CHOP and PERK, which are also involved in ER-mediated apoptosis when ER homeostasis cannot be restored (Yan *et al*., 2002). Ladiges *et al*., and Oyadomari *et al*., through the use of DNAJC3 knockout mouse model illustrated that the depletion of DNAJC3 triggers ER-mediated apoptosis, reducing the amount of pancreatic β cells and affecting functionality which gradually results in the onset of diabetes (Ladiges *et al*., 2005, Oyadomari *et al*., 2006). However, Rutkowski *et al*., have reported that the diabetic phenotype observed in DNAJC3 knockout mice is considerably mild compared to the knockdown of essential UPR pathway regulatory proteins such as ATF6, IRE1 or PERK (Rutkowski *et al*., 2007).

1.7.3 Structural organisation and properties of DNAJC3

DNAJC3 is a member of the DNAJ protein family. The protein is comprised of three different functional domains, the J domain at the C-terminus, the middle region has nine TPR motifs which are arranged in a tandem array and make up approximately 60 % of the protein's sequence and a cleavable ER signal peptide of about 25 amino acids at the N terminus (Figure 1.8) (Barber *et al*., 1994, Lee *et al*., 1994, Tao *et al*., 2010, Svärd *et al*., 2011).

The J domain of DNAJC3, composed of residues 393 to 455 and located at the extreme C-terminus (Svärd *et al*., 2011), has been shown to be able to interact and stimulate the ATPase activity of both Hsp70 (Melville *et al*., 1997) and Grp78 (Tao *et al*., 2010, Svärd *et al*., 2011). The J domain of DNAJC3 has four helices (I, II, III, and IV). Helix I and VI are shorter compared to helix II and III. The canonical HPD motif conserved in DNAJ family members is located between helices II and III (Figure 1.8) (Svärd *et al*., 2011). The HPD motif is essential for the stimulation of Hsp70 ATPase activity as shown by numerous mutational studies of the motif (Feldheim *et al.,* 1992; Wall *et al.,* 1994; Tsai and Douglas, 1996).

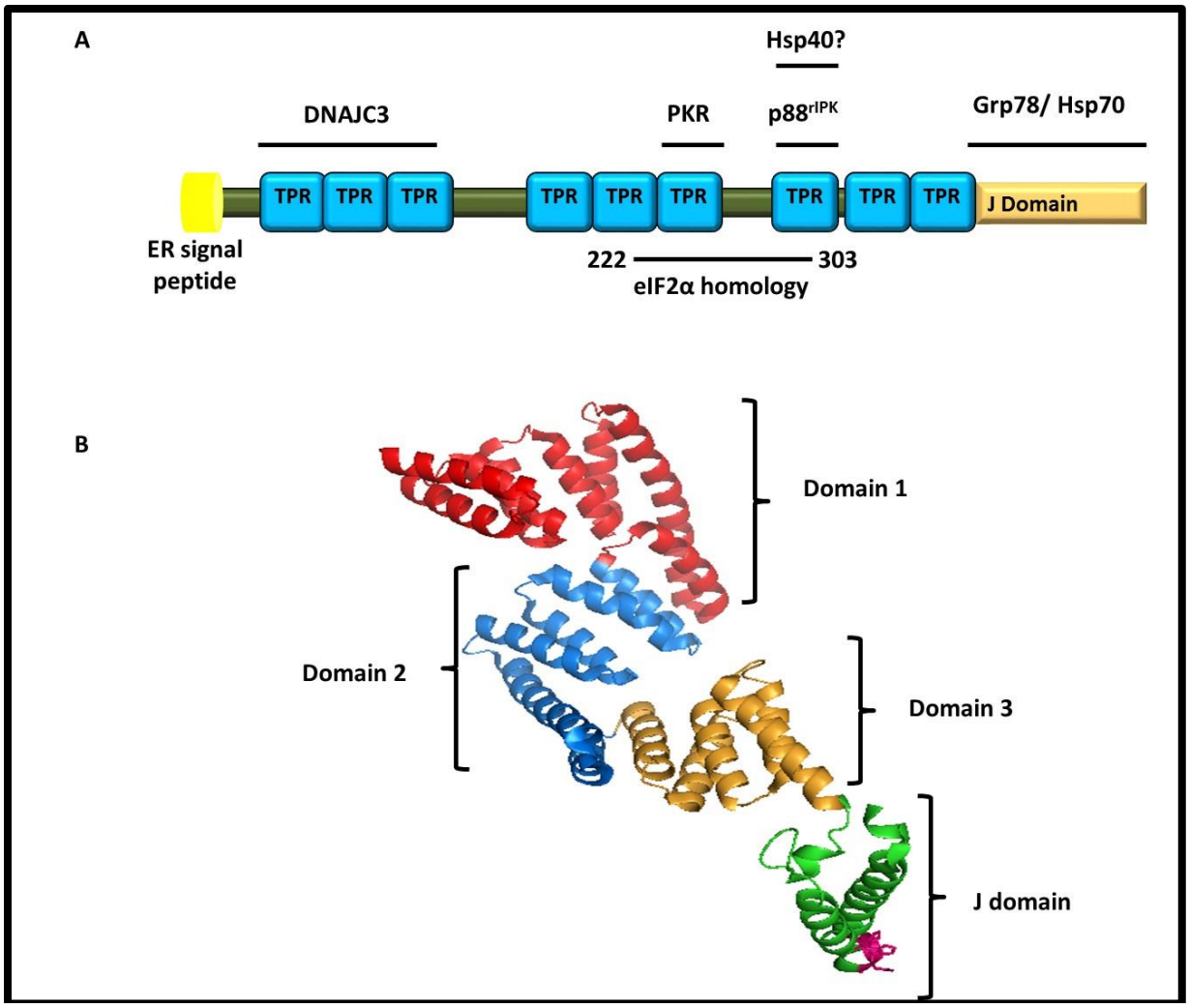

Figure 1.8: Structural organisation of DNAJC3 (A) Schematic representation of DNAJC3 domains. A cleavable ER signal peptide (yellow) is located at the N-terminus, the 9 TPR motifs (blue) make up the middle domain and the J domain (orange) is located at the C-terminus. Highlighted on the upper side by the black bars are the regions where known DNAJC3 associating proteins bind. These include PKR, p88^{rIPK}, Grp78/ Hsp70, Hsp40/DNAJ and the self-interacting region of DNAJC3. Also included are the central regions of homology to eIF2α, the natural substrate of PKR (B) The resolved 3D structure of DNAJC3 (pdb id: 2Y4T) represented in ribbon form. The cleavable ER signal peptide is missing from the structure, the 3 TPR domains made up from the 9 TPR motifs are coloured red, blue and orange, representing TPR domains 1, 2 and 3, respectively. The J domain located at the C-terminus is coloured green and the HPD motif is coloured purple (adapted from Gale *et al*., 1996, Melville *et al*., 1999, Tao *et al*., 2010, Svärd *et al*., 2011).

Tetratricopeptide repeat (TPR) motif

Protein-protein interactions form the foundation of numerous biological functions within the cell. The interaction between these proteins can be facilitated by structural, chemical or even physical means. Proteins with unique motifs that function as mediators or scaffolds between proteins have been identified, such as the WW domain that specifically binds sequences that are proline rich and

contain tyrosine (Bork and Sudol, 1994, Blatch and Lässle, 1999). Out of all the scaffolding motifs or domains, the tetratricopeptide repeat (TPR), is one of the best studied. The TPR motif was first identified by Sikorski *et al.* (1990) when they discovered that several proteins in yeast contained a repeated degenerate amino acid sequence that was 34 amino acid long (Sikorski *et al*., 1990). It was observed that the numbers of TPR motifs within a protein sequence varies, between three and sixteen being most common, and are usually arranged one after the other into domains, although single TPR motifs have been found within proteins (Lamb *et al*., 1995, Blatch and Lässle, 1999, D'Andrea and Regan, 2003, Allan and Ratajczak, 2010, Zeytuni and Zarivach, 2012).

To date, there are over 5000 TPR-containing proteins identified from different organisms through the use of bioinformatics analysis. Over a 100 resolved structures are currently available in the Protein Data bank (Zeytuni and Zarivach, 2012). TPR-containing proteins have been found to be part of numerous multiprotein complexes and play a role in cellular processes such transcriptional regulation, co-chaperone functions, protein translocation to the mitochondria, chloroplast and peroxisome activity, as well as the regulation of cell cycle and kinase activity (Goebl and Yanagida, 1991, Lamb *et al*., 1995, Brocard and Hartig, 2006, Baker *et al*., 2007, Mirus *et al*., 2009). TPR-containing proteins are not only present and required in eukaryotic cells, but are also found in bacteria (Gatsos *et al*., 2008, Zeytuni *et al*., 2011) and viral pathogens (Callahan *et al*., 1998). The subcellular localization of TPR-containing proteins is also diverse, as proteins have been found in the cytosol, nucleus, mitochondria, peroxisomes, ER and chloroplasts (Blatch and Lässle, 1999).

TPR motif primary structure

The TPR motifs are described as highly degenerate 34 amino acid repeats usually found in tandem arrays, but singular motifs have been found to occur in some proteins (Lamb *et al*., 1995, Blatch and Lässle, 1999, D'Andrea and Regan, 2003). The sequences of the various single TPR motifs when aligned illustrate a consensus pattern of small and large hydrophobic amino acid residues that are mostly conserved at positions 4, 7, 8, 11, 20, 24, 27 and 32 (Figure 1.9A) (Lamb *et al*., 1995, Blatch and Lässle, 1999, D'Andrea and Regan, 2003, Zeytuni and Zarivach, 2012). However, residues at positions 8, 20 and 27 favour alanine/glycine, alanine and alanine residues, respectively, whereas the other sites favour residues with either small, large or aromatic characteristics rather than a specific amino acid (D'Andrea and Regan, 2003, Zeytuni and Zarivach, 2012). However, residue conservation can be found outside the above listed site,

between TPR motifs that are functionally similar or equivalent (Blatch and Lässle, 1999). It has also been suggested that residue conservation at the turns between two helices or adjacent helices can play an important role in both structure and function (D'Andrea and Regan, 2003, Zeytuni and Zarivach, 2012).

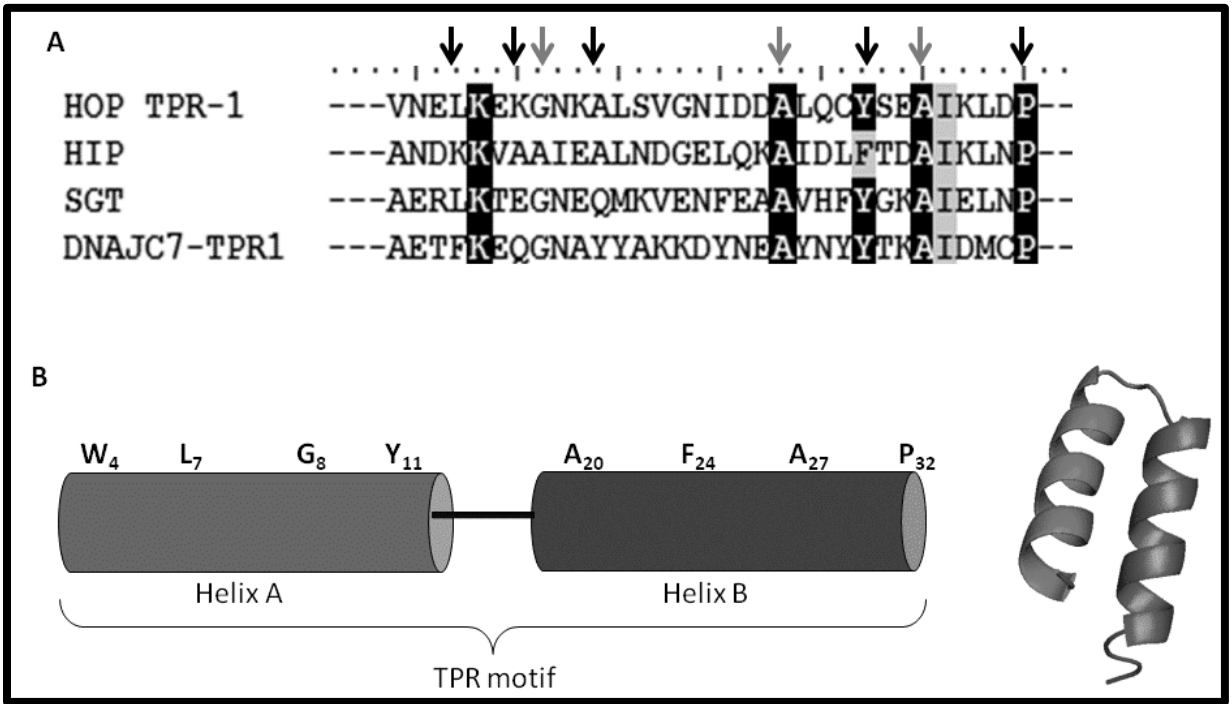

Figure 1.9: TPR motif sequence and structure. (A) Sequence alignment of the first TPR motif of Hsp70 binding proteins (HOP; AAA58682.1, HIP; NP_003923.2, SGT; NP_003012.1 DNAJC7; NP_003306.3). (B) Schematic representation of the secondary structure of the TPR motif highlighting the position of the conserved amino acid residues. The ribbon cartoon depicts the helix turn helix confirmation adopted by the TPR motif. Black arrows indicate the position of the conserved residues, while the grey arrows indicate the highly conserved residues at positions 8 (glycine/alanine), 20 (alanine) and 27 (alanine) (adapted from D'Andrea and Regan, 2003).

TPR secondary and tertiary structure

Through the use of secondary structural predictions, the TPR motif was proposed to be made up of two alpha-helical structures, namely helix A and helix B (Figure 1.9 B). The conserved consensus residues at position 4, 7, 8 and 11 are located on helix A, while residues 20, 24, 27 and 32 are found on helix B (Figure 1.9B) (Blatch and Lässle, 1999, D'Andrea and Regan, 2003). The two helical units (A and B) of TPR motifs adopt a basic helix-turn-helix fold (Figure 1.9B). Adjacent motifs are arranged in a parallel fashion, which results in a spiral repeat of anti-parallel alpha-helices that form a super helical structure (D'Andrea and Regan, 2003, Zeytuni and

Zarivach, 2012). Initially the TPR motifs were thought to form a "knob and hole" structure that was made up of two amphipathic alpha helices that were separated by a spacer region (Hirano *et al*., 1990, Sikorski *et al*., 1990). This structure was regarded as a snap helix and was thought to mediate protein-protein interactions between TPR-containing proteins and ligands through the knob of the TPR domain snapping into the hole of the ligand. In addition, the helix A and B of a single TPR motif was thought to be arranged in a linear formation and the anti-parallel arrangement was observed between adjacent TPR motifs (Hirano *et al*., 1990, Sikorski *et al*., 1990). However, the resolution of the TPR domain of PP5 (Das *et al*., 1998) proved that the predicted arrangement of the helical subunits and TPR motif arrangement was incorrect, and the helical structure of the TPR motif adopted an anti-parallel arrangement. Furthermore, an additional elongated helix was found to be located at the C-terminus of the TPR domain; this extra helix is present in numerous resolved TPR structures and is thought to act as a capping or stabilizing helix that is essential for the solubility or solubilisation of the isolated TPR domains (Das *et al*., 1998, D'Andrea and Regan, 2003).

To date, several crystal structures of the TPR domain of other proteins have been solved and this has highlighted the variability found in the packing of the TPR helical domains. TPR structures of proteins such as peroxin 5 (PEX5), TOM20 and Cyp40 have been shown to have dramatic differences in the way the TPR domains fold, compared to most of the TPR domains from other proteins such as HOP and PP5. In, PEX5, the six TPR motifs do not fold into a super helical structure but form independent TPR clusters that do not conform to the canonical super helical structure (Gatto *et al*., 2000). In the case of Cyp40, TOM20 and *Trypanosoma brucei* PEX5, the two helical structures of the TPR motif do not fold into the helix turn helix structure, but instead form a single elongated helix (Abe *et al*., 2000, Kumar *et al*., 2001, Taylor *et al*., 2001).

Ligand binding diversity of TPR domains

TPR-containing proteins have been shown to be able to bind to a vast number of diverse ligands. This ability is linked to the concave and convex surfaces that result from the unique super helix fold, and also the different properties of the amino acid residues that are located within those surfaces (Zeytuni and Zarivach, 2012). What is interesting is that the ligands usually do not share sequence or structural similarities; rather the binding between TPR domain and ligand is usually highly specific. However, in some cases, the TPR domain displays surface residues within its binding cleft which will interact in a specific manner with its chosen ligand (Zeytuni and Zarivach,

2012, Cortajarena and Regan, 2006, Cortajarena *et al*., 2008). For other interactions, ligand specificity can be linked to the electrostatic potential of the binding surface which is imparted by the properties of the amino acid residues within that area, or the hydrophobicity and size of the residues which might support hydrophobic interactions between the ligand and the TPR domain (Zeytuni and Zarivach, 2012, Cortajarena and Regan, 2006, Cortajarena *et al*., 2008). Through the study of several TPR-ligand interactions, it should be noted that binding specificity cannot be attributed to a single specific property but rather that several factors in different combinations are required and this cooperation gives TPR domains the ability to bind to diverse ligands. An example of ligand diversity and function of TPR domains can be observed in TPR-containing proteins that interact with Hsp90 and or Hsp70, such as HOP. HOP TPR domains have five highly conserved residues that form the carboxylate clamp with is required for the interaction with the EEVD motif of Hsp90 or Hsp70. In addition, it has been reported that within the HOP TPR domains are residues that confer binding specificity to either Hsp90 or Hsp70, resulting in TRP-1 binding Hsp70 binding and TPR-2A binding Hsp90 (Odunuga *et al*., 2003).

1.7.3.1 DNAJC3 TPR motifs

Structurally, the TPR motifs of DNAJC3 follow the same helix-turn- helix conformation for each individual motif and adjacent motifs are arranged in a parallel fashion (D'Andrea and Regan, 2003). The first resolved structure of DNAJC3 was from mice (Tao *et al*., 2010), however the structure lacked the J domain. The crystal structure showed that a monomer of DNAJC3 has nineteen helices that form three TPR domains which are grouped in clusters of six helices linked by an elongated helix (Tao *et al*., 2010). The domains are arranged in a head to tail fashion and this arrangement differs from that of many TPR proteins which have multiple TPR motifs as they are normally packed into a super-helix (D'Andrea and Regan, 2003, Zeytuni and Zarivach, 2012). A human DNAJC3 crystal structure was resolved in 2011 by Svärd and colleagues which included the J domain that was lacking in the murine structure. This structure showed that although there was sequence conservation between the murine and human DNAJC3 protein, the shape of the structures differed. It is unclear, however, whether this difference in shape is important to any physiological functions of the protein (Svärd *et al*., 2011). The TPR domains of DNAJC3 share structural homology with several TPR-containing proteins such as HOP (Scheufler *et al*., 2000), PP5 (Das *et al*., 1998), CHIP (Zhang *et al*., 2005) and the N-terminal domain of TOM70 (Wu and Sha, 2006). Despite the structural conservation, the primary amino acid sequences of the different

TPR domains differ vastly. The listed proteins have all been shown to interact with their ligands through a large groove and these grooves are also present in all three DNAJC3 TPR domains. Although all TPR domains form and interact through the groove, which can also be referred to as the concave surface, the properties of this groove differ significantly. An example is the electrostatic potential of the concave surface; in TPR-containing proteins that interact with Hsp90 and Hsp70 such as HOP and PP5, the electrostatic potential of the groove is mainly positive (Das *et al*., 1998, Scheufler *et al*., 2000).

1.7.3.1.1 Interactions of DNAJC3 TPR motifs

Inhibitors of DNAJC3

Different TPR motifs of DNAJC3 are known to associate with various proteins (Figure 1.8). An example of this is seen for $p88^{rIPK}$, is a natural negative regulator of DNAJC3 activity (Luig *et al*., 2010). $p88^{rIPK}$ inhibits DNAJC3 through a direct interaction with the seventh TPR motif (in TPR3). Mutational studies of TPR motif 7 resulted in the mutant DNAJC3 being a better kinase inhibitor than the wild type, proving the mutated protein lacked the negative regulatory domain. It is interesting to note that a region of $p88^{rIPK}$ has been shown to share limited homology with the charged linker region of Hsp90, although it is unknown whether this region is involved in the interaction with TPR motif 7 of DNAJC3 (Gale *et al*., 2002). An unknown member of the Hsp40/DNAJ family has also been identified as a possible inhibitor of DNAJC3 activity (Melville *et al*., 1997, 1999, Guan *et al*., 2010). The Hsp40 was identified in a purified lysates fraction and its inhibition activity verified *in vitro* (Melville *et al*., 1997). Melville *et al*. (1997) demonstrated that in influenza infected cells, dissociation of Hsp40 and DNAJC3 is required to inhibit the function of PKR. At the same time, the same association between DNAJC3 and Hsp40 was found to be disrupted during the recovery process after heat shock, suggesting a regulatory role for DNAJC3 independent of viral infection (Melville *et al*., 1999). Recently, the inhibitory effect of DNAJC3 on PKR during influenza virus infection has been linked to the formation of a complex between DNAJC3 and influenza matrix proteins (M1 and M2) that is mediated by Hsp40 (Guan *et al*., 2010). Although the actual binding site for Hsp40 on DNAJC3 is currently unknown, mutational studies conducted on the seventh TPR motif of DNAJC3 strongly suggest that the motif might be the binding site for Hsp40, as mutations resulted in stronger inhibitory effects of DNAJC3. If the Hsp40 bound to a different region it would have probably negated the effects

observed with the loss of p88^{rIPK} binding site (Melville *et al*., 1997, 1999). However, it should be noted that the removal of TPR motif 5 was also shown to increase the inhibitory functions of DNAJC3, implying that this site could also be a potential binding site for DNAJC3 inhibitors (Tang *et al*., 1996).

Kinase binding

TPR motif 6 of DNAJC3 (in TPR2) is the binding site of PKR and this region has been identifies as being crucial for its inhibitory functions (Lee *et al*., 1994, Gale *et al*., 1996). Mutational studies on TPR motif 6 negated the ability of DNAJC3 to inhibit PKR functions *in vivo* and *in vitro* (Lee *et al*., 1994, Gale *et al*., 1996). Interestingly, the region within DNAJC3 found to share homology with eIF2α, the natural substrate of PRK, includes TPR motif 6 (Lee *et al*., Melville *et al*., 2000). The eIF2α protein is required for translation initiation within the cell; the initiation factor is phosphorylated on serine 51 (Merrick, 1992, Samuel, 1993) by PKR when activated by interferons or by the presence of highly structured RNA molecules or dsRNA (Dauber and Wolff, 2009). The phosphorylation of eIF2α eventually leads to the attenuation of protein synthesis and this acts as a defence mechanism in virus infected cells, since it prevents or limits the synthesis of viral proteins or the spread of viral infection. The shared homology between eIF2α and the region encompassing DNAJC3 TPR motif 6 could explain why TPR motif 6 is the binding site for PKR.

Self-association

Another interesting region of DNAJC3 identified was the N-terminus 166 amino acids region which includes TPR motif 1 to TPR motif 3 (TPR1) and parts of TPR motif 4 (in TPR2). This region shares significant homology with another TPR-containing protein, PP5 (Melville *et al*., 2000). This region mediates interactions between DNAJC3 molecules (Gale *et al*., 1996). This ability of the TPR domain to allow self-interaction has also been found in other TPR-containing proteins (Nyarko *et al*., 2007, Krachler *et al*., 2010). However, although studies show that TPR motif 1-3 allowed self-association, the oligomeric state of DNAJC3 *in vivo* has not been extensively studied and it remains unclear whether it is important for function and regulation. Nevertheless, truncations of TPR motifs 1-3 have been shown to be non-essential for the interaction with and inhibition of PKR (Polyak *et al*., 1996). Despite these published interactions, there have been no studies conducted on the interactions of DNAJC3 with chaperones, Hsp90 or Hsp70, despite the presence of the TPR domain in this protein.

1.8 Motivation

DNAJC3 is one of only two DNAJ proteins to have TPR domains, the other being DNAJC7. DNAJC7 has seven TPR domains and a J domain located at the C-terminus of the protein, while DNAJC3 has nine TPR motifs together with the J domain at the C-terminus. DNAJC7 has been shown to interact with both Hsp70 and Hsp90 (Brychzy *et al*., 2003) and can regulate the functions of Hsp70 through its J domain and TPR domains and Hsp90 through the TPR domain (Brychzy *et al*., 2003, Moffatt *et al*., 2008). DNAJC3 and DNAJC7 are known to localize to different compartments of the cell, namely the cytosol in the case of DNAJC7, the ER lumen in the case of DNAJC3, although a subpopulation of the latter has been found in the cytosol, the majority of the protein resides in the ER lumen (Rutkowski *et al*., 2007). Similar to DNAJC7, the J domain of DNAJC3 is able to stimulate the ATPase activity of cytosolic Hsp70 leading to the inhibition of PKR (Melville *et al*., 1999). DNAJC3 also stimulates the ATPase activity of Grp78 during UPR caused due to ER stress, where it helps to restore ER homeostasis (Oyadomari *et al*., 2006, Rutkowski *et al*., 2007, Tao *et al*., 2010; Svärd *et al*., 2011).

At present, there have not been any studies conducted to demonstrate an interaction between DNAJC3 TPR domains and Hsp90 or Hsp70, even though this domain is present in known co-chaperones of Hsp90 and or Hsp70. The only proposed co-chaperone function for DNAJC3 TPR domains is linked to TPR1, which binds selectively to unfolded protein through its hydrophobic peptide-binding groove. The J domain of DNAJC3 is able to stimulate the ATPase activity of Grp78 (Tao *et al*., 2010). Since DNAJC3 is proposed to have three functional TPR domains (Tao *et al*., 2010, Svärd *et al*., 2011), and a function has been proposed for only one of the domains, this begs the question as to the purpose or functions of the other TPR domains. The ER homologues of Hsp90 and Hsp70, Grp94 and Grp78, do not possess the EEVD motif of their cytosolic counterparts which is normally required for the interaction with TPR domains (Argon and Simen, 1999, Fewell *et al*., 2010). Hence the mechanism of interaction of Grp94/Grp78 with the TPR domains may be different to that of cytosolic proteins such as the Hsp70/Hop/Hsp90 machinery. Therefore it is possible that DNAJC3 may represent an example of new and unique interactions of TPR domains with chaperones. In addition, there are currently no known co-chaperones of Grp94, although DNAJC3 was recently found to be in a complex with Grp94 along with other proteins (Jansen *et al*., 2012), raising the question as to whether DNAJC3 could possibly be the missing Grp94 co-chaperone.

1.9 Hypothesis

The TPR domains of DNAJC3 are involved in non-canonical interactions with Hsp70 and Hsp90 chaperones.

1.10 Aims and objectives

1.10.1 Aim

Characterization of the structure and function of DNAJC3 TPR domains

1.10.2 Objectives

- *In silico* analysis of DNAJC3 TPR domains
- Development of bacterial systems to over-express DNAJC3 and other chaperones for functional studies.
- *In vitro* analysis of protein-protein interactions of DNAJC3 TPR domains
- Preliminary *ex vivo* analysis of DNAJC3 in mammalian cells

Chapter 2: Materials and Methods

2.1 Sequence retrieval and analysis

The amino acid sequence for *Homo sapiens* DNAJC3 (Accession number NP_006251.1) was retrieved from the National Centre of Biotechnology Information (NCBI) database. Using the retrieved *Homo sapiens* DNAJC3 amino acid sequence, pBLAST (Basic local Sequence Alignment Tool) (Altschul *et al*., 1990) and Psi-BLAST (Position-Specific Iterative BLAST) (Altschul *et al*., 1997) were conducted to identify DNAJC3 homologues from various species (Table 3.1). Reverse BLAST was conducted on every amino acid sequence identified in the first round of BLAST and Psi-BLAST to ensure that the retrieved sequences represented the protein DNAJC3 in the selected species. Sequence selection was based on two criteria; namely an E-value of 0 or close to 0 and sequence percentage coverage higher than 75 %.

2.2 Multiple sequence alignment

To eliminate or reduce the chances of receiving biased results, four multiple sequence alignment programs were used to align the DNAJC3 amino acid sequences, namely ClustalW (Thompson *et al*., 1994), MAFFT (Katoh *et al*., 2002), T-COFFEE (Notredame *et al*., 2000) and Promals3D (Pei *et al*., 2008). Each program uses specific algorithms to elucidate the different interrelations that exist between a set of sequences. For each program, a FASTA format file was uploaded to the web servers, and alignment conducted under the default parameters. After the completion of the alignment, the resulting output was edited using the BioEdit software (Hall, 1999).

2.3 Phylogenetic analysis

The Promals3D DNAJC3 multiple sequence alignment result obtained in section 2.2 was used to construct a phylogenetic tree in order to infer the evolutionary relationships between the different DNAJC3 sequences from different species (Table 3.1). The tree was constructed using the Molecular Evolutionary Genetics Analysis 5 (MEGA5) program (Tamura *et al*., 2011). Evolutionary models were calculated and the best two models selected based on low Bayesian information criterion (BIC) score. The selected models were used for phylogenetic analysis, while the tree was generated using the Maximum Likelihood analysis (Tamura *et al*., 2011) with the following parameters: bootstrap consensus tree surmised from 1000 replicates and any tree

partitions replicated in less than 75 % of the bootstrap analyzes were collapsed. For the calculation of the evolutionary distances, the MEGA5 program used the Jones-Taylor-Thornton (JTT) evolutionary model (Jones *et al*., 1992).

2.4 Motif identification and comparison

Several TPR-containing co-chaperones of Hsp90 and Hsp70 were selected based on literature (Caplan, 2003) and the amino acid sequences were retrieved from NCBI. The following co-chaperones were selected for analysis; DNAJC7 (NP_003306.3), CHIP (NP_005852.2), TOM34 (NP_006800.2), SGT (NP_003012.1), HIP (NP_003923.2), HOP (AAA58682.1) and PP5 (NP_006238.1). The co-chaperones and DNAJC3 sequences were submitted to several motif identification programs; namely Simple Modular Architecture Research Tool (SMART) (Schultz *et al*., 1998 and Letunic *et al*., 2012), Eukaryotic Linear Motifs (ELM) (Dinkel *et al*., 2012), Multiple Em for Motif Elucidation (MEME) (Bailey *et al*., 2009) and PROSITE (Sigrist *et al*., 2002). Multiple programs were used to maximise the identification of all possible motifs within a protein. All programs were used under the default parameters. The identified motifs from all four programs were compiled and protein domains were represented using DOG 2.0 software (Ren *et al*., 2009).

2.5 TPR domain alignment and comparison

Using the sequences of co-chaperones listed above (section 2.4), the amino acid sequences for the TPR domains were manually isolated from the rest of the sequence and grouped based on the chaperone (Hsp90, Hsp70 or both) with which they are known to interact. Multiple sequence alignment was conducted using the Promals3D program.

2.6 HHpred structural homologue detection, retrieval and alignment

The Protein Data Bank (pdb) coordinate file for *Homo sapiens* DNAJC3 (PDB id: 2Y4T) was retrieved from the RCSB Protein Data Bank, an online repository for three-dimensional (3-D) structures of various biological molecules such as proteins and nucleic acids (Berman *et al*., 2000). The 2Y4T.pdb file was manually manipulated using the free word processor gedit software, separating DNAJC3 into the three identified TPR domains, yielding 2Y4T_domain1.pdb, 2Y4T_domain2.pdb and 2Y4T_domain3.pdb which represented DNAJC3 TPR1, 2 and 3, respectively (numbering from the N to the C-terminus of the protein). The three TPR domain files (2Y4T_domain1.pdb, 2Y4T_domain2.pdb and 2Y4T_domain3.pdb) were loaded into the HHpred

server (Söding *et al*., 2005) to identify putative structural homologues. The best structural homologues were selected based on E-value, structure resolution and template range. The retrieved structures were subjected to multiple sequence alignment using the Promals3D program, which is able to utilise both the FASTA and pdb format for alignments. The resulting alignments were analyzed using BioEdit software. Structural alignment of the structural homologues and DNAJC3 TPR domains was conducted using the Pymol Molecular Graphics system (DeLano and Lam, 2005).

2.7 Structural modelling of DNAJC7 and DNAJC3 TPR domain mutations

The *Homo sapiens* DNAJC7 sequence was submitted to the internet based modelling server HHPred to identify templates. A model for DNAJC7 was constructed by MODELLER under HHpred (Sali *et al*., 1995) using DNAJC3 (2Y4T) as a template. Mutation of DNAJC3 TPR domain amino acids was selected based on the residues shown by Odunuga *et al*. (2003) to play a crucial role in the formation of the carboxylate clamp between HOP TPR domains and Hsp70/Hsp90 chaperone EEVD motif interactions, namely (K8, N12, N43, K73, R77) in TPR-1 of HOP and K229, N233, N264, K301, R305 in TPR-2A of HOP. The residue numbers correspond to the alignment conducted in section 2.4. The five residues were mutated in all three DNAJC3 TPR domains (TPR1: L8K, K12N, R59N, A96K and Q100R, TPR2: R8K, Q12N, L59N, E96K and K100R and TPR3:I8K, E12N, R59N, E96K and D100R.) and the models built using MODELLER under HHpred with DNAJC3 (2Y4T) as the template. Model validation was conducted by submitting the generated models to the online based MetaMQAP server (Pawlowski *et al*., 2008) and Verify3D (Eisenberg *et al*., 1997).

2.8 Electrostatic potential analysis

Electrostatic potential analysis of DNAJC3 TPR domains and structural homologues was conducted using the freeware DeepView/Swiss-PdbViewer with default parameters (Guex and Peitsch, 1997).

2.9 Mammalian cell lines and growth conditions

The MCF-7 breast carcinoma cell line (ATCC accession number HTB-22) and the HEK293T cell line (ATCC accession number CRL-1573) were a kind gift from Prof Sharon Prince (Department of Human Biology, University of Cape Town). The cells were cultured in Dulbecco's Modified Eagle Medium (DMEM) containing Glutamax™ and supplemented with 10 % (v/v) heat-

inactivated fetal calf serum (FCS), 100 $U.ml^{-1}$ penicillin-streptomycin-amphotericin (PSA) (Gibco, Invitrogen UK) and incubated at 37 °C in a 10 % CO_2 incubator. The HEK293T cells were cultured in Dulbecco's Modified Eagle Medium (DMEM) containing Glutamax™ and supplemented with 10 % (v/v) heat-inactivated fetal calf serum (FCS), 100 $U.ml^{-1}$ penicillin-streptomycin-amphotericin (PSA), 500 µg/ml Geneticin (G418) and incubated at 37 °C in a 5 % CO_2 incubator.

2.10 Total RNA extraction from MCF-7 carcinoma cell line

MCF-7 breast carcinoma cells were grown to confluency in a 75 cm^2 cell flask. The cells were rinsed twice with phosphate buffered saline (PBS) (140 mM NaCl, 2.7 mM KCl, 10 mM Na_2PO_4, 1.8 mM KH_2PO_4, pH 7.4). Cells were lifted with 1 % (v/v) trypsin supplemented with 0.3 % (w/v) ethylenediaminetetraacetic acid (EDTA) and were stained with equal volume of trypan blue (Sigma-Aldrich, Germany) and counted using a haemocytometer. For total RNA extraction, MCF-7 cells were lysed in 1 ml TRI® Reagent (Sigma-Aldrich, Germany) per 5 – 10 x 10^{-6} cells. The homogenate was incubated at 30 °C for 5 minutes, after which 0.2 ml of chloroform per 1 ml of TRI® Reagent was added. The mixture was vigorously shaken for 15 seconds and incubated at 30 °C for 3 minutes. Samples were centrifuged at speeds not higher than 12000 x *g* for 15 minutes at 4 °C, with the samples separating into three distinct layers. The upper aqueous layer which contained RNA was transferred to a new eppendorf tube and 0.5 ml of isopropanol per 1 ml of TRI® Reagent was added to precipitate the RNA. The mixture was incubated at 30 °C for 10 minutes and centrifuged at 12000 x *g* for 15 minutes at 4 °C. The resulting supernatant was decanted and the pellet was washed in 75 % (v/v) ethanol prepared with RNAse free water (1 ml per 1 ml TRI® Reagent used). The pellet was resuspended by vortexing and centrifuged for 5 minutes at 4 °C at 7500 x *g*. After centrifugation, the supernatant was decanted and the pellet air dried. The dried pellet was dissolved in 50 µl of RNAse-free water, incubated at 55 °C for 10 minutes and stored at -70 °C for long-term storage or -20 °C for short-term storage.

2.11 Generation of bacterial expression plasmid for DNAJC7

The complementary deoxyribonucleic acid (cDNA) was synthesized from total RNA isolated in section 2.10 through reverse transcription polymerase chain reaction (RT-PCR) using the RevertAid™ Premium first Strand cDNA Synthesis Kit (Fermentas, USA), according to manufacturer's instructions. The primer pair LZMC7-1F (5'-

AAAGGATCCATGGCGGCTGCCGCGAGTGCG-3') and LZMC7R (5'-AAAGTCGACTTAGCCAAATTGAAAAAAGAAATTCCCTGG-3'), which introduced restriction sites *Bam*H1 and *Sal*1 at the 5' and 3' ends, respectively, were used to amplify the DNAJC7 coding sequence from the synthesized cDNA. The PCR product was excised from a 1 % (w/v) agarose gel in Tris-acetate-EDTA (TAE [40 mM Tris acetate, 1 mM EDTA]) buffer and cleaned and concentrated using the ZymoClean™ Gel DNA Recovery kit (Zymo Research, USA), according to manufacturer's instructions. The resultant PCR product was ligated into the cloning vector, pGEM-T-Easy® (Promega, USA), to generate the intermediate plasmid, pGEMDNAJC7. Restriction digest with *Bam*H1 and *Sal*1 was conducted to verify the success of the ligation procedure. The pGEMDNAJC7 and the pGEX 4T-1 vector were digested with *Bam*H1 and *Sal*1, to introduce compatible ends and resolved on a 1 % (w/v) agarose gel in TAE buffer. The insert (DNAJC7) and the pGEX 4T-1 backbone vector were gel purified using the ZymoClean™ Gel DNA Recovery kit. The coding sequence for DNAJC7 was ligated into pGEX 4T-1, resulting in the expression vector pLZMC7 that encoded GST-tagged DNAJC7. Verification of the plasmids was conducted by sequencing with pGEX5' and pGEX3' primers (Inqaba Biotechnology).

2.12 Generation of bacterial expression plasmids for DNAJC3

Mammalian expression plasmids mP58.FL1-pCDNA3 (Addgene, 21883) and mP58.dJ1-pCDNA3 (Addgene, 21884), carrying the coding sequence for full length DNAJC3 (including ER signal peptide, TPR and J domains) and DNAJC3 that was lacking the J domain (but contained the ER signal peptide and TPR domains) was constructed by Oyadomari *et al*., 2006. The mP58.FL1-pCDNA3, mP58.dJ1-pCDNA3 and pGEX 4T-1 plasmids (the vector chosen for bacterial expression) were digested with *Bam*H1 and *Xho*1, to generate compatible sticky sites. The digested coding sequences of DNAJC3 were ligated into pGEX 4T-1, resulting in the expression vectors, pLZMC3FL and pLZMC3dJ that encoded GST-tagged DNAJC3FL and DNAJC3dJ. In addition, constructs coding for DNAJC3 lacking the ER signal peptide were also constructed. This was accomplished by designing primers, DNAJC3F (5'-AAAGGATCCGCGGATGTGGAGAAGCATC-3', DNAJC3R (5'-AAACTC GAGTTAATTGAAGTGGAACTTAAATCTGAAC-3') and DNAJC3dJR (5'-AAACTCGAGTTATCGTTTCTGTGACTGCTTCAGTAAC-3') that amplified DNAJC3 coding region from mP58.FL1-pCDNA3 eliminating the N-terminal region that coded for the ER signal peptide. The resulting PCR products were ligated into pGEM-T-Easy® and then subcloned into

the expression vector pGEX 4T-1 using *Bam*H1 and *Xho*1 restriction sites, resulting in the expression vectors, pLZMC3ΔER and pLZMC3ΔJ/ER. The new pLZMC3FL, pLZMC3ΔER, pLZMC3dJ and pLZMC3ΔJ/ER constructs were verified by restriction digest analysis and sequencing with pGEX5' and pGEX3' primers (Inqaba Biotechnology).

2.13 Optimization and Over expression of GST- tagged DNAJC3 constructs

Recombinant expression constructs pGEX 4T-1, pLZMC3FL, pLZMC3ΔER, pLZMC3dJ and pLZMC3ΔJ/ER were transformed separately into various competent *E. coli* cell strains (Table 2.1) and incubated overnight at 37 °C. Single colonies were inoculated into 2X Yeast Tryptone (YT) broth (1.6 % [w/v] tryptone, 1 % [w/v] yeast extract and 0.5 % [w/v] NaCl) supplemented with appropriate antibiotics at final concentrations listed in Table 2.1 and grown overnight with shaking at 37 °C. A total of 1 ml of the overnight culture was inoculated into fresh 100 ml 2X YT broth (supplemented with antibiotics) and grown at 37 °C with shaking until the culture reached an OD_{600} reading of between 0.4 and 0.8. At this point, various expression conditions were utilised to determine the optimum conditions for the expression of GST-tagged DNAJC3 proteins. Protein expression was induced by the addition of isopropyl β-D-1-thiogalactopyranoside (IPTG) to a final concentration of either 1 mM or 0.5 mM. A total of 1 ml samples were collected at 0-4 hours post induction and used to determine optimum protein expression time. In addition to the 2X YT broth, four different growth medium were also to express the protein, 2X YT broth with 2 % (w/v) glucose, 2X YT broth with 0.5 M sorbitol, glucose minimal medium (0.4 % [w/v] glucose, 2 mM $MgSO_4$, 0.1 mM $CaCl_2$, 33.7 mM Na_2HPO_4, 22 mM KH_2PO_4, 8.55 mM NaCl, 9.35 mM NH_4Cl) and auto-induction medium (1 % [w/v] tryptone, 0.5 % [w/v] yeast extract, 25 mM Na_2HPO_4, 25 mM KH_2PO_4, 50 mM NH_4Cl, 5 mM Na_2SO_4, 2mM $MgSO_4$, 0.5 % [v/v] glycerol, 0.05 % [w/v] glucose and 0.2 % [w/v] α-lactose). Using the normal 2X YT broth, cells were also expressed under four different conditions: 20 °C for 4 hours with 1 mM IPTG, 37 °C for 0.5 hours with 1 mM IPTG, 37 °C for 4 hours with 0.5 mM IPTG and 37 °C with 1 mM IPTG for 4 hours. For post expression treatments, cell were harvested by centrifugation at 4 °C for 10 minutes at 6000 x *g* and the pellet resuspended in PBS (2.5 ml of PBS per 1 g of cells) containing lysozyme and phenylmethylsulfonyl fluoride (PMSF) at a final concentration of 1 mg/ml and 1 mM, respectively. The resuspended mixture was divided equally into six tubes (a total of 1 ml per tube). For the treatments, five of the tubes were treated with one of the following detergents, Nonidet-P 40 (NP40), N-Laurylsarcosine (Sac), Triton-X, Tween-20 and Durrapol 2000 at concentrations

ranging between 1- 10 % (v/v), with the remaining untreated tube serving as a control. Samples were incubated with shaking at 37 °C for 1 hour and frozen at -80 °C overnight. The frozen lysates were thawed on ice, followed by 10 rounds of sonication for 30 seconds with 15 second cooling periods in between. Lysate clarification was done by centrifuging at 10000 x *g* for 30 minutes at 4 °C after which total protein, pellet and supernatant fractions were collected. All samples were analyzed by sodium dodecyl sulphate polyacrylamide gel electrophoresis (SDS-PAGE) using a 12 % (v/v) polyacrylamide gel, followed by Coomassie blue staining and Western analysis.

2.14 Batch purification of GST-tagged DNAJC3 proteins

E. coli cells expressing the different GST-tagged DNAJC3 proteins were treated as previously described in section 2.12. The clarified cell lysate was added to pre-washed Protino® Glutathione Agarose resin (Thermo Scientific, USA) and the mixture incubated for 30 minutes at room temperature with gentle shaking. Sedimentation of the mixture was done by centrifuging at 500 x *g* for 5 minutes. The supernatant was decanted, and the resin washed three times with 10 bead volumes of PBS. Each wash step was followed by centrifugation at 500 x *g* for 5 minutes. After the wash steps, 1 bead volume of GST elution buffer (50 mM Tris pH 8, 10 mM glutathione) was added to the agarose resin and incubated with gentle shaking at room temperature for 10 minutes, followed by centrifugation at 500 x *g* for 5 minutes. The elution step was repeated three more times, with the resulting supernatant being transferred to fresh eppendorf tubes. The success of the purification protocol was evaluated by SDS-PAGE and Coomassie blue staining.

2.15 Over expression and batch purification of His-tagged peptides Grp78 and Grp94$_{284\text{-}543}$

His-tagged Grp78 (BiP) (pQE10-BiP, kind donation from Professor Zimmermann, Universität des Saarlandes, Germany) and His-tagged middle domain of Grp94$_{284\text{-}543}$ (HSP90B1- Addgene, 30976) were expressed in M15 *[pREP4]* and BL21 (DE3) *E. coli* cells, respectively. Protein expression for His-tagged Grp78 and His-tagged Grp94$_{284\text{-}543}$ was induced with IPTG at a final concentration of 1 mM at 37 °C and 0.5 mM at 18 °C, respectively. Cells were harvested by centrifuging at 6000 x *g* at 4 °C for 20 minutes. The resulting pellet was resuspended in cold His lysis/wash buffer (10 mM Tris pH 7.4, 300 mM NaCl, 50 mM imidazole), lysozyme and PMSF were added to a final concentration of 1 mg/ml and 1 mM, respectively and the pellet frozen at -80 °C overnight. The following day, the pellet was thawed on ice and sonicated five times for 30 seconds bursts, followed by 30 seconds cooling periods. The sample was clarified by centrifuging

at 16000 x *g* for 30 minutes at 4 °C. The supernatant was added to nickel charged Chelating Sepharose™ Fast Flow resin (GE HealthCare, UK) and binding was conducted at 4 °C overnight with shaking. The overnight mixture was centrifuged at 1500 x *g* for 2 minutes, the supernatant discarded and the beads washed three times with lysis/wash buffer, followed by centrifugation at 1500 x *g* for 2 minutes. His-tagged proteins were eluted twice with cold His elution buffer (10 mM Tris pH 7.4, 300 mM NaCl, 400 mM imidazole) and the supernatant containing the eluted protein stored at -20 °C until further use. The success of the purification protocol was once again evaluated by SDS-PAGE and Coomassie blue staining.

Table 2.1: Genotype of *E. coli* strains used in this study

Strain	Genotype
DH5α	*F^- endA1 glnV44 thi-1 recA1 relA1 gyrA96 deoR nupG Φ80dlacZΔM15 Δ(lacZYA-argF)U169, hsdR17(r_K^- m_K^+), λ–*
JM109	*endA1 glnV44 thi-1 relA1 gyrA96 recA1 $mcrB^+$ Δ(lac-proAB) e14- [F' traD36 $proAB^+$ $lacI^q$ lacZΔM15] hsdR17($r_K^-m_K^+$)*
BL21(DE3)	*$F^–$ ompT gal dcm lon $hsdS_B$(r_B^- m_B^-) λ(DE3 [lacI lacUV5-T7 gene 1 ind1 sam7 nin5])*
BL21 C41 (DE3)	*$F^–$ ompT gal dcm $hsdS_B$(r_B^- m_B^-)(DE3)*
BL21 C43 (DE3)	*$F^–$ ompT gal dcm $hsdS_B$(r_B^- m_B^-)(DE3)*
XL1 Blue	*endA1 gyrA96(nal^R) thi-1 recA1 relA1 lac glnV44 F'[::Tn10 $proAB^+$ $lacI^q$ Δ(lacZ)M15] hsdR17(r_K^- m_K^+)*
M15*[pREP4]*	*lac,ara,gal,mtl,recA+,uvr+ [pREP4,lacI,$kana^r$]*
BB1994	*MC4100 dnaK52 sidB1::Tc pDMI,1::CmR KanR*

2.16 Sodium dodecyl sulphate polyacrylamide gel electrophoresis (SDS-PAGE) and Western analysis

All samples analyzed by SDS-PAGE were resolved on a 12 % (v/v) polyacrylamide gel run at 200V, stained with either Coomassie staining solution (0.1 % [w/v] Coomassie brilliant blue R-250, 50 % [v/v] methanol, 10 % [v/v] glacial acetic acid) or Colloidal Coomassie staining solution (20 % [v/v] ethanol, 10 % [v/v] phosphoric acid, 0.12 % [w/v] Coomassie Brilliant blue G-250, 10 % [w/v] ammonium sulphate). For Western analysis, proteins were transferred onto nitrocellulose membrane (Bio-Rad Laboratories, USA) for 50 minutes at 400 mA in transfer buffer (25 mM Tris-HCl pH 7.4, 192 mM glycine, 20 % [v/v] methanol). Ponceau stain (0.1 % [w/v] Ponceau stain in 1 % [v/v] acetic acid) was used to verify protein transfer. The stain was removed by rinsing the membrane in water and then Tris buffered saline with 1 % (v/v) Tween-20 (TBS-T

150 mM NaCl, 50 mM Tris-HCl pH 7.6). The membrane was incubated for 1 hour in blocking solution (TBS-T containing 5 % [w/v] bovine albumin serum [BSA]), followed by an overnight incubation with primary antibody in blocking solution (dilutions summarized in Table 2.2). The membrane was washed three times for 15 minutes in TBS-T. For secondary antibody incubation, the membrane was incubated in species specific HRP- conjugated secondary antibody (1:5000) for 1 hour, followed by three 15 minutes washes with TBS-T. Secondary antibodies were detected using Clarity™ Western ECL Substrate (Bio-Rad Laboratories, USA) and visualised using AGFA Medical X-Ray Film Blue (AGFA Healthcare NV, Belgium) or Version™ Model 4000 imaging system (Bio-Rad Laboratories, USA).

Table 2.2: Description of primary antibodies utilized for Western analysis

Antibody/ Cat #	Dilution	Type/ Species	Source
Anti-DNAJC3/SC-100717	1:1000	Monoclonal/ Mouse	Santa Cruz Biotech, USA
Anti-DNAJC3/ ab70840	1:1000	Polyclonal/ Rabbit	Abcam, UK
Anti-Hsp70/Hsc70/ SC-24	1:1000	Monoclonal/ Mouse	Santa Cruz Biotech, USA
Anti-Hsp90α/β/ SC-13	1:1000	Monoclonal/ Mouse	Santa Cruz Biotech, USA
Anti-Grp78/ SMC-196D	1:1000	Monoclonal/ Mouse	StressMarq, Canada
Anti-Grp94/ SMC-105B	1:1000	Monoclonal/ Rat	StressMarq, Canada
Anti-HOP/ SRA-1500	1:1000	Monoclonal/ Mouse	Assay Designs, USA
Anti-p-p38/ SC-166182	1:200	Monoclonal/ Mouse	Santa Cruz Biotech, USA
Anti-pJNK/ SC-6254	1:200	Monoclonal/ Mouse	Santa Cruz Biotech, USA
Anti-p44/42 MAPK (T202/Y204)	1:2500	Polyclonal/ Rabbit	Cell Signalling Tech, USA
Anti-GAPDH/ SC-25778	1:1000	Polyclonal/ Rabbit	Santa Cruz Biotech, USA
Anti-GST/ SC-459	1:5000	Polyclonal/ Rabbit	Santa Cruz Biotech, USA
Anti-Histone /H3 #9715	1:2500	Polyclonal/ Rabbit	Cell Signalling Tech, USA

2.17 Preparation of MCF-7 carcinoma cell lysates

MCF-7 carcinoma cells were grown to confluency in 150 cm^2 dishes and the cell rinsed twice with PBS. The cells were lysed by incubating in 1 ml radioimmunoprecipitation assay buffer (RIPA; 50 mM Tris-HCl, pH 7.4, 150 mM NaCl, 1 mM EDTA, 1 mM Na_3VO_4, 1 % (v/v) NP40, 1 mM Na deoxycholate, 1 mM PMSF, 2 µg/ml Protease inhibitor cocktail [Sigma-Aldrich, Germany]) at 4 °C for 1 hour. The lysed cells were centrifuged at 4 °C at 16000 x *g* for 20 minutes and the supernatant stored at -20 °C.

2.18 Pull down assay

2.18.1 MCF-7 carcinoma lysate pull down assay

A total of 20 µg of purified protein (GST protein, GST- tagged mSTI1 and GST-tagged DNAJC3ΔJ/ER) in 1 ml PBS, was incubated with 100 µl resuspended pre-washed Protino® Glutathione Agarose resin at 4 °C for 2 hours, with gentle agitation. The reaction was washed three times with PBS and centrifuged for 5 minutes at 5000 *x g*. The bound purified proteins were incubated overnight with 500 µl of MCF-7 carcinoma cell lysate as prepared in section 2.16. The reaction was washed three times with PBS and centrifuged for 5 minutes at 5000 x *g* and resuspended in SDS sample buffer (50 mM Tris-HCl, pH 6.8, 2 % SDS, 10 % glycerol, 1 % β-mercaptoethanol, 12.5 mM EDTA, 0.02 % bromophenol blue) prior to Western analysis for Hsp90, Hsp70, Grp78 and Grp94.

2.18.2 Purified protein pull down assay

The purified protein pull down assay protocol was a modified from that published by Staron *et al*., 2011. A total 10 µg of purified protein (GST protein, GST- tagged mSTI1 and GST-tagged DNAJC3ΔJ/ER) was bound to Protino® Glutathione Agarose as previously described in section 2.17.1. The bound proteins were incubated separately with 1 µg of recombinant Hsp90 (StressMarq, Canada), Hsp70 (StressMarq, Canada), Grp94 (Abcam, UK), His-tagged Grp78 or His-tagged $Grp94_{284\text{-}543}$ at 4 °C with shaking in binding buffer (20 mM HEPES pH 7.2, 50 mM KCl, 5 mM $MgCl_2$, 20 mM Na_2MO_4, 0.5 % (v/v) NP40, 1 mM ATP). The reactions were washed three times in binding buffer before being analyzed by SDS-PAGE and Colloidal Coomassie staining.

2.18.3 Assessment of substrate binding by ELISA

Malate dehydrogenase (MDH, Roche Diagnostics GmbH, Germany) and β-galactosidase (Sigma Aldrich, Germany) were used as model substrate (Freeman and Morimoto, 1996, Rampelt *et al*., 2012) and heat denatured for 1 hour at 50°C and 30 minutes at 65 °C, respectively. A total of 50 µg/ml of native and heat denatured MDH or β-galactosidase was coated onto the surface of 96 well medium binding ELISA microplates (Greiner Bio-ONE GmbH, Germany) by incubating overnight at 4 °C. Nonspecific binding was blocked by incubating the coated wells in ELISA blocking solution (5 % [w/v] BSA in buffer A [20 mM Tris-HCl (pH 7.4), 150 mM NaCl, 5 mM $CaCl_2$, 0.05 % (v/v) Tween-20, 1 mM ATP]) overnight at 4 °C. Varying concentrations (10 µg/ml,

50 µg/ml, and 100 µg/ml) of GST, GST-DNAJC3ΔJ/ER and His-Grp78 in blocking solution were added to wells and incubated for 12 hours at 4 °C. Wells were washed three times in wash buffer (1 % (w/v) BSA in buffer A), followed by incubation in anti-GST or anti-His primary antibody (1:1000) in blocking solution for 1 hour at room temperature. The wells were washed three times in wash buffer before being incubated with secondary antibody (1: 2000) in blocking buffer for 1 hour at room temperature and subsequently washed again five times with wash buffer. The 3,3',5,5'-Tetramethylbenzidine (TMB) substrate (0.1 mg/ml TMB in 0.05 M phosphate-citrate buffer, pH 5) was added to each well and incubated in the dark for 20 minutes. After incubation, the reaction was stopped by the addition of 2 M H_2SO_4 and absorbance read at 450 nm.

2.18.4 Complex formation assay

Pull down assay

A total of 10 µg of purified protein (GST protein, GST-DNAJC3ΔJ/ER and His-Grp78) was bound to Protino® Glutathione Agarose or nickel charged Chelating Sepharose™ Fast Flow resin for 3 hours in 1 ml PBS or His lysis/binding buffer. The reaction was washed three times with PBS or His lysis/binding buffer and centrifuged for 5 minutes at 5 000 *x g*. The bound proteins were incubated with 10 µg/ml heat denatured β-galactosidase and either 5 µg/ ml GST, GST-DNAJC3ΔJ/ER or 2 µg/ml Grp94 in binding buffer. The reactions were incubated at 4 °C overnight with gentle shaking, followed by three washes with binding buffer. The reactions were analyzed by SDS-PAGE and Colloidal Coomassie staining.

ELISA

A total of 50 µg/ml of His-Grp78 was coated onto the surface of 96 well medium binding ELISA microplates by incubating overnight at 4 °C. Nonspecific binding was blocked by incubating the coated wells in ELISA blocking solution overnight at 4 °C. Varying concentrations (50 µg/ml and 100 µg/ml) of heated denatured β-galactosidase and 20 µg/ml of GST or GST-DNAJC3ΔJ/ER were added and incubated for 12 hours at 4 °C. Wells were washed three times with wash buffer, followed by incubation in anti-GST antibody (1:1000) in blocking solution for 1 hour at room temperature. The wells were washed three times wash buffer before being incubated in secondary antibody (1: 2000) in blocking buffer for 1 hour at room temperature, after which the wells were washed five times in wash buffer. Reactions were analyzed as described in section 2.17.3.

2.18.5 Luciferase refolding assay

The protocol for the refolding of chemically denatured luciferase was modified from that published by Buchberger *et al* 1994 and Freeman *et al*., 1995. A stock solution of QuantiLum® recombinant luciferase (Promega. USA) was prepared at 4 mg/ml in 1 M glycylglycine (pH 7.4). Chemical denaturation of luciferase was conducted by 2-fold dilution of the substrate into 1 M glycylglycine (pH 7.4), followed by a 6.4-fold dilution into denaturation buffer (25 mM HEPES pH 7.5, 50 KCl, 5 mM $MgCl_2$, 5 mM β-mercaptoethanol, 6 M guanidine-HCl) and incubated at 37 °C for 30 minutes. The denatured luciferase was diluted 125-fold into refolding buffer (25 mM HEPES pH 7.5, 50 mM KCl, 5 mM $MgCl_2$, 10 mM dithiothreitol [DTT], 1 mM ATP) supplemented with different combinations of GST, GST-DNAJC3ΔJ/ER and His-Grp78 at 3.2 µM. The refolding procedure was initiated by adding 2 µl of denatured luciferase to a 50:50 mixture (100 µl) of refolding buffer and firefly luciferase assay reagent (FLAR) buffer (20 mM Tris-HCl (pH 7.8), 100 µM EDTA, 1.07 mM $MgCO_3$, 2.67 mM $MgSO_4$, 17 mM DTT, 250 µM ATP and 250 µM D-luciferin [Promega. USA]) in a white 96 high binding well plates (Greiner Bio-ONE GmbH, Germany). The refolding reactions were monitored by measuring luminescence (luciferase activity) at 10 minute intervals for 2 hours at 37 °C using the Synergy Mx Multi-Mode Reader (BioTek, Instruments, Inc., USA) .Native luciferase was used as a positive control and diluted to the same extent as denatured luciferase. Luciferase activity in the refolding reactions was calculated as a percentage of the activity of denatured luciferase without the addition of GST, GST-DNAJC3ΔJ/ER or His-Grp78

2.19 Analysis of expression of DNAJC3 under induced stress conditions

To determine the expression profile of DNAJC3 under different stress conditions, HEK293T cells were treated as listed in Table 2.3. After each treatment, cells were harvested and resuspended in 5X SDS sample buffer and equal amount of protein was analyzed by SDS-PAGE and Western analysis.

Table 2.3: Description of various treatments used to simulate a variety of stress conditions

Stress Condition	Treatment*	Concentration (mM)	Treatment time (Hours)	Recovery time (Hours)
Normal	Untreated	-	-	24
ER Stress	Tunicamycin (Tun)	2.38	24	-
ROS	H_2O_2	0.5	0.25	2
Hypoxia	$CoCl_2$	0.1	24	-
Tumor inducer	PMA	5×10^{-5}	2	24
Proteosome Inhibition	MG132	0.01	2	24
Heat Shock	Heat (42 °C)	-	2	2
UV stress	Short UV (254 nm)	-	0.02	2
UV stress	Long UV (366 nm)	-	0.02	2

* Tunicamycin (Sigma-Aldrich, Germany), Phorbol 12-myristate 13-acetate (PMA [Sigma-Aldrich, Germany]), Z-Leu-Leu-Leu-al (MG132 [Sigma-Aldrich, Germany])

2.20 Effects of Novobiocin (NOVO) and Geldanamycin (GA) on the expression of DNAJC3 in MCF-7 carcinoma cells

MCF-7 carcinoma cells were grown to 90 % confluency and treated with, 0.1, 1 and 10 µM of GA (Biomol International Inc, USA) or 5, 50 and 500 µM of NOVO (Sigma-Aldrich, USA). Cells were also treated with DMSO, the vehicle used to resuspend GA, in order to ensure the effects observed were not due to DMSO. At 24 hours post treatment cells were collected and analyzed by SDS-PAGE and Western analysis.

2.21 Transient siRNA transfections for knockdown of DNAJC3

For transient knockdown of DNAJC3, MCF-7 carcinoma cells were grown to 80 % confluency and transfected with negative control siGENOME Non-Targeting siRNA Pool #2 (cat # D-001206-14-05) and siGENOME SMARTpool Human DNAJC3 (cat # M-012251-00-0005) (Dharmacon Technologies, UK) to a final concentration of 25 nM using Dharmafect 1 transfection reagent (Thermo Scientific, USA) according to manufacturer's specifications. Cells were harvested at 0 hours, 48 hours and 72 hours post-transfection and analyzed by Western analysis.

2.22 Transient transfections of HEK293T cells with HRas plasmids

mEGFP-HRas (Addgene, 18664), mEGFP-HRas G12V (Addgene, 18666) and mEGFP-HRas S17N (Addgene, 18665) plasmids, which coded for EGFP-tagged wild type Ras, EGFP-tagged constituently active Ras, and EGFP-tagged dominant negative Ras, respectively, were extracted using the GenElute™ endotoxin-free plasmid midiprep kit (Sigma-Aldrich, Germany) according

to manufacturer's specifications. HEK293T cells were grown to 80 % confluency overnight in 24 well plates. At 2 hours prior to transfection, spent media was replaced with 500 µl fresh complete media without PSA. For each well, 0.5 µg of plasmid DNA was incubated with 1µl PureFection™ transfection reagent (System Biosciences, USA) in 50 µl complete media. The reaction tubes were vortexed for 10 minutes, centrifuged briefly and incubated for 15 minutes at room temperature, after which the reaction was added to the wells. Transfection mixtures were incubated with cells for 48 hours at 37 °C in a 5 % CO incubator. The transfections were analyzed by Western blot and confocal microscopy.

2.23 Indirect immunofluorescence staining and confocal microscopy

Cells grown on glass coverslips and treated accordingly were fixed in ice cold 100 % ethanol, and washed in PBS. Cells were permeabilized in PBS containing 0.1 % (v/v) Tween-20 for 20 minutes with shaking at room temperature (all subsequent steps were conducted at room temperature with shaking unless stated otherwise). Cells were rinsed twice for 10 minutes in wash buffer (PBS containing 0.1 % [w/v] BSA) and blocked in blocking solution (PBS containing 1 % [w/v] BSA) for 30 minutes. Cells were incubated in primary antibodies (mouse anti-DNAJC3 [1:200], rat anti-Grp94 [1:200] and goat anti-Hsp90 [1:100]) prepared in blocking solution overnight at 4 °C. Cells were washed twice for 10 minutes in wash buffer and then incubated in species-specific Alexa-Fluor 488, Alexa-Fluor 546 (Molecular probes, Invitrogen, UK) or Dylight 660 (Abcam, UK)-conjugated secondary antibodies for 30 minutes. Three 10 minute washes in wash buffer were conducted with the third wash containing 1 µg/ml Hoechst 33342 (Pierce Biotechnology, Inc Thermo Scientific, USA) to stain the cell nucleus. Coverslips were mounted onto glass slides using Dako fluorescence Mounting Medium (Dako North America, Inc, CA, USA) and stored at 4 °C.

Cells were visualized using the inverted LSM 510-Meta confocal laser scanning microscope (Carl Zeiss, Germany) using the 60x oil immersion objective lens. The lasers at wavelengths 405, 488, 543, 633 nm were used to excite Hoechst 33342, Alexa-Fluor 488, Alexa-Fluor 546 and Dylight 660, respectively. Images were analyzed using the Axionvision LE/SE freeware software (Carl Ziess, Germany). Quantification of colocalization analysis was conducted using the Image J software and processed using Microsoft Office PowerPoint 2007.

Chapter 3: *In silico* analysis of DNAJC3 TPR domains

3.1 Introduction

This chapter describes the bioinformatics analysis of the different TPR domains of DNAJC3. DNAJC3, also known as $p58^{IPK}$, has a cleavable ER retention signal at the N-terminus, nine TPR motifs and a J-domain at the C-terminus. Currently there are two resolved structures of DNAJC3 available, mouse DNAJC3, which is missing the ER signal peptide and the J domain (Tao *et al*., 2010) and human DNAJC3 with the J domain included (Svärd *et al*., 2011). The availability of these structures enabled the prediction of the protein's function based on analysis on the various domains making up its tertiary structure. DNAJC3 was selected for study due to the fact that two of its domains, the TPR and J domain, are well characterized domains commonly found in the co-chaperones of Hsp90 and Hsp70. DNAJC3 is only one of two DNAJ proteins to have TPR domains, the other being DNAJC7 (Kampinga and Craig, 2010).

DNAJC7, or TPR2, is a member of the DNAJC group that was first discovered during a screening process for proteins that interacted with the GAP-related domain of neurobromin, a protein that regulates Ras (Murthy *et al*., 1996). Structurally, DNAJC7 has seven TPR domains and a J domain located at the C-terminus of the protein. Through a yeast two-hybrid system, DNAJC7 was identified as a cytosolic protein that could interact with both Hsp70 and Hsp90 (Brychzy *et al*., 2003). The ability of DNAJC7 to interact with both Hsp90 and Hsp70 was examined during the refolding of the glucocorticoid receptor. Brychzy *et al* (2003) found that during the refolding of the receptor, the J domain of DNAJC7 stimulated the ATPase activity of Hsp70 which resulted in ATP hydrolysis, increasing the binding affinity of Hsp70 for its substrate. However, DNAJC7 caused the dissociation of Hsp90 from the substrate, which did not occur with Hsp70. Mutational studies identified the TPR domains of DNAJC7 as being responsible for mediating the dissociation, leading Brychzy and co-workers to conclude that the TPR domains induced an ATP-independent disassociation of Hsp90 from substrates (Brychzy *et al*., 2003, Moffatt *et al*., 2008).

Although structurally similar, DNAJC3 and DNAJC7 are localized in different compartments of the cell. DNAJC7 is cytosolic, while DNAJC3 is found mainly in the ER lumen, although a subpopulation of the protein can be found in the cytosol due to the fact that the ER signal peptide

is somewhat inefficient in mediating the translocation of DNAJC3 to the ER (Rutkowski *et al*., 2007). In addition, while the TPR domains of DNAJC7 have been shown to be able to interact with both Hsp90 and Hsp70, this has not been proven for DNAJC3. The only co-chaperone related function currently proposed for DNAJC3 TPR domains is that TPR1 of the protein binds selectively to unfolded protein through its hydrophobic peptide-binding groove, while functioning as a co-chaperone to Grp78 via the J domain (Tao *et al*., 2010). Similar to DNAJC7, the J-domain of DNAJC3 has been shown to be able to stimulate the ATPase activity of Grp78 during UPR caused due to ER stress, where it helps to restore ER homeostasis (Oyadomari *et al*., 2006, Rutkowski *et al*., 2007, Tao *et al*., 2010; Svärd *et al*., 2011). Since DNAJC3 is proposed to have three functional TPR domains (Tao *et al*., 2010 and Svärd *et al*., 2011), and currently there has only been a proposed function for one of these domains, the function of the other two domains are unknown. The objective of this study was to use various bioinformatics tools to analyse the TPR domains and predicted possible functions of the protein not yet discovered. The specific objectives were:

- To conduct multiple sequence analysis and phylogenetic analysis on DNAJC3 from various species;
- To conduct motif identification for DNAJC3 and known Hsp90 and Hsp70 TPR-containing co chaperones and conduct multiple sequence alignment on the TPR domains;
- Determine sequence, structural and electrostatic potential similarities between DNAJC3 TPR domains and structural homologues.

3.2 Results

3.2.1 DNAJC3 is a highly conserved protein found in numerous species

3.2.1.1 DNAJC3 Multiple sequence alignment

In order to determine the conservation of DNAJC3 across a wide range of species, multiple sequence alignment was conducted on DNAJC3 amino acid sequences from 35 different species identified through BLAST and Psi-BLAST (Table 3.1). The selected species represented different groups including mammals, fish, birds, insects, fungi and plants.

Table 3.1: Accession number, E-value, sequence identity and sequence percentage coverage of DNAJC3 amino acid sequences from 35 species used in the study.

Accession number	Species	Common name	E value	Sequence identity	% Coverage
NP_006251.1	*Homo Sapiens*	Human	0	100	100
XP_001138934.1	*Pan troglodytes*	Chimpanzee	0	99	100
XP_003257442.1	*Nomascus leucogenys*	White-cheeked gibbon	0	99	100
NP_001253333.1	*Macaca mulatta*	Rhesus monkey	0	99	100
XP_003832176.1	*Pan paniscus*	Bonobo	0	99	95
XP_002752533.1	*Callethrix jacchus*	Marmoset	0	98	100
XP_003928253.1	*Saimiri boliviensis*	Squirrel monkey	0	98	100
XP_002918691.1	*Ailuropoda melanoleuca*	Panda	0	98	100
NP_032955.2	*Mus musculus*	Mouse	0	97	100
NP_001177113.1	*Sus scrofa*	Wild boar	0	97	100
NP_001011485.1	*Xenopus tropicalis*	Clawed frog	0	97	100
XP_534166.3	*Canis lupus familiaris*	Dog	0	97	95
NP_777181.1	*Bos Taurus*	Cow	0	96	100
XP_003495288.1	*Cricetulus griseus*	Hamster	0	96	94
XP_001492322.1	*Equus caballus*	Horse	0	96	95
XP_003409693.1	*Loxodonta Africana*	Elephant	0	95	95
NP_071568.1	*Rattus norvegicus*	Rat	0	94	100
XP_002824422.1	*Pongo abelii*	Orangutan	0	94	100
XP_003765831.1	*Sarcophilus harrisii*	Tasmanian devil	0	92	100
XP_001366332.1	*Monodelphis domestica*	Opossum	0	91	100
XP_003430813.1	*Orinithorhynchus anatinus*	Platypus	0	90	94
XP_003203294.1	*Meleagris gallopavo*	Turkey	0	80	95
NP_001008437.1	*Gallus*	Chicken	0	80	100
XP_003218715.1	*Anolis carolinensis*	Carolina anole	0	80	100
NP_955904.2	*Danio rerio*	Zebrafish	0	71	100
NP_001134029.1	*Salmo salar*	Atlantic salmon	0	70	84
XP_003699497.1	*Megachile rotundata*	Leafcutter bee	0	48	93
EFN69747.1	*Campontus floridanus*	Carpenter ant	0	47	96
XP_312173.2	*Anopheles gambiae*	Mosquito	0	46	94
NP_649916.1	*Drosophila melanogaster*	Fruit fly	0	44	94
XP_001824393.1	*Aspergillus oryzae*	Yellow koji mold	2 e-178	31	98
XP_002152681.1	*Penicillium marneffei*	Mold	8 e-169	29	95
NP_001234332.1	*Solamun lycpersicum*	Tomato	4 e-150	32	80
NP_195936.1	*Arabidopsis thaliana*	Thale cress	2 e -138	30	87
AAP41819.1	*Nicotiana benthamiana*	Wild tobacco	1 e- 127	29	83

Sequence alignment was conducted using four different multiple sequence alignment programs, namely ClustalW, MAFFT, T-COFFEE and Promals3D. Alignment results obtained using the Promals3D program were selected for further analysis. BioEdit was use to annotate and present the results (Figure 3.1).

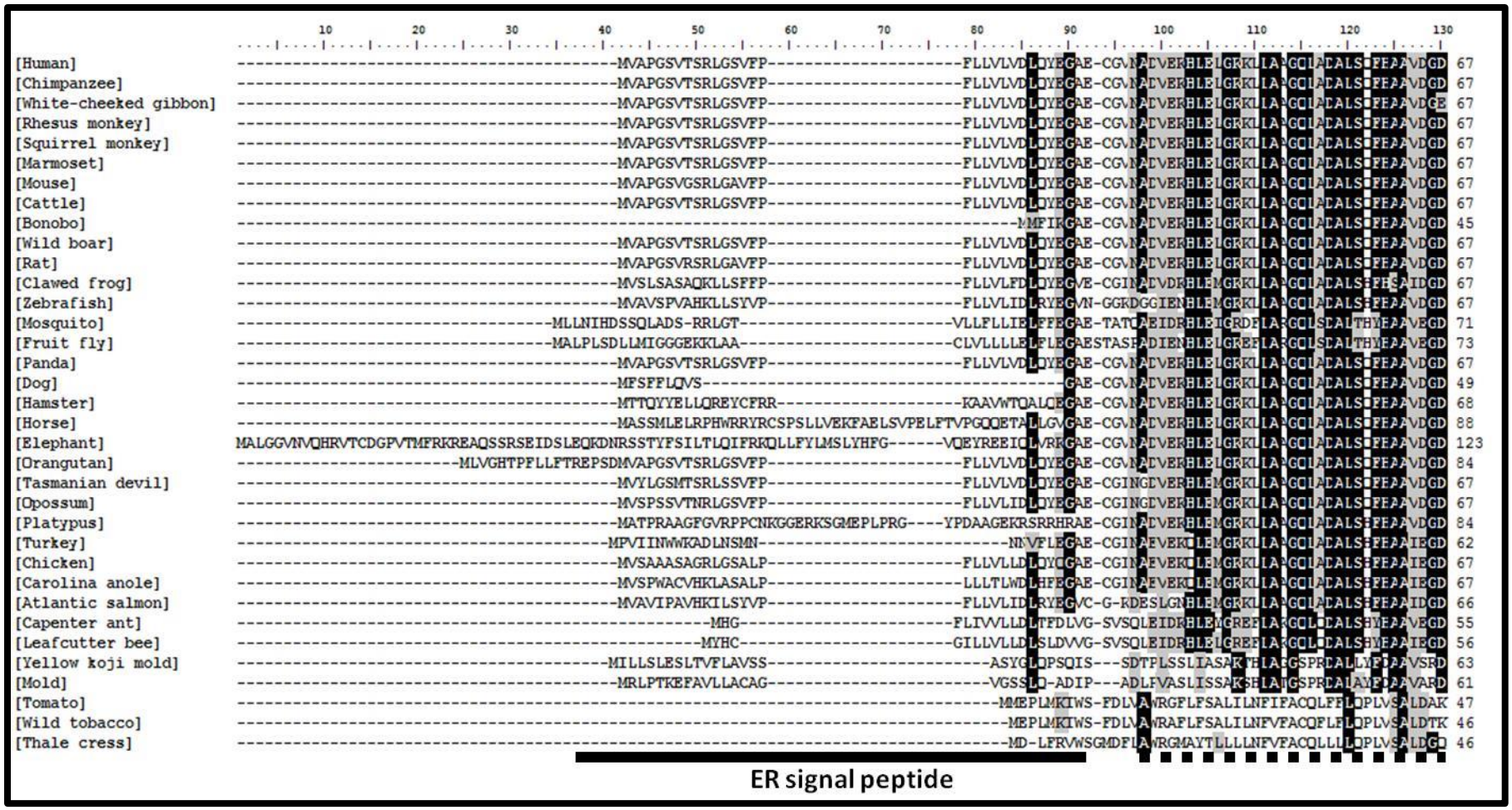
ER signal peptide

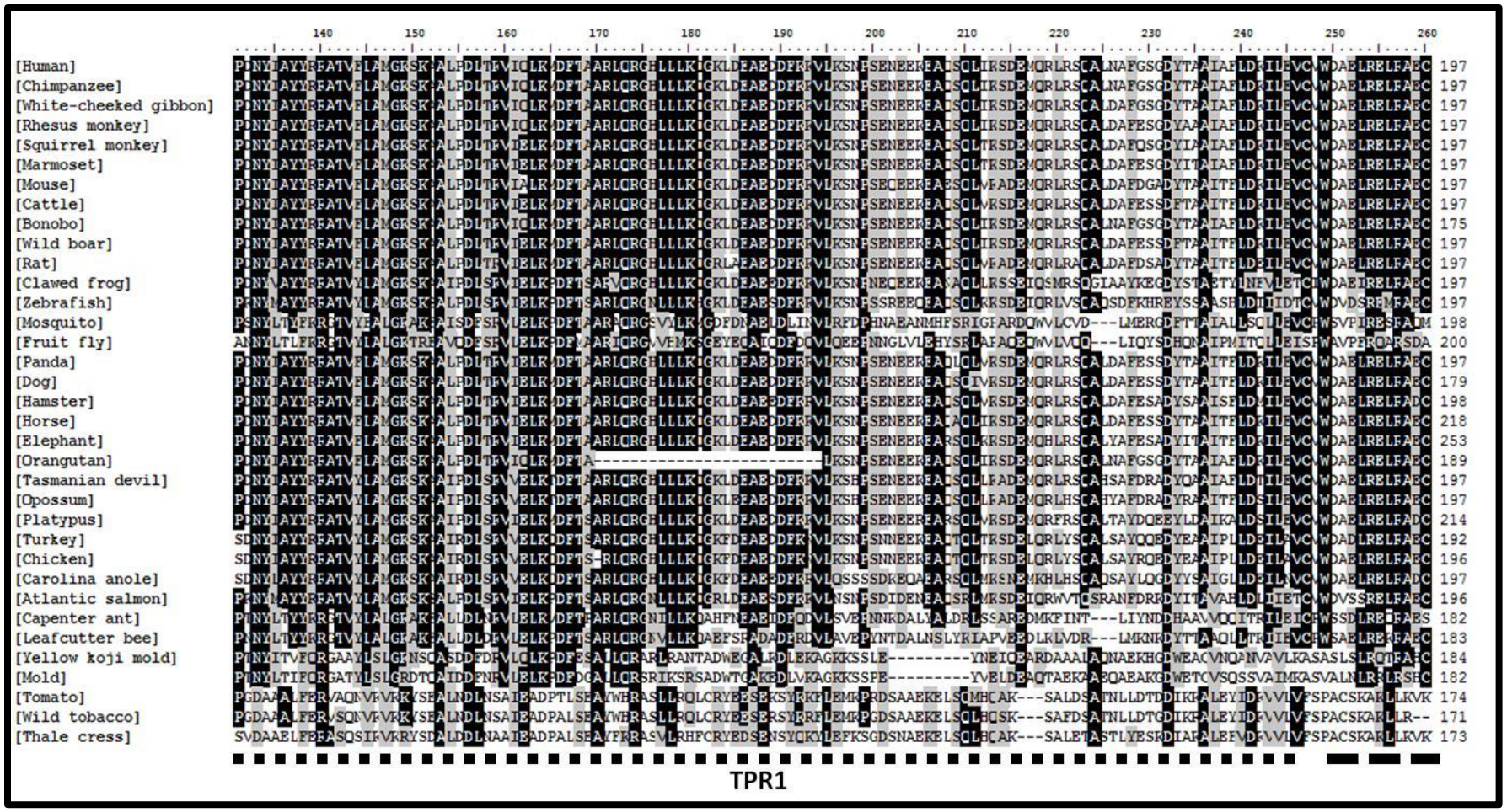
TPR1

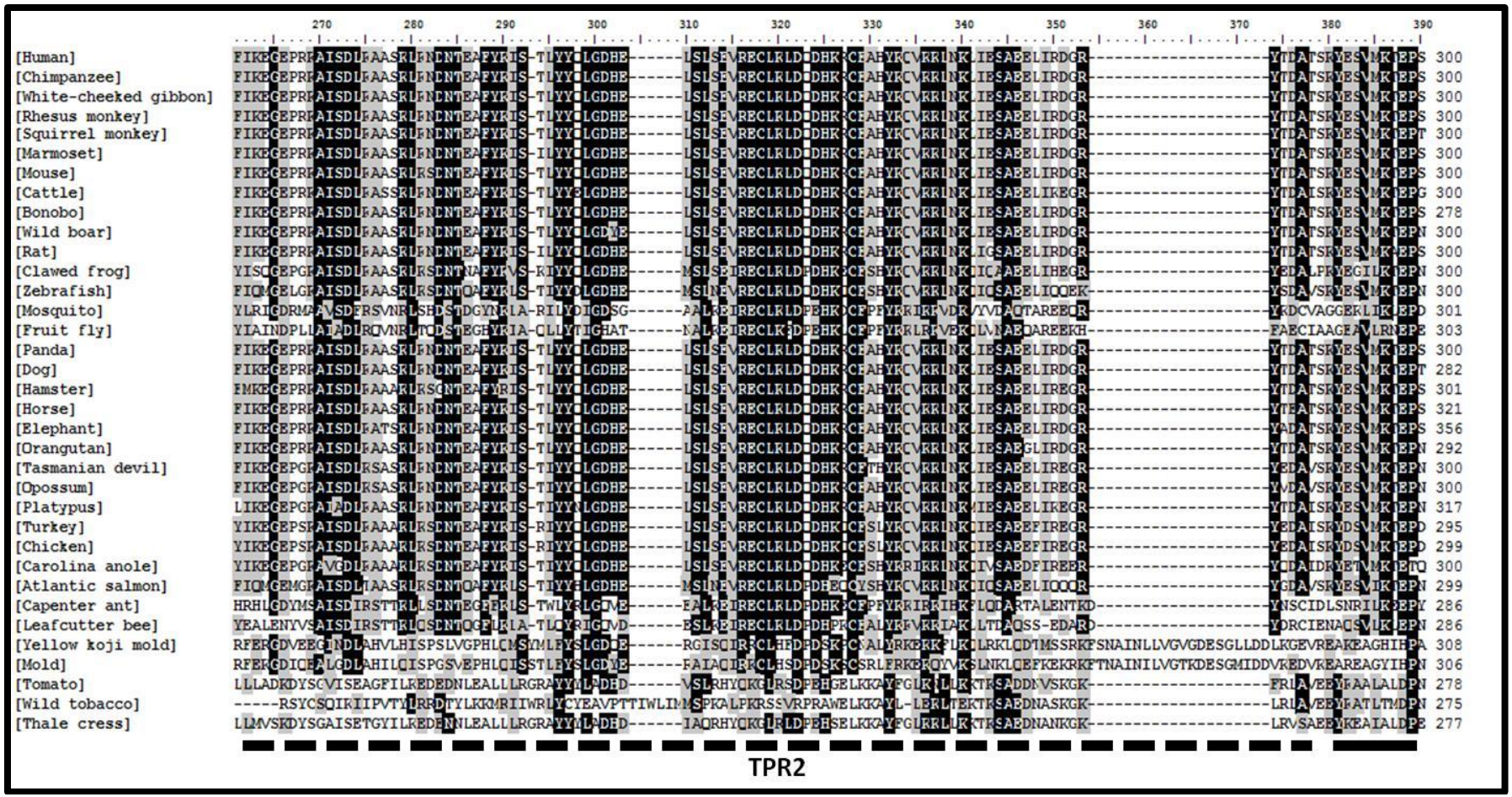
TPR2

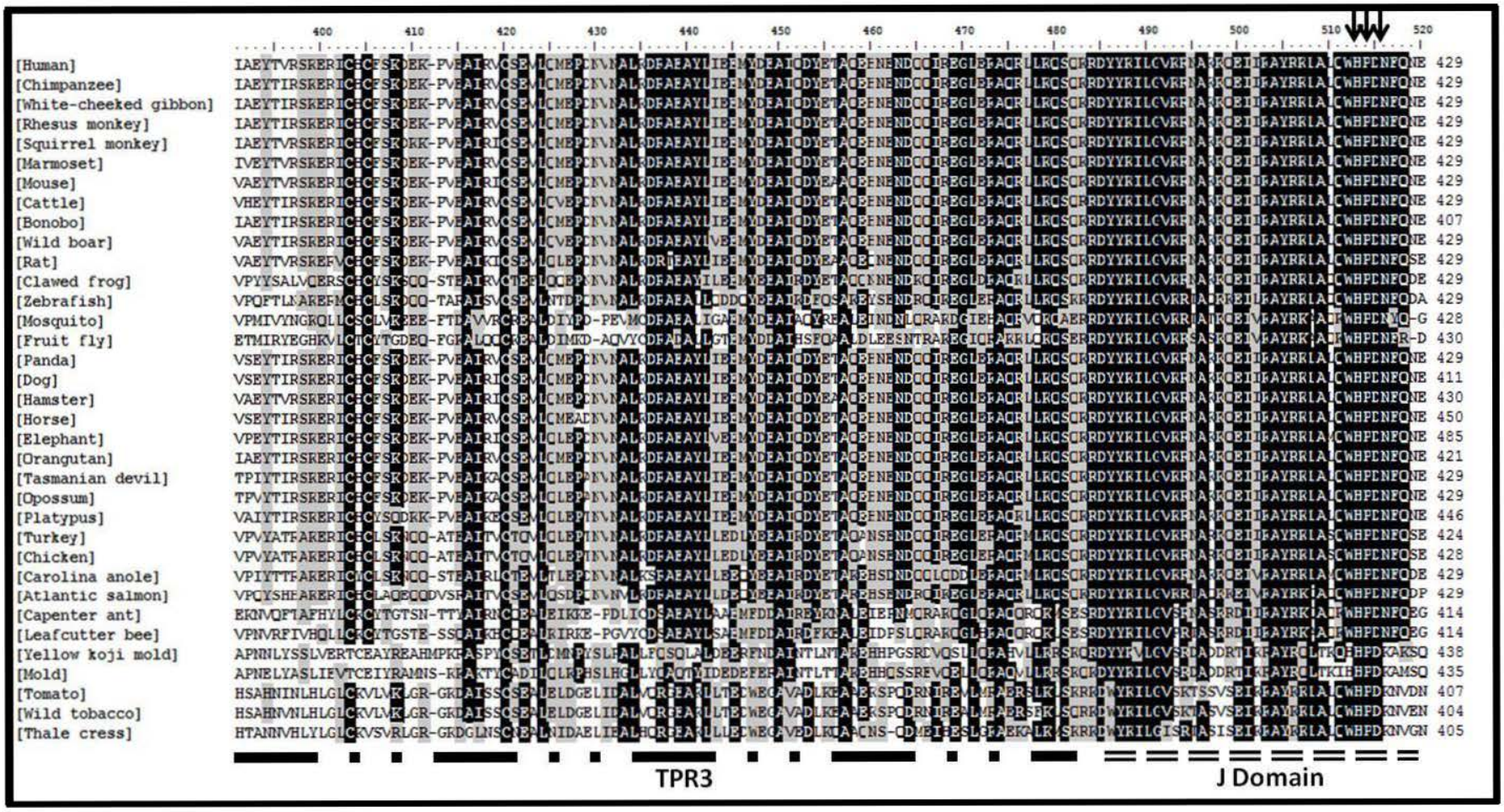
TPR3
J Domain

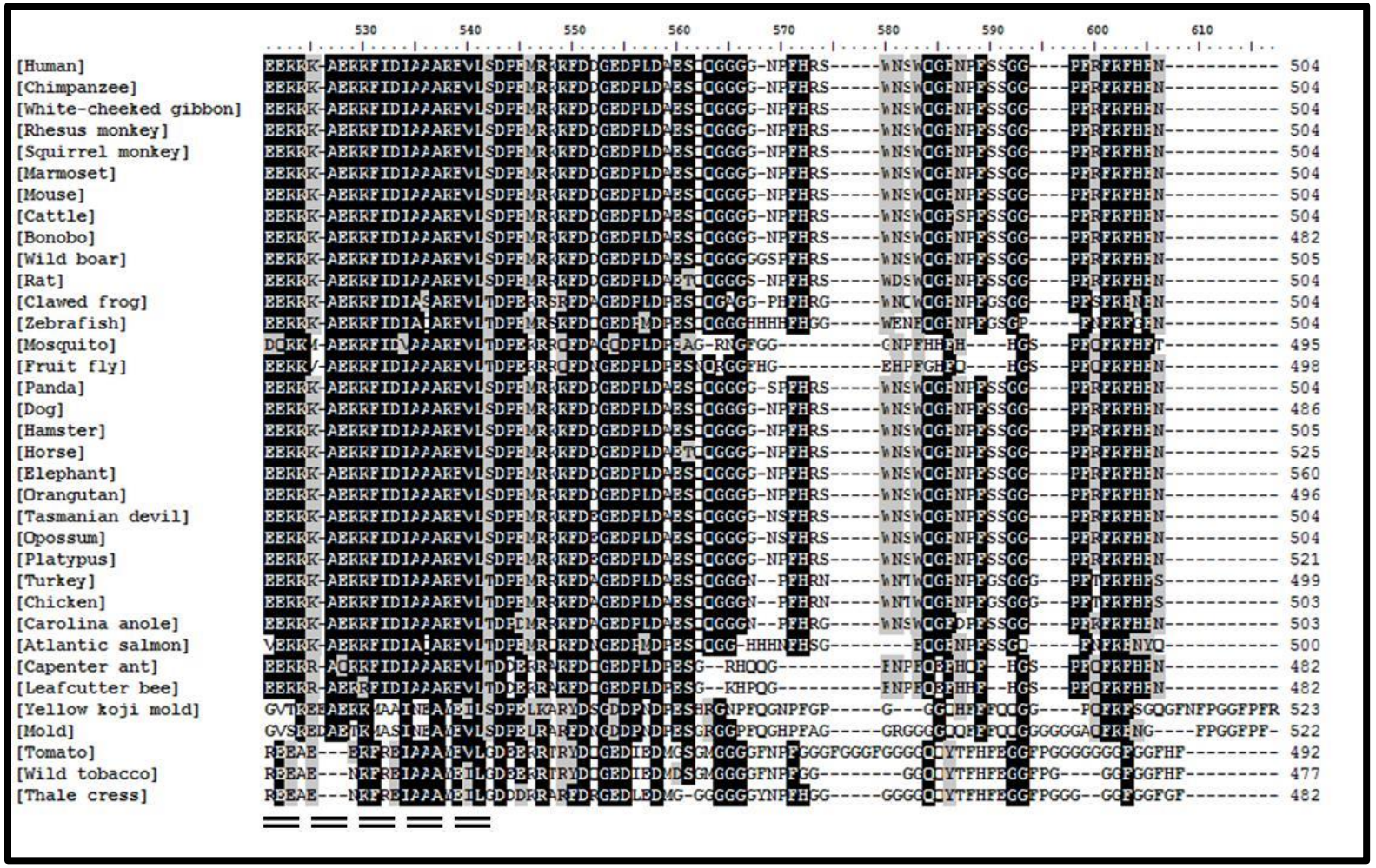

Figure 3.1: Multiple sequence alignment of DNAJC3 amino acid sequence from 35 species. Multiple sequence alignment generated by Promals3D and edited using BioEdit. Residues highlighted as follows; black shading represents identical residues and grey shading represents similar residues. The Hsp40 defining domain, the J domain is underlined double broken black line and the HPD residues involved in stimulation of the ATPase activity of Hsp70 (Tsai and Douglas, 1996), are indicated by black arrows. The ER signal peptide and TPR1, 2 and 3 are underlined by different black lines.

DNAJC3 has three distinct TPR domains located at the N terminus of the protein which are underlined by different black lines (Figure 3.1). An ER signal peptide located at the N-terminus of the sequence, is underlined black. The ER signal peptide is cleaved once the protein has translocated to the ER, resulting in DNAJC3 being an ER lumen residential protein (Rutkowski *et al*., 2007). The J domain, the domain that defines a protein as a member of the DNAJ family is underlined by a double black line, while the HPD motif, known to be required for the stimulation of the ATPase activity of Hsp70 (Tsai and Douglas,1996), is indicated by black arrows (Figure 3.1). The black and grey shading represents identical and similar amino acid residues, respectively, the conservation of which illustrated that the DNAJC3 protein was highly conserved amongst the species analyzed. This was also depicted by the percentage identity matrix, with percentage similarity ranging from 98 % to 85 % between the human protein and other mammalian protein (results not shown). DNAJC3 protein sequences from insects (leafcutter bee, carpenter ant, mosquito and fruit fly), plants (tomato, wild tobacco and thale cress) and fungi (mold and yellow koji mold) were an exception. This was indicated by the numerous amino acid residue substitutions, deletions and additions (Figure 3.1) as well as the low identity percentage, with plant proteins sequences having as low as 30% sequence identity (data not shown). The limited sequence conservation seen in Figure 3.1 for insects, plants and fungi correlated with the limited sequence identity percentage and low E value score results from the BLAST and Psi-BLAST analysis (Table 3.1). To further examine the relationship between the DNAJC3 proteins of the 35 species in this study, a phylogenetic analysis was conducted.

3.2.1.2 DNAJC3 phylogenetic analysis

Based on the results obtained from the multiple sequence alignment, additional analysis was conducted to examine the interrelationship of the DNAJC3 proteins across the various species. The results obtained from the Promals3D alignment (Figure 3.1) was utilized for the phylogenetic analysis, which was conducted using MEGA5.1 (Figure 3.2).

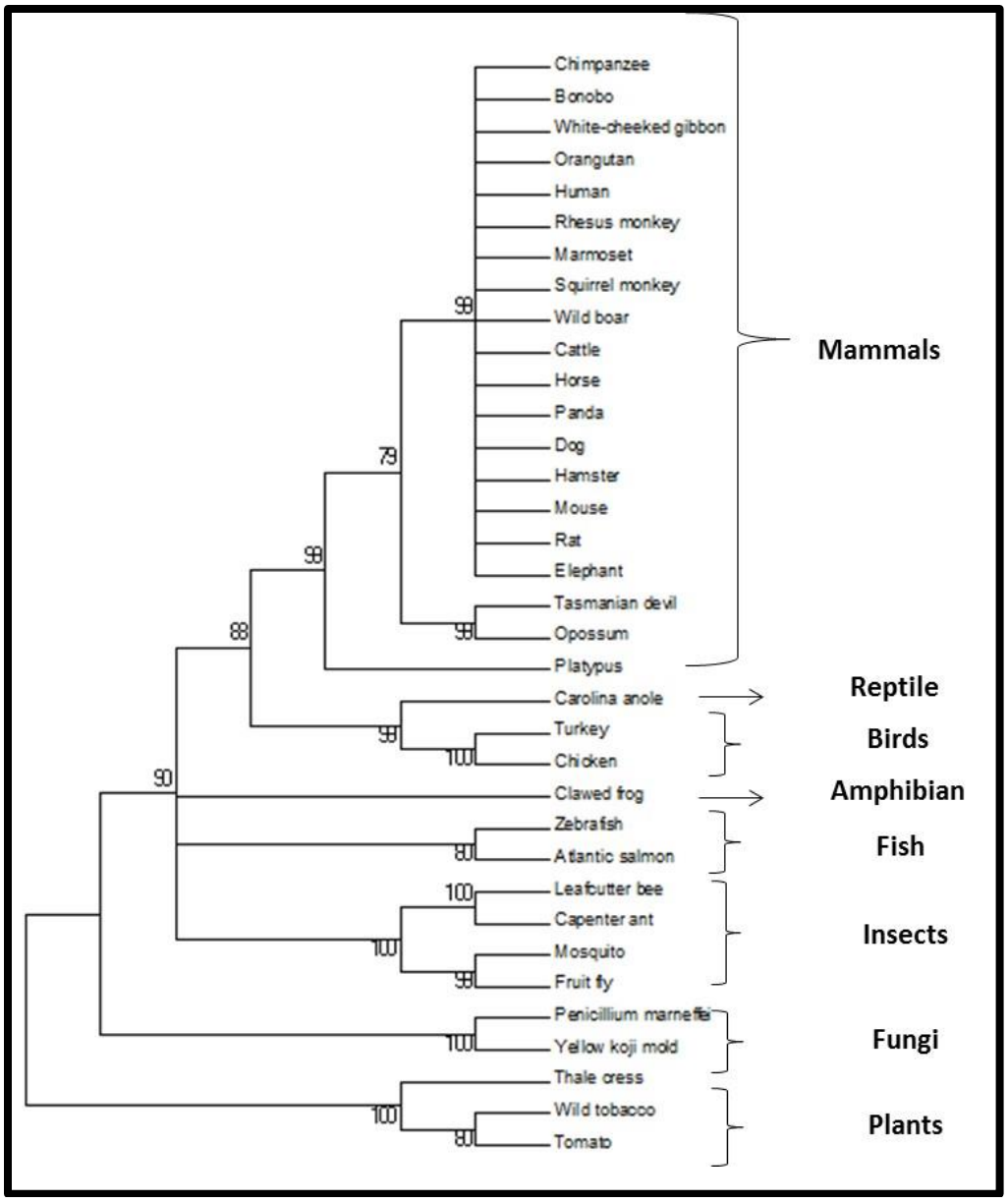

Figure 3.2: Evolutionary relationships of DNAJC3 proteins from various species. The evolutionary history was generated using the Maximum likelihood statistical method. The bootstrap consensus tree inferred from 1000 replicates was taken to represent the evolutionary history of the taxa analyzed. The percentage of replicate trees in which the associated taxa clustered together in the bootstrap test (1000 replicates) is shown next to the branches. Branches partitions replicated in less than 75% of the bootstrap analyzes were collapsed The evolutionary distances were computed using the Jones-Taylor- Thornton (JTT) model and are in the units of the number of amino acid substitutions per site. The analysis involved 35 amino acid sequences. All positions containing gaps and missing data were eliminated. There were a total of 396 positions in the final dataset. Evolutionary analyses were conducted in MEGA5.1.

Several branches can be observed from the phylogenetic tree. The mammals formed a monocluster that separated them from other families, with the high bootstrap value of, 99 % illustrating the

significance of the split. The Tasmanian devil and opossum formed an additional monocluster that split from the main mammalian clade, while the same was observed for the platypus which had a branch that split from the rest of the mammals earlier, possibly indicating an evolutionary difference between the proteins in higher and lesser mammals (Figure 3.2). A similar trend was observed for the other species within the same family, which formed their own clades as seen in the case of birds (turkey and chicken, 100%), fish (zebra fish and salmon, 80%) and insects (mosquito, fruit fly, carpenter ant and leafcutter bee, 100%).Interestingly the insects split into subclades which separated the ant and bee from the mosquito and fruit fly, representing a divergence that separated non winged insects from winged insects. The most interesting observation from the phylogenetic tree was the outlier branch that separated the plants (tomato, wild tobacco and thale cress) from the rest of the species. The difference in the plant DNAJC3 protein from the human protein was also observed with the alignment analysis, where these sequences had the lowest sequence identity to all the other protein sequences analyzed.

3.2.2 DNAJC3 TPR domains differ from TPR domain that interact with Hsp90 and Hsp70 and are more similar to TPR domains with functions independent of Hsp90 and Hsp70

3.2.2.1 Domain identification

Literature lists the number of different domain types present within DNAJC3 as three, an ER signal peptide, TPR domains and a J domain (Tao *et al*., 2010 and Svärd *et al*., 2011). The TPR domain and J domain are defined as co-chaperone domains, although the TPR domain can have other functions not linked to co-chaperoning activity (Lamb *et al*., 1995, D'Andrea and Regan, 2003). Only one other DNAJ protein, DNAJC7, is known to contain TPR domains and a J domain in combination, both of which function as co-chaperone domains. The TPR domains of DNAJC7 interact with both Hsp90 and Hsp70 in a co-chaperone capacity (Brychzy *et al*., 2003, Moffatt *et al*., 2008). Due to the similarity of DNAJC3 and DNAJC7 further analysis was conducted in an attempt to elucidate the possible functions of DNAJC3 using published data on DNAJC7. Also included in the analysis were TPR-containing proteins known to co-chaperone either Hsp90, Hsp70 or both chaperones. In order to identify specific domains of DNAJC3, DNAJC7 and known co-chaperones of Hsp90 and or Hsp70, amino acid sequences were submitted to four different motif identification software programs to increase the probability of identifying all possible motifs. The results from the programs were compiled and represented using the DOG 2.0 software (Figure 3.3).

Selected for analysis were known TPR-containing co-chaperones of Hsp70 (HIP), Hsp90 (PP5 and TOM34) and of both Hsp90 and Hsp70 (HOP, DNAJC7, CHIP and SGT). Figure 3.3 showed that DNAJC3 protein was composed of three different types of motif, namely an ER signal peptide at the N-terminus, eight TPR motifs in the middle and a J domain at the C-terminus, which involved in Hsp70 and DNAJ interactions (Tsai and Douglas, 1996). The domain identification analysis results reported here are similar to previous findings (Kampinga and Craig, 2010), although the majority of studies list the number of TPR motifs as nine (Tao *et al*., 2010 and Svärd *et al*., 2011). The TPR motif was found in all the co-chaperones of Hsp90 and Hsp70 analyzed; however the number and position of the motif differed (Figure 3.3). A functional TPR domain is comprised of three or more TPR motif clustered in a group (Lamb *et al*., 1995), and the domain is known to mediate protein-protein interactions. DNAJC3 and DNAJC7 follow the same pattern with the exception of the middle motifs, in which only two or a single TPR motif were predicted, respectively (Figure 3.3). The identification of eight TPR motifs suggested that DNAJC3 potentially has two functional TPR domain as opposed to the proposed three, or that one of the three domains is incomplete (Tao *et al*., 2010, Svärd *et al*., 2011). DNAJC3 and DNAJC7 also have the J domain at the C-terminus in common. HIP and HOP, as well as HIP and CHIP also share common domains, namely the DP domain and the coiled coil domain, respectively. The phosphatase and Ubox domains were only found in PP5 and CHIP, respectively.

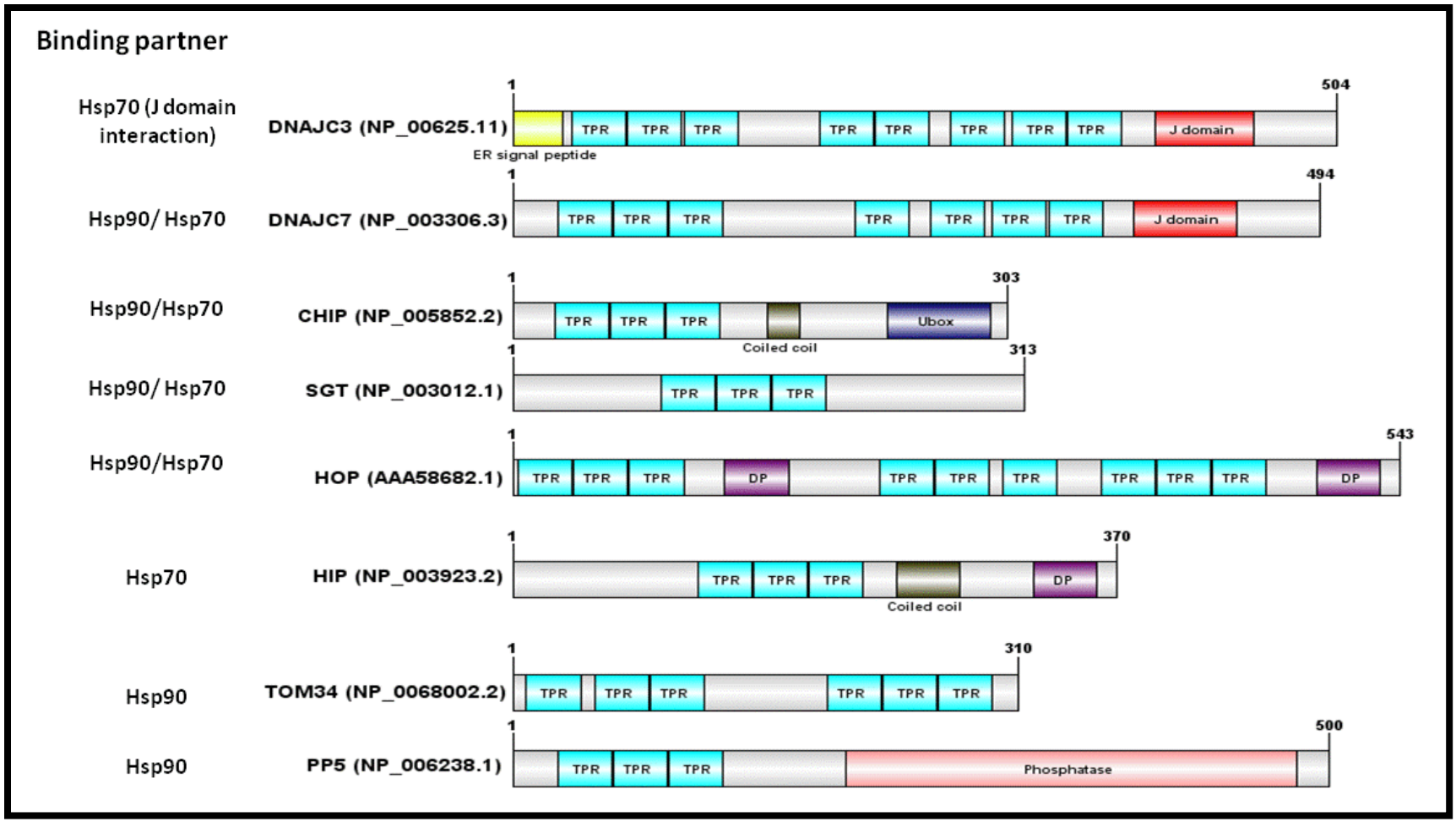

Figure 3.3: Domain identification of DNAJC3, DNAJC7 and selected Hsp90 and Hsp70 co-chaperones. The number on the top left of each protein indicate the N-terminus and the number at the top right indicate the C-terminus. Domain architecture was constructed using the DOG 2.0 software

3.2.2.2 TPR domain multiple sequence alignment

Based on the motif identification and comparison conducted in section 3.2.2.1, the TPR domain was identified as the common feature amongst all the analyzed co-chaperones of Hsp90 and Hsp70 and DNAJC3. Multiple sequence alignment was conducted on the TPR domains of known Hsp90 and Hsp70 interacting co-chaperones as well as the three TPR domains of DNAJC3 (Figure 3.4).

The TPR motif consensus sequence, W_4, G_8, Y_{11}, G_{15}, Y_{17}, A_{20}, Y_{24}, A_{27} and P_{32} (D'Andrea and Regan, 2003), was identified after the alignment. However, apart from the TPR motif consensus sequence, no sequence conservation or similarity was observed between the co-chaperones and DNAJC3 TPR domains (Figure 3.4). The residues involved in the formation of the carboxylate clamp with the C-terminal EEVD of Hsp90 or Hsp70 (boxed red, Figure 3.4), usually a positively charged residue (K, N or R), was observed to be conserved in Hsp70 and Hsp90 interacting proteins and absent in all three DNAJC3 TPR domains. The same was observed for the residues involved in determining the binding specificity between of TPR binding and Hsp90 or Hsp70. Interestingly, although the residues involved in determining specificity between Hsp90 and Hsp70 differed, the topological position of the residues was identical (boxed blue, Figure 3.4). However, although it was noted that there was no sequence conservation, the Promals3D alignment also included structural prediction of TPR domains and from the analysis it was suggested that the analyzed TPR domains were made up of helical structures (red arrows, Figure 3.4). From the latter analysis, each TPR motif (34 amino acid residues) appeared to form two alpha helical structures, which is similar to previous observations of TPR domains (D'Andrea and Regan, 2003).

Since the carboxylate clamp residues were identified to be important in the TPR domain for Hsp90/Hsp70 interaction and found to be lacking in DNAJC3 TPR domains, additional analysis was conducted to understand the consequence of the lack of the clamp residues in DNAJC3 TPR domains.

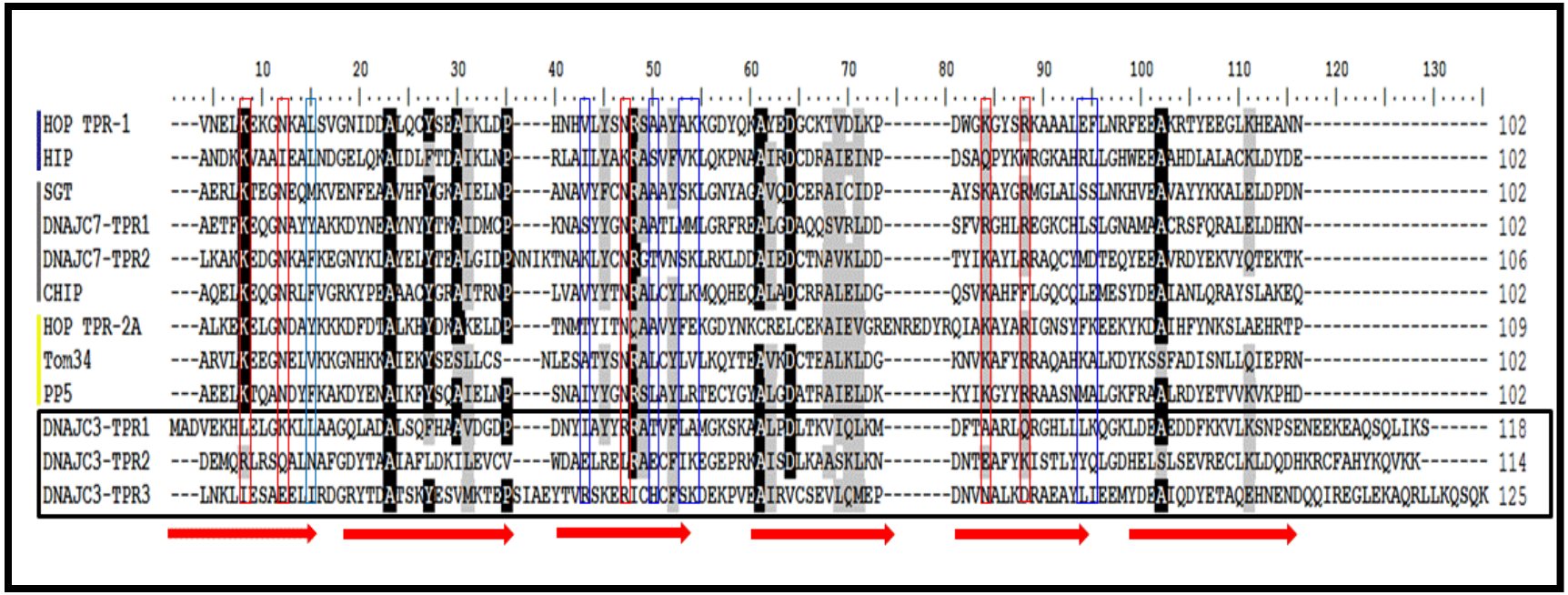

Figure 3.4: Multiple sequence alignment of DNAJC3 TPR domains and TRP domains of known Hsp90 and Hsp70 co-chaperones. Amino acid sequence of TPR domains involved in the interaction with Hsp90 and or Hsp70 were isolated and alignment against DNAJC3 TPR domains 1-3 using Promals3D and analyzed using the BioEdit software. Black box highlights DNAJC3 TPR domains; red box highlights amino acid that form the carboxyl clamp and blue box highlights amino acid residues shown in HOP to be involved in determining specificity for either Hsp90 or Hsp70 (Odunuga *et al.*, 2003). Black and grey shading indicate identical and similar amino acids, respectively. The blue, grey and yellow lines indicate co-chaperone proteins known to interact with Hsp70, Hsp90 / Hsp70 and Hsp90, respectively. The red arrows represent predicted helical secondary structure.

3.2.2.3 Electrostatic potential analysis of TPR domains, interaction analysis of the TPR domains and EEVD motif and mutational studies of DNAJC3 TPR domains

Based on the multiple sequence alignment conducted in section 3.2.2.2 between DNAJC3 TPR domains and Hsp90 and Hsp70 co-chaperones, it was noted that DNAJC3 TPR domains were missing five residues (K8, N12, N59, K96, R100), that were highly conserved in both Hsp90 and Hsp70 co-chaperones (Figure 3.4). These five residues form the carboxylate clamp, which is essential for the interaction of the TPR domain with the C–terminal EEVD motif of Hsp90 and Hsp70 (Scheufler *et al*., 2000, Odunuga *et al*., 2003). Mutational analyses were conducted on the TPR domains of DNAJC3, in which the aforementioned five residues in the three DNAJC3 TPR domains were mutated *in silico* as follows; DNAJC3 TPR1: L8K, K12N, R59N, A96K and Q100R; DNAJC3 TPR2: R8K, Q12N, L59N, E96K and K100R; and DNAJC3 TPR3 :I8K, E12N, R59N, E96K and D100R. These mutations were conducted to introduce the five carboxylate clamp residues. DNAJC3 TPR domain mutation models were constructed using HHpred and using the original DNAJC3 sequence as the template, models were verified using MetaMQAP and Verify3D.

Electrostatic potential analysis (at pH 7 and default protonation state for all residues) of the interacting TPR domain grooves of HOP, DNAJC7 (modelled using DNAJC3 as template), DNAJC3 and mutated DNAJC3 TPR domains, was conducted to examine the different charge distribution of the TPR interacting groove (Figure 3.5). For TPR domains, the groove is mostly known as the interface for protein-protein interaction (D'Andrea and Regan, 2003), thus the electrostatic potential analysis and comparison was focused on that area. Electrostatic potential for each protein was determined by submitting the corresponding pdb file to Deepview/Swiss-PdbViewer (Guex and Peitsch, 1997). The program assigns a numerical value to each amino acid residue based on its charge and represents the assigned charge in a color code; namely blue to represent positively charged residues, white for neutral residues and red for negatively charge residues.

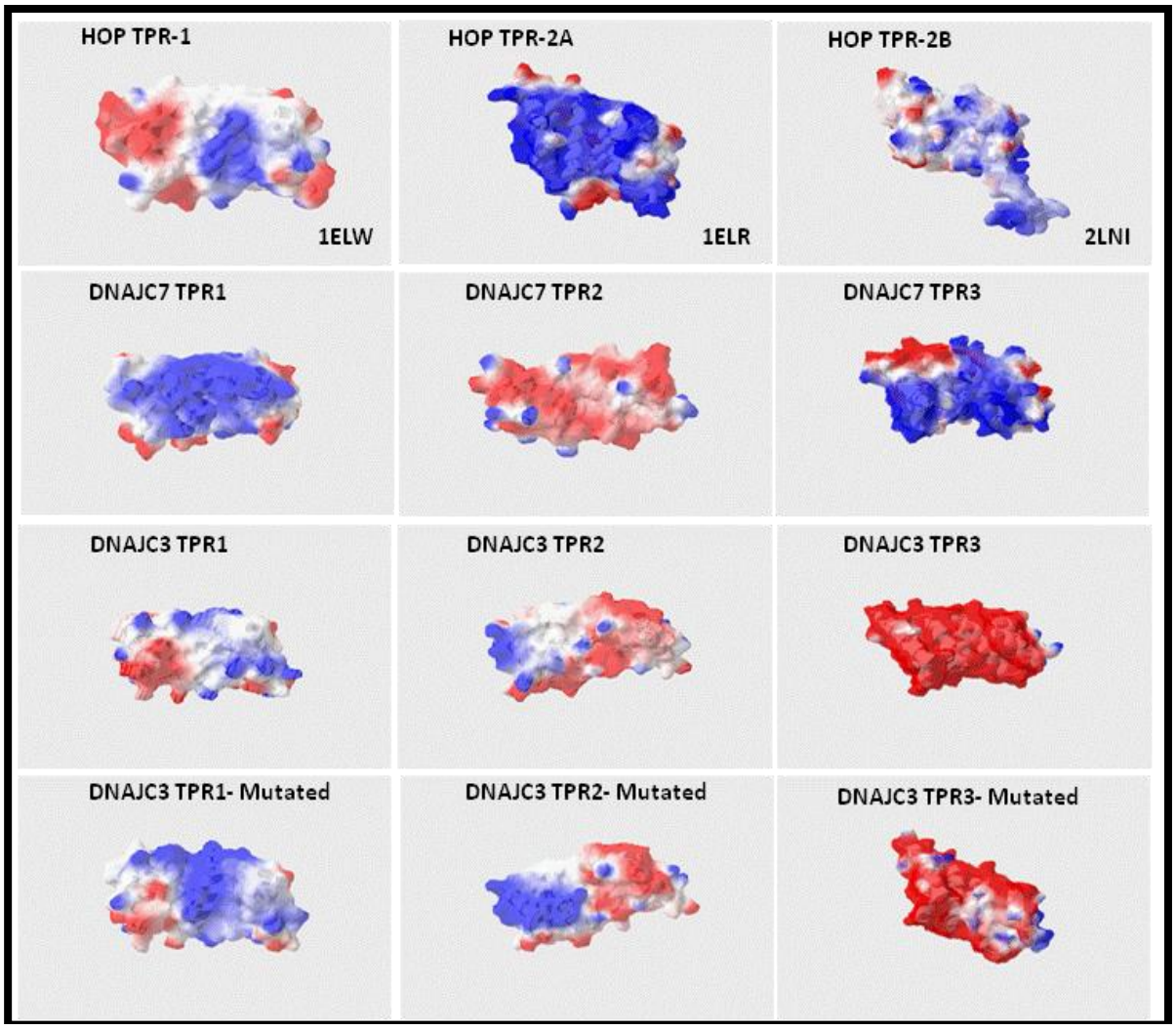

Figure 3.5: Electrostatic potential analysis and comparison of TPR domains from HOP, DNAJC7, DNAJC3 and TPR mutated DNAJC3. Red represents negatively charged regions, blue represents positively charged regions and white shading represents neutral areas

The TPR domains of HOP were included in the comparison (Figure 3.5, top panels), as they have been extensively characterized (Odunuga *et al.*, 2003), the structures resolved (Scheufler *et al.*, 2000) and are known to interact with both Hsp90 and Hsp70. Two out of the three TPR domains of HOP had a positively charged groove (Figure 3.5). The groove of HOP TPR-1 was surrounded by neutral regions and the centre of the groove was highly positive. HOP TPR-2A had an overall positive charge, even on areas outside of the TPR groove. The electrostatic distribution TPR-2B was a mixture of neutral, positive and negative charged regions. TPR1 and TPR3 of DNAJC7 were mainly positively charged at the TPR groove, while TPR2 was negatively charged (Figure 3.5, upper middle panels). DNAJC3 TPR1 domain was mainly neutrally charged at the groove, while

TPR2 and TPR3 (in particular) were negatively charged (Figure 3.5, lower middle panels). The presence of the carboxylate clamp residues results in a positively charged TPR groove that is responsible for the interaction with the negatively charged EEVD motif, ensuring a stable interaction (Scheufler *et al*., 2000). The lack of the positively charged groove in DNAJC3 TPR domains is at least partly due to the absence of the five residues forming the carboxylate clamp. The *in silico* mutation of DNAJC3 TPR domains to include the carboxylate clamp residues altered the electrostatic charge distribution drastically, especially for DNAJC3 TPR1 (Figure 3.5 lower panels). TPR1 of the mutated DNAJC3 had a positively charged groove, while the second TPR domain groove had a mixture of both positive and negative regions. TPR3 was still mainly negatively charged but the inner centre of the groove was neutral (Figure 3.5, lower panels). Comparing the mutated DNAJC3 TPR domains, the mutation of the five residues in DNAJC3 TPR1, altered the electrostatic charge distribution of the groove to closely resemble that of HOP TPR-1 and DNAJC7 TPR1 and 3, which all have positive TPR grooves. The mutation of TPR2 of DNAJC3 resulted in a domain with one side being negatively charged and the other positive; none of the other TPR domains exhibited this trait. After mutation, DNAJC3 TPR3 changed from being mostly negatively charged to having a slightly neutral TPR groove, similar to that of DNAJC7 TPR2.

The carboxylate clamp residues of a TPR domain are not only involved in creating the charged groove that ensures a stable interaction with an EEVD motif. Direct residue interactions in the form of hydrogen bonds occur between the side chains of the carboxylate clamp residues and EEVD motif residues (Scheufler *et al*., 2000). The orientation and charge of the carboxylate clamp residues were analyzed in relation to the EEVD motif by superimposing the resolved structure of HOP TPR1 in complex with the Hsc70 EEVD motif (1ELW, Scheufler *et al*., 2000) to that of DNAJC7 TPR1, DNAJC3 TPR1 and mutated DNAJC3 TPR1 (Figure 3.6). The orientation of the EEVD motif present in these structural alignments is therefore not a true representation of the orientation or placement of the EEVD in complex with the mentioned TPR domains, but was utilized to illustrate the general area or space the EEVD motif might occupy if in complex with the TPR domains. DNAJC3 TPR1 was selected for further analysis based on the electrostatic charge distribution results (Figure 3.5), where the mutation studies suggested that this domain was more similar to that of known Hsp70/90 interacting TPR domains.

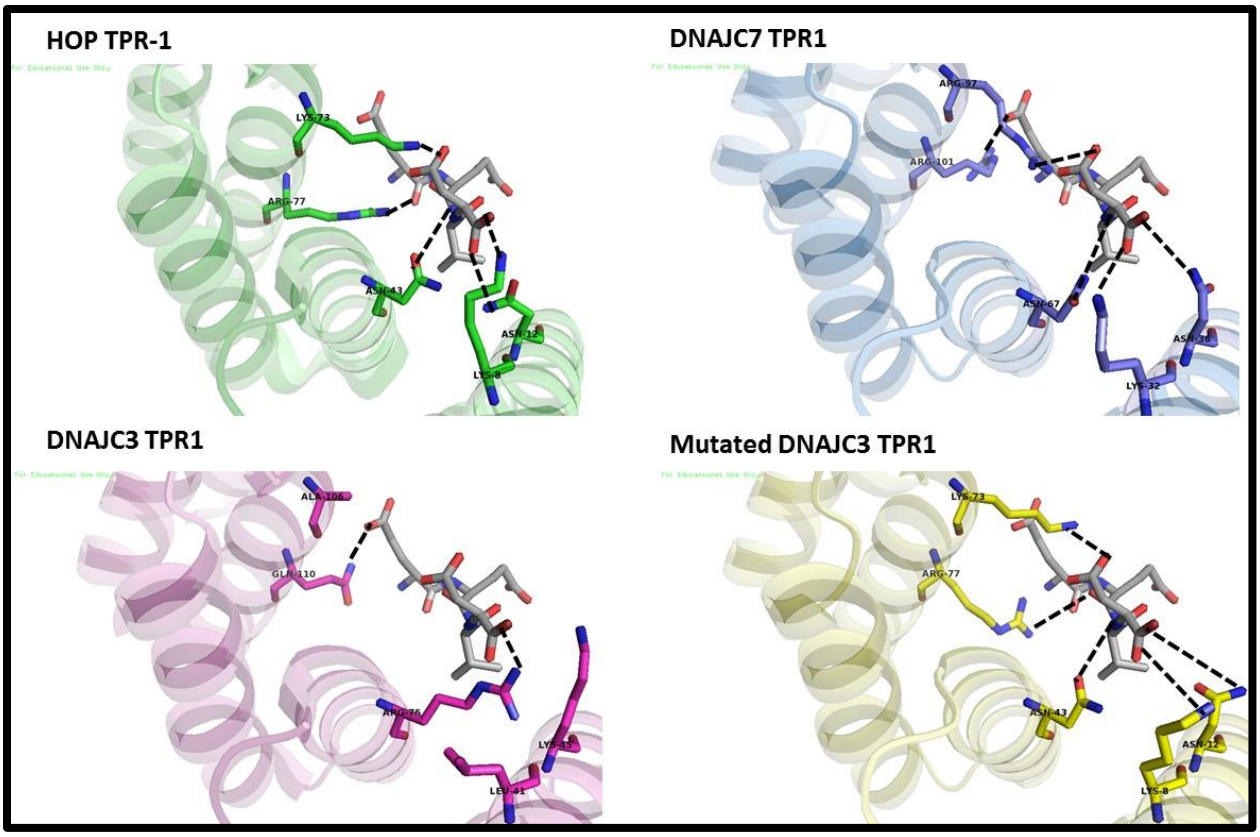

Figure 3.6: Analysis of the orientation and charge of the sidechain of the carboxylate clamp residues in complex with Hsp70 EEVD motif. Analysis was conducted aligning the resolved structure of HOP TPR1 in complex with Hsp70 EEVD motif (1ELW, green) to that of DNAJC7 TPR1 (blue), DNAJC3 TPR1 (purple) and mutated DNAJC3 TPR1 (yellow). The EEVD motif from Hsc70 (as in the 1ELW structure) is represented in grey sticks and the carboxylate residues or corresponding residues represented in stick form and black dotted lines represent hydrogen bonds.

The resolved structure of HOP TRP1 in complex with the EEVD motif of Hsp70 (Figure 3.6, shown in green) was used as the template to illustrate how the carboxylate clamp residues or equivalent residues of DNAJC7 TPR1 (blue), DNAJC3 TPR1 (purple) and mutated DNAJC3 TPR1 (yellow), would appear when in complex with the EEVD residues of Hsp70, as no resolved structures are available. Both HOP TPR1 and DNAJC7 TPR1 have been shown to have the conserved carboxylate clamp residues and, in the case of HOP, the charge of the side chains of those residues are known to form hydrogen bonds with the E, E and D residues of the EEVD motif, as well as interactions with residues upstream of the EEVD motif (Scheufler *et al*., 2000. Odunuga *et al*., 2003). Since DNAJC7 has been shown to interact with Hsp70 in a similar manner to HOP, the latter interactions are also likely for DNAJC7 (Brychzy *et al*., 2003). The bulk size of the carboxylate clamp residues (K, R), results in the residues being able to extend into the space where

the EEVD motif docks, permitting a physical interaction. The residues on DNAJC3 TPR1 (Figure 3.6, purple) that correspond to those of the carboxylate clamp residues are either too short and uncharged (A, V) or are polar but uncharged (Q). The consequence of differences is the lack of the ability to form hydrogen bonds with the EEVD motif that is required for the interaction. The mutation of the corresponding residue on DNAJC3 TPR1 to those that form the carboxylate clamp (Figure 3.6 yellow), resulted in the formation of hydrogen bonds with the EEVD motifs (data not shown). This suggested that the absence of these conserved residues at the exact positions in DNAJC3 TPR1 would not permit interaction with the EEVD motif. However, it should be noted that the mutation of DNAJC3 TPR2 and TPR3 to introduce the carboxylate clamp residues, did not infer the ability of these domains to form physical interactions with the EEVD motif (data not shown). Also the introduction of the mutations did not change the electrostatic charge distribution to that required for a stable interaction to occur, especially for TPR3 (Figure 3.5, lower panels). These results suggest that DNAJC3 TPR1 might be the only TPR domain to possibly interact with the EEVD motif, but only if the carboxylate clamp residues occurred naturally on the domain.

DNAJC3 TPR domains were predicted not to be able to interact with both Hsp70 and Hsp90 due to the absence of the carboxylate clamp residues, therefore additional analysis was conducted to identify possible alternative binding sites.

3.2.2.4 Repressor of DNAJC3, p88^{rIPK} ,shares limited structural homology with the charged linker region of both Hsp90 and Grp94 introducing a potential alternative binding site for DNAJC3 TPR domains

The ER homologues of Hsp70 and Hsp90, Grp78 and Grp94, respectively lack the EEVD motif that is required to interact with TPR domains (Argon and Simen, 1999, Fewell *et al*., 2004). The alignment of cytosolic and organelle Hsp90, Grp94 and TRAP1, demonstrates that Grp94 and TRAP1 lack the EEVD motif. GRP94 has the ER retention motif, KDEL instead, although Grp94 also has an EEVD-like motif upstream of the KDEL motif (Figure 3.7). However, whether this EEVD-like motif of Grp94 is able to interact with TPR domains has not been demonstrated.

DNAJC3 is usually inactive in the cell under normal conditions due to its association with its own repressor protein, p88^{rIPK}, which inhibits DNAJC3's inhibitory effects on PKR activity by binding to the seventh TPR motif via an unknown mechanism (Gale *et al*., 1998, 2002, Luig *et al*., 2010). Previous studies have shown that a region at the N-terminus of p88^{rIPK} shared limited structural homology with the charged linker region of Hsp90 (Gale *et al*., 1998). From the multiple sequence

alignment of Hsp90 isoforms, both Grp94 and the cytosolic Hsp90 isoforms have a charged linker region and this region is highly conserved (Figure 3.7).

The identified region on $p88^{rIPK}$ (86 – 200 amino acids) and the charged linker regions of Hsp90 (170 – 300 amino acids) and Grp94 (231 – 346 amino acids) (Figure 3.8, A) were aligned using Promals3D to determine whether $p88^{rIPK}$ shared structural homology with Grp94 (Figure 3.8, B). The alignment results illustrated a lack of primary sequence conservation between the three proteins as illustrated by the absence of numbers above the alignment representing the degree of conservation between aligned residues. However, the region of $p88^{rIPK}$ seemed to share some degree of structural homology with both Hsp90 and Grp94 as indicated by the red residues and the highlighted "h" under the alignment, which represent predicted alpha helical structures (Figure 3.8, B).

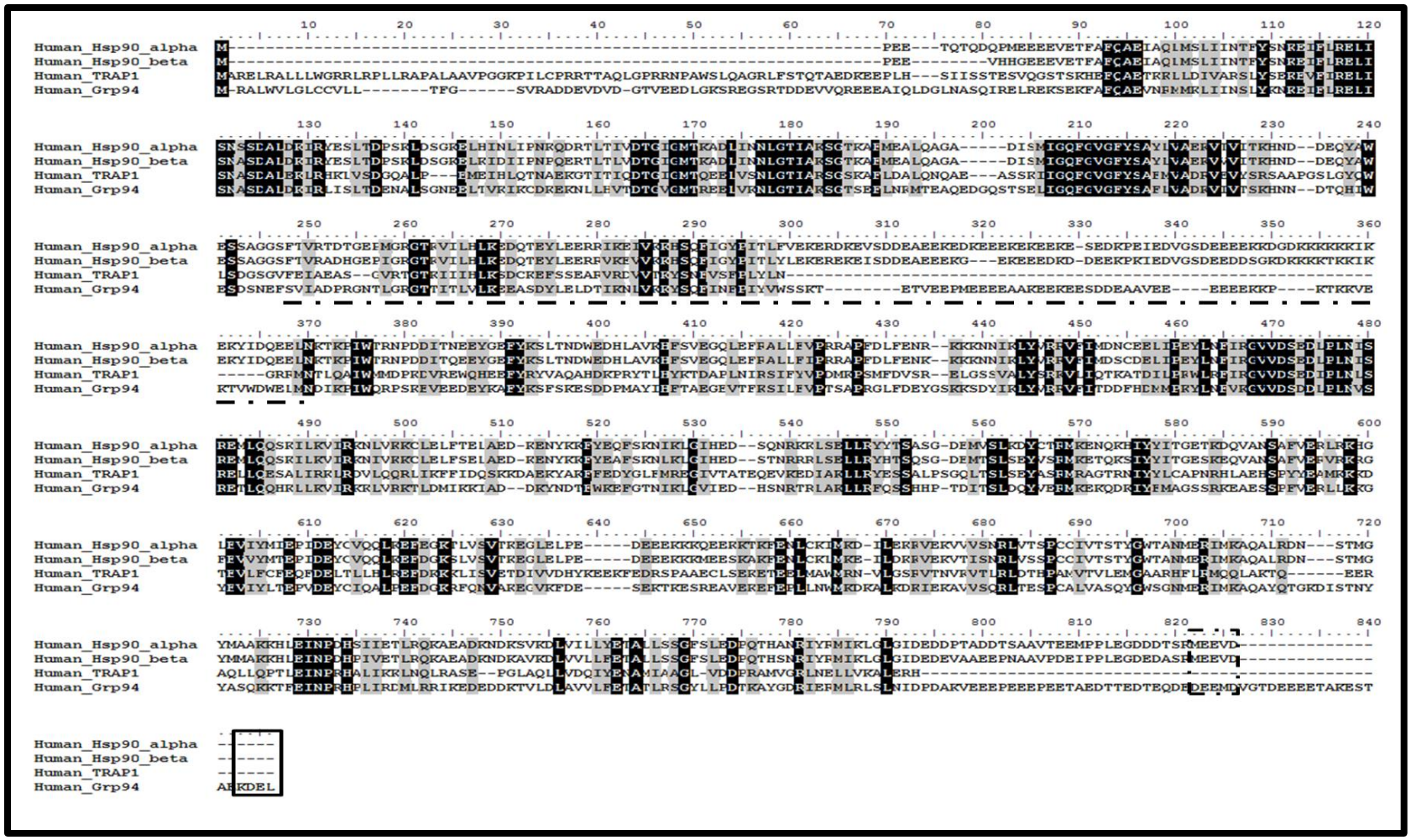

Figure 3.7: Multiple sequence alignment of Hsp90 protein sequences. Multiple sequence alignment generated by Promals3D and edited using BioEdit. Residues highlighted as follows: black shading represents identical residues and grey shading represents similar residues. The charged linker region is underlined by a dashed black line, the EEVD motif and EEVD-like motif in Grp94 is indicated by a dashed black box and the KDEL by a solid black box.

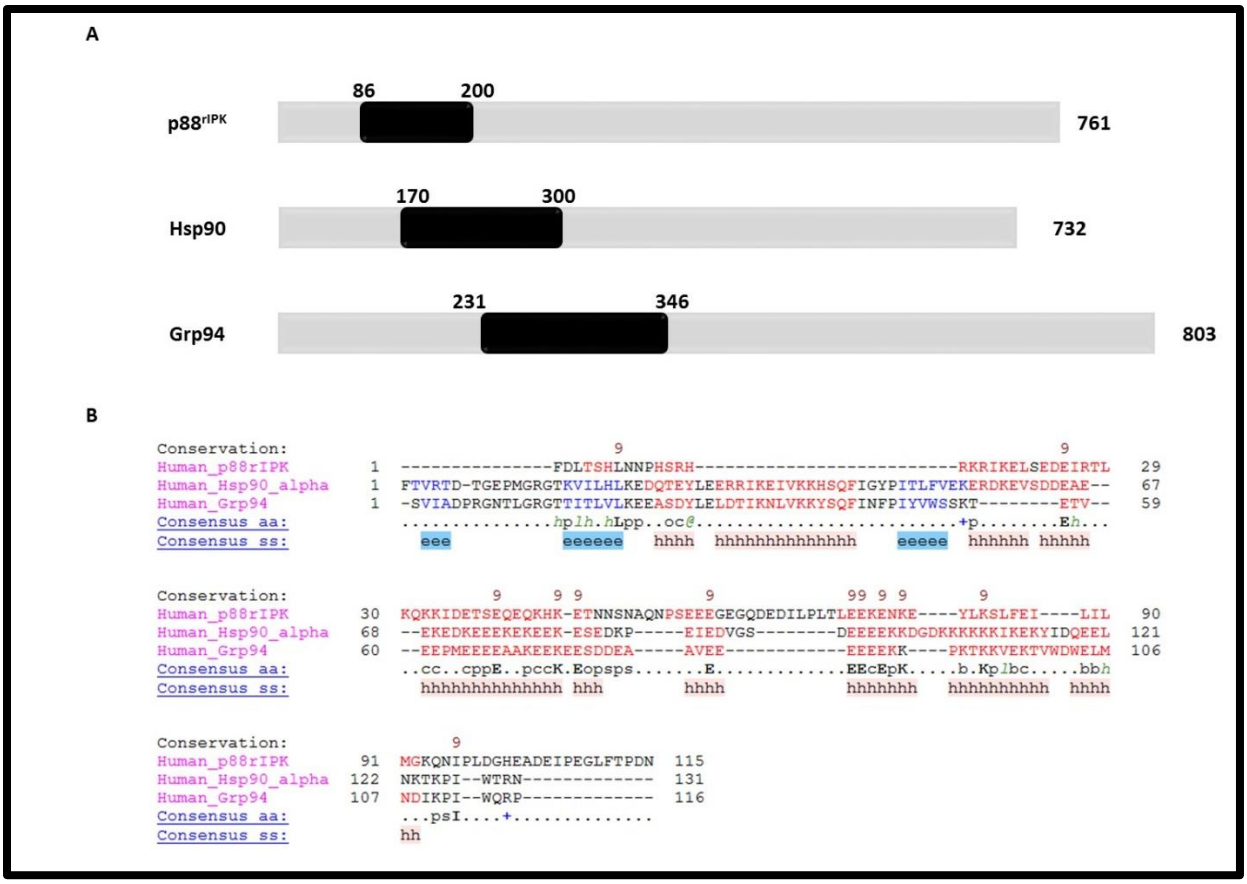

Figure 3.8: DNAJC3 inhibitor p88^{rIPK} shares limited structural homology with the charged linker regions of Hsp90 and Grp94. (A) Schematic representation of structural homology between p88^{rIPK}, Hsp90 and Grp94. The area highlighted in black indicates the region of p88^{rIPK} (residues 86 – 200) that shares limited homology with the charged linker region of Hsp90 (residues 170 – 300) and Grp94 (residues 231 – 346). (B) Multiple sequence alignment of p88^{rIPK} and the charged linker regions of Hsp90 and Grp94. Residues in blue (e highlighted in blue) and red (h highlighted in pink) represent beta sheets and alpha helices, respectively. Highly conserved residues are marked by bold uppercase letters, + represent positively charged residues, b represents bulky residues, h represents hydrophobic residues, l represents aliphatic residues p represents polar residues, c represents charged residues, s represents small residues, o represents alcohol residues and the number above the residues represent degree of conservation.

3.2.2.5 Analysis of DNAJC3 TPR domains and structural homologues

The bioinformatics analyses conducted on the TPR domains of DNAJC3, suggested that the domains cannot interact with the EEVD motifs of Hsp90 and Hsp70 due to the absence of the carboxylate clamp forming residues. We therefore conducted analysis into deducing possible alternative functions of the three TPR domains of DNAJC3 based on structural information. Structural homologues of each TPR domain were identified using the HHpred server. Majority of identified homologues have functions independent of Hsp90 and Hsp70 such as peptidyprolyl isomerase, PEX-5, PEX-related protein, MamA, PcrH and SycD. However, known co-chaperones

of Hsp90 and Hsp70, HOP and SGT were also identified as structural homologues of DNAJC3 TPR domains (Table 3.2).

The first analysis conducted was multiple sequence alignment using Promals3D, alignment was conducted for each DNAJC3 TPR domain and its identified structural homologues (Figure 3.9, 3.10, 3.11).

Table 3.2: Summary of the identified structural homologues of DNAJC3 TPR domains

PDB ID	Protein name	Function	Reference
1A17	PP5	Serine/threonine phosphatase protein, responsible for the dephosphorylation of various proteins, ensuring the regulation of numerous cellular processes.	Barford, 1996, Das *et al.*, 1998
1ELR	HOP TPR-2A	TPR domain in HOP known to interact with Hsp90	Scheufler *et al*., 2000, Odunuga *et al*., 2003, Southworth and Agard, 2011, Lee *et al*., 2012
1ELW	HOP TPR-1	TPR domain in HOP known to interact with Hsp70	Scheufler *et al*., 2000, Southworth and Agard, 2011, Lee *et al*., 2012
1HXI	PEX-5	Receptor involved in protein import into the peroxisomal matix.	Schliebs *et al*., 1999, Kumar *et al*., 2001
1ZU2	TOM20	Importer receptor involved in the import of proteins from the cytosol into the mitochondria	Lithgow *et al*., 1995, Perry *et al*., 2006
2C2L	CHIP	Ubiqutin protein ligase, known to modulate the chaperone activity of Hsp90 and Hsp70	Ballinger *et al*., 1999, Zhang *et al*., 2005
2LNI	HOP TPR-2B	Third TPR domain in HOP, function unknown but though to contribute to the dimerization of HOP	Longshaw *et al*., 2009, Southworth and Agard, 2011, Lee *et al*., 2012, Tang *et al*., Unpublished (pdb structure)
2VGX	SycD	Cytosolic protein necessary for the secretion of the YopE and YopH proteins in Yersinia	Woestyn *et al*., 1996, Neyt and Cornelis, 1999, Büttner *et al*., 2008, Schreiner and Neimann, 2012
2XCB	PcrH	Pseudomonas translocator chaperone	Job *et al*., 2010
3RKV	Peptidylprolyl isomerase	Known to catalyze the *cis-trans* isomerisation of proline peptide bonds in folded and unfolded proteins	Fischer *et al*., 1989, Osipuik *et al*., Unpublished (pdb structure)
3SZ7	SGT	Known to interact and modified by parvovirus non-structural proteins	Cziepluch *et al*., 1998, Chartron *et al*., 2011
3VTX	MamA	Involved in controlling the assemble of biomineralized magnotosomes in magnetotatic bacteria	Zeytuni *et al*., 2011
4EQF	PEX-5 related protein	Accessory subunit for the hyperpolarization-activated cyclic nucleotide-gate (HCN) channels	Santoro *et al*., 2011, Bankston *et al*., 2012
4GA2	E3 SUMO-protein ligase	Involved in the SUMOylation of various proteins	Chu and Yang, 2011, Kussube *et al*., 2012

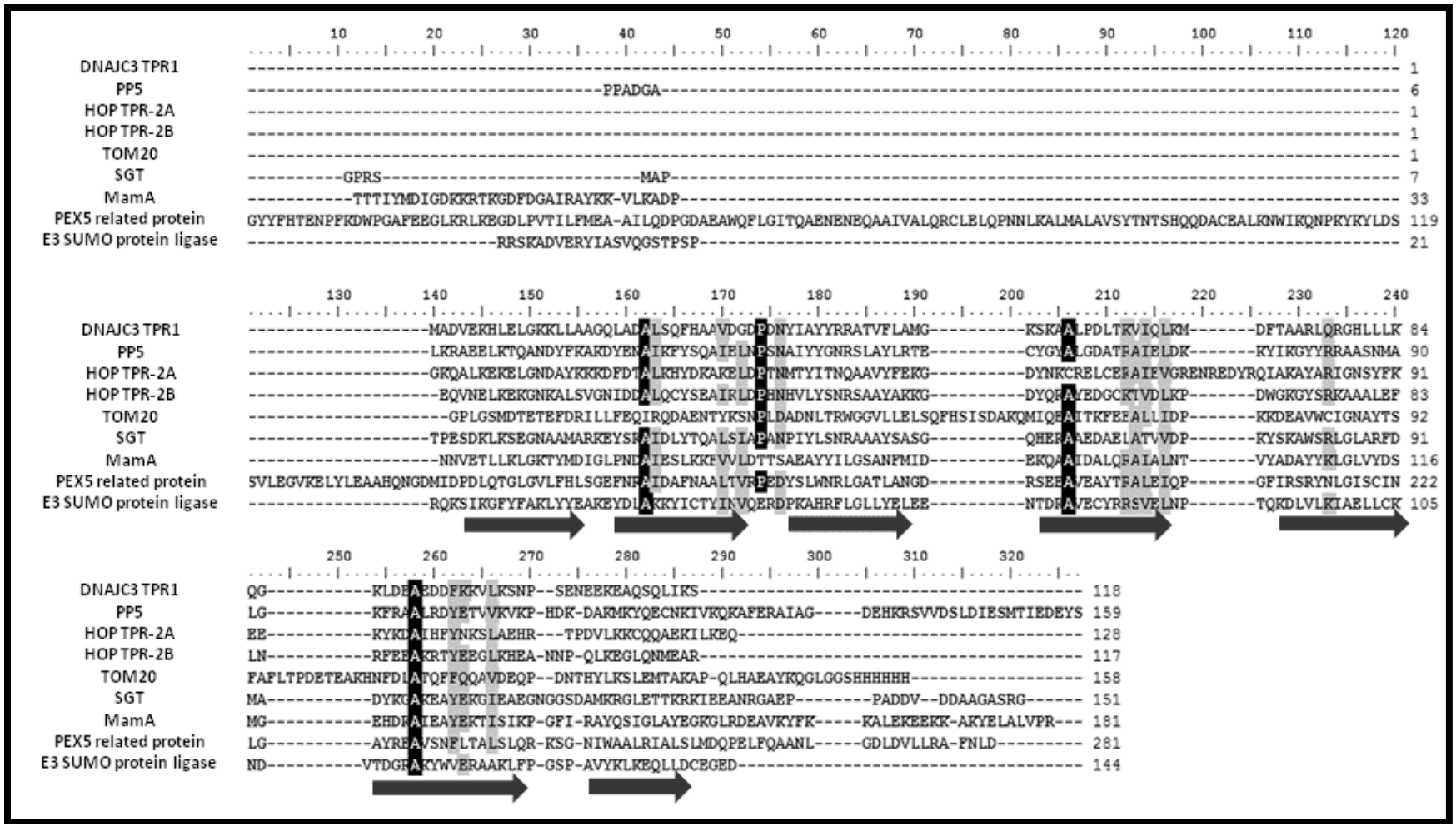

Figure 3.9: Promals3D multiple sequence alignment of DNAJC3 TPR1 and structural homologues retrieved from HHPred. Multiple sequence alignment of DNAJC3 TPR1 and homologues: 1A17 (PP5), 1ELR (HOP TPR-2A), 1ELW (HOP TPR-1), 1ZU2 (TOM20), 3SZ7 (SGT), 3VTX (MamA) and 4EQF (PEX-related protein) and 4GA2 (E3 SUMO-protein ligase). Black and grey highlight identical and similar amino acids, respectively. The black arrows represent predicted helical secondary structure.

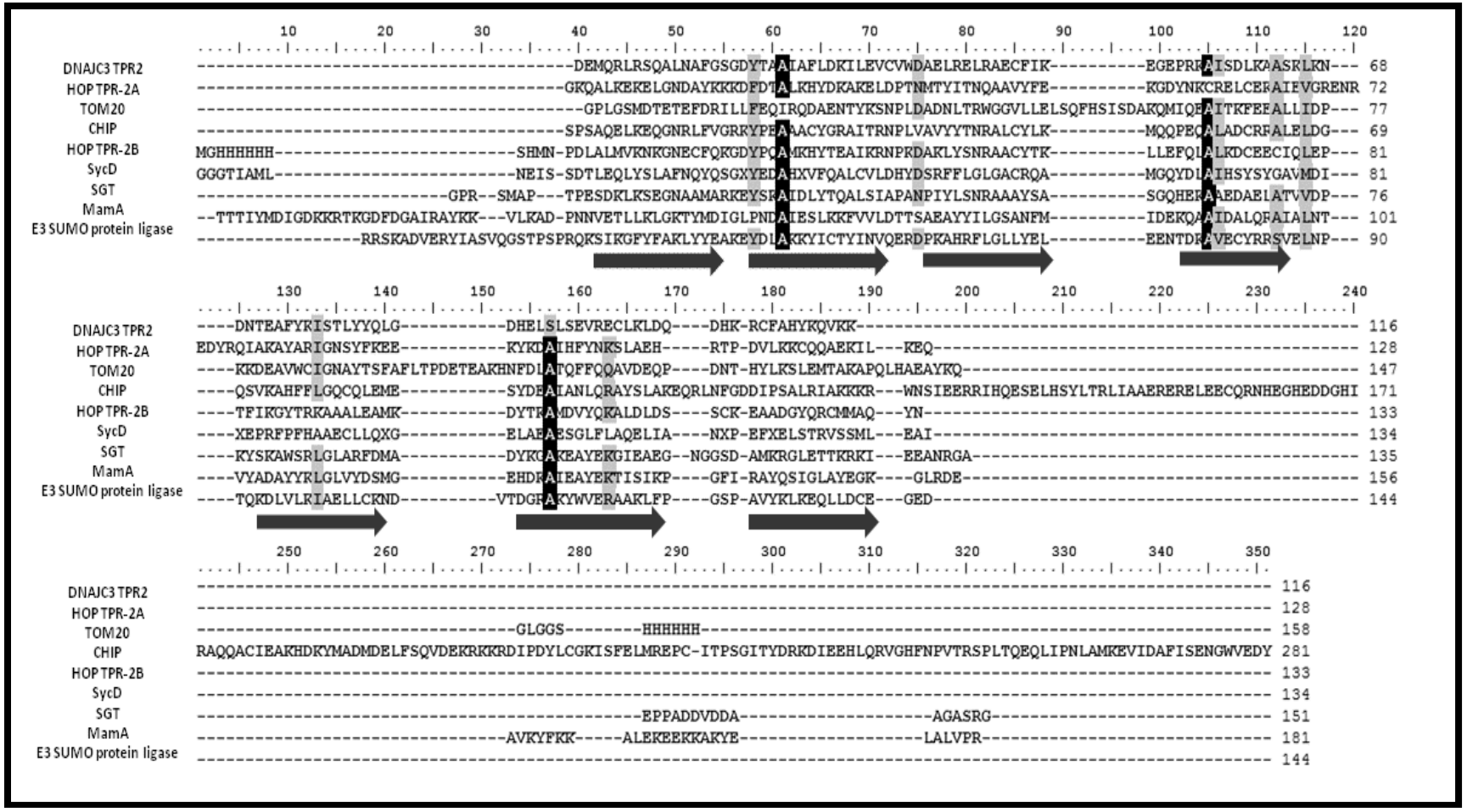

Figure 3.10: Promals3D multiple sequence alignment of DNAJC3 TPR2 and structural homologues retrieved from HHPred. Multiple sequence alignment of DNAJC3 TPR2 and homologues: 1ELR (HOP TPR-2A), 1ZU2 (TOM20), 2C2L (CHIP), 2LNI (HOP TPR-2B), 2VGX (Chaperone SycD), 3SZ7 (SGT), (3VTX MamA) and 4GA2 (E3 sumo-protein ligase). Black and grey highlight identical and similar amino acids, respectively. The black arrows represent predicted helical secondary structure.

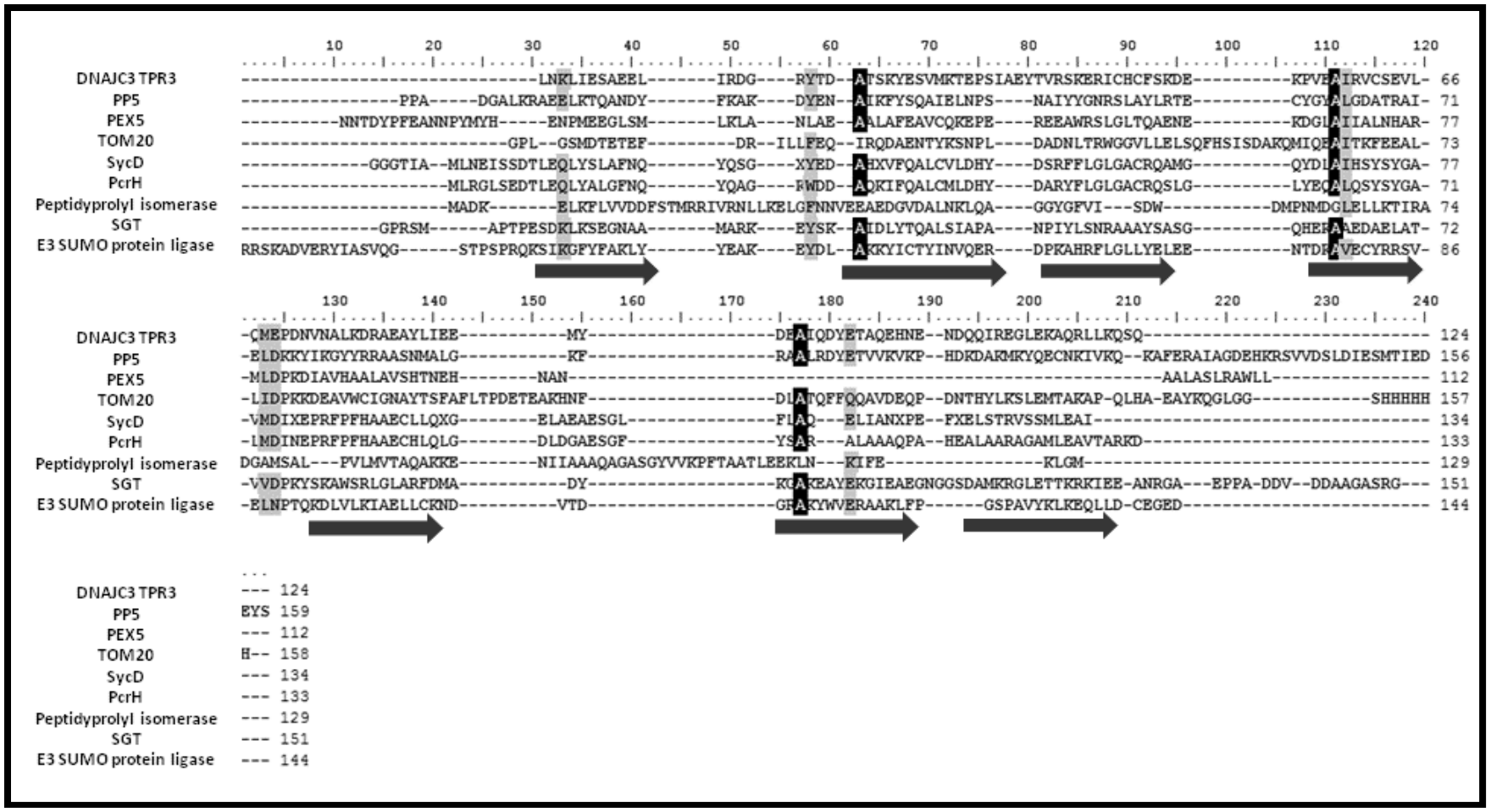

Figure 3.11: Promals3D multiple sequence alignment of DNAJC3 TPR3 and structural homologues retrieved from HHPred. Multiple sequence alignment of DNAJC3 TPR3 and homologues: 1A17 (PP5), 1HX1 (PEX-5), 1ZU2 (TOM20), 2VGX (Chaperone SycD), 2XCB (Regulatory protein PcrH), 3RKV (Peptidyprolyl isomerase), 3SZ7 (SGT), 4GA2 (E3 sumo-protein ligase). Black and grey highlight identical and similar amino acids, respectively. The black arrows represent predicted helical secondary structures.

Multiple sequence alignment was conducted to determine sequence conservation between DNAJC3 TPR domains and their identified structural homologues. Sequence conservation could indicate similarities between DNAJC3 TPR domains and structural homologues absent in the alignment previously conducted with known co-chaperones of Hsp90 and Hsp70 (Figure 3.4). Some of the identified homologues (PP5, HOP TPR-1 and HOP TPR-2A), had previously been aligned with DNAJC3 TPR domains. It was pertinent to determine whether the presence of additional TPR-containing proteins with different functions could alter the alignment and illustrate sequence similarities that were not detected in the previous alignments. Similar to the previous analysis, there was no sequence conservation observed (Figure 3.9, 3.10, 3.11). However, the alignment indicated that the sequences seemed to be grouped in large clusters followed by smaller ones. Promals3D results output identified these clusters as alpha helices (black arrows, Figure 3.9, 3.10, 3.11), suggesting that there was conservation of the proteins at the secondary structure level, despite the lack of identity or similarity at the primary sequence level. The absence of sequence conservation or similarity observed in this analysis was similar to that found in literature. TPR domains are known to not share sequence conservation or similarity with the exception of the TPR motif consensus sequence (D'Andrea and Regan, 2003). In light of this observation, it was decided to analyze conservation at secondary and tertiary structure level. Structural alignments of the putative structural homologues to DNAJC3 TPR domains was conducted, analyzed and visualized in Pymol. The root mean square deviation (RMSD) value obtained for each structural alignment is also illustrated (Figure 3.12, 3.13, 3.14).

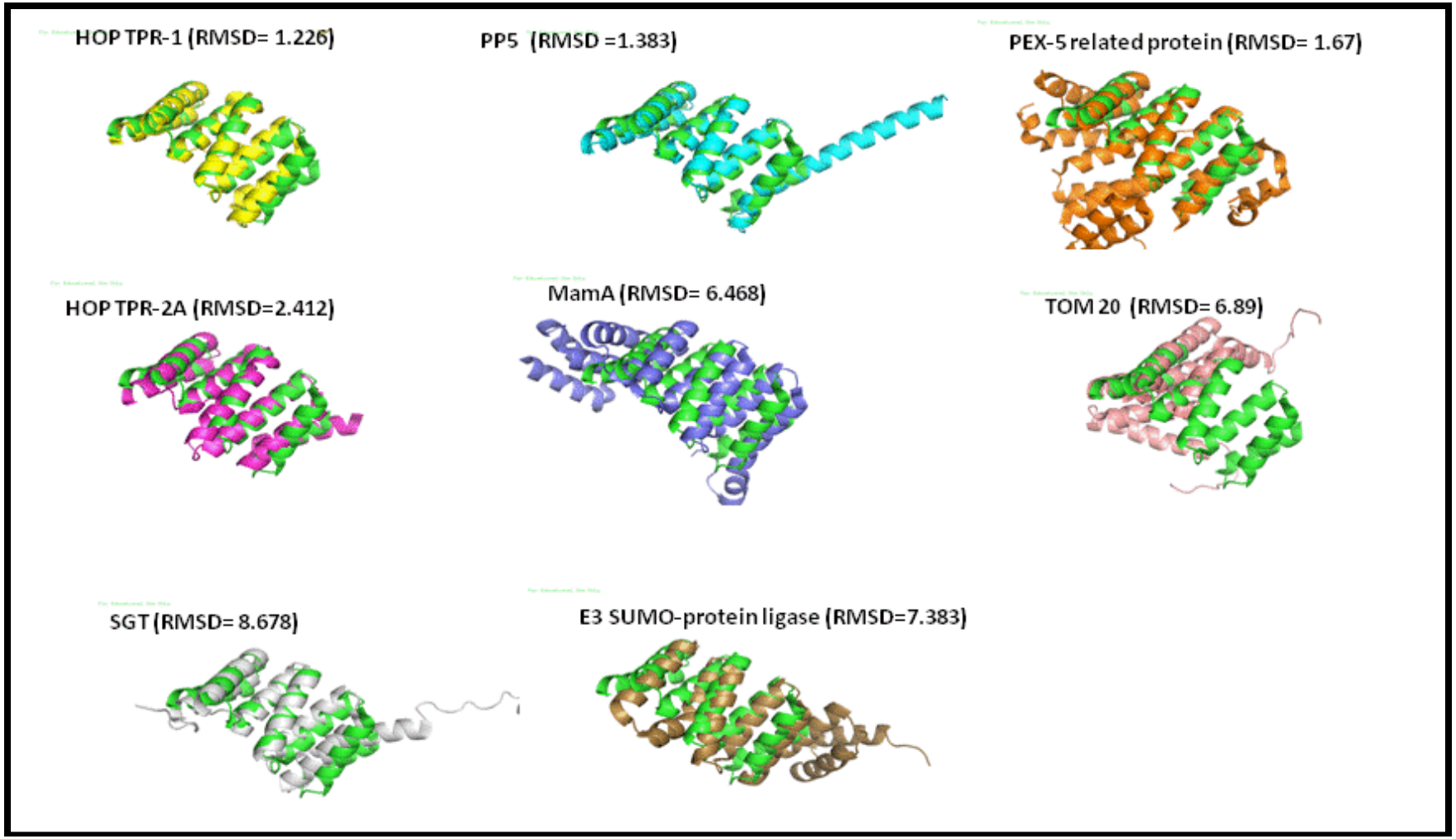

Figure 3.12: Structural alignment of HHpred identified homologues and DNAJC3 TPR1 domain in Pymol. DNAJC3 TPR1 domain (green) and structural homologues: PP5/ 1A17 (light blue), HOP TPR-1/ 1ELW (yellow), SGT/3SZ7 (grey), MamA/3VTX (blue), PEX-5 related protein/4EQF (orange), TOM20/1ZU2 (pink), E3 SUMO-protein ligase/4GA2 (sand) and HOP TPR-2A/1ELR (light purple). The RMSD value for each alignment is also presented with the structural alignment.

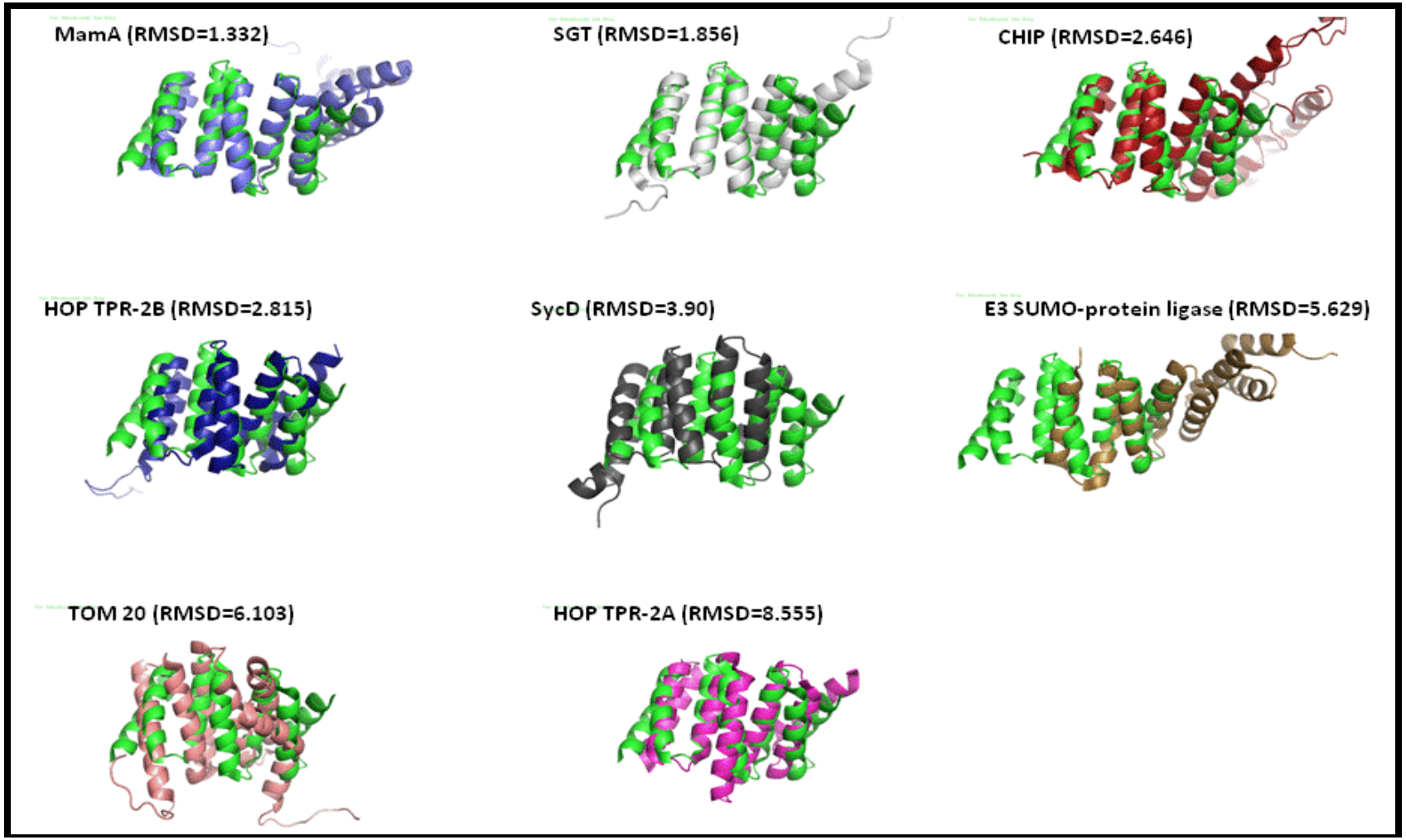

Figure 3.13: Structural alignment of HHpred identified homologues and DNAJC3 TPR2 domain in Pymol. DNAJC3 TPR2 (green) and structural homologues: TOM20/1ZU2 (pink), HOP TPR-2A/1ELR (light purple), CHIP/2C2L (maroon), HOP TPR-2B/2LNI (dark blue), chaperone SycD/2VGX (dark grey), SGT/3SZ7 (grey), MamA (blue) and E3 SUMO-protein ligase/4GA2 (sand). The RMSD value for each alignment is also presented with the structural alignment.

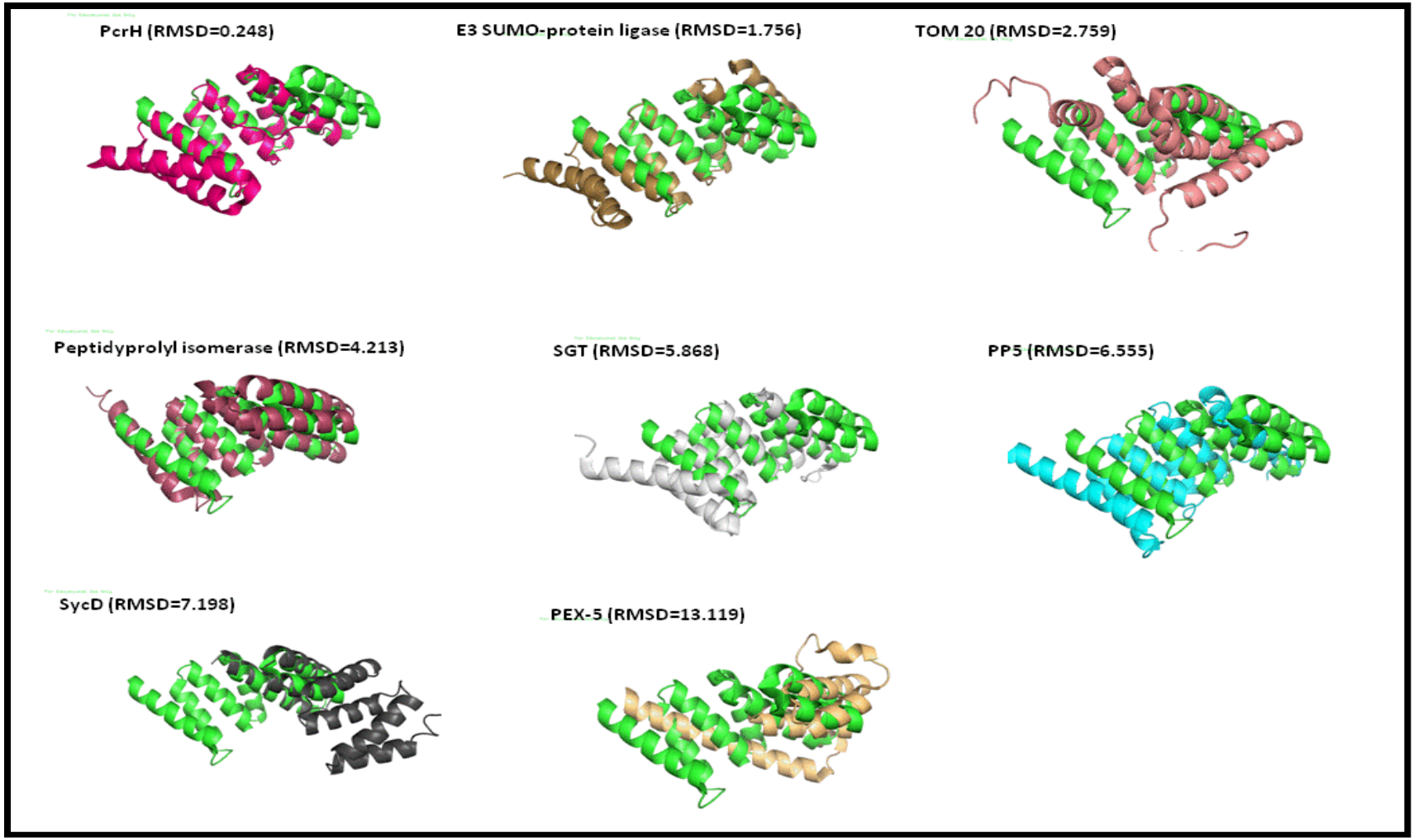

Figure 3.14: Structural alignment of HHpred identified homologues and DNAJC3 TPR3 domain in Pymol. DNAJC3 TPR3 (green) and structural homologues: PP5/1A17 (light blue), TOM20/1ZU2 (pink), chaperone SycD/2VGX (dark grey), regulatory protein PcrH/2XCB (magenta), peptidylprolyl isomerase/3RKV (dark pink), SGT/3SZ7 (grey), E3 SUMO-protein ligase/ 4GA2 (sand) and PEX-5/1HXI (peach). The RMSD value for each alignment is also presented with the structural alignment.

When a structural alignment is conducted between two structures, a root mean-square deviation (RMSD) value is generated as an indicator of structural similarity. The RMSD is a quantitative measurement of the similarity between equivalent atoms from two protein structures (Carugo and Pongor, 2001). RMSD values of 0 indicates identical structures or a good alignment, while an increase in the value represents structural differences between molecules (Carugo and Pongor, 2001).

Out of the eight structural homologues of DNAJC3 TPR1, HOP TPR-1 and STG displayed the lowest and highest RMSD value of 1.226 and 8.555, respectively (Figure 3.12). For DNAJC3 TPR2, MamA (1.332) and HOP TPR-2A (8.555) displayed the highest and lowest RMSD values (Figure 3.13), while PcrH (0.248) and PEX-5 (13.119) had the highest and lowest RMSD values, respectively out of DNAJC3 TPR3 identified homologues (Figure 3.14).

Although the RSMD value is considered a dependable measurement of structural similarity between aligned structures, visual analysis of the alignment also needs to be considered to ensure that RMSD value is a true representation of the alignment. RMSD values generated during the alignments are influenced by the number of alpha carbon atoms aligned between the structures (Carugo and Pongor, 2001). If few atoms are aligned, the RMSD generated might be closer to 0 which could give the false impression that the two structures align perfectly, whilst only a small portion of the structures align and the majority of the structures are not aligned or have poor alignment. In contrast, although a RMSD value greater than 5 usually represents poor alignment, depicting poor alignment of the overall structure, visual analysis might be able to identify small regions within the alignment that are significant to the study and may have been missed if considering the RMSD value alone. Structural analysis was conducted and presented using Pymol (Figure 3.12, 3.13, 3.14).

DNAJC3 and structural homologues TPR domains are made up of alpha helices joined by short loops, with the only difference between the structures being the number and length of the different helices (Figure 3.12, 3.13, 3.14). This observation coincides with the known structural features of TPR motifs, where each motif is arranged as a helix turn helix structure (D'Andrea and Regan, 2003). The structures with the least structural alignment to DNAJC3 TPR1 based on visual analysis were MamA, PEX-5 related protein, TOM20 and SGT (Figure 3.12). The best alignment was observed for the co-chaperones PP5 and HOP TPR-1, while the alignment for E3 SUMO-protein ligase and HOP TPR-2A were considered acceptable (Figure 3.10). Visual analysis of DNAJC3

TPR2 and homologue alignment (Figure 3.13), illustrated that, while all the alignments were poor, HOP TPR-2A, HOP TPR-2B and MamA, had better structural alignment to DNAJC3 TPR2, while TOM20, SycD and SGT had the worst alignment (Figure 3.13). Unlike the other domains, DNAJC3 TPR3 had only two homologues that showed acceptable structural alignment, PcrH and E3 SUMO-protein ligase, although only a small part of the structures aligned (Figure 3.14). The remaining homologues showed little to no alignment to DNAJC3 TPR3, as illustrated by the absence of any contact between the two structures (Figure 3.14). When compared, the RMSD values and visual structural alignment results seemed to correlate in terms of best and worst alignments, although there were some discrepancies between the RMSD value and the visual analysis.

3.2.2.6 Electrostatic potential analysis of identified structural homologues of DNAJC3 TPR domains

Subsequent to the structural alignment results (section 3.2.2.5), electrostatic potential analysis was conducted on identified homologues, as electrostatic charge distribution is known to participate in protein-protein interaction between TPR domains and substrates. Electrostatic potential analysis was conducted in a manner similar to that described in section 3.2.2.5. Analysis was focused on the groove of the TPR domain (Figure 3.15). The electrostatic charge distribution of the analysed TPR domain grooves varied vastly (Figure 3.5). TOM20, PEX-5, PEX-5 related protein, SycD and regulatory protein PcrH had had negatively charged grooves, while SGT, HOP TPR-1/2A, E3 SUMO-protein ligase and PP5 had positively charged TPR grooves and MamA and HOP TPR-2B were the only proteins with TPR grooves that were mainly neutral (Figure 3.5). It was observed that HOP TPR-1/2A, SGT, PP5, and CHIP, which are known co-chaperones of Hsp90 and Hsp70, possessed positively charged grooves. Based on electrostatic potential analysis, DNAJC3 TPR1 was found to be more similar to HOP TPR-1, while DNAJC3 TPR3 was most similar to TOM20 and PcrH. However, none of the electrostatic distribution patterns of structural homologues resembled that of DNAJC3 TPR2. Overall, based on the electrostatic charge potential analysis and structural alignment (visual analysis and RMSD value), HOP TPR-1, MamA and PcrH were thought to be more similar to DNAJC3 TPR1, TPR2 and TPR3, respectively (Figure 3.16). These results suggested that DNAJC3 TPR domains may function in a similar manner to the identified structural homologues. It was also interesting to note that for DNAJC3 TPR2 and TPR3, the homologues identified to be most similar have functions independent of Hsp90 and Hsp70.

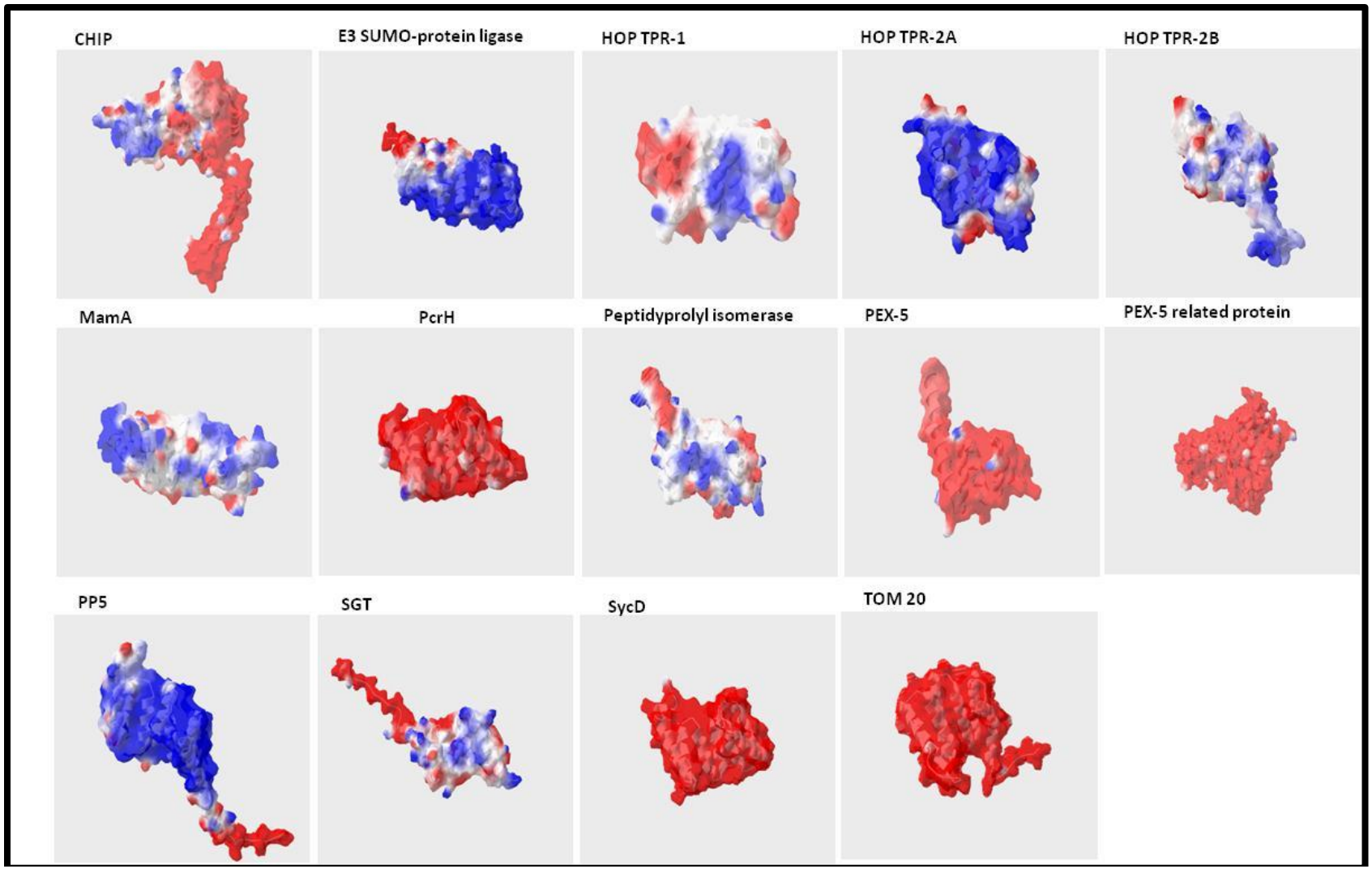

Figure 3.15: Electrostatic potential analysis of DNAJC3 TPR domains structural homologues. Red represents negative charged regions, white represents neutral regions and blue represents positively charged regions.

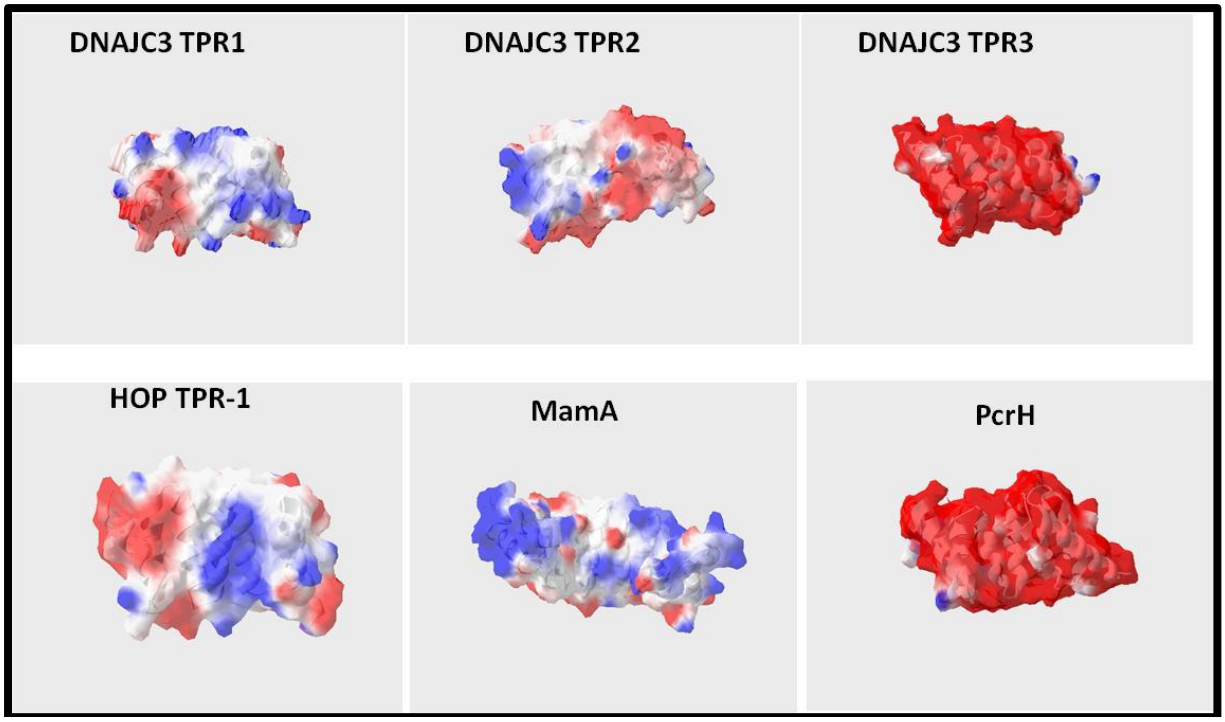

Figure 3.16: DNAJC3 TPR domains are more similar to TPR-containing proteins that have independent functions to Hsp90 and Hsp70, with the exception of DNAJC3 TPR1. Red represents negatively charged regions, white represents neutral regions and blue represents positively charged regions of the protein.

3.3 Discussion

Analysis of DNAJC3 from various species through multiple sequence alignment and phylogenetic analysis revealed that the protein was highly conserved, although that of species from the insect and plant families were least similar to that of mammals, with sequence similarity as low as 45 % and 30 %, respectively. Although, there were differences found in the DNAJC3 proteins from various species, it was noted that the structural arrangement of the protein domains was highly similar. This high degree of structural conservation could suggest functional similarity of the protein within different species. Motif identification of DNAJC3 identified an ER signal peptide at the N-terminus, eight TPR motifs in the middle and a J domain at the C terminus, similar to the findings of Kampinga and Craig (2004), although most literature list the number of TPR motifs as nine (Tao *et al*., 2010 and Svärd *et al*., 2011). The discrepancy in the number of TPR motifs could be linked to the middle TPR domain. Each TPR motif is made up of two helical structures and a TPR domain made up of three or more TPR motifs. When looking at the structure of DNAJC3, the middle domain was only composed of five helical structures and the sixth helical structure usually counted as part of this domain is an extended helix between the first and middle TPR domains. This extended helix has been shown to function more as stabilizing, solubilizing or capping helix at the C terminus of a TPR

domain. Although first discovered in PP5, it has been shown that the extended helix is not unique to PP5 but has been seen in almost all TPR structures resolved to date (D'Andrea and Regan, 2003). This possibly suggests that DNAJC3 has only two functional domains, TPR1 and TPR3, since they are made up of three TPR motifs, which is one of the requirements for a TPR domain to be considered functional (Lamb *et al*., 1995). This suggested that DNAJC3 TPR2 might function more as a linker region responsible for structural flexibility rather than a functional domain and could explain how an elongated protein like DNAJC3 could possibly pass substrates bound by TPR1 to Grp78 during its co-chaperoning activities (Tao *et al*., 2010). However, even though TPR2 of DNAJC3 could possibly be non-functional, it can still be involved in protein-protein interactions, as TPR motif 6 has been shown to be the possible binding site for PKR during the inhibitory function of DNAJC3 during viral infection (Gale *et al*., 1996).

Multiple sequence alignment of the three identified DNAJC3 TPR domains with TPR domains of known Hsp90 and Hsp70 co-chaperones (Figure 3.4), revealed that although DNAJC3 TPR domains contained the majority of the TPR consensus sequence (D'Andrea and Regan, 2003), conserved residues necessary for the formation of the carboxylate clamp involved in the protein-protein interaction with the EEVD of Hsp90 or Hsp70 and Hsp90 and Hsp70 specificity residues (Scheufler *et al*., 2000, Odunuga *et al*., 2003), were absent. Tao *et al*. (2010) found similar results when they aligned mouse DNAJC3 TPR domains to that of HOP TPR-1, TOM70, PP5 and CHIP (Tao *et al*., 2010). The carboxylate clamp residues have been shown to be necessary for the formation of a positively charged TPR groove that is needed to for stable interactions with the EEVD motif as the clamp residues are involved in direct physical contact with the EEVD motif through hydrogen bonds (Scheufler *et al*., 2000 and Odunuga *et al*., 2003).

Electrostatic potential analysis showed that similar to the analysis conducted by Tao *et al*., (2010) the groove of DNAJC3 TPR1 was mainly neutral, while both TPR2 and three grooves were negatively charged (Figure 2. 5) suggesting that the absence of a positively charge groove prevented DNAJC3 TPR domains from creating the necessary environment needed to form a stable interaction with the EEVD motifs. Also, the absence of the carboxylate clamp residues would prevent the formation of physical contact in the form of hydrogen bonds between DNAJC3 TPR domains, due to the clamp corresponding residues being mostly uncharged and in addition, the size of the side chains lacked the bulk of the clamp residues preventing the residues from protruding further into the region were the interaction occurred (Figure 3.6). However, when the corresponding clamp residue on DNAJC3 TPR domains were mutated to

carboxylate clamp residues, the electrostatic potential distribution of DNAJC3 TPR1 changed to resemble that of HOP TPR-1, containing a positively charge groove in the middle, and also the charge and bulky size of the mutated residues extend into the space where the EEVD motif was docked, increasing the chances of a physical interaction occurring. Since the positive charge of HOP TPR-1 groove is known to play a vital role in the interaction with the negatively charges EEVD motif of Hsp70 (Kajander *et al*., 2009), the change in the groove of DNAJC3 TPR1 to resemble that of HOP TPR-1 might suggest that the mutated domain has the potential to interact with the EEVD motif.

Since the Hsp70 and Hsp90 ER homologues, Grp78 and Grp94, are known to lack the EEVD motif at the C-terminus, the absence of the carboxylate forming clamp residues might be a direct response and an adaptation for DNAJC3 to form other interactions with Grp78 and Grp94 that do not involve the EEVD motif. Alternatively, the absence of those residues suggested that the TPR domains of DNAJC3 might be adapted for protein-protein interactions that might be not be linked to co-chaperoning activity. However, the charged linker regions of Hsp90 has been shown to share limited structural homologue with the N terminal region of $p88^{rIPK}$, the natural repressor of DNAJC3 (Gale *et al*., 2002) and this study extended that known observation to include the linker region of Grp94 (Figure 3.8, B).This may be a possible alternative binding site between Hsp90 or Grp94 and DNAJC3 TPR domains which is independent of the EEVD motif and carboxylate clamp forming residues. Full length DNAJC3 has been shown to be part of a complex with Grp94 through a pull down assay (Jansen *et al*., 2012), but whether this is due to a direct or indirect interaction remains unclear.

The lack of sequence conservation or similarity between DNAJC3 TPR domains and known TPR co-chaperones suggests that the DNAJC3 TPR domains might be involved in protein-protein interactions independent of Hsp90 or Hsp70. Multiple sequence alignment of DNAJC3 TPR domains and TPR-containing structural homologues highlighted the lack of sequence conservation or similarity, however when structural alignment was conducted, conservation was observed in the helical structure of the TPR domain as previously shown within all TPR domains (D'Andrea and Regan, 2003). Although all TPR domains are known to have a helical structure, structural alignment, along with the RMSD values, also identified HOP TPR-1, MamA and the regulatory protein, PcrH as the homologues with the highest degree of structural similarity to DNAJC3 TPR1, 2 and 3, respectively.

Several studies have indicated that certain protein-protein interactions involving TPR domains were mediated by the electrostatic distribution on the surface of the proteins, as seen in the case of interactions between TPR domains and Hsp90/70 EEVD motifs. When compared to the

electrostatic potential of the structural homologues, DNAJC3 TPR1 domain was mostly similar to HOP-TPR-1, the TPR domain on HOP known to interact with the EEVD motif of Hsp70 (Scheufler *et al*., 2000, Odunuga *et al*., 2003). The electrostatic potential of DNAJC3 TPR2 was found to be more similar to that of MamA, an adaptor protein involved in controlling the assembly of biomineralized magnotosomes in magnetotatic bacteria (Zeytuni *et al*., 2011), suggesting it functions as a scaffolding protein. The electrostatic potential of DNAJC3 TPR3, which was mainly negative, was found to be similar to a large array of the analyzed structural homologues. The electrostatic distribution pattern of the latter was similar to that of PEX-5, TOM20, PcrH, SycD and PEX-5 related protein. Since the function and interacting partners of the listed proteins varies immensely, which hints at a large array of potential binding partners for DNAJC3 TPR3. Based on structural alignment, RMSD values and electrostatic potential distribution, PcrH was found to be most similar to DNAJC3 TPR3. PcrH is known to function as a chaperone for translocator proteins PopB and PopD, the end result being a functional translocon that ensures efficient substrate translocation (Page and Parsot, 2002, Parsot *et al*., 2003). Since DNAJC3 is known to translocate from the cytosol to the ER lumen, the presence of a TPR domain such as TPR3, that is highly similar to translocator TPR proteins, could suggest that DNAJC3 might also function as a chaperone for translocator proteins that are involved in the translocation of substrates from the cytosol to the ER lumen. However, no studies have been conducted to determine whether DNAJC3 can function as a chaperone, independent of Hsp70 and or Hsp90 nor have there been reports of additional functions and binding properties of its TPR domains.

Chapter 4: Development of bacterial systems to over-express DNAJC3 and other chaperones for functional studies.

4.1 Introduction

Similar to other DNAJ proteins, the J-domain of DNAJC3 has been shown to be able to stimulate the ATPase activity of Grp78 during UPR caused due to ER stress, where it helps to restore ER homeostasis (Oyadomari *et al*., 2006, Rutkowski *et al*., 2007, Tao *et al*., 2010; Svärd *et al*., 2011). DNAJC3 also stimulates the ATPase activity of Hsp70 during Influenza virus infection (Melville *et al*., 1999). In addition, although DNAJC3 is known to also have three functional TPR domains, at present a proposed function for these domains is limited to TPR1, which is thought to interact with denatured proteins (Tao *et al*., 2010 and Svärd *et al*., 2011). In order to elucidate additional functions of DNAJC3 TPR domains, recombinant proteins were required. Hence, the main aim of this chapter was to engineer bacterial constructs for the expression of DNAJC3 for utilization in biophysical characterization analysis. The objectives were to:

- Construct bacterial expression systems for DNAJC3
- Overexpress and purify GST-tagged DNAJC3FL and DNAJC3dJ protein
- Overexpress and purify of chaperone proteins for interaction studies

4.2 Results

4.2.1 Cloning, overexpression and purification of GST-tagged DNAJC3 recombinant proteins

In order to generate GST-tagged DNAJC3FL and DNAJC3dJ bacterial expression vectors, from mammalian expression vectors, the mP58.FL1-pCDNA3 (Addgene, 21883) and mP58.dJ1-pCDNA3 (Addgene, 21884) plasmids were first verified by restriction analysis using the enzymes *Bam*H1 and *Xho*1 (Figure 4.1, A and B).

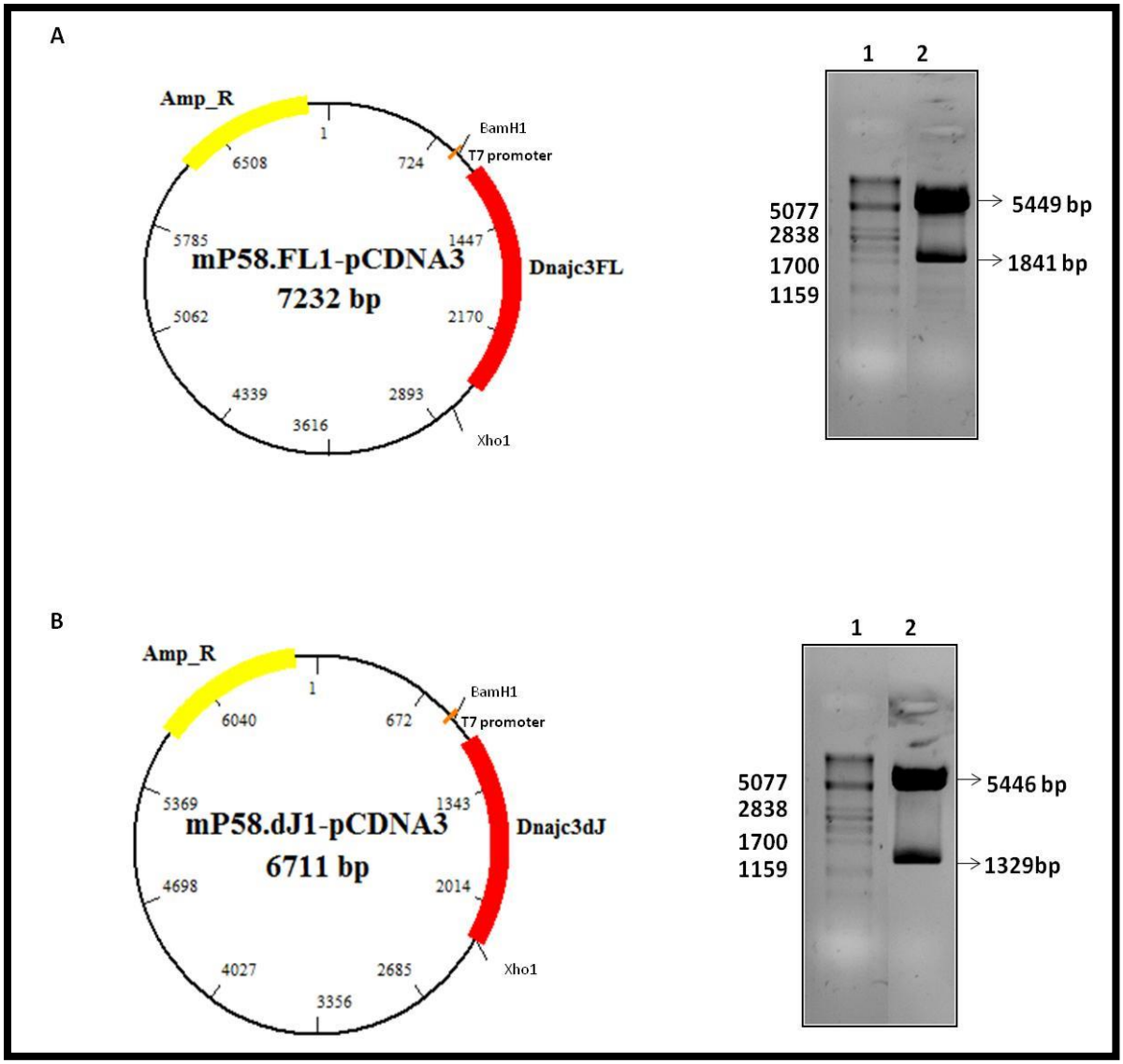

Figure 4.1: Verification of mP58.FL1-pCDNA3 and mP58.dJ1-pCDNA3 constructs by restriction analysis. Plasmid map of (A) mP58.FL1-pCDNA3 and (B) mP58.dJ1.pCDNA3 constructed using BioEdit software. The pCDNA vector has an ampicillin resistance gene (Amp_R) used for selective screening. The construct is lacking a tag on either side of the insert, which is flanked between the restriction enzyme sites, *Bam*H1 and *Xho*1. Restriction analysis of the (A) mP58.FL1-pCDNA3 and (B) mP58.dJ1.pCDNA3 plasmid using the restriction enzymes *Bam*H1 and *Xho*1. The restriction plasmid DNA was resolved on a 1% agarose gel. Lane 1: Lambda DNA digested with *Pst*1, Lane 2: mP58.FL1-pCDNA3 or mP58.dJ1.pCDNA3 digested with *Bam*H1 and *Xho*1. The arrows indicate the pCDNA3 backbone and the DNAJC3FL or DNAJC3dJ DNA fragment. The expected sizes of the pCDNA3 vector and DNAJC3FL and DNAJC3dJ DNA fragment are 5446 bp, 1841 bp and 1329 bp respectively.

The coding regions for DNAJC3FL and DNAJC3dJ were digested from mP58.FL1-pCDNA3 and mP58.dJ1-pCDNA3 plasmids using the restriction sites (*Bam*H1 and *Xho*1) and ligated into pGEX4T-1 vector in frame with the GST tag resulting in the expression vectors pLZMC3FL and pLZMC3dJ (Figure 4.2), which encoded for GST-tagged DNAJC3FL and DNAJC3dJ. The resulting GST-tagged DNAJC3FL and DNAJC3dJ expression constructs

were confirmed by restriction digest analysis (Figure 4.2, A and B) and sequencing (data not shown).

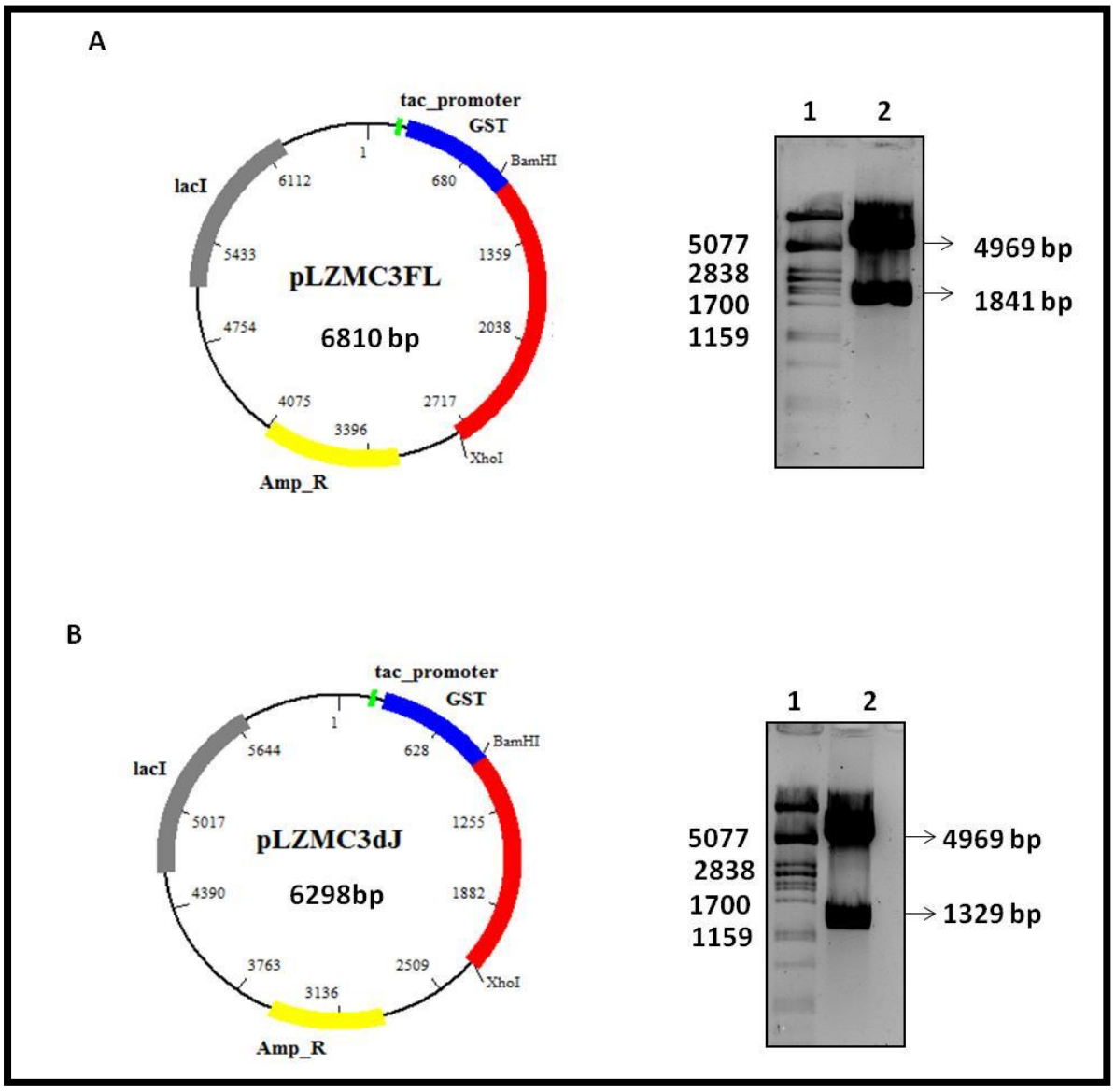

Figure 4.2: Verification of the GST-tagged DNAJC3FL and DNAJC3dJ expression constructs pLZMC3FL and pLZMC3dJ by restriction analysis. Plasmid map of (A) pLZMC3FL and (B) pLZMC3dJ constructed using BioEdit software. The pGEX4T-1 vector has an ampicillin resistance gene (Amp_R) used for selective screening. The GST tag is located upstream of the PCR fragment, which is shown between the restriction enzyme sites, *Bam*H1 and *Xho*1, used for ligation. Restriction analysis of the (A) pLZMC3FL and (B) pLZMC3dJ plasmid using the restriction enzymes *Bam*H1 and *Xho*1. The restriction plasmid DNA was resolved on a 1% agarose gel. Lane 1: Lambda DNA digested with *Pst*1, Lane 2: pLZMC3FL or pLZMC3dJ digested with *Bam*H1 and *Xho*1. The arrows indicate the pGEX4T-1 backbone and the DNAJC3FL or DNAJC3dJ DNA fragment. The expected sizes of the pGEX4T-1 vector and DNAJC3FL and DNAJC3dJ DNA fragment is 4960 bp, 1841 bp and 1329 bp respectively.

Expression of GST-tagged DNAJC3FL and DNAJC3 proteins was optimised in *various E. coli* expression strains (Table 2.2, Figure 4.3, A-E) and using a range of IPTG concentrations and expression temperatures. Examples of the expression profiles from selected optimization

treatments are shown in Figure 4.3. Despite repeated efforts at optimization, substantial protein expression was not observed.

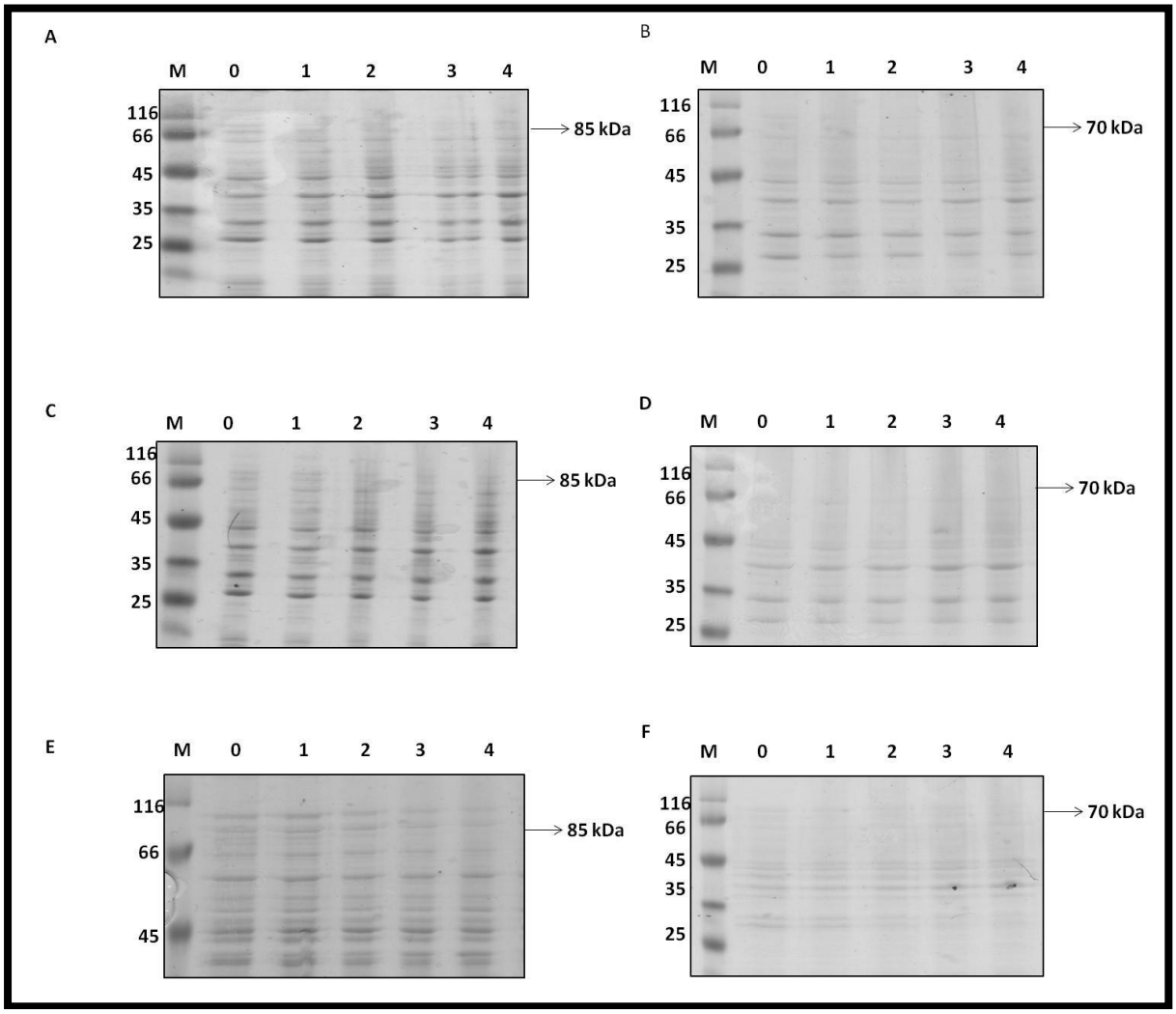

Figure 4.3: SDS-PAGE analysis of the expression profile of GST-tagged DNAJC3FL and GST-tagged DNAJC3dJ proteins in various *E. coli* expression strains. Expression of GST-tagged DNAJC3Fl and GST-tagged DNAJC3dJ in (A and B) BL21 (DE3) cells, (C and D) BL21 C43 (DE3) cells and (E and F) BB1994 cells. Lane M: Molecular marker, Lanes 0-4: DNAJC3FL and DNAJC3dJ protein samples collected at hourly intervals from 0 to 4 hours post induction with 1mM IPTG.

SDS-PAGE and Western blot analysis of both proteins samples at 0 to 3 hours post induction in a selected expression strains (BL21 C41 (DE3) *E. coli* cells) using GST specific antibodies indicated the presence of bands at 26 and 30 kDa band and not the expected bands at 85 kDa and 70 kDa, which should have corresponded to GST-tagged DNAJC3FL and DNAJC3dJ, respectively (Figure 4.4, A and B).

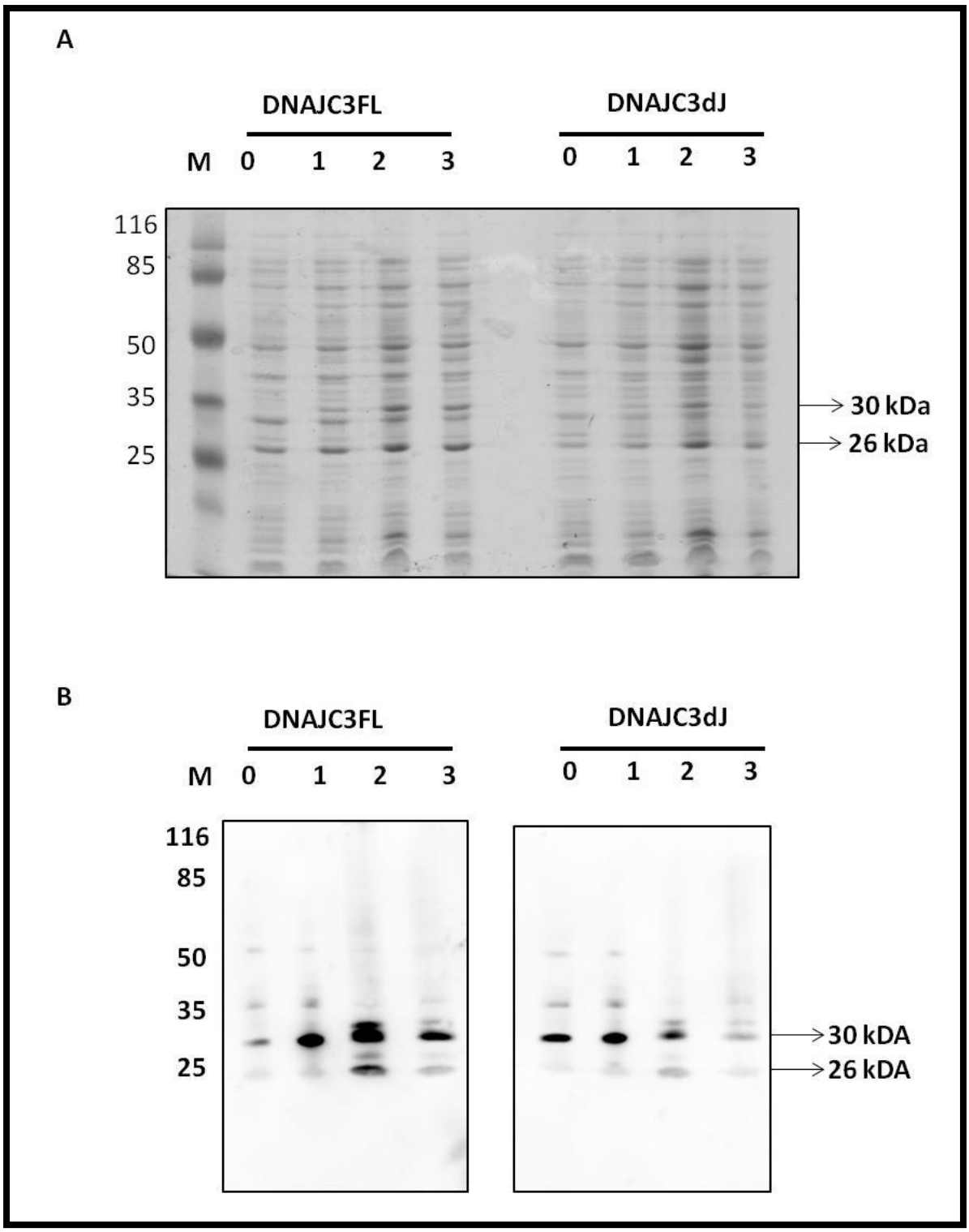

Figure 4.4: SDS-PAGE and Western analysis of GST-tagged DNAJC3FL and DNAJC3dJ in BL21 C41 (DE3) cells. (A) SDS-PAGE and (B) Western analysis of the expression profile of GST-tagged DNAJC3FL and DNAJC3dJ using anti-GST antibodies. Lane M: Molecular marker, Lanes 0-3: DNAJC3FL and DNAJC3dJ protein samples collected at hourly intervals from 0 to 3 hours post induction with 1 mM IPTG.

The lack of GST-tagged DNAJC3FL and DNAJC3dJ protein detected following induction suggested that there was a problem in expressing both proteins in the current form. The DNAJC3 protein is known to have a cleavable ER signal peptide at the N terminus, a signal

peptide which was present in the initial construct (Figure 4.5, A and B, Rutkowski *et al*., 2007). The cleavage of the ER signal peptide after protein synthesis in *E. coli* could explain the observation of only a 30 kDa protein during western blot analysis (Figure 4.4, B). This band could possible represent the GST tag and the ER signal peptide (Figure 4.5, A), since the pGEX4T-1 vector used encoded an N-terminal GST tag (Figure 4.2). This suggests that the remaining protein of the DNAJC3FL and DNAJC3dJ proteins were not detected using GST specific antibodies since it was no longer tagged. Alternatively, the truncated protein observed could be a consequence of the physical properties of the ER signal peptide, which consists of numerous hydrophobic amino acids as indicated by the Kyte and Doolittle plot (Figure 4.5, C). Regions above 0 represent hydrophobic residues and regions below 0 represent hydrophilic regions (Kyte and Doolittle, 1982). It was observed that the first 25 amino acid residues of DNAJC3 which code for the ER signal peptide, display values above 0 (Figure 4.5 C). This hydrophobic nature of the ER signal peptide could be causing early termination of protein synthesis, resulting in truncated GST-tagged DNAJC3 proteins.

An alternative strategy for obtaining GST-tagged DNAJC3FL and DNAJC3dJ protein was formulated, and this involved removing the 25 amino acids at the N-terminus of the protein that made up the cleavable ER signal peptide Primers were designed to PCR amplify the coding regions of DNAJC3FL and DNAJC3dJ from the mP58.FL1-pCDNA3 plasmid, excluding the region that coded for the cleavable ER signal peptide (henceforth the coding regions lacking the ER signal peptide will be referred to as DNAJC3ΔER and DNAJC3ΔJ/ER) (Figure 4.6, A and C). The PCR fragments of DNAJC3ΔER and DNAJC3ΔJ/ER were ligated into the expression vector pGEX4T-1 using the restriction sites *Bam*H1 and *Xho*1 introduced during the PCR procedure. Verification of the resulting constructs was conducted by restriction digest (Figure 4.6, B and D) and sequencing (data not shown).

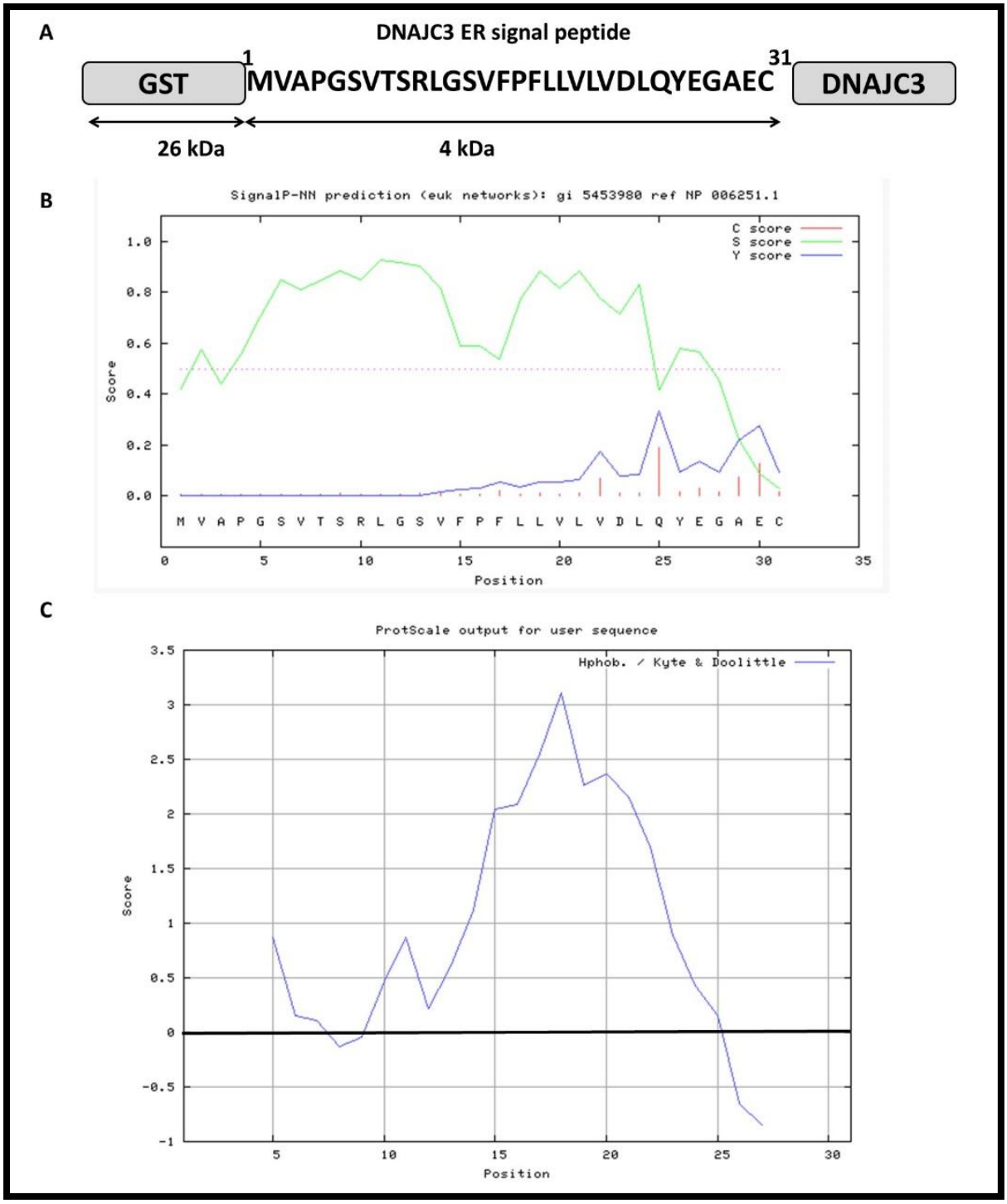

Figure 4.5: DNAJC3 has a cleavable ER signal peptide that is highly hydrophobic. (A) Schematic representation of GST tagged DNAJC3 ER signal peptide. (B) SignalP3.0 prediction for the DNAJC3 signal peptide (green line/region above pink dotted line), cleavable region (blue line) and cleavable site/residue (red line). (C) Kyte and Doolittle plot indicating the hydrophobic (values above 0) and hydrophilic regions (values below 0) of the DNAJC3 ER signal peptide

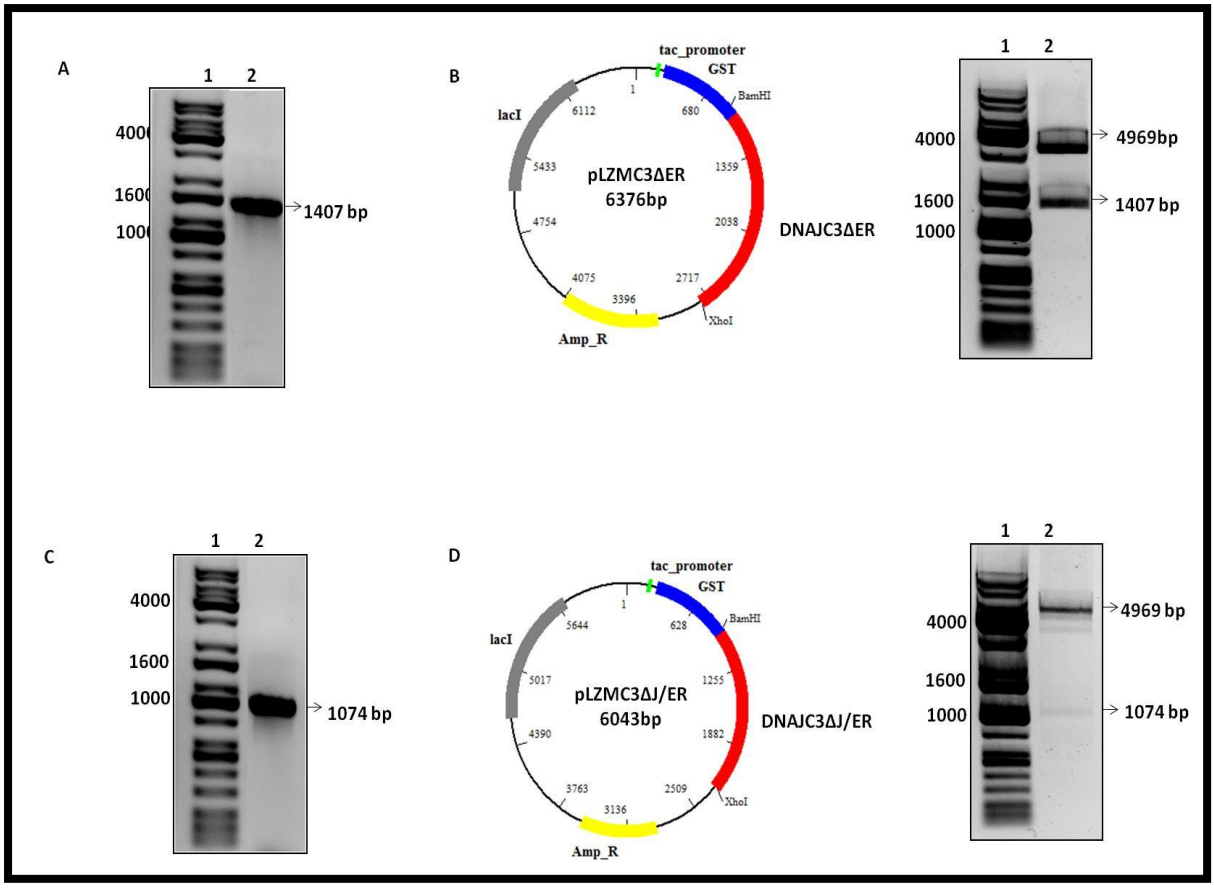

Figure 4.6: PCR cloning of bacterial expression vectors for DNAJC3ΔER and DNAJC3ΔJ/ER. PCR amplification of the coding region of (A) DNAJC3ΔER and (C) DNAJC3ΔJ/ER which excluded the ER signal peptide region. Lane 1: Lambda DNA digested with *Pst*1, Lane 2: PCR product. Plasmid map of (B) pLZMC3ΔER and (D) pLZMC3ΔJ/ER constructed using BioEdit software. The pGEX4T-1 vector has an ampicillin resistance gene (Amp_R) used for selective screening. The GST tag is located upstream of the PCR fragment, which is shown between the restriction enzyme sites, *Bam*H1 and *Xho*1, used for ligation. Restriction digest analysis was carried out for the (B) pLZMC3ΔER and (D) pLZMC3ΔJ/ER plasmids using the restriction enzymes *Bam*H1 and *Xho*1. The restriction digestion of the plasmid DNA was resolved on a 1% agarose gel. Lane 1: Lambda DNA digested with *Pst*1, Lane 2: pLZMC3ΔER or pLZMC3ΔJ/ER digested with *Bam*H1 and *Xho*1. The arrows indicate the pGEX4T-1 backbone and the DNAJC3ΔER or DNAJC3ΔJ/ER DNA fragment at the expected size of 4969 bp, 1700 bp and 1150 bp, respectively.

Plasmids coding for the N terminus GST-tagged DNAJC3ΔER and DNAJC3ΔJ/ER proteins were transformed into competent *E. coli* BL21 (DE3) cells and 1 mM IPTG used to overexpress the proteins over 4 hours and the expression profile analyzed by SDS-PAGE (Figure 4.7, A and B). Analysis of the gel representing the expression profile of GST-tagged DNAJC3ΔER (Figure 4.7, A) showed a faint increase in the expression of a protein which resolved to a similar position as the 85 kDa marker band at 1 hour post induction. The expected size of GST-tagged DNAJC3ΔER was 75 kDa. The protein band observed could possibly represent DNAJC3ΔER being expressed, as the equivalent band is absent in the sample collected before induction (0 hours). The expression profile gel of GST-tagged DNAJC3ΔJ/ER (Figure 4.7, B), in contrast showed an increase in protein resolving around 70 kDa, from 1 hour post induction. Since the

expected size of GST-tagged DNAJC3ΔJ/ER was 65 kDa, strongly suggesting that the protein observed around 70 kDa was the GST-tagged DNAJC3ΔJ/ER. Initial attempts to purify both GST-tagged DNAJC3ΔER and DNAJC3ΔJ/ER proteins revealed that the proteins were located in the pellet fraction, suggesting that the proteins were insoluble (Figure 4.7, C and D).

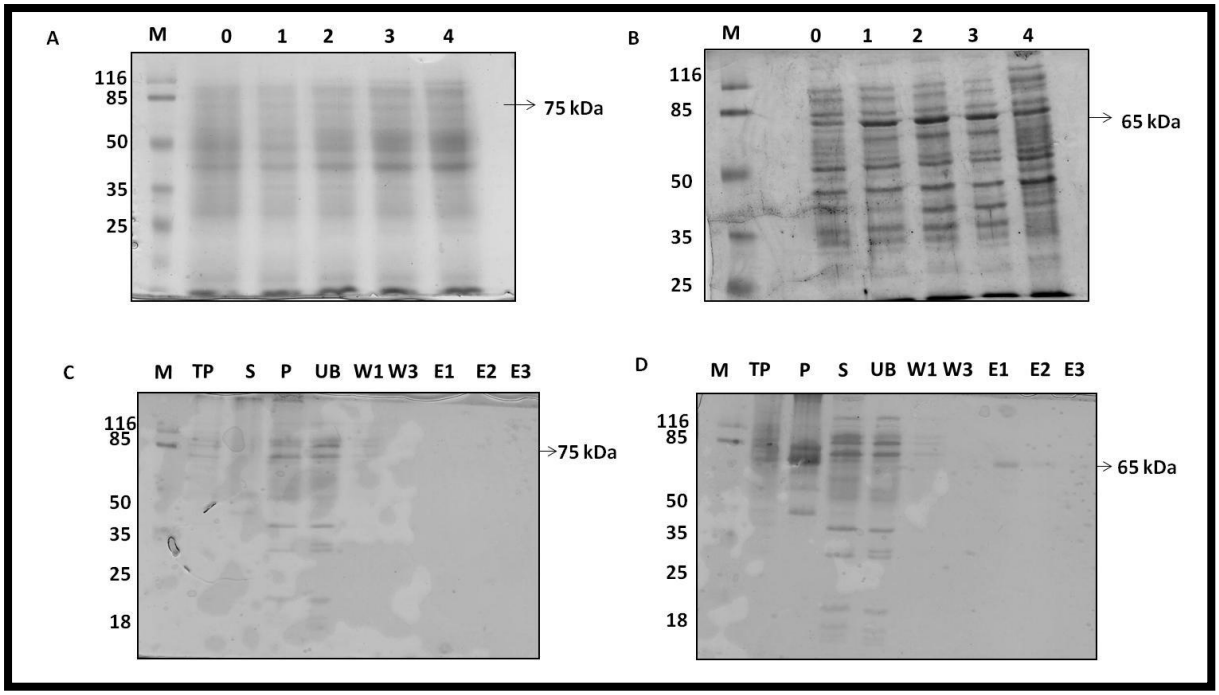

Figure 4.7: Expression and purification of GST-tagged DNAJC3ΔER and GST-tagged DNAJC3ΔJ/ER. (A and B) Induction profile of GST-tagged DNAJC3ΔER and GST-tagged DNAJC3ΔJ/ER, respectively. Lane M: Molecular marker, Lanes 0-5: protein samples collected at hourly intervals from 0 to 4hours post induction with 1mM IPTG. (C and D) GST batch purification of GST-tagged DNAJC3ΔER and GST-tagged DNAJC3ΔJ/ER. Lane M: Molecular weight marker, Lane TP: total protein fraction, Lane P: insoluble fraction, Lane S: soluble fraction, lane UB: unbound protein fraction, Lane W1-W3: wash fractions and Lane E1-E3: elution fractions.

A solubility study was conducted using various modifications of the expression protocol or lysate preparation conditions in order to increase the yield of soluble protein. These modifications included the addition of various detergents (N-Laurylsarcosine [Sac], Nonidet-P 40 [NP40], Tween-20 and Durrapol-2000 [Schlager *et al*., 2012]), modification of growth medium (glucose MM and auto-induction medium), use of additives including 2% (w/v) glucose (San-Miguel *et al*., 2013) and 0.5 M sorbitol (Sandee *et al.*, 2005) and induction and growth conditions including reducing the inducer concentration to 0.5 mM IPTG (Winograd *et al*. 1993) and using a lower induction temperature of 20 ˚C (Vasina and Baneyx, 1997) and a shorter induction time of 0.5 hours (for further details see section 2.12).

SDS-PAGE analysis of the insoluble and soluble fractions from the treatments suggested that the protein was still located mainly in the insoluble protein fraction (Figure 4.8). Although not

obvious on the SDS-PAGE gels, western blot analysis of the soluble fractions from the various treatments proved that with the exception of the detergent treated samples, all other treatments resulted in an increase in soluble protein (Figure 4.9). Three GST-tagged bands were detected in the soluble fraction, one at 65 kDa, which was the expected size for GST-tagged DNAJC3ΔJ/ER, a second at 50 kDa, which could represent a truncated GST-tagged DNAJC3ΔJ/ER and the third at 26 kDa, which is the expected size of the GST tag.

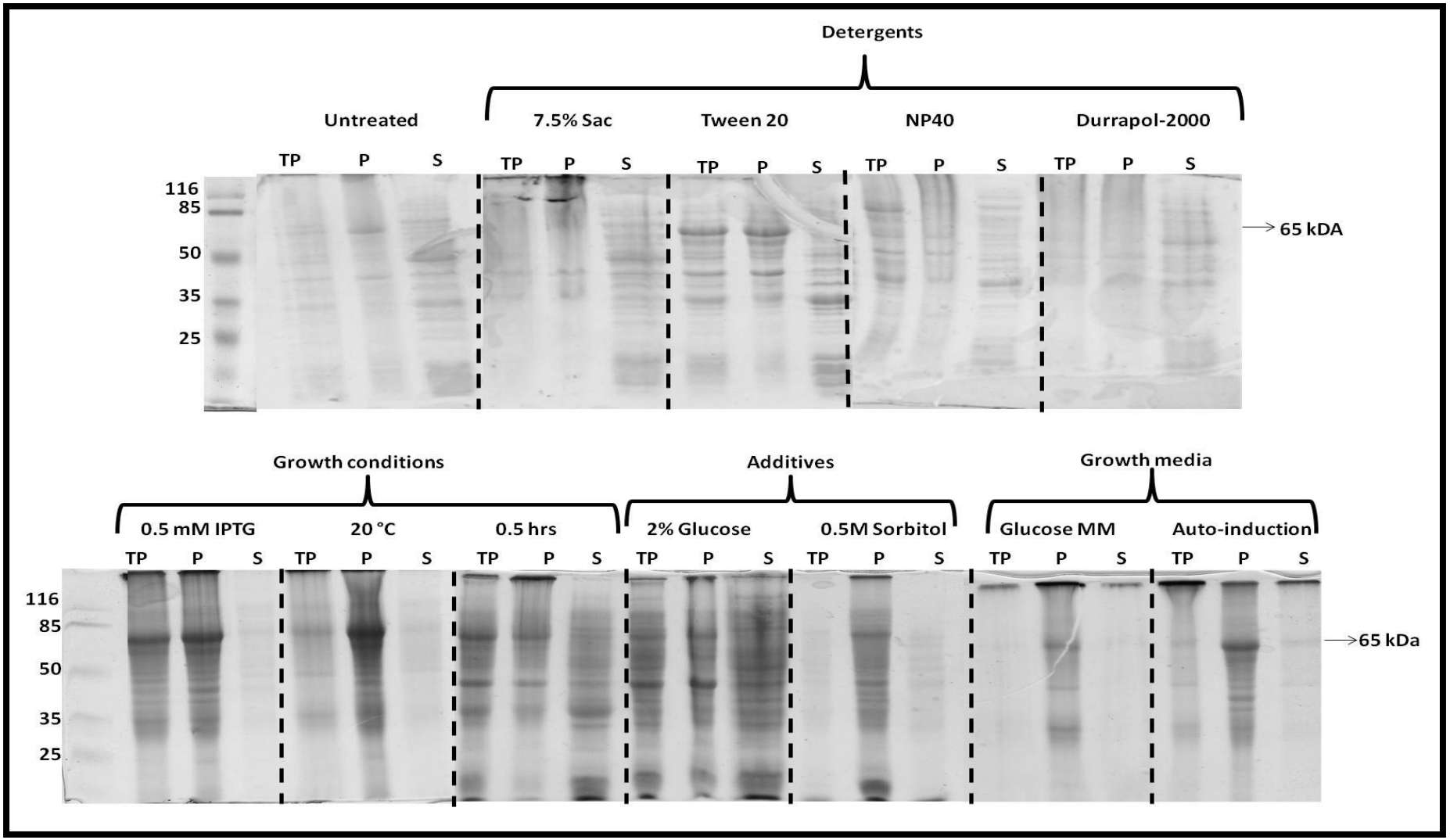

Figure: 4.8: SDS-PAGE analysis of the optimization of GST-tagged DNAJC3ΔJ/ER protein solubility by means of various treatments and growth conditions. TP: total protein, P: pellet fraction and S: soluble fraction.

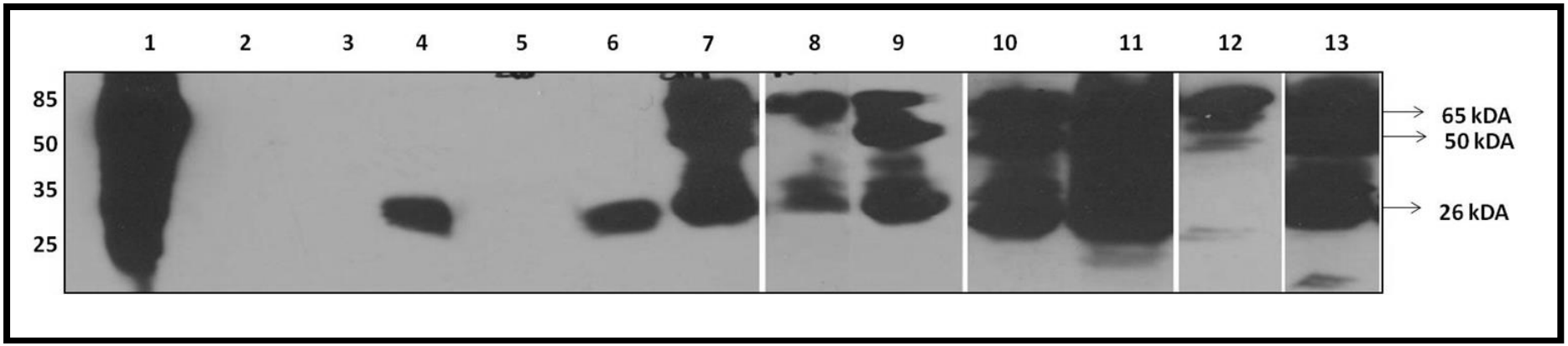

Figure 4.9: Western analysis of the optimization of GST-tagged DNAJC3ΔJ/ER protein solubility by means of various treatments. Equivalent volume of soluble fraction derived from the same number of bacterial cells was loaded. Anti-GST antibodies were used for Western analysis. Lane 1: Pellet fraction from untreated sample. Lanes 2-13 represent the soluble fraction (Supernatant) from the following: Lane 2: Standard protocol (untreated), Lane 3: 7.5 % (v/v) Sac, Lane 4: Tween-20, Lane 5: NP40, Lane 6: Durrapol-2000, Lane 7: expression for 0.5 hours, Lane 8: induced by 0. 5 mM IPTG, Lane 9: expressed at 20 ˚C, Lane 10: 2X YT supplemented with 2 % (w/v) glucose, Lane 11: 2X YT supplemented with 0.5 M sorbitol, Lane 12: Auto-induction medium and Lane 13: Glucose MM medium.

After optimization, expression of the GST-tagged DNAJC3ΔER and DNAJC3ΔJ/ER was induced at 18°C for 0.5 hours using 0.5 mM IPTG and purified as previously described. The success of the purification procedure was analyzed by SDS-PAGE and Western analysis. Despite numerous attempts at optimization, there was no improvement in the expression of GST-tagged DNAJC3ΔER protein (data not shown), which resulted in no protein being observed at the end of the purification procedure. In the case of DNAJC3ΔJ/ER, the combination of changing the expression temperature, time and inducer concentration, resulted in an increase in the solubility of GST-tagged DNAJC3ΔJ/ER, allowing better purification as indicated in SDS-PAGE and Western analysis by the presence of a protein band of about 65 kDa in the elution fraction after purification (Figure 4.10, A and B). Additional protein bands were also observed in the purified samples (Figure 4.10, A and B, Lanes 8-9), namely a 50 kDa protein which could represent a truncated GST-tagged DNAJC3ΔJ/ER and a 26 kDa protein, which could be the GST protein itself as it is known that this tag is 26 kDa in size.

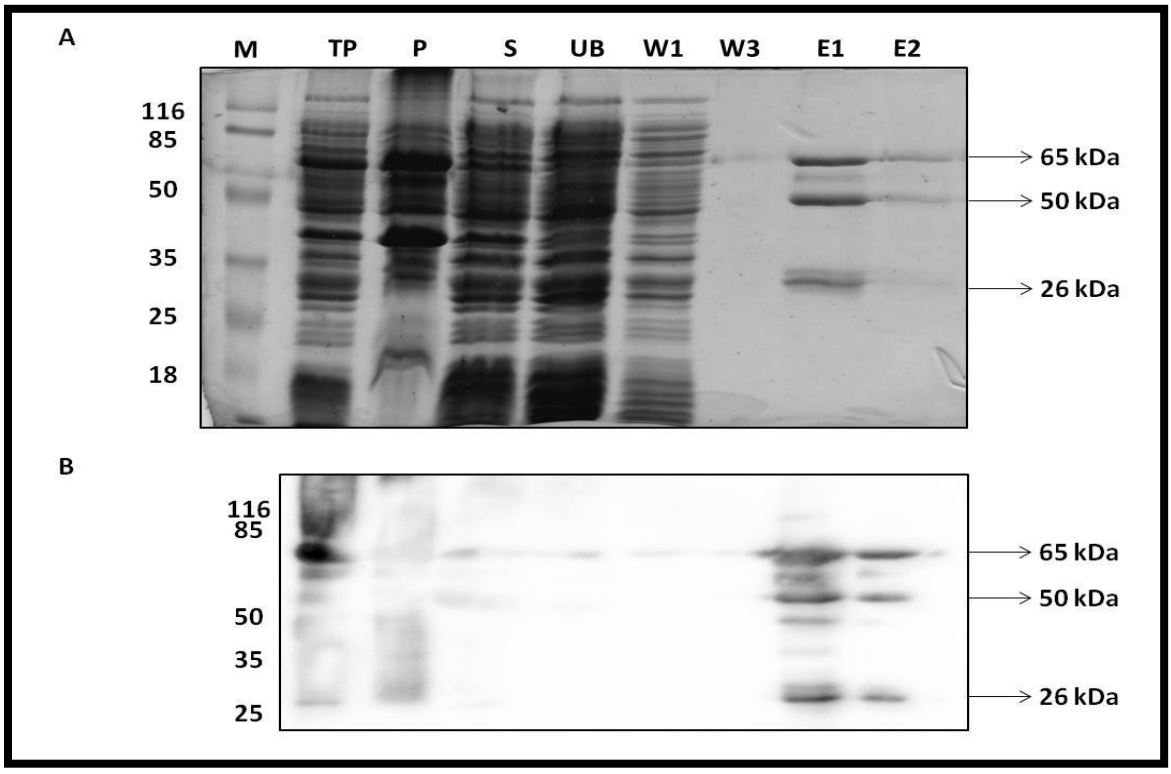

Figure 4.10: Batch purification of GST-tagged DNAJC3ΔJ/ER. (A) SDS-PAGE and (B) Western analysis using anti-GST antibodies. Lane M: Molecular weight marker, Lane TP: total protein fraction, Lane P: insoluble fraction, Lane S: soluble fraction, lane UB: unbound protein fraction, Lane W1-W3: wash fractions and Lane E1-E2: elution fractions.

4.2.2 Cloning, overexpression and purification of GST-tagged DNAJC7

DNAJC7 is a known TPR-containing DNAJ similar to DNAJC3, which interacts with both Hsp90 and Hsp70 (Brychzy *et al*., 2003, Moffatt *et al*., 2008). Because DNAJC7 is highly similar to DNAJC3, recombinant DNAJC7 protein would make an appropriate positive control during the binding interaction characterization of DNAJC3 TPR domains.

Total RNA was successfully extracted from MCF-7 carcinoma cells using Trizol Reagent® (Figure 4.11, A). The isolated RNA was used to synthesize cDNA through RT-PCR and the resulting cDNA was used in the PCR amplification of the DNAJC7 gene. The PCR reaction was analyzed by agarose gel electrophoresis and two DNA products of approximately 1480 bp and 850 bp were observed (Figure 4.10, B). The expected size of the DNAJC7 gene was 1484 bp, suggesting that the larger and fainter band observed on the gel was likely DNAJC7 and the smaller and brighter band might represent an alternative amplicon. The PCR product of DNAJC7 was inserted into the N-terminus GST-tagged expression vector pGEX4T-1 as previously described. Using the restriction sites introduced during the PCR procedure the coding region of DNAJC7 was ligated into pGEX4T-1 in frame with the GST tag resulting in the expression vector pLZMC7 (Figure 4.11, C), which encoded GST-tagged DNAJC7. The pLZMC7 expression vector was verified by restriction digest analysis (Figure 4.11, D) and sequencing (data not shown).

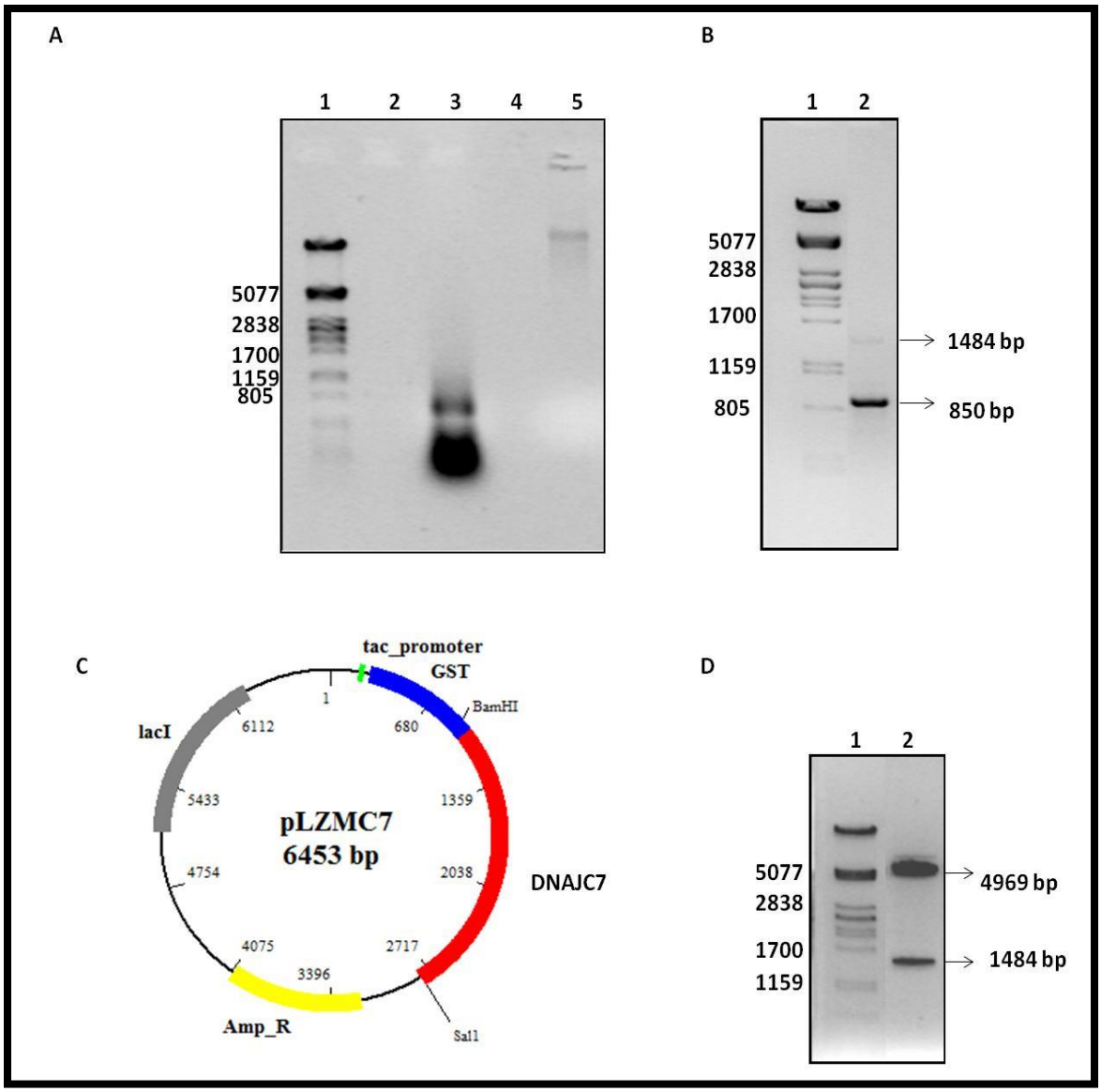

Figure 4.11: Generation of a bacterial expression system for the over expression and purification of GST- tagged DNAJC7. (A) 1 % (w/v) agarose gel analysis of total RNA and DNA isolated from MCF-7 breast carcinoma. Lane 1: Lambda DNA digested with *Pst*1, Lane 3: Isolated total RNA, Lane 5: Isolated MCF-7 DNA. (B) PCR amplification of DNAJC7 gene. Lane 1: Lambda DNA digested with *Pst*1, Lane 2: DNAJC 7 PCR product. The expected size of DNAJC7 fragment was 1484 bp. (C) Plasmid map of pLZMC7 constructed using BioEdit software. The pGEX4T-1 vector has an ampicillin resistance gene (Amp_R) used for selective screening. The GST tag is located upstream of the DNAJC7 gene, which is shown between the restriction enzyme sites, *Bam*H1 and *Sal*1, used for ligation. (D) Restriction analysis of the pLZMC7 plasmid using the restriction enzymes *Bam*H1 and *Sal*1. The resulting plasmid DNA fragments were resolved on a 1% (w/v) agarose gel. Lane 1: Lambda DNA digested with *Pst*1, Lane 2: pLZMC7 digested with *Bam*H1 and *Sal*1. The expected sized of pGEX4T-1 vector and DNAJC7 DNA fragment were 4690 bp and 1483 bp, respectively.

Expression of the GST protein (as a control) and GST-tagged DNAJC7 was conducted by transforming *E. coli* XL1 Blue cells with the pGEX4T-1 and pLZMC7 plasmids, and inducing protein production using 1 mM IPTG at 37 °C. Expression of the GST protein and GST-tagged

DNAJC7 was analyzed by SDS-PAGE (Figure 4.12, A and B). Protein expression for both proteins was observed from 1 hour post induction as indicated by the presence of a 26 kDa band on the GST protein expression gel (Figure 4.12, A) and a 85 kDa band on the GST-tagged DNAJC7 expression profile acrylamide gel (Figure 4.12, B). Purification of the GST protein and GST-tagged DNAJC7 was attempted using the GST affinity batch purification method. The success of the purification method was analyzed by SDS-PAGE (Figure 4.12, C and D). For the GST protein, the majority of the protein was soluble as indicated by the prominent band at 26 kDa in the supernatant fraction (Figure 4.12, C). However, purification of the GST-tagged DNAJC7 protein was unsuccessful since most of the protein was found to be insoluble as indicated by the presence of the bulk of the protein in the pellet fraction (data not shown). The addition of the detergent N-Lauroylsarcosine (Sac) at a final concentration of 7.5% (v/v), which is known to increase protein solubility (Schlager *et al*., 2012), did not improve the solubility or purification of DNAJC7 (Figure 4.12, D).

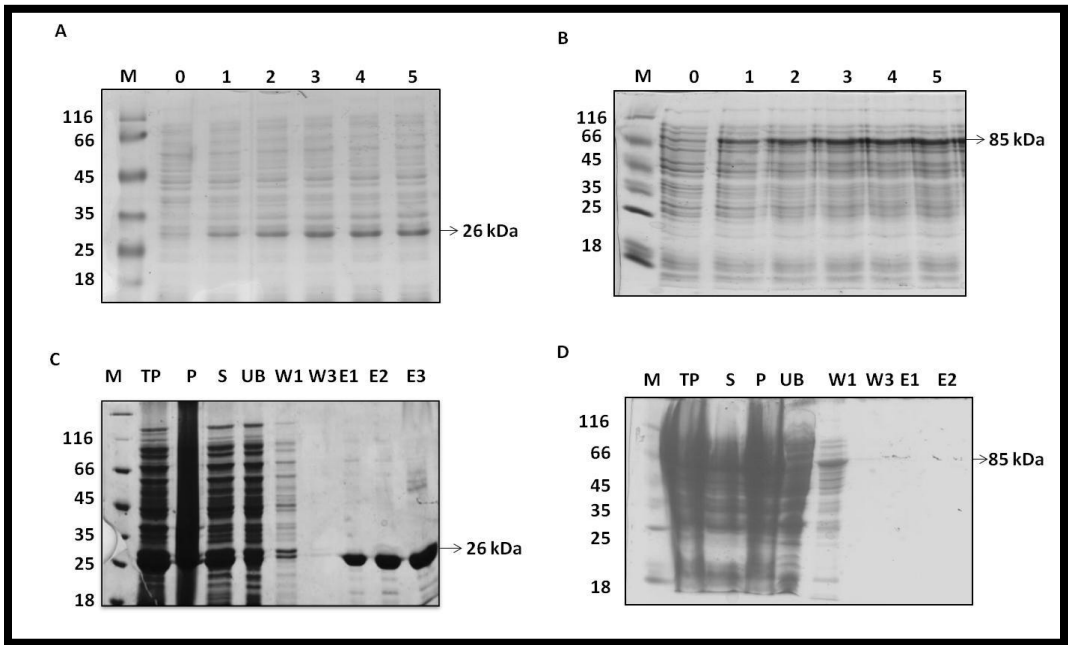

Figure 4.12: Overexpression and batch purification of GST-tagged DNAJC7. (A and B) Expression profile of GST and GST-tagged DNAJC7, Lane 1: Molecular marker, Lanes 0-5: protein samples collected at hourly intervals from 0 to 5 hours post induction with 1mM IPTG. (C and D) GST batch purification of GST and GST-tagged DNAJC7, Lane M: Molecular weight marker, Lane TP: total protein fraction, Lane P: insoluble fraction, Lane S: soluble fraction, lane UB: unbound protein fraction, Lane W1-W3: wash fractions and Lane E1-E2: elution fractions.

4.2.3 Overexpression and purification of His-tagged Grp78 and Grp94$_{284-543}$

Plasmids coding for N terminal His-tagged Grp78/BiP and His-tagged Grp94$_{284-543}$ (pQE10-BiP, a kind donation from Prof. Richard Zimmermann (Universität des Saarlandes, Germany) and HSP90B1 (Addgene plasmid, 39076), encoding the middle domain of Grp94 from residues 284-543)) were transformed into M15 *[pREP4]* and BL21 (DE3) competent cells, respectively and protein production induced by addition of 1 mM IPTG at 37 °C for Grp78 and 0.5 mM IPTG at 18 °C for Grp94$_{284-543}$. SDS-PAGE was used to analyze the expression profile of the proteins (Figure 4.13, A and B). An increase in the expression of protein of molecular weights of approximately70 kDa and the 40 kDa were observed for Grp78 and Grp94$_{284-543}$, respectively. These sizes corresponded to the expected sizes for both the latter proteins, which suggested that the protein bands represented His-tagged Grp78 and His-tagged Grp94$_{284-543}$. Nickel affinity purification was successful in purifying both proteins as illustrated by the large amount of protein recovered in the elution fractions (Figure 4.13 C and D).

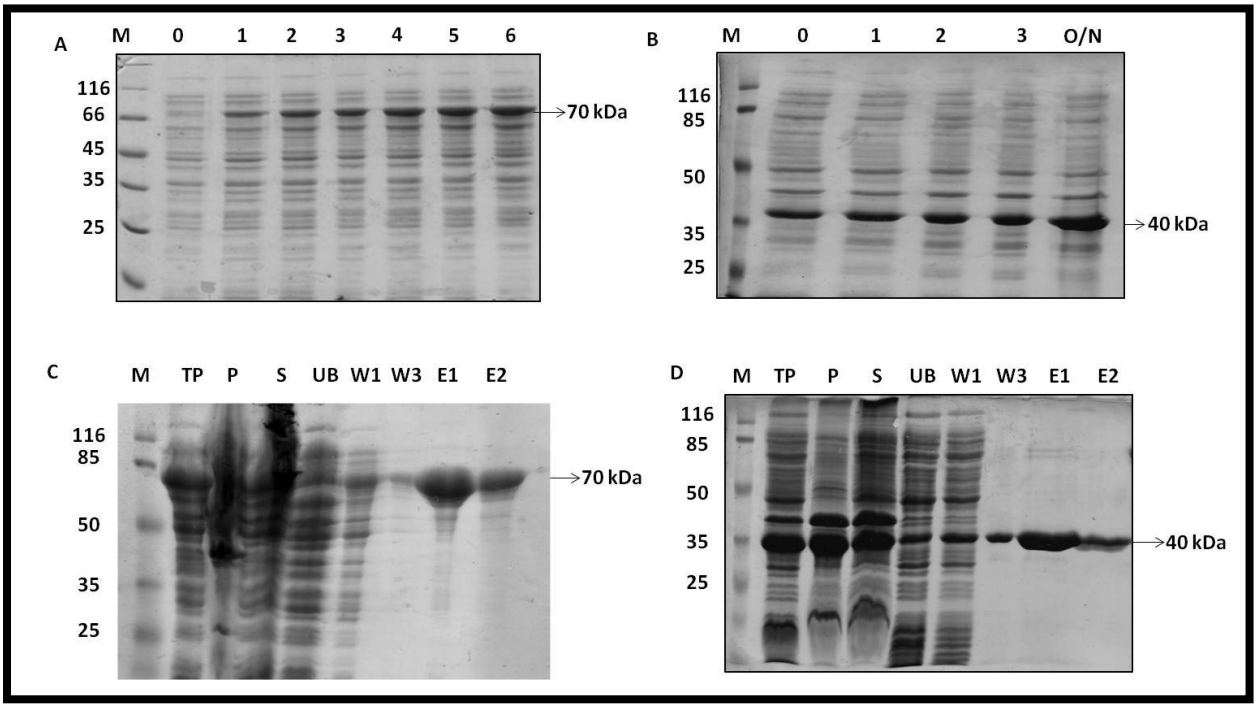

Figure 4.13: Expression and purification of His-tagged Grp78 and His-tagged Grp94$_{284-543}$
(A) Expression profile of His-tagged Grp78. Lane M: Molecular marker, Lanes 0-6: protein samples collected at hourly intervals from 0 to 6 hours post induction with 1mM IPTG. (B) Expression profile of His-tagged Grp94$_{284-543}$. Lane M: Molecular marker, Lanes 0-O/N: protein samples collected at hourly intervals from 0 to 3 hours and overnight post induction with 1mM IPTG. (C and D) Nickel affinity purification of His-tagged Grp78 and His-tagged Grp94$_{284-543}$ Lane M: Molecular weight marker, Lane TP: total protein fraction, Lane P: insoluble fraction, Lane S: soluble fraction, lane UB: unbound protein fraction, Lane W1-W3: wash fractions and Lane E1-E2: elution fractions.

4.3 Discussion

In order to conduct biophysical characterization of DNAJC3, recombinant proteins had to be produced. Expression of recombinant proteins in bacterial systems followed by affinity purification is one of the ways utilized to accomplish this (Smith and Johnson, 1988, Guan and Dixon, 1991). For this study, two types of affinity purification tags, namely GST and His, were utilized to make purification of the proteins of interest possible from bacterial lysates. The use of different tags was required for the subsequent interaction studies, which required the bait and prey proteins to have different tags. The His tag is generally preferred as it is small, does not usually impact on the protein conformation and permits both native and denaturing purification procedure (Terpe, 2003). Although the GST tag is larger and known to dimerize, this tag was selected for the DNAJC3 constructs because it has been shown to increase protein solubility and improve protein folding (Kaplan *et al*., 1997), leading to good expression and recovery of expressed proteins. Despite this however, this was not the observed outcome in this study, as all GST-tagged proteins (DNAJC7, DNAJC3FL and DNAJC3dJ, DNAJC3ΔER and DNAJC3ΔJ/ER) were highly insoluble. The addition of the detergent, N-Laurylsarcosine during the lysis step of GST-tagged DNAJC7 expressing cells did not improve the protein solubility of the protein resulting in no protein being purified.

Initial attempts were made to express both GST-tagged DNAJC3FL and DNAJC3dJ with the ER signal peptide still present at the N-terminus of the proteins. However it was observed in SDS-PAGE analysis that full length GST-tagged DNAJC3FL and GST-tagged DNAJC3dJ were not being expressed, but rather a 30 kDa protein was observed in different expression strains (Figure 4.3). Western analysis using GST specific antibodies (Figure 4.4, B) illustrated that the 30 kDa protein was GST-tagged, suggesting that this protein consisted of the GST tag (26 kDa) and the ER signal peptide (4 kDa), which has been shown to be cleavable at least in mammalian cell lines, and might be undergoing the same process in bacterial cells (Rutkowski *et al*., 2007, Figure 4.5, A and B). Alternatively, the hydrophobic nature of the ER signal peptide (Figure 4.5, C) could be causing early protein synthesis termination, as hydrophobic proteins like membrane proteins have been shown to promote protein unfolding and aggregation resulting in protein degradation (Schwarz *et al*., 2008). Cell-free expression systems have been used successfully in the production of hydrophobic recombinant proteins (membrane proteins) due to their ability to create an artificial hydrophobic environments which is able to maintain hydrophobic proteins in their soluble state

(Schwarz *et al*., 2008). Therefore, this may be a possible alternative method to use in the production of other proteins with large patches of hydrophobic residues such as the ER signal peptide of DNAJC3 (Figure 4.5, C).

Alternative constructs (pLZMC3ΔER and pLZMC3ΔJ/ER) that removed the ER signal peptide were constructed, resulting in GST-tagged DNAJC3ΔER and DNAJC3ΔJ/ER, respectively. Both GST-tagged DNAJC3ΔER and DNAJC3ΔJ/ER were successfully expressed in BL21 (DE3) cells (Figure 4.7, A and B), although expression of GST-tagged DNAJC3ΔER was low. Initial attempts to purify GST-tagged DNAJC3ΔER and DNAJC3ΔJ/ER were unsuccessful (Figure 4.7, C and D), as most of the expressed protein was found to be in the insoluble fraction (pellet), prompting the need to improve the solubility of the proteins through various methods.

Several methods are usually adopted when attempting to improve protein solubility, these could include changing expression strains, lowering expression time and temperature, altering concentration of the inducer, addicting additives to the media, co-expressing recombinant proteins with chaperones, cofactors or special plasmids (i.e. pRARE), changing the composition or type of media or using fusion proteins (Fox and Waugh, 2003, Golovanov *et al*., 2004, Sørensen and Mortensen, 2005, Kobayashi *et al*., 2009, San-Miguel *et al*., 2013, Voulgaridou *et al*., 2013). In this study, several of the listed modifications were attempted to improve protein solubility. The first method tried was the use of various detergents, which are known to permeabilize membranes and release trapped proteins (Schlager *et al*., 2012). The following modification involved reducing the concentration of the inducer (IPTG), reducing the expression temperature and expression time. Reducing the inducer concentration, expression time or temperature is known to decrease the rate of protein synthesis, ensuring that synthesized proteins are folded correctly, preventing protein aggregation that normally occurs as a result of protein overcrowding caused by rapid protein synthesis and protein misfolding (Winograd *et al*., 1993, Vasina and Baneyx, 1997). The other modifications exploited were changing growth medium (auto induction medium and glucose minimum medium) or supplementation with additives such as sorbitol and glucose. Auto induction medium ensures that the rate of protein expression is reduced, while glucose minimum medium ensures tight regulation of the lac promoter, controlling expression. Addition of glucose to growth medium has been shown to repress induction of the lac operon by lactose thereby having a tighter control on the protein expression, in a way similar to that of glucose minimal medium (San-Miguel

et al., 2013), while sorbitol is known to stabilize the native structure of the protein, preventing unfolding and aggregation (Sandee *et al*., 2005).

In this study, the addition of detergents did not improve the solubility of GST-tagged DNAJC3ER. However, solubility of DNAJC3ΔJ/ER was slightly improved by changing the growth medium and growth conditions. This suggested that GST-tagged DNAJC3ΔJ/ER was insoluble as a result of protein aggregation, rather than being trapped in membranes, since detergents which are known to permeabilize membranes (Bhairi and Mohan, 2007) were unable to improve DNAJC3ER solubility.

In literature, a few studies have successfully expressed and purified the full length and truncated (without J domain) DNAJC3 with the ER signal peptide using a bacterial expression system. The majority of the studies used alternative tags such as the His-tag (Lee *et al*., 1994, Bilgin *et al*., 2003, Svärd *et al*., 2011, Wen *et al*., 2011), HA-tag (Oyadomari *et al*., 2006), (GAL4 DNA binding domain) BD-tag (Gale *et al*., 1996) or (DNA activation domain) AD-tag (Bilgin *et al*., 2003). Lee *et al*., also found DNAJC3 to be highly insoluble, and since they used the His-tag, they were able to use a denaturing and refolding purification protocol (Lee *et al*., 1994). However this approach cannot be used with a GST-tagged protein because the GST tag will also be denatured since it is a proteins that relies on the three-dimensional structure in order to bind to its ligand during affinity chromatography.

In the few studies that have been able to purify GST-tagged DNAJC3 (Lee *et al*., 1994, Tan and Katze, 1998), the expression of DNAJC3 was induced with 0.1 or 1 mM IPTG at 37 °C for 3-4 hours, which was similar to the original protocol utilized in this study. Studies have used the expression and purification protocol from Lee *et al*., for producing recombinant GST-tagged DNAJC3 (Gale *et al*., 1996, 1998, Melville *et al*., 1997, 1999, Yan *et al*., 2010), however none of these studies have ever published their purification results, making it difficult to compare the yield and purity of the purified protein. YanLong *et al* (2009) were able to express and purify a GST-tagged DNAJC3 recombinant protein by using a specialized *E. coli* expression strain Rosetta (YanLong *et al*., 2009), however attempts to express DNAJC3 in specialized expression strains (BL21 C41 [DE3] and BL21 C43 [DE3]) were unsuccessful.

Ultimately, the combination of lowering the expression temperature, time and IPTG concentration, resulted in increased solubility of the GST-tagged DNAJC3ΔJ/ER protein which allowed purification of sufficient quantities of the protein to be possible. Although GST-tagged

DNAJC3ΔJ/ER was purified successfully, two proteins at 50 kDa and 26 kDa were consistently being co-purified with DNAJC3ΔJ/ER, and through Western analysis with GST specific antibodies, were found to be GST-tagged (Figure 4.9). Although not conducted in this study, size exclusion chromatography could be performed on the elution fractions to remove the co-eluting contaminants. The presence of co-eluting contaminants in the elution fractions could negatively impact subsequent interaction assays as the contaminants have the potential to participate and influence the interaction results. However, the co-eluting contaminants in this study were determined to be GST tagged, suggesting that they were truncations of DNAJC3ΔJ/ER, hence size exclusion chromatography was not conducted. Since the focus of the study was to evaluate binding by the TPR motifs within DNAJC3, these results were deemed sufficient to allow the *in vitro* interaction analysis using the DNAJC3ΔJ/ER protein.

Chapter 5: *In vitro* analysis of protein-protein interactions of DNAJC3 TPR domains

5.1 Introduction

DNAJC3 TPR domains lack the residues required to form the carboxylate clamp and the electrostatic charged environment necessary to form and maintain a stable interaction with the EEVD motifs of Hsp90 and Hsp70 (Figure 3.4, 3.5, 3.6) (Tao *et al*., 2010). The ER homologues of Hsp90 and Hsp70, Grp94 and Grp78 lack the EEVD motif at the C-terminal required to interact with TPR domains of co-chaperones such as HOP (Argon and Simen, 1999, Scheufler *et al*., 2000, Odunuga *et al*., 2003, Fewell *et al*., 2004). Although DNAJC3 interacts with and stimulates the ATPase activity of Hsp70 (Melville *et al*., 1999) and Grp78 (Oyadomari *et al*., 2006, Rutkowski *et al*., 2007, Tao *et al*., 2010; Svärd *et al*., 2011), this interaction is mediated by the J domain. DNAJC3 exists in a complex with Grp78 and Grp94 (Jansen *et al*., 2010), but it is unknown whether DNAJC3 and Grp94 interact directly. The protein $p88^{rIPK}$, a known inhibitor of DNAJC3, has been shown to share limited structural homology with the charged linker region of Hsp90 (Gale *et al*., 1998) and in this study we have expanded this analysis to include the charged linker region of Grp94 (Figure 3.8, B). This chapter sought to test *in vitro* whether the TPR domains of DNAJC3 to interact with chaperones. The specific objectives were to:

- Determine whether DNAJC3 TPR domains interact with purified chaperones
- Determine whether DNAJC3 TPR domains bind native and heat denatured substrates
- Determine whether DNAJC3 TPR domains form complexes with heat denatured substrate, Grp78 and/or Grp94 *in vitro*
- Determine whether DNAJC3 TPR domains have refoldase activity

5.2 Results

5.2.1 DNAJC3 TPR domains do not form a direct interaction with Grp94 or Hsp90

DNAJC3 TPR domains lack the residues crucial for the interaction with Hsp90 through the EEVD motif, while at the same time the ER homologue of Hsp90, Grp94 lacks the EEVD motif. (Argon and Simen, 1999) DNAJC3 and Grp94 have been shown to exist in a complex together (Jansen *et al*., 2012) and multiple sequence alignment has illustrated that the charged linker region of both Hsp90 and Grp94 shared limited structural homology with $p88^{rIPK}$, an inhibitor of DNAJC3. A pull down assay was conducted to determine whether DNAJC3 TPR domains interact with both Grp94 and Hsp90, independent of the carboxylate clamp residues and the EEVD motif. A total of 10 µg of GST tagged bait protein (GST, mSTI1 DNAJC3ΔJ/ER) was incubated overnight at 4 °C with 1 µg of Hsp90, Grp94 or $Grp94_{284\text{-}543}$ (encoding the middle domain and the C-terminal end of the charged linker region of Grp94), washed and the pull down reactions analyzed by SDS-PAGE and Colloidal Coomassie staining (Figure 5.1). mSTI1 is the mouse homologue of HOP, a TPR-containing protein know to interact with both Hsp90 and Hsp70 through the TPR domains (Scheufler *et al*., 2000, Odunuga *et al*., 2003), similar to DNAJC7. As the purification of GST-DNAJC7 was unsuccessful (Figure 4.12, D), recombinant GST-tagged mSTI1 was utilized as a positive control.

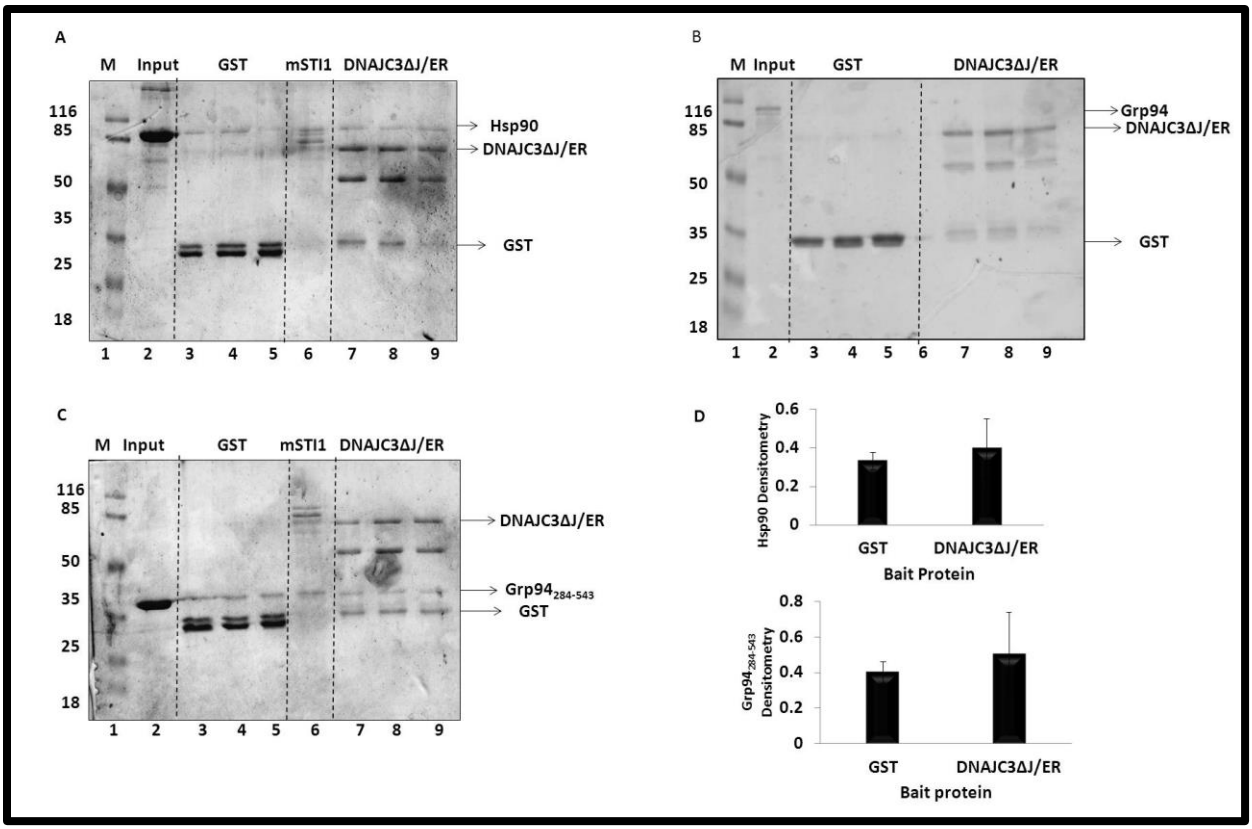

Figure 5.1: DNAJC3 TPR domains do not interact directly with Hsp90 or Grp94. DNAJC3ΔJ/ER protein-protein pull down assay with (A) Hsp90 (B) Grp94 (C) Grp94$_{284-543}$. Lane 1: Marker, Lane 2: Input. Lane 3-5: triplicate pull down reactions with GST protein, Lane 6: GST tagged mSTI1 and Lane 7-8: triplicate pull down reactions with GST tagged DNAJC3ΔJ/ER. (D) Densitometry analysis of interaction between bait proteins and (upper) Hsp90 and (lower) Grp94 middle domain

DNAJC3ΔJ/ER did not interact directly with purified Hsp90, Grp94 or Grp94$_{284-543}$ in this study (Figure 5.1, A, B and D, Lane 7-9). Although bands were observed in the DNAJC3ΔJ/ER lanes that correlated to Hsp90 and Grp94$_{284-543}$ (compared to the input lane), bands were present in GST samples, which served as a negative control (Figure 5.1, A and C, compare lanes 3-5 and lanes 7-8). GST protein has previously been shown to bind indiscriminately to various purified proteins, prompting the need to conduct densitometry analysis to determine the total amount of Hsp90 or Grp94$_{284-543}$ bound directly to DNAJC3ΔJ/ER and not the GST tag. The value of Hsp90 or Grp94$_{284-543}$ bound to the GST protein was subtracted from the value of Hsp90 or Grp94$_{284-543}$ bound to GST-tagged DNAJC3ΔJ/ER (Figure 5.1, D). The difference was taken as a representation of the amount Hsp90 and Grp94$_{284-543}$ bound directly to DNAJC3ΔJ/ER. Based on the densitometry analysis, the difference in levels of Hsp90 or Grp94$_{284-543}$ bound to GST compared to GST-tagged DNAJC3ΔJ/ER was not significant.

5.2.2 DNAJC3 TPR domains interacted with both native and denatured substrate

Interaction of full length DNAJC3 with Grp78 and Hsp70 is mediated by the J domain (Melville *et al*., 1999, Oyadomari *et al*., 2006, Rutkowski *et al*., 2007, Tao *et al*., 2010; Svärd *et al*., 2011). In order to determine whether DNAJC3 TPR domains could interact with Hsp70 and Grp78 independent of the J domain, a pull down assay was conducted. A total of 10 µg of GST tagged bait protein (GST, mSTI1 or DNAJC3ΔJ/ER) was incubated overnight at 4 °C with 1 µg of either Hsp70 or Grp78, washed and the reactions analyzed by SDS-PAGE and Colloidal Coomassie staining (Figure 5.2).

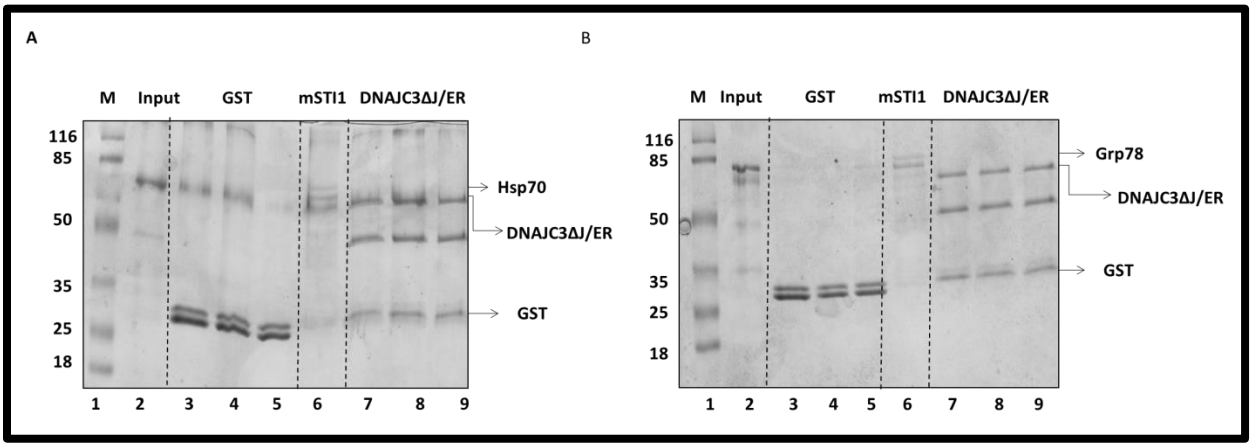

Figure 5.2: DNAJC3 TPR domains do not interact directly with Hsp70 or Grp78. DNAJC3ΔJ/ER protein-protein pull down assay with (A) Hsp70 (B) Grp78. Lane 1: Marker, Lane 2: Input. Lane 3-5: triplicate pull down reactions with GST protein, Lane 6: GST tagged mSTI1 and Lane 7-8: triplicate pull down reactions with GST tagged DNAJC3ΔJ/ER.

DNAJC3ΔJ/ER did not interact in this assay with either purified Hsp70 or Grp78 as illustrated by the absence of a band below the 85 kDa marker (Figure 5.2, A and B, Lane 7-9). However, mSTI1 was able to interact with Hsp70 but not with Grp78, as Grp78 lacks the EEVD motif needed to mediate the interaction (Fewell *et al*., 2004) (Figure 5.2, A and B, Lane 6).

The TPR1 domain of DNAJC3 TPR1 has been shown to bind denatured proteins through its hydrophobic pocket during its co-chaperone functions to Grp78 during UPR (Tao *et al*., 2010). Previously, DNAJC3 TPR domains were shown been to have selective binding affinity for chemically denatured luciferase compared to native luciferase (Tao *et al*., 2010). An ELISA was conducted to determine whether the three DNAJC3 TPR domains bound discriminately to heat denatured or native substrates, using two model substrates, MDH and β-galactosidase (Figure 5.3).

As previously stated, the GST protein is known to bind indiscriminately to purified proteins, therefore GST alone was included in the ELISA as a negative control and His-tagged Grp78 was used as a positive control for substrate binding as it has been shown to bind to denatured substrate (Tao *et al*., 2010).

Grp78 bound both denatured and native substrates, although the chaperone had greater binding affinity for heat denatured MDH than β-galactosidase (Figure 5.3, A and B). DNAJC3ΔJ/ER bound both native and heat denatured β-galactosidase and MDH (Figure 5.3 A and B). DNAJC3ΔJ/ER bound denatured β-galactosidase with greater affinity than native β-galactosidase (Figure 3.3 A), however there was no substantial difference in the binding affinity between native or denatured MDH (Figure 3.3, B). there was a dose dependent increase in the binding of both native and denatured MDH to the TPR domains of DNAJC3, while β-galactosidase binding was dose dependent up to 50 μ/ml (Figure 5.3, A and B).

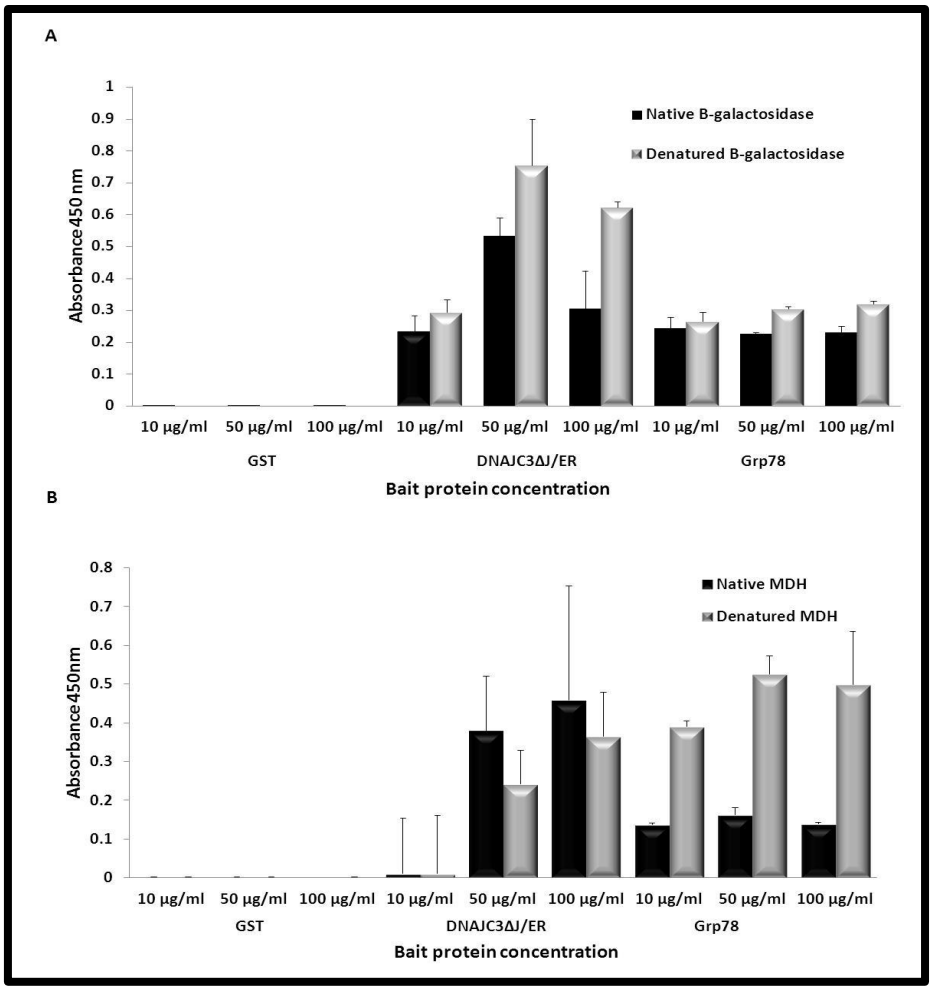

Figure 5.3: DNAJC3 TPR domains interacted with both native and heat denatured model substrate proteins. 50 µg/ml of native and heat denatured substrate (A) β-galactosidase and (B) MDH were coated onto high binding 96 well plates, none specific binding was blocked with 5 % BSA, followed by incubation with different concentrations (10 – 100 µg/ml) of bait proteins (GST, DNAJC3ΔJ/ER and His-Grp78). Wells were incubated with GST or His specify primary and secondary antibodies. TMB substrate solution and H_2SO_4 were used to develop and stop the reaction, respectively, absorbance was read at 450 nm.

To further characterize the functions of DNAJC3 TPR domains, complex formation analysis was conducted to determine the ability of DNAJC3 TPR domains to form complexes with Grp78 and or Grp94 and denatured substrate *in vitro*. The complex formation assay was conducted using two methods, namely purified proteins pull down assay and ELISA. For the ELISA analysis, two different concentrations of heat denatured β-galactosidase (50 and 100 µg/ ml) were incubated with fixed concentrations of His-Grp78 (50 µg/ ml) and DNAJC3ΔJ/ER (20 µg/ ml) and the capacity of DNAJCΔJ/ER to bind Grp78 was compared in the presence or absence of heat denatured β-galactosidase. For the pull down method, different combinations as DNAJC3ΔJ/ER, Grp78 and Grp94 where incubated in the presence or absence of heat denatured β-galactosidase,

with GST being used as a negative control. However, DNAJC3ΔJ/ER was unable to form a complexes with either Grp94 or Grp78 or a combination of both in the presence or absence of heat denatured β-galactosidase *in vitro* (data not shown), although full length DNAJC3, Grp94 and Grp78 have been found in a complex together *in vitro* (Jansen *et al*., 2012). A guanidine-HCl denatured luciferase refolding assay was conducted in an attempt to further characterize a potential refoldase function for the of DNAJC3 TPR domain. However, DNAJC3ΔJ/ER was unable to refold chemically denatured luciferase into a functional enzyme or enhance the refolding capacity of Grp78 (data not shown), suggesting that DNAJC3 TPR domains do not exhibit refoldase activity.

5.2.3 DNAJC3 TPR domains are able to pull down Hsp90 and Grp94 from MCF-7 carcinoma cell lysates

DNAJC3 has previously been shown to be part of a complex consisting of Grp94 and Grp78, through a lysate pull down reaction using Grp78 as the bait protein (Jansen *et al*., 2012). A lysate pull down was conducted using DNAJC3ΔJ/ER to determine whether DNAJC3 TPR domains could mediate interacts with cytosolic and ER Hsp90 and Hsp70 proteins *ex vivo*.

The expression levels of DNAJC3, Hsp90 and Hsp70, and the ER homologues Grp94 and Grp78, was examined in five different cancerous cell lines (Figure 5.4). The chaperones were found to be expressed in detectable amounts in all cell lines analyzed, however the expression levels of the chaperones differed between the cell lines. The MCF-7 carcinoma cell line was chosen for use in subsequent experiments, although the expression level of Hsp90 in this cell line was low compared to the other cell lines.

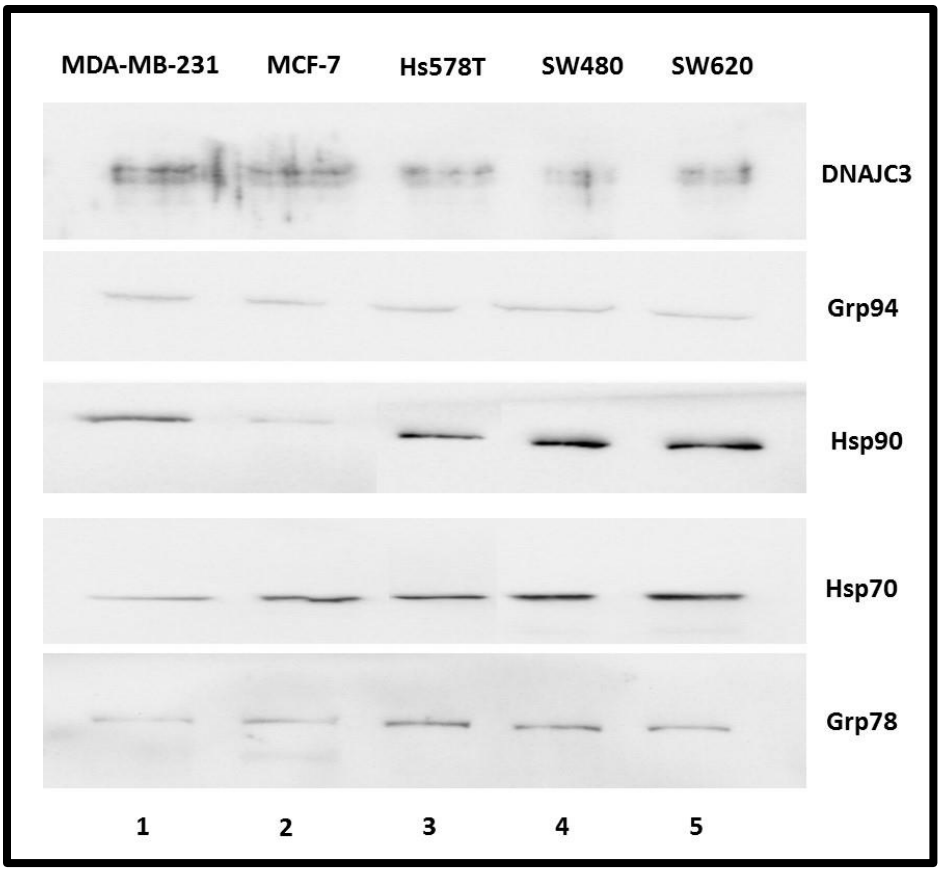

Figure 5.4: Expression profile of chaperones in five mammalian cancer cell lines: An equal amount of total protein (50 µg) from each cell line was analyzed. Expression levels of Hsp90, Hsp70, Grp78, Grp94 and DNAJC3 were detected using monoclonal mouse anti-Hsp90, anti-Hsp70 and anti-Grp78, monoclonal rat anti-Grp94 and polyclonal rabbit anti-DNAJC3.

To conduct the lysate pull down assay, 20 µg of purified recombinant protein, GST (negative control), GST-tagged mSTI1 (positive control, kind donation from Samantha Beckley, Rhodes University) and GST-tagged DNAJC3ΔJ/ER were incubated with MCF-7 cell lysates overnight at 4 °C, washed and analyzed by Western analysis for the presence of Hsp90, Hsp70, Grp78 and Grp94 (Figure 5.5).

Negative control GST showed no signal for the analyzed proteins with the exception of a faint signal for Hsp70 and Grp94 in one of the independent replicate samples (Figure 5.5, Lane 3). As expected, mSTI1 was able to pull down Hsp70 as previously illustrated (Odunuga *et al*., 2003), however Hsp90 which has also been shown to interact with mSTI1 was not detected in the same samples (Figure 5.5, lane 5-6). GST-tagged DNAJC3ΔJ/ER was unable to pull down both Grp78 and Hsp70 as previously shown (Rutkowski *et al*., 2007). However, the protein was able to pull down both Hsp90 and Grp94 (Figure 5.5, lane 7-8). Previous studies have shown that endogenous

full length DNAJC3 can be pulled down in a complex that consists of both Grp78 and Grp94 (Jansen *et al*., 2012).

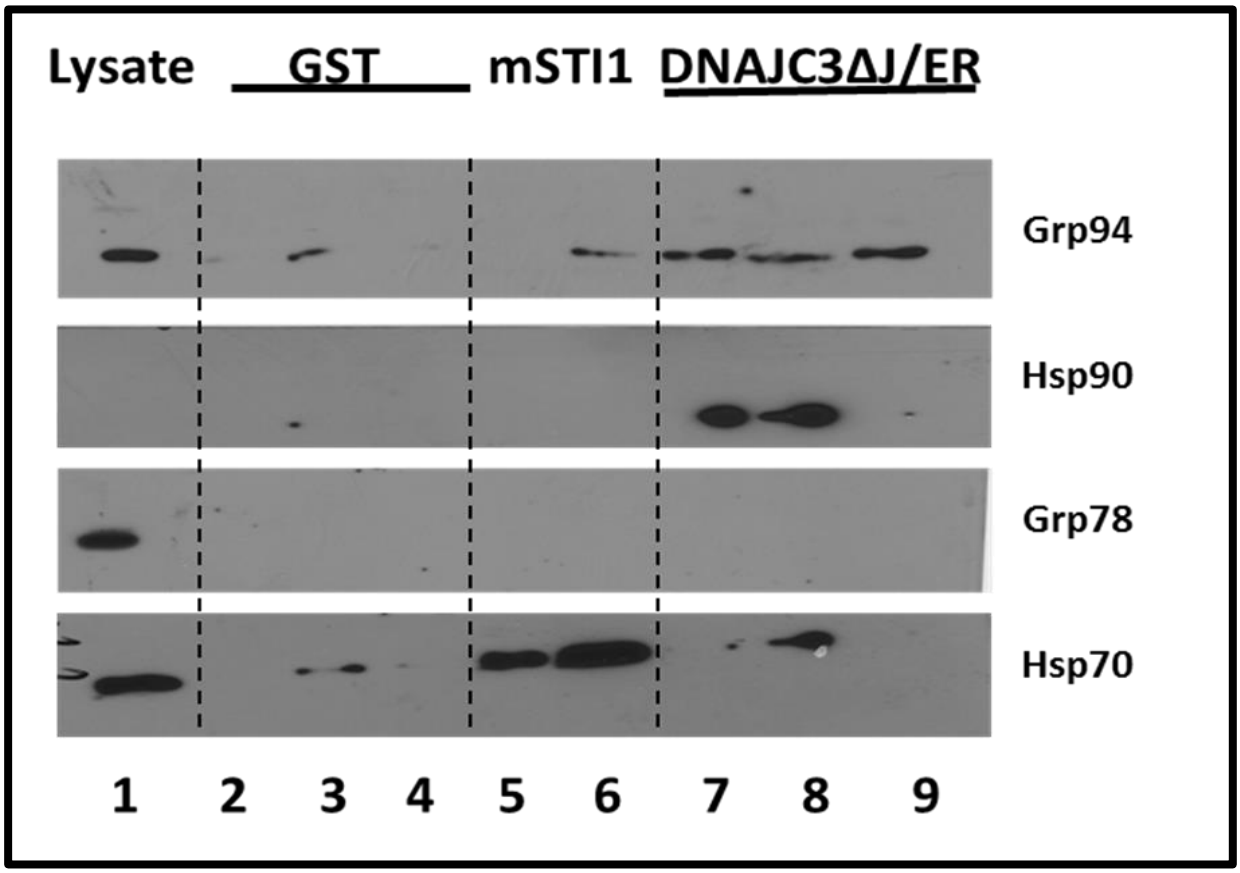

Figure 5.5: DNAJC3 TPR domains are able to pull down Hsp90 and Grp94 and not Hsp70 or Grp78 from MCF-7 cell lysates. Pull down assays were conducted by incubating 20 µg of purified bait protein (GST and GST-DNAJC3ΔJ/ER) with MCF-7 lysates overnight and analyzed by Western analysis. Lane 1: MCF-7 cell lysate, Lane 2-4: GST protein, Lane 5-6, GST-mSTI1 and Lane 7-9: GST-DNAJC3ΔJ/ER. n=3.

5.3: Discussion

This chapter described the *in vitro* interaction analysis of DNAJC3 TPR domains with chaperones. DNAJC3 TPR domains did not interact directly with purified Hsp90, Hsp70 or the ER homologues, Grp94 and Grp78, although the TPR domains were able to pull down Grp94 and Hsp90, but not Hsp70 or Grp78, from MCF-7 carcinoma cell lysates. In addition, DNAJC3 TPR domains were able to bind both native and heat denatured substrates but could not form complexes with denatured substrates, Grp78 and/or Grp94 and did not exhibit independent refoldase activity.

Previously, full length DNAJC3 has been shown to be in a multicomplex with Grp94 and other chaperones such as Grp78 and refolding enzyme, PDI (Jansen *et al*., 2012), but whether this interaction was due to direct binding was unknown. This study showed experimentally that DNAJC3 TPR domains cannot interact directly with either Hsp90 or Grp94. Interaction between Hsp90 with TPR containing co-chaperones such as HOP is dependent of the interaction of the carboxylate clamp forming residues of TPR domains and the EEVD motif located on the C-terminal domain of Hsp90 (Odunuga *et al*., 2003). However, Grp94 lacks the EEVD motif (Figure 3.7) (Argon and Simen, 1999, Tastan Bishop *et al*., 2013). In addition, DNAJC3 TPR domains lack the carboxylate forming residues found in co-chaperones such as HOP (Figure 3.4) (Tao *et al*., 2010), suggesting that any potential interactions that occur between DNAJC3 and Grp94 and or Hsp90 would be EEVD motif and carboxylate clamp independent. We initially predicted that the limited structural homology of $p88^{rIPK}$ with the charged linker region of Hsp90 (Gale *et al*., 1998) and of Grp94 (Figure 3.8), might indicate a possible alternative interaction site between DNAJC3 TPR domain and Hsp90 and or Grp94. However, our data suggest that DNAJC3 TPR domains cannot interact directly with Hsp90 or Grp94, irrespective of the EEVD motif, and the charged linker region of both Grp94 and Hsp90 is not a possible alternative binding site for DNAJC3 via its TPR domain. These observations suggest that the interaction between DNAJC3 and Grp94 with in the isolated complex was mediated by other proteins present in the complex such as Grp78 and PDI or the client protein (Jansen *et al*., 2012). Cytosolic Hsp90 chaperone activity is dependent on the assistance of numerous co-chaperones such as p23, Aha1 and Cdc37, there are no known co-chaperones of Grp94. Although DNAJC3 was found not to interact directly with Grp94 *in vitro* in this study, their co-existence in a complex could suggest DNAJC3 acts a co-chaperone to Grp94 in concert with other proteins. Cyclophilin B, an ER isoform of Hsp90 co-chaperone Cyp40 that lacks the TPR domain was pulled down in a multiprotein complex that contained several chaperones including Grp94. (Meunier *et al*., 2002). These two examples of proteins with known co-chaperoning activity existing in complexes with Grp94, strongly suggests that the later protein could have potential co-chaperones that have yet to be identified. Cell lysate pull down using Grp94 as bait protein, along with mass spectrometry could be conducted to identify proteins that interact with the chaperone that could possible function as co-chaperone. Assays such as ATPase, substrate aggregation suppression, refolding and complex formation assay

could be conducted to determine if the identified protein do determine whether they exhibit co-chaperone activity towards by assisting and enhancing Grp94 chaperoning activity.

DNAJC3 TPR domains in the absence of the J domain were also unable to interact directly with either Hsp70 or Grp78 in vitro. The TPR domains of DNAJC3 are known to bind denatured proteins through the hydrophobic pocket of TPR1 (Tao *et al*., 2010) while the J domain stimulates the ATPase activity of both Hsp70 (Melville *et al*., 1999) and Grp78 (Oyadomari *et al*., 2006, Rutkowski *et al*., 2007, Tao *et al*., 2010; Svärd *et al*., 2011). This suggested that the J domain is required to mediate interactions between DNAJC3 and Hsp70 or Grp78 (Green *et al*., 1998, Kampinga and Craig, 2010, Gao *et al*., 2012). mSTI1, known to interact through the carboxylate clamp residue with the EEVD motif found in cytosolic Hsp70 (Odunuga *et al*., 2003) was able to interact with Hsp70. Grp78 also lacks the EEVD motif found in cytosolic Hsp70 and was found to not interact with both mSTI1 and DNAJC3ΔJ/ER, illustrating the importance of both the EEVD motif and the carboxylate clamp forming residues to mediate binding.

DNAJC3ΔJ/ER was however found to be able to bind both native and heat denatured model substrates, MDH and β-galactosidase (Figure 5.3). Mouse DNAJC3 TPR1 has been shown to have higher binding affinity toward chemically denatured luciferase than native luciferase (Tao *et al*., 2010). The human DNAJC3 TPR domains used in this study, were able to bind both native MDH and β-galactosidase at levels comparable to heat denatured MDH and β-galactosidase (Figure 5.3). Mouse and human DNAJC3 proteins are highly conserved at both the primary (Figure 3.1) and secondary structural levels (Svärd *et al*., 2011) which strongly suggests functional similarities. The ability of human DNAJC3 TPR domains to bind to both native and denatured substrates observed in the mouse counterparts could possibly be linked to the subtle difference observed between in the overall shape of the TPR domains in mouse and human DNAJC3 proteins (Svärd *et al*., 2010). The differences were found to be a result of the rotations of the long seventh and thirteenth helices that connect TPR1 to TPR2 and TPR2 to TPR3, respectively. The rotations brought the three human TPR domains closer, resulting the DNAJC3 having a more curved shape than mouse DNAJC3 (Svärd *et al*., 2011). However the possibility that the structural difference observed could affect the physiological function of the proteins is yet to be determined. Alternatively, the indiscriminate binding to both native and denatured substrates, could be linked to substrate specificity, as even between the two different substrates, DNAJC3ΔJ/ER seemed to bind β-galactosidase with greater affinity compared to MDH (Figure 5.3). Therefore, the human DNAJC3

TPR domains can bind denatured substrates, MDH and β-galactosidase, similar to mouse DNAJC3 TPR1 domain which bound luciferase (Tao *et al*., 2010). Human DNAJC3 TPR2 and TPR3 could possibly be selectively binding to native MDH and β-galactosidase, with greater affinity for β-galactosidase, illustrating substrate specify. However, this suggestion is purely conjecture as substrate binding capabilities of TPR2 and TPR3 of DNAJC3 have not been studied. We can conclude from the murine study that it is likely that TPR2 and 3 of human DNAJC3 act in a similar manner to TPR1. *In silico* analysis conducted in Chapter 3 of this study strongly suggested that DNAJC3 TPR2 and TPR3 had the capability to interact with diverse substrates. The domains were demonstrated to share structural (Figure 3.12, 3.13, 3.14) and chemical (Figure 3.16) similarities to TPR-containing proteins such as MamA, a known adaptor protein involved in the assembly of proteins in magnetotatic bacteria (Zeytuni *et al*., 2011) and PcrH, a chaperone of PopB and PopD, translocator proteins involved in the translocation of protein across membranes (Page and Parsot, 2002, Parsot *et al*., 2003).

DNAJC3ΔJ/ER could not form a complex with Grp78 and or Grp94 in the absence or presence of denatured β-galactosidase (data not shown) and altering the range of concentrations of denatured substrate did not improve binding (data not shown). These observations suggested that although DNAJC3 TPR domains were capable of binding denatured β-galactosidase (Figure 5.3, A), they could not mediate the formation of substrate complexes with Grp78 and or Grp94. Indeed, the presence of DNAJC3 may have prevented binding of chaperones to substrate proteins. The J domain is known to be crucial for the interaction of DNAJ and Hsp70 proteins (Greene *et al*., 1998, Kampinga and Craig, 2010, Gao *et al*., 2012), and DNAJ and Hsp70 through their interaction, are components of the early complex in Hsp90 mediated substrate folding or maturation (Figure 1.2) (Mahalingam *et al*., 2009, Li *et al*., 2013). These data might suggest DNAJC3 TPR domain cannot induce substrate-chaperone interactions in the absence of the J domain. Alternately, the formation of complexes between DNAJC3, Grp78 and or Grp94 could be substrate specific, especially in the case of Grp94. Unlike Grp78, which was shown by use to be able to bind denatured model substrates, Grp94 is known to be highly selective of the client protein it chaperones (Randow and Seed, 2001, Yan *et al*., 2005, Morales *et al*., 2009). This might suggest that the substrate used in this study β-galactosidase, could not mediate the formation of a complex because it was not a true representation of substrates that require DNAJC3, Grp78 and or Grp94 for its maturation. Follow up studies could attempt the complex formation assay using a known

client of Grp78 and Grp94, however majority of Grp94 client proteins are transmembrane and secretory proteins and these proteins are known to be difficulty to express in *E.coli* cells (Melnick *et al*., 1994, Randow and Seed, 2001, Marzec *et al*., 2012).

Despite being previously shown to bind denatured luciferase, DNAJC3ΔJ/ER did not exhibit any refoldase activity or enhance the refoldase activity of Grp78 (data not shown). Several members of the DNAJA and DNAJB proteins have been shown to have chaperone activity independent of Hsp70 and Hsp90, where they can bind newly synthesised protein and supress protein aggregation or maintain them in a conformation favourable for folding (Langer *et al*., 1992, Cyr, 1995, Freeman and Morimoto, 1996, Meacham *et al*., 1999, Lee *et al*., 2002). Numerous TPR-containing protein have also been shown to have chaperoning activity independent of Hsp90 or Hsp70, such as PcrH, a chaperone for translocator protein PopB and PopD in *Pseudomonas aeruginosa* (Page and Parsot, 2002, Bröms *et al*., 2003, 2006, Parsot *et al*., 2003, Jobs *et al*., 2010) and another chaperone SycD also involved in chaperoning translocator protein YopD and YopB in *E. coli* (Neyt and Cornelis, 1999, Schreiner and Neimann, 2012. The observed results suggested that DNAJC3 TPR domains do not have refoldase activity, observed in other DNAJ proteins. However, at present Hsp90 and Hsp70 independent chaperone activity has only been detected in members of DNAJA and DNAJB proteins and not DNAJC proteins (Langer *et al*., 1992, Cyr, 1995, Freeman and Morimoto, 1996, Meacham *et al*., 1999, Lee *et al*., 2002). DNAJC3 is a member of the DNAJC family, which possibly indicated that the likelihood of DNAJC3 exhibit ATP dependent chaperoning activity similar to DNAJA and DNAJB members was improbable. The incapability of DNAJC3ΔJ/ER to enhance Grp78 refoldase activity observed could be linked to the absence of the J domain, which is known to stimulate Grp78 ATPase dependent protein refolding (Freeman *et al*., 1995, Oyadomari *et al*., 2006, Galam *et al*., 2007, Rutkowski *et al*., 2007). Although DNAJC3 TPR domains were illustrated to not exhibit refoldase in this study, other chaperoning activities such as substrate aggregation suppression or translocation could be examined in the future.

Pull down assay experiments conducted in this study showed that DNAJC3 TPR domains did not interact with Grp94, Grp78, Hsp90 or Hsp70 *in vitro.* Therefore, we conducted a mammalian cell lysate pull down assay. As previously shown by Odunuga and colleagues, mSTI1, mouse homologue of HOP used as a positive control was able to pull down Hsp70 (Odunuga *et al*., 2003) but not Grp78. DNAJC3ΔJ/ER was unable to consistently pull down either Hsp70 or Grp78 from MCF-7 carcinoma cell lysate (Figure 5. 5, lanes 5-6 and 7-9), coinciding with the findings of

Rutkowski *et al*., 2007. This observation further supported the idea that DNAJC3 and Grp78 interaction is mediated and dependent on the J domain.

Although full length DNAJC3 has been shown to be part of a complex with Grp78 and Grp94 *in vivo* through a pull down assay using Grp78 as bait protein (Jansen *et al*., 2012), the current study was the first to demonstrate the ability of DNAJC3 TPR domains to pull down both Hsp90 and Grp94 from a cell lysate. However, our data suggest that the ability of DNAJC3 TPR domains to pull down both Hsp90 and Grp94 is not a result of direct interaction between with the chaperones. This suggested that DNAJC3 and Grp94 or Hsp90 might be components of a complex that is Grp78 or Hsp70 independent and mediated by DNAJC3 TPR domains. The interaction between DNAJC3 and Grp94 might be facilitated by a specific cellular substrate protein, distinct from the as the model substrate β-galactosidase which was unable to mediate the formation of a complex between DNAJC3 TPR domains and isolated Grp94 *in vitro* (data not shown). Grp94 is known to be highly discriminate with respect to client proteins (Ostrovsky *et al*., 2009, 2010).

The absence of Grp78 from the complex could possibly be a result of the chaperone not being required for the folding or maturation of the unknown substrate. The maturation of IGF, a known Grp94 client, has been shown to require the chaperoning activity of Grp94 without assistance from Grp78 (Ostrovsky *et al*., 2009, 2010). Alternatively, a number of proteins have been shown to require assistance from Grp78 and Grp94 at different stages of their maturation or folding (Eletto *et al*., 2010). To further understand the interaction between DNAJC3 TPR domains and Hsp90 or Grp94, the pull down assay could be repeated in the presence of known Hsp90 and Grp94 inhibitors such as GA and NOVO to determine whether the inhibition of Hsp90 and Grp94 ATPase activity affects the interaction. In addition to inhibition studies, the pull down assay could be repeated and the co-precipitating proteins identified by mass spectrometry in an attempt to identify the substrate mediating the interaction between DNAJC3 TPR domains and Hsp90 or Grp94. Mass spectrometry analysis of the pull down assay could also potentially identify additional proteins that might interact with DNAJC3 TPR domains directly or indirectly.

Chapter 6: Preliminary *ex vivo* analysis of DNAJC3 in mammalian cells

6.1 Introduction

This chapter describes the preliminary analysis of DNAJC3 functions in mammalian cells. Studies have shown that DNAJC3 plays a role in diseases such as cancer, diabetes and viral infection. The upregulation or downregulation of DNAJC3 appers to have different consequences in different diseases. In mice, the knockdown of DNAJC3 has been shown to activate apoptosis genes, leading to an increase in β-cell failure, which has been shown to result in moderate diabetic phenotypes (Ladiges *et al*., 2005). DNAJC3 has also been implicated in a variety of cancers such as colon cancer (Ghosh *et al*., 2011) and breast cancer (Gao *et al*., 2012). Overexpression of DNAJC3 has been found to induce malignant tumor formation in mice (Barber *et al*., 1994) and in colon cancer, DNAJC3 expression was reported to be upregulated in the metastatic cell line (SW620) compared to the primary tumor (SW480). (Ghosh *et al*., 2011). Due its inhibitory activity on PRK/PERK activity, DNAJC3 has been shown to have anti-apoptotic properties in several cancers (Tang *et al*., 1999, Gao *et al*., 2012, Huber *et al*., 2013). Additionally, DNAJC3 has also been found to regulate or be regulated by the phosphorylation of kinases downstream of the RAS signalling pathway such as p-38 during influenza virus infection (Luig *et al*., 2010) or AKT during CBV3 infection (Zhang *et al*., 2010b). In order to further understand the role of DNAJC3 in these diseases, it is important to first understand its basic functions and any links to other chaperones and signalling pathways. The specific objectives were to:

- Determine the effects of various stress conditions on the expression and localization of DNAJC3 in HEK293T cells
- Determine the effects of Hsp90 inhibitors GA and NOVO, on DNAJC3 expression in MCF-7 carcinoma cells
- Determine effects of HRas and HRas mutants on the localization and expression of DNAJC3 in HEK293T cells
- Determine the effects of DNAJC3 knockdown on the expression profile of different chaperones and co-chaperones in MCF-7 carcinoma cells

6.2 Results

6.2.1 DNAJC3 is expressed in numerous mammalian cancer cell lines from different tissues

Previous analysis has shown that DNAJC3 is conserved in numerous species (Figure 3.1). Through Western analysis, endogenous DNAJC3 was found to be expressed in nine cancer cell lines from different tissues (Figure 6.1). Tissues represented in the analyses were; breast (Hs578T, MCF-7 and MDA-MB-231), colon (SW620 and SW480), lung (A549), monocytes cell (U937), cervix (HeLa) and kidney (HEK293T).

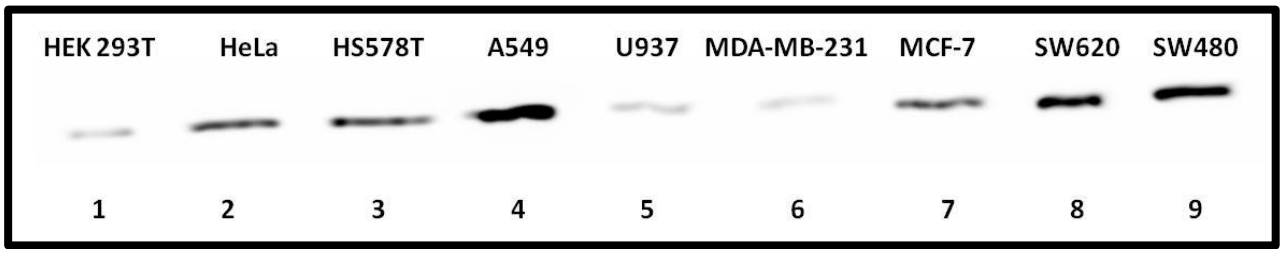

Figure 6.1: Expression of endogenous DNAJC3 in various mammalian cancer cell lines. DNAJC3 was detected in a variety of mammalian cancer cell lines by Western analysis using mouse monoclonal anti-DNAJC3 antibodies. Cell lysate from each cell line was loaded as following: Lane 1: HEK293T, Lane 2: HeLa, Lane 3: Hs578T, Lane 4: A549, Lane 5: U937, Lane 6: MDA-MB-231, Lane 7: MCF-7, Lane 8: SW620 and Lane 9: SW480

6.2.2 Effects of different stress conditions on the expression and localization of DNAJC3 in mammalian cells

DNAJC3 is known to localize and be retained mainly in the ER due to the cleavable ER signal peptide located at the N- terminus of the protein, although a sub population has also been found in the cytoplasm and this is due to the inefficiency of the signal peptide (Rutkowski *et al*., 2007). In order to determine whether localization of DNAJC3 is altered by different stresses, HEK293T cells were subjected to various treatments to induce a wide variety of stress conductions (Table 6.1).

Table 6.1: Summary of treatments used to induce stress in HEK293T cells

Stress Condition	Treatment	Concentration (mM)	Treatment time (Hours)
Normal	Untreated	-	-
ER Stress	Tunicamycin (Tun)	2.38	24
ROS	H_2O_2	0.5	0.25
Hypoxia	$CoCl_2$	0.1	24
Tumor inducer	PMA	5×10^{-5}	2
Proteosome Inhibition	MG132	0.01	2
Heat Shock	Heat (42 °C)	-	2
UV stress	Short UV (254 nm)	-	0.02
UV stress	Long UV (366 nm)	-	0.02

The changes in DNAJC3 localization during stress were compared to that of the control (untreated) cells and Grp94 and Hsp90 were used as indicators of ER and cytoplasmic localization, respectively (Figure 6.2,). In the control cells, DNAJC3 signal was found to be mainly localized around the nucleus with some cytoplasmic staining in all analyzed samples (Figure 6.2, red column). Grp94, a known ER resident protein was also found to be localized around the nucleus (Figure 6.2, green column) similar to DNAJC3. Hsp90 signal was found to be mostly cytoplasmic with faint perinuclear staining in a few cells (Figure 6.2, purple column).

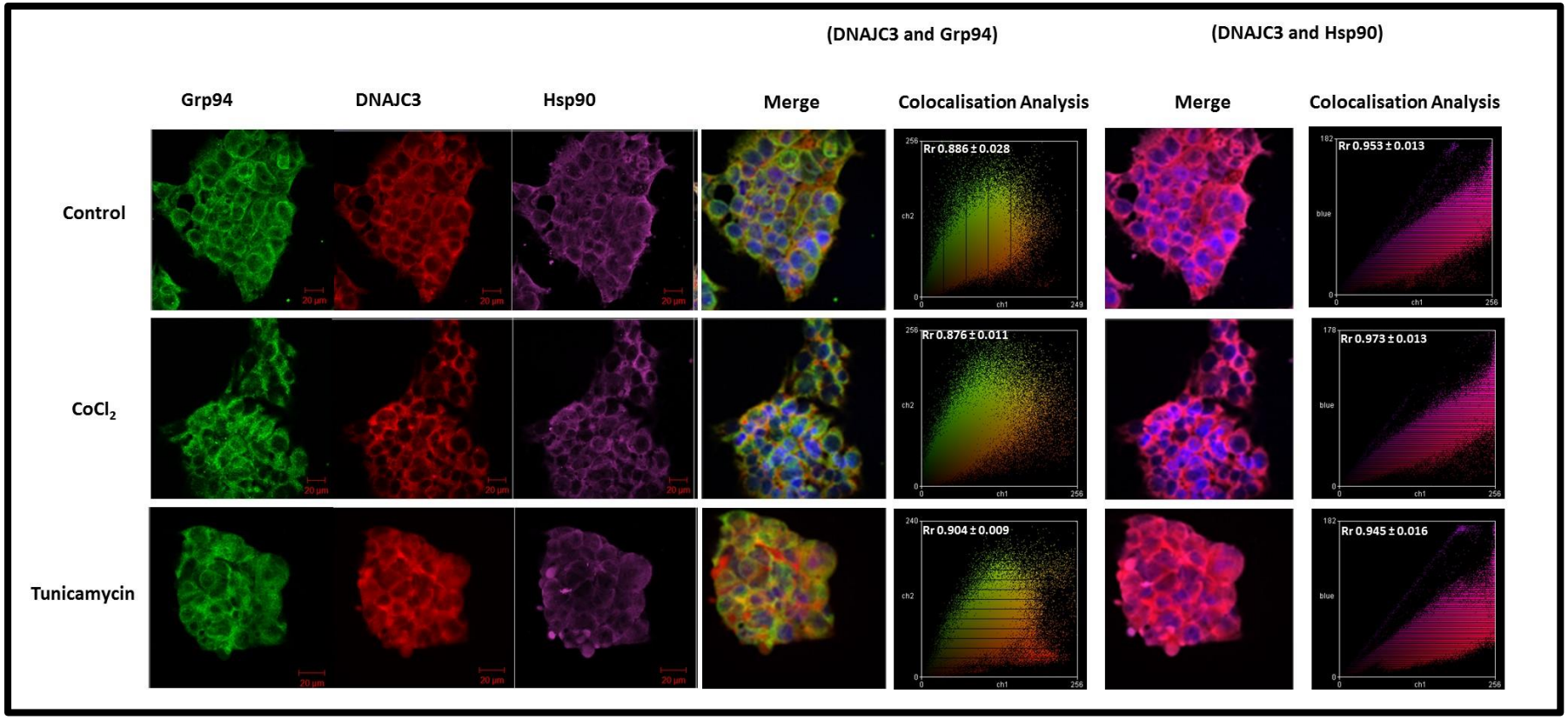
(DNAJC3 and Grp94)
(DNAJC3 and Hsp90)
Grp94
DNAJC3
Hsp90
Merge
Colocalisation Analysis
Merge
Colocalisation Analysis
Control
CoCl2
Tunicamycin
Rr 0.886 ± 0.028
Rr 0.953 ± 0.013
Rr 0.876 ± 0.011
Rr 0.973 ± 0.013
Rr 0.904 ± 0.009
Rr 0.945 ± 0.016
20 µm
ch1
ch2
blue

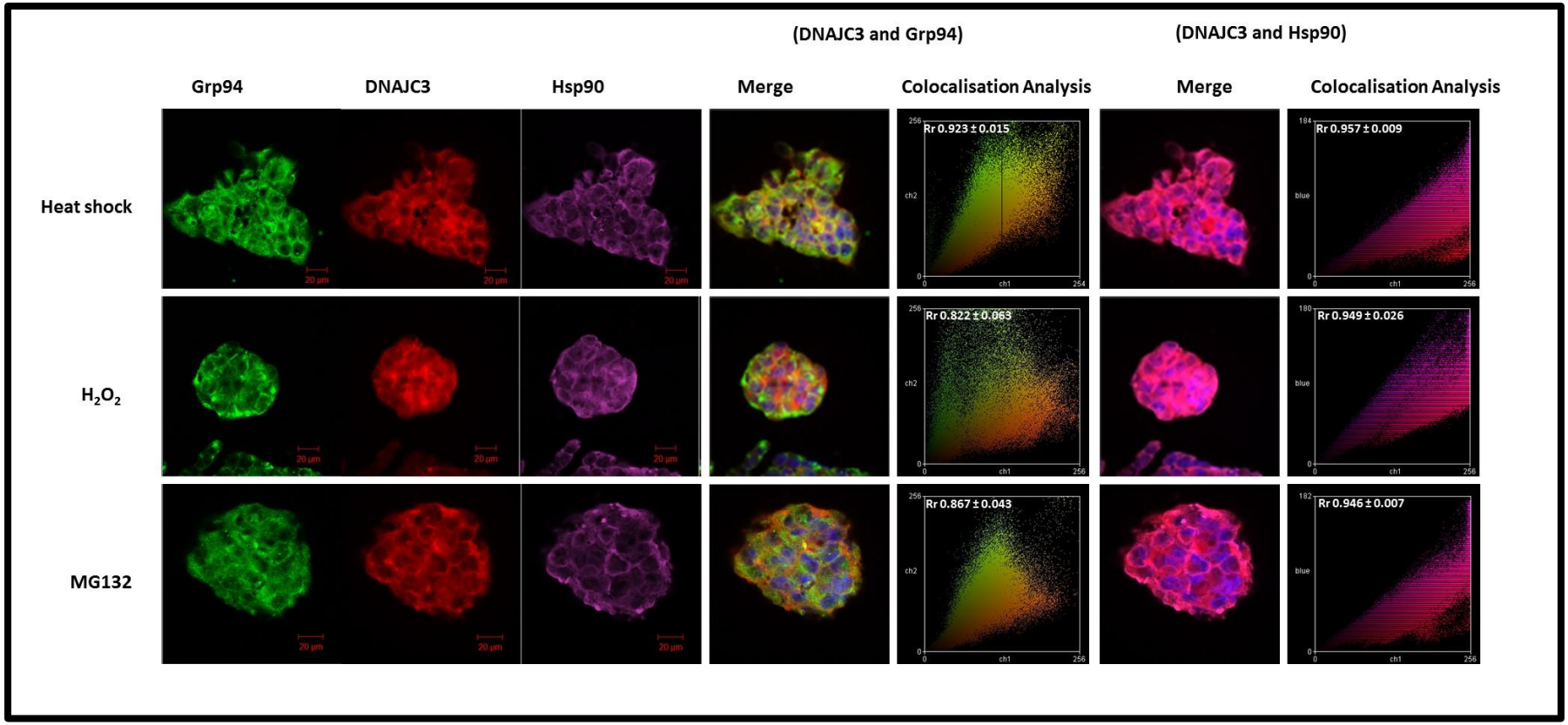
(DNAJC3 and Grp94)
(DNAJC3 and Hsp90)
Grp94
DNAJC3
Hsp90
Merge
Colocalisation Analysis
Merge
Colocalisation Analysis
Heat shock
H2O2
MG132
Rr 0.923 ± 0.015
Rr 0.957 ± 0.009
Rr 0.822 ± 0.063
Rr 0.949 ± 0.026
Rr 0.867 ± 0.043
Rr 0.946 ± 0.007
20 µm
ch1
ch2
blue

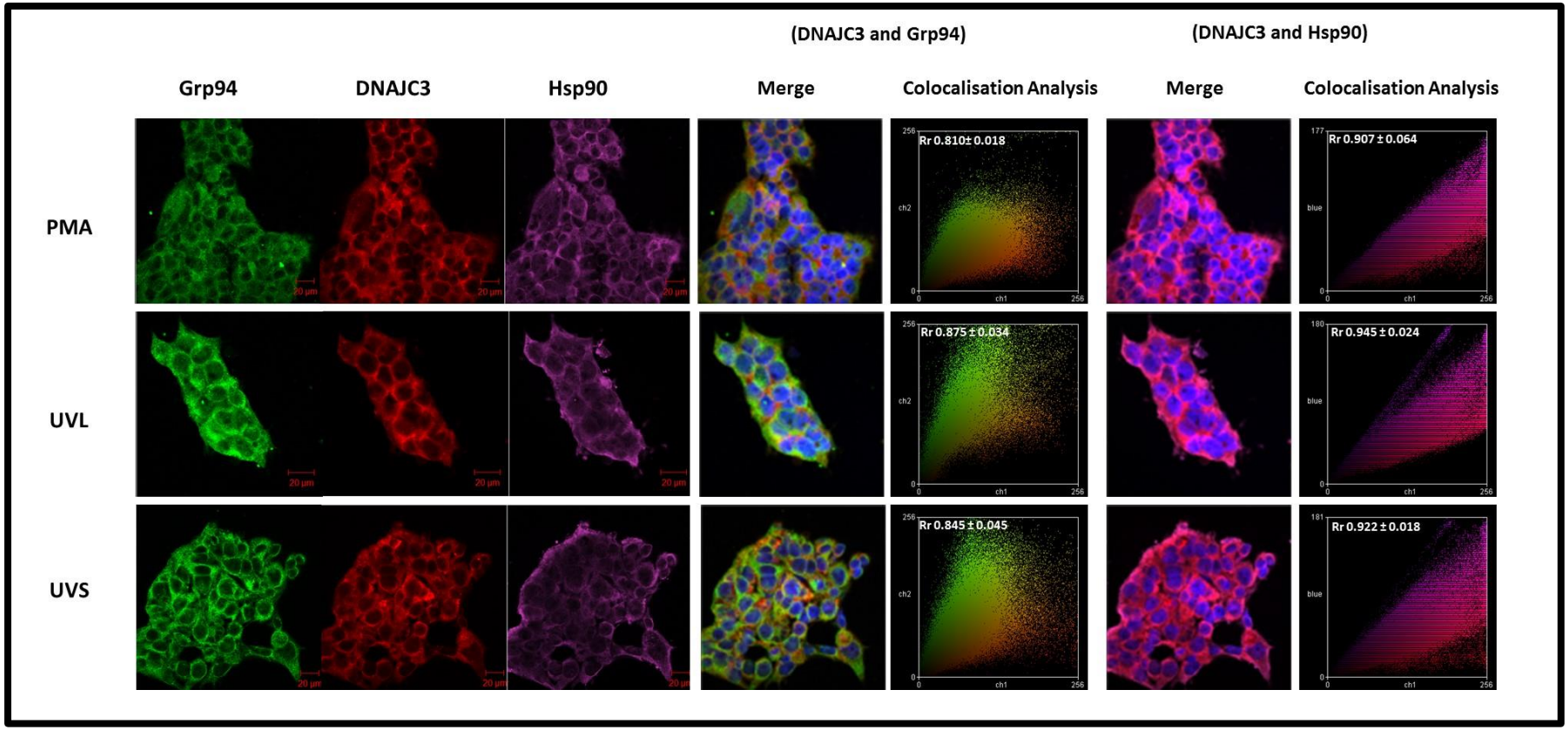

Figure 6.2: Colocalization analysis of DNAJC3, Grp94 and Hsp90 under various stress conditions in HEK293T cells. HEK293T cells were grown on glass coverslips for 24 hours and subjected to various stress conditions as indicated in Table 2.1. After each treatment cells were fixed in ice-cold ethanol, permeabilized and stained with anti-DNAJC3, anti-Grp94 and anti-Hsp90 antibodies. Primary antibodies were detected with species specific Alexa Fluor 546- conjugated secondary antibodies for DNAJC3, Alexa Fluor 488- conjugated secondary antibodies for Grp94 and Alexa Fluor 660- conjugated secondary antibodies for Hsp90. Colocalization analysis was done using ImageJ according to published methods (Zinchuk *et al*., 2010)

Colocalization analysis using ImageJ was also conducted as an additional method to determine whether DNAJC3 and Grp94 or Hsp90 localized to the same organelles or compartments. The analysis was done by determining the signal intensity of the fluorescence signals (DNAJC3 and Grp94 or DNAJC3 and Hsp90) to establish points where they overlap, which could be used as quantitative analysis of colocalization (Zinchuk *et al*., 2010). For this study, fluorescence scattergrams (Figure 6.2) were used to demonstrate the degree of colocalization between DNAJC3 and Grp94 and DNAJC3 and Hsp90. Perfect colocalization using the scattergrams can be described as the alignment or overlap of both signals at the linear line of progression. (Zinchuk *et al*., 2010). In the control cells, the scattergram for DNAJC3 and Hsp90 signals (Figure 6.2, far right column [red and purple]), aligned on the linear line of progression, suggesting pixel on pixel colocalization between the two signals. When compared to the various stress treatments, no changes were observed to the DNAJC3 fluorescence scattergrams suggesting that the various stress conditions analyzed did not affect the localization of DNAJC3 relative to Hsp90. Similar to DNAJC3 and Hsp90, in the scattergram for DNAJC3 and Grp94 (Figure 6.2, far left column [red and green]), the two signals overlapped at the linear line of progression which suggested colocalization. The pattern of the fluorescence scattergram did not change substantially in cells subjected to hypoxia ($CoCl_2$), heat shock (42 °C), proteasome inhibition (MG132) and tumour promoting (PMA) stress conditions. This observation suggested that these stress conditions did not alter the localization of DNAJC3 in relation to Grp94. However, cells exposed to ER stress (Tun), ROS (H_2O_2) and DNA damage (UVL and UVS) dispalyed fluorescence scattergrams that showed a different pattern to that of the unstressed (untreated) cells, suggesting a change in localisation of DNAJC3 in relation to Grp94. It could thus be interpreted that these stress conditions have an effect on the ER, as the cytosolic localization (DNAJC3 and Hsp90 scattergrams) were not altered by the same treatments. In addition to changes in localization, changes in expression levels of DNAJC3 were also analysed by Western analysis to determine whether the expression pattern of DNAJC3 differed under the different stress conditions compared to untreated cell (Figure 6.3. A). Hsp70 was used as marker of stress, as it has been shown to be upregulated in cells during stress conditions (Lindquist and Craig, 1988).

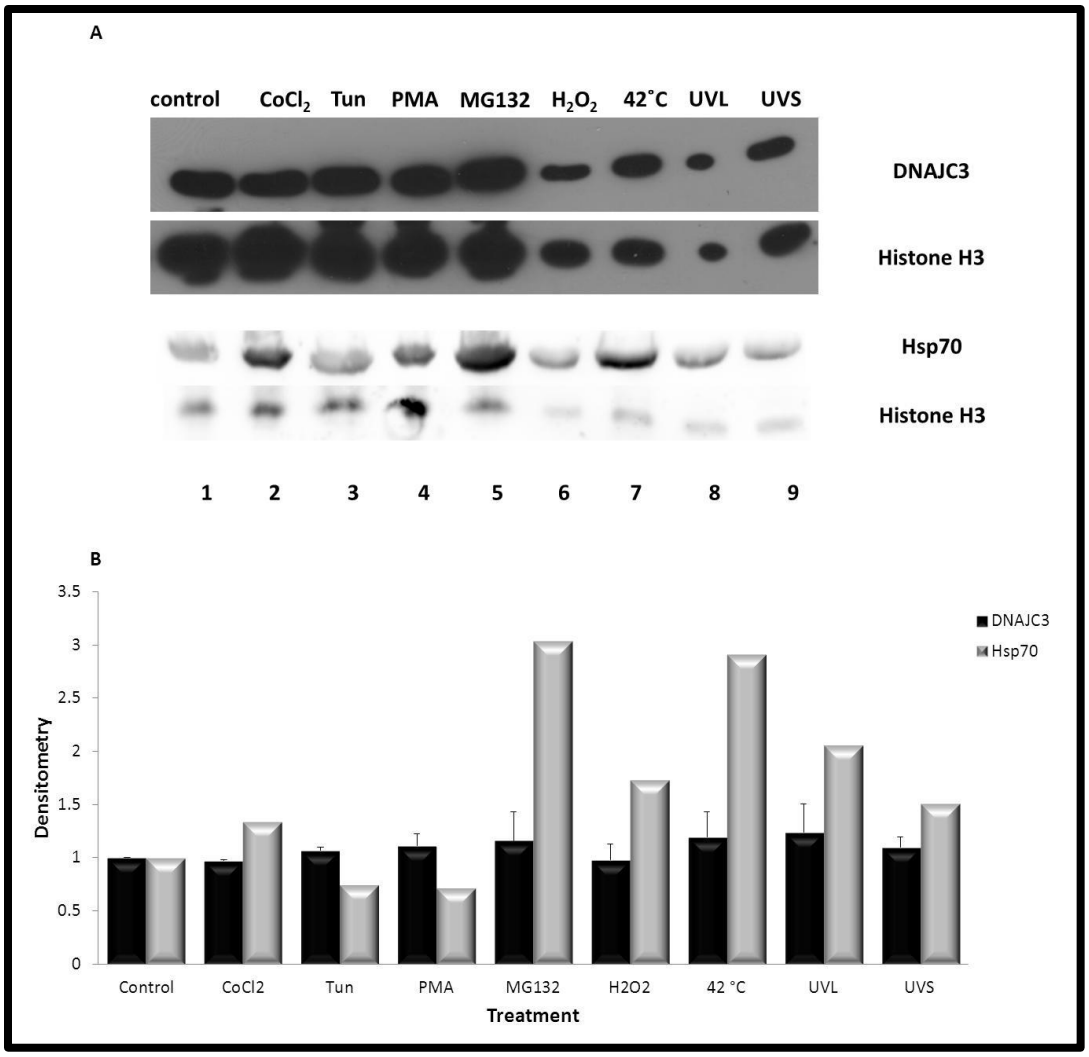

Figure 6.3 Expression levels of DNAJC3 under different stress conditions. (A). Levels of DNAJC3 and Hsp70 were detected by Western analysis in HEK293 T cell lysates subjected to various treatments to stimulate different stress conditions using mouse monoclonal anti-DNAJC3 and mouse monoclonal anti-Hsp70, Histone H3 was used as a loading control and detected using rabbit polyclonal anti-Histone H3. (B) Densitometry analysis used to compare the expression levels of DNAJC3 and Hsp70 under various stress conditions, where the ratio of DNAJC3 or Hsp70 to histone was normalized to the untreated sample which was taken as 1. Data shown are representatives of duplicate experiments with similar results.

Densitometry analysis of the expression levels of DNAJC3 in stressed cells compared to normal unstressed cells, illustrated that none of the stress treatments substantially altered the expression levels of DNAJC3 (Figure 6.3, B). Looking at the expression levels of Hsp70 in the stressed samples in comparison to the unstressed cells, it appeared that the Tun (ER stress) and PMA (tumor promoter) concentrations utilized in this study did not elicit a stress response, while the other treatment did induce an increase in Hsp70 expression, suggesting the stress response was induced (Figure 6.3, B). The lack of a stress response in Tun treated cells might be the reason why an

expected increase in DNAJC3 expression was not observed, as it has been shown that treatment with Tun results in ER stress which should lead to the upregulation of DNAJC3 (Oyadomari *et al*., 2006, Rutkowski *et al*., 2007).

It was interesting to note that there was no apparent correlation in the changes in DNAJC3 localization and expression. As mentioned, no changes were observed in the expression profile of DNAJC3 in stressed samples when compared to the control. However, a few of the stress treatments did alter the localization of DNAJC3 in relation to ER Grp94, although none was observed in its relation to the cytosolic Hsp90.

6.2.3 High concentrations of the Hsp90 inhibitor NOVO decrease DNAJC3 protein levels

GA is a known inhibitor of Hsp90 and Grp94 ATPase activity, that binds to the N-terminal ATP sites of the proteins (Chavany *et al*., 1996, Grenert *et al*., 1997, Prodromou *et al*., 1997a, Schulte *et al*., 1998, 1999). NOVO is known to bind to the ATP site at the C-terminus of Hsp90 (Marcu *et al*., 2000). The sequence associated with NOVO binding to Hsp90 is not conserved in Grp94, however it has been suggested that binding of NOVO to Hsp90 and its inhibition of ATPase activity could be linked to the conformation state of the protein rather than the sequence itself (Dollins *et al*., 2007, Marzec *et al*., 2012). Therefore, as Grp94 demonstrations identical conformational states to Hsp90, NOVO may be predicted to interact with this chaperone (Ratzke *et al*., 2010).

MCF-7 carcinoma cells were treated with different concentrations of GA and NOVO for 24 hours and the lysates analyzed by Western analysis to determine the consequence of Hsp90 and Grp94 inhibition on DNAJC3 protein levels (Figure 6.4). The preliminary results showed that, at all tested concentrations GA did not affect the protein levels of DNAJC3 compared to the DMSO sample, which was used as the vehicle control (Figure 6.4, A). NOVO did not alter the protein levels of DNAJC3 at the lower concentrations of 5 and 50 µM, when compared to the untreated sample. However, a dramatic decrease in the protein levels of DNAJC3 was observed in cells treated with 500 µM of NOVO. Since these results are from a single experiment, additional replicates will however need to be conducted to determine if the observed trends are a true representation of the inhibitors effects on DNAJC3 protein levels.

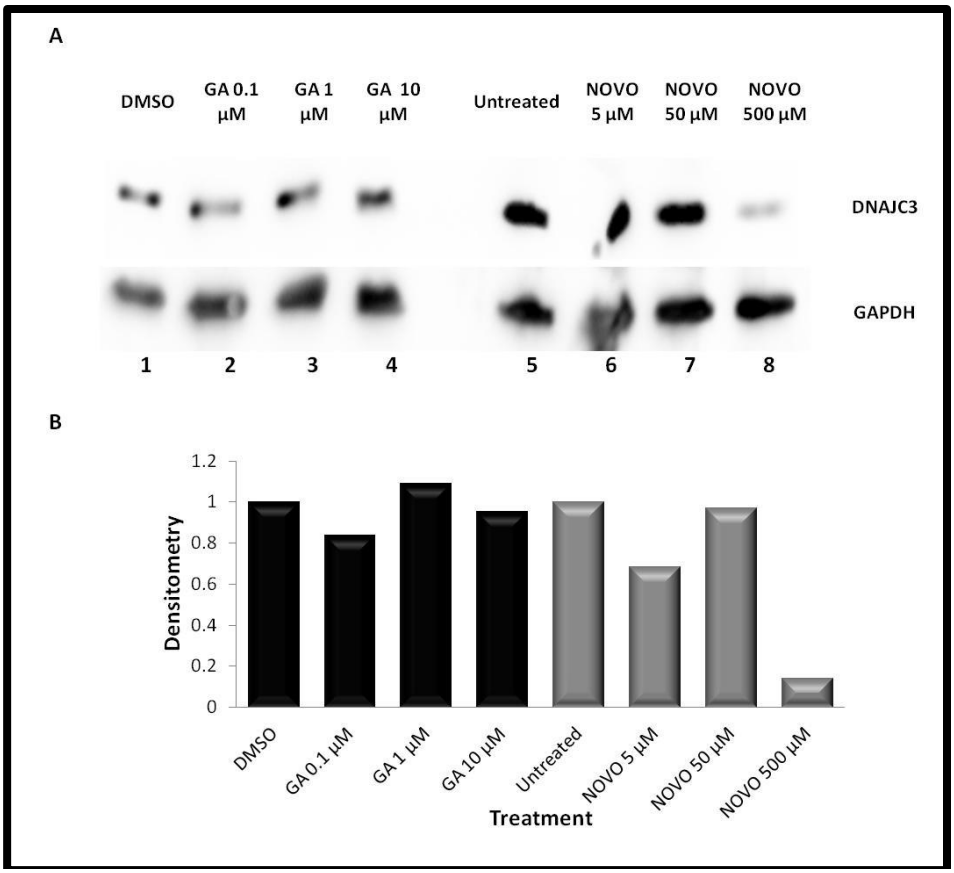

Figure 6.4: Preliminary analysis showed that DNAJC3 expression is reduced by high concentrations of novobiocin (NOVO) but not geldanamycin (GA). (A) Levels of DNAJC3 and were detected by Western analysis in MCF-7 carcinoma cell lysates treated with different concentrations of GA (0.1, 1, 10 µM) and NOVO (5, 50, 500 µM) for 24 hours using mouse monoclonal anti-DNAJC3, Histone H3 was used as a loading control and detected using rabbit polyclonal anti-Histone H3. (B) Densitometry analysis used to compare the expression levels of DNAJC3 after treatment with different concentrations of GA and NOVO, where the ratio of the DNAJC3 relative to Histone was calculated and normalized against the untreated sample, which was taken as 1.

6.2.4 DNAJC3 expression and localization is not affected by expression of HRas

HRas is a protein translated from the Harvey rat sarcoma viral oncogene homolog gene and is involved mainly in regulating cell division, by relaying signals (growth factor stimulation) from outside the cell to the nucleus through a process called signal transduction (McCormick , 1996, Ayllón and Rebollo 2001).

Several mutations have been identified on the HRAS gene. HRas G12V is a mutation at the twelfth amino acid, which results in the HRas protein being constitutively active within the cell (Seeburg *et al*., 1984). HRas S17N is a mutation that occurs at the seventeenth amino acid residue which results in a dominant negative mutant HRas protein (Stacey *et al*., 1991).

HEK293T cells were transfected with EGFP tagged HRas and mutant plasmids for 48 hours. Images were taken at 24 hours post transfection to determine the success of the procedure. An EGFP signal was detected in HRas, HRas G12V and HRas S17N cells and not the untreated cells (Figure 6.5, A). The transfection efficiency of all 3 plasmids appeared to be comparative. At 24 hours post transfection, the EGFP signal was mainly diffuse in the cytosol for all 3 HRas plasmids, although a few cells showed the EGFP signal concentrated next to the nucleus (Figure 6.5, A white arrow).

At 48 hours post transfection, cells were fixed, stained for DNAJC3 and analyzed by confocal microscopy (Figure 6.5, B). In the control cells (Figure 6.5, B upper panels), DNAJC3 signal was found mainly surrounding the nucleus in a punctate pattern, with faint staining in the cytosol and no EGFP signal detected. The distribution pattern of EGFP in HRas and HRas mutant transfected cells differed to the pattern observed 24 hours post transfection. In HRas transfected cells, the EGFP signal had an elongated fibril-like pattern, HRas G12V cells showed a more diffuse and grainy pattern and in HRas S17N cells the EGFP signal diffused uniformly in the cytoplasm (Figure 6.5, B). The concentrated EGFP signal found around the nucleus at 24 hours post transfection was absent in HRas and HRas G12V transfected cells and only a small population in HRas S17N cells still exhibited the staining pattern (Figure 6.5, B lower panels, yellow arrow). However, the presence of HRas and HRas mutated proteins did not alter substantially the localization of DNAJC3 (Figure 6.5, B middle column) and colocalization between DNAJC3 and the HRas proteins was not observed as illustrated by the lack of overlapping signals (Figure 6.5, B, Merge).

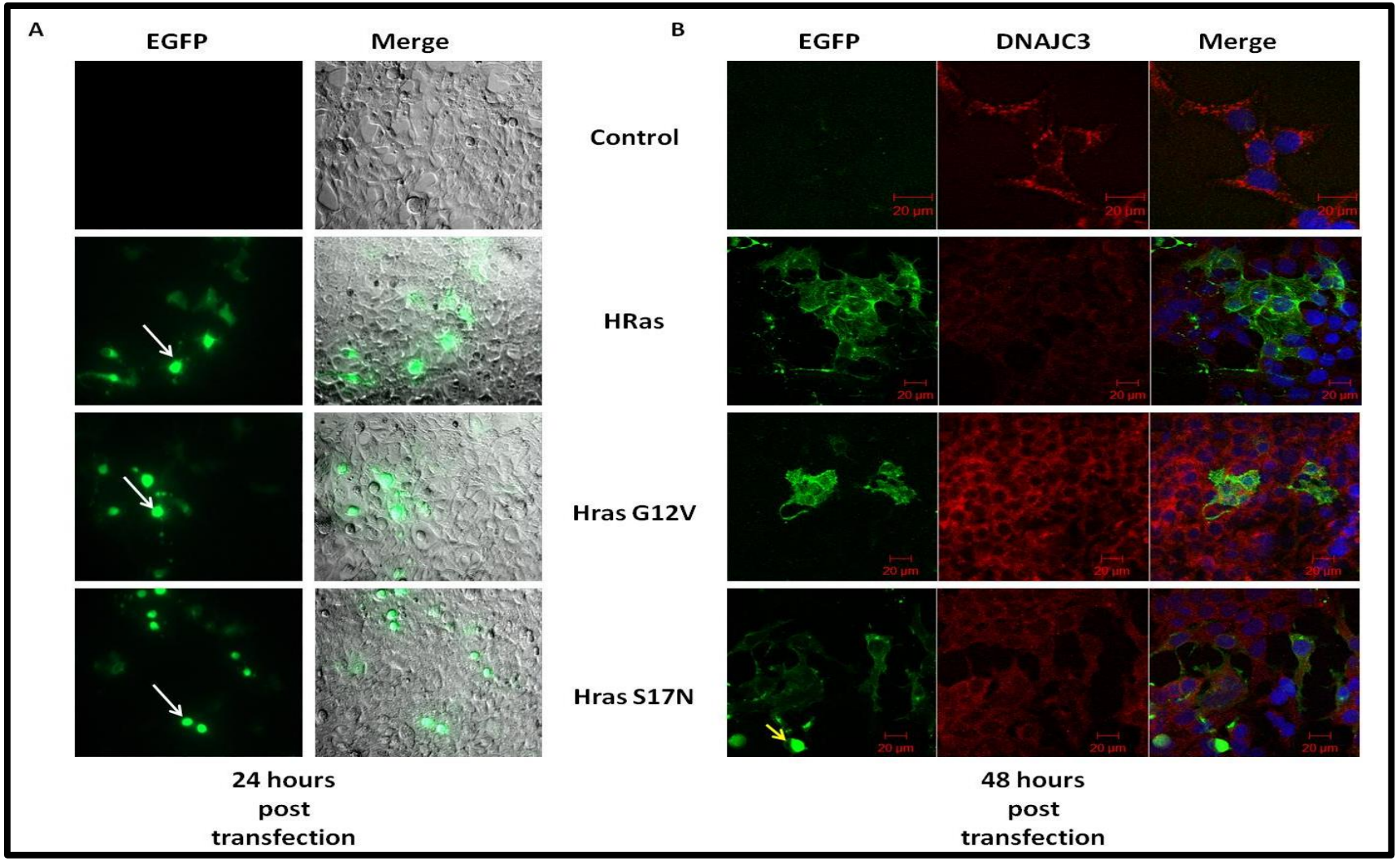

Figure 6.5: HRas, HRas G12V and HRas S17N plasmids did not alter the subcellular localization of DNAJC3 in HEK293T cells. HEK293T cells were grown on glass coverslips for 24 hours and transfected with EGFP- tagged HRas, HRas G12V and HRas S17N plasmids. After 24 hours (A), images of each transfection were captured to determine the success of the procedure. After 48 hours (B) cells were fixed in cold ethanol, permeabilized and stained with anti-DNAJC3. DNAJC3 primary antibody was detected with species specific Alexa Fluor 546- conjugated secondary**.**

The expression of DNAJC3 and the phosphorylation of selected proteins downstream of the Ras signalling pathway, namely ERK, JNK and p38 was analyzed by Western blot in HEK293T cells transfected with HRas and mutant plasmids for 48 hours (Figure 6.6). From the preliminary analysis, the expression levels of DNAJC3 were not affected by the expression of HRas or the mutants HRas G12V and S17N. The expression of HRas and HRas mutants had little to no effect on the levels of phosphorylated ERK. However, subtle changes were observed in the levels of phosphorylated JNK and p38 in cells transfected with the HRas S17N plasmid, were a decrease in phosphorylated protein levels can be observed (Figure 6.6).

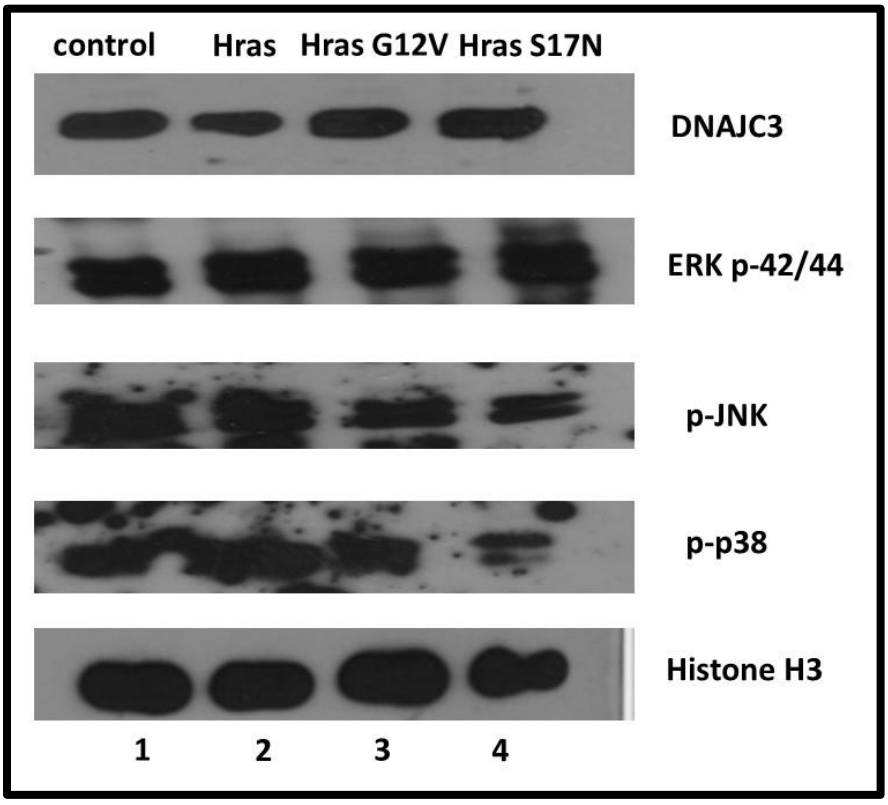

Figure 6.6: The effect of HRas, HRas G12V and HRas S17N plasmids on the expression levels of DNAJC3 and the activation (phosphorylation) of proteins, p**42/44 ERK, JNK and p38 in HEK293T cells.** Expression levels of DNAJC3 and the levels of phosphorylated proteins ERK, JNK and p38 was determined by western analysis in HEK293T cells transfected with HRas, HRas G12V and HRas S17N plasmids using mouse monoclonal anti-DNAJC3, anti-pJNK, anti-p-p38 and rabbit polyclonal Anti-p44/42 MAPK (T202/Y204). Histone H3 was used as a loading control and detected with rabbit polyclonal anti-Histone H3 antibodies.

6.2.5 Transient DNAJC3 knockdown reduced levels of the co-chaperone HOP

DNAJC3 is a known co-chaperone of Grp78 in the ER and Hsp70 in the cytosol, where it stimulates the ATPase activities of the two proteins, assisting them in their chaperoning functions

(Melville *et al*., 1999, Oyadomari *et al*., 2006, Rutkowski *et al*., 2007, Tao *et al*., 2010; Svärd *et al*., 2011). In order to determine the consequence of reducing protein levels of DNAJC3 on the protein levels of chaperones and co-chaperones, MCF-7 carcinoma cells were treated with DNAJC3 targeting small interfering RNA (siRNA) and non-targeting (NT) siRNA for 72 hours and analyzed by western analysis (Figure 6.7, A).

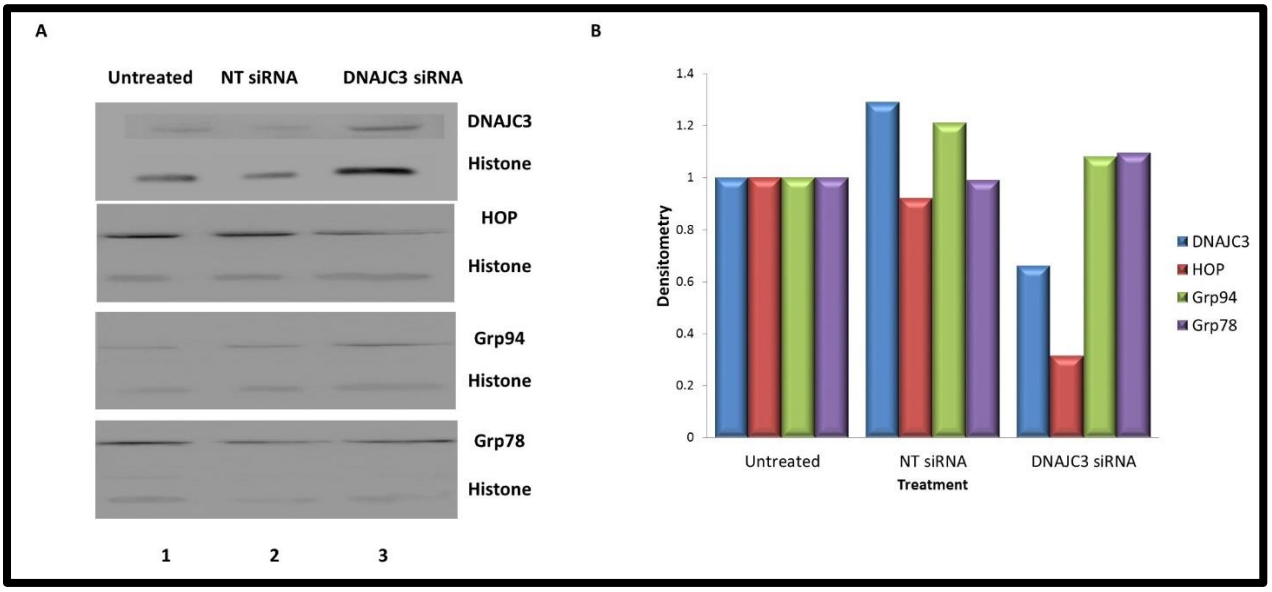

Figure 6.7: DNAJC3 knockdown decreased the expression of the co-chaperone HOP but not the ER chaperones, Grp78 and Grp94. (A) Levels of DNAJC3, HOP, Grp94 and Grp78 were detected by Western analysis in MCF-7 carcinoma cell lysates treated with DNAJC3 siRNA and NT siRNA for 72 hours using mouse monoclonal anti-DNAJC3, anti-Grp78 and anti-HOP and rat monoclonal anti-Grp94. Histone H3 was used as a loading control and detected using rabbit polyclonal anti-Histone H3. (B) Densitometry analysis was used to compare the expression levels of DNAJC3, HOP, Grp78 and Grp94 after DNAJC3 siRNA treatment, where the ratio of the chaperone or co-chaperone relative to Histone was calculated and normalized against the untreated sample, which was taken as 1.

After treating with DNAJC3 siRNA for 72 hours, DNAJC3 protein levels were reduced to about 60 % compared to the untreated sample, although a slight increase in DNAJC3 was observed in NT siRNA treated cells (Figure 6.7, B, blue column). The knockdown of DNAJC3 did not seem to have altered the protein levels of Grp94 (Figure 6.7, B, green column) and Grp78 (Figure 6.7, B, purple column). However, the knockdown of DNAJC3 resulted in a drastic reduction of HOP protein compared to the untreated and NT siRNA sample (Figure 6.7, B, red column).

However, the consistent knockdown of DNAJC3 in the MCF7 cell line was not reproducible and therefore to analyze the relationship between HOP and DNAJC3 further, DNAJC3 expression

levels were analyzed by Western analysis in HEK293T cells in which HOP had been depleted by RNA interference (Figure 6.8, A)

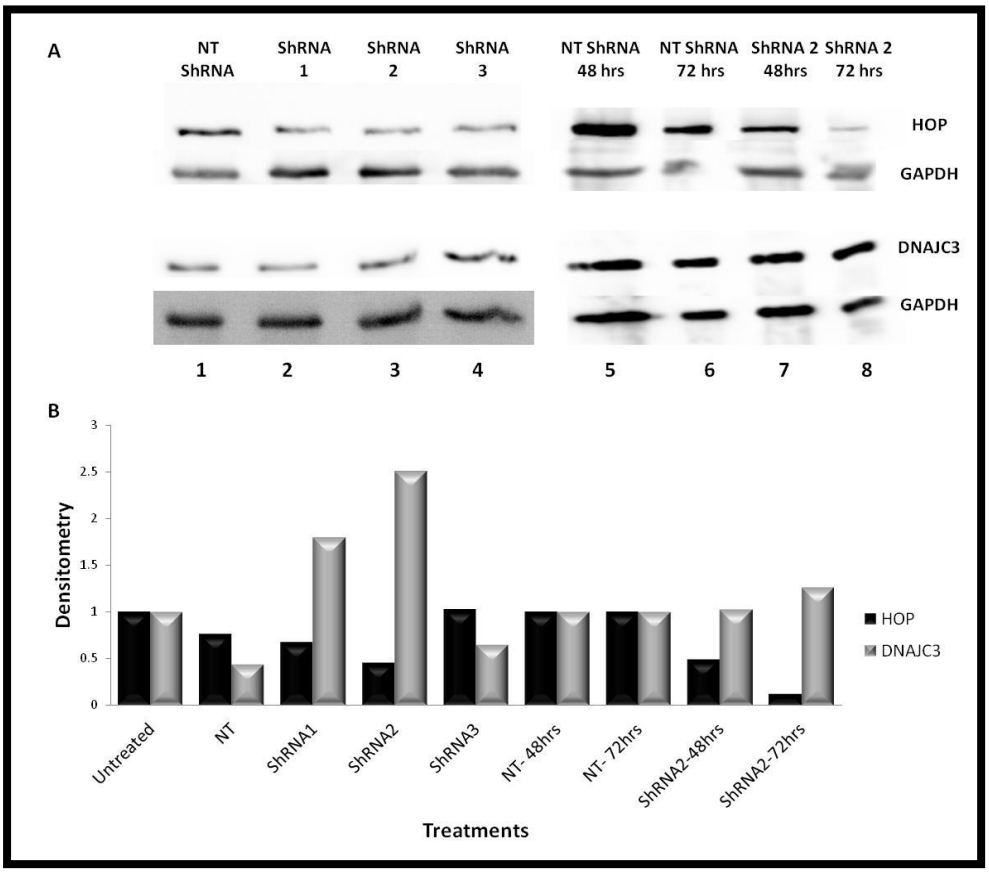

Figure 6.8: Knockdown of the co-chaperone HOP increased the expression levels of DNAJC3 in HEK293T cells. (A) Levels of HOP and DNAJC3 and were detected by Western analysis in HEK293T lysates transfected with HOP shRNA and non-targeting (NT) shRNA for 48 hours and 72 hours using mouse monoclonal anti-HOP and anti-DNAJC3. GAPDH was used as a loading control and detected using rabbit polyclonal anti-GAPDH. (B) Densitometry analysis used to compare the expression levels of HOP and DNAJC3 after HOP knockdown using shRNA, where the ratio of HOP or DNAJC3 to GAPDH loading control was normalized to the untreated sample which was taken as 1. Data is representative of duplicate experiments with similar results.

Triplicate HOP shRNA knockdown cells, along with a control NT shRNA cells were analyzed to determine the level of HOP knockdown and its effect on DNAJC3 expression. HOP knockdown was found to be greater in cells transfected with HOP shRNA 1 and 2, with shRNA 3 showing lower levels of HOP knockdown compared to the controls (Figure 6.8, B). The same lysates were analyzed to determine the expression levels of DNAJC3 when HOP proteins levels were low

(Figure 6.8). It was observed that in cells with greater HOP knockdown (shRNA 1 and 2), the protein levels of DNAJC3 increased compared to untreated and NT cells (Figure 6.8, B).

A stable polyclonal cell line expressing HOP shRNA 2 was created as part of another study (Lara Contu, unpublished). After transfection, expressions of the HOP shRNA 2 construct which has a puromycin selection marker and a TurboRFP fluorescence marker was induced with doxycycline. Puromycin was used to select for successful transfectants which were expanded, while the TurboRFP fluorescence tag was used to assess HOP shRNA expression (data not shown). A time course study using the stable HOP knockdown polyclonal cell line showed that HOP expression was reduced significantly after 72 hours induction with doxycycline compared to 48 hours. At 72 hours post induction, protein levels of DNAJC3 increased slightly compared to the NT control and 48 hours post induction samples.

6.3 Discussion

The focus of this chapter was to analyze DNAJC3 in mammalian cells. This was accomplished by examining the expression of endogenous DNAJC3 in cancer cell lines, determining the effects of different stress conditions on the localization and expressions of DNAJC3, determining the effect of HRas and two HRas mutants on the expression and localization of DNAJC3 and determining the consequences of knocking down DNAJC3 on chaperones and other co-chaperones. DNAJC3 did not appear to be generally stress inducible, nor was its expression or localization effected by the HRas oncogene. However, some of the stress conditions induced an apparent re-distribution of the protein in cells. DNAJC3 was found to be sensitive to NOVO treatment and slightly increased in Hop knockdown cells, while Hop was putatively decreased in DNAJC3 knockdown cells.

Endogenous DNAJC3 was found to be expressed in nine cancer cell lines from various tissues, including breast, cervix, colon and blood. DNAJC3 has previously been reported to be expressed in some of the cell lines analysed herein, such as MCF-7, MDA-MB-231 (Gao *et al*., 2012), SW620 and SW480 (Ghosh *et al*., 2011). Although endogenous DNAJC3 was detected in all tested cell lines, the level of protein expression was undetermined. Follow up experiments should analyze the levels of DNAJC3 expression as it has been shown that overexpression or knockdown of the protein has different consequences in different cancers (Barber *et al*., 1994, Gao *et al*., 2012, Huber *et al*., 2013). By determining and comparing the expression levels of DNAJC3 in paired cell lines such as SW620 and SW480 or different types of cancers from the same tissues such as MCF-7,

MBA-MB-231 and Hs578T (breast), the role of DNAJC3 in cancer biology may be better understood.

Numerous heat shock proteins have been shown to be upregulated and undergo a change in localization under stress conditions (Bagatell and Whitesell, 2004). DNAJC3 is known to localize to the ER lumen, with a subpopulation in the cytosol (Rutkowski *et al*., 2007). Compared to the untreated cells, none of the various stress conditions altered the cytosolic localization of DNAJC3 in relation to Hsp90 (Figure 6.2). However, the ER localization of DNAJC3 was altered slightly by ER stress (Tun), ROS (H_2O_2) and DNA damage (UVL and UVS) (Figure 6.2). However, when the protein levels of DNAJC3 under the different stress condition were compared to the untreated control, no changes were observed (Figure 6.3). Using Hsp70 as an indicator of stress, it was observed that the Tun and PMA treatments did not induce any stress response at the concentration used. This lack of stress induction could be the possible explanation as to why no upregulation of DNAJC3 was observed in the treatments meant to resemble ER stress, as it has been shown that ER stress induces the upregulation of ER chaperones including DNAJC3 (van Huizen *et al*., 2003). In literature Tun concentrations as low as 1 µg/ml (Zinszner *et al*., 1998) or lower (100 ng/ml) (Ming-Zhi *et al*., 2010) have been shown to induce ER stress; while double that concentration (2 µg/ml) was utilized in this study. Although ER stress was induced for 24 hours with double the concentration of Tun listed in literature, the HEK293T cells seemed to have been resistant to chemically induced ER stress at this concentration. Future experiments will have to include dose and time course studies to determine the appropriate concentration and treatment period in this cell line.

In addition to stress conditions, preliminary experiments were conducted to determine the effects of known Hsp90 inhibitors GA and NOVO on the protein levels of DNAJC3. Both drugs are known to bind and inhibit Hsp90 ATPase activity by binding to the ATP site at the N and C terminus domains of Hsp90, respectively (Grenert *et al*., 1997, Prodromou *et al*., 1997, Marcu *et al*., 2000). Currently, only GA has been established to bind to both Grp94 and Hsp90 (Chavany *et al*., 1996) and binding of NOVO to Grp94 has not yet been reported. However, the NOVO binding site in Hsp90, ^{559}KKQEEKK^{564} (Matts *et al*., 2011) is not conserved in Grp94 (Tastan Bishop *et al*., 2013). However, binding of NOVO to the C-terminal ATP site of Hsp90 resulting in the inhibition of the chaperone's ATPase activity is thought to not be dependent on the primary sequence but conformation state of the protein and Grp94 and Hsp90 are known to undergo

identical conformational changes as part of their ATP dependent chaperone activity (Prodromou *et al*., 1997a; 1997b; 2000).

GA did not affect the expression levels of DNAJC3 at all tested concentrations (01, 1 and 10 µM), while only the highest concentration of NOVO (500 µM) dramatically decreased the protein levels of DNAJC3 compared to the loading control (Figure 6.4). Both inhibitors are known to bind and inhibit Hsp90 (Whitesell *et al*., 1994, Grenert *et al*., 1997, Prodromou *et al*., 1997, Marcu *et al*., 2000) and GA also inhibits Grp94 (Chavany *et al*., 1996). The ability of NOVO to alter the protein levels of DNAJC3 suggested that DNAJC3 and Hsp90 and/or Grp94 might have an interaction, direct or indirect, that is dependent on the C-terminal domain of the protein, as the inhibitor is known to bind the C-terminal ATP binding site (Marcu *et al*., 2000). In literature and in our study, Grp94 was found to be in a complex with DNAJC3 in a pull down assay, although our data suggest that this interaction is indirect (Jansen *et al*., 2012). NOVO may be destabilizing the complex, affecting the complex between Hsp90 and/or Grp94 and DNAJC3. Marcu *et al*., (2000) and Yun *et al*., (2004) found similar results, where NOVO reduced the amounts of p23, a Hsp90 co-chaperone, that co-immunoprecipitated with Hsp90 in a dose dependent manner, suggesting that NOVO affects Hsp90s ability to interact with co-chaperones (Marcu *et al*., 2000, Yun *et al*., 2004). However, the decrease in DNAJC3 protein levels observed resemble the effects mostly associated with Hsp90 client proteins when cells are treated with NOVO, as NOVO inhibition of Hsp90 has been shown to cause destabilization of the Hsp90 multi-chaperone complex, resulting in degradation of the client proteins within the complex (Donnelly and Blagg, 2007). In addition to being an Hsp90 inhibitor, NOVO is also known to bind and inhibit the activity of topoisomerases such as DNA gyrase which is involved in introducing and relaxing negative supercoils in DNA (Reece and Maxwell, 1991). Therefore, the effects on DNAJC3 protein levels observed in NOVO treated cells might not be limited to its effect on Hsp90 or Grp94.The role of topoisomerase in DNAJC3 stability could be addressed using known inhibitors like etoposide (Bromberg *et al*., 2003).

The involvement of DNAJC3 in the Ras signal transduction pathway was also analyzed by determining the effects of HRas and HRas mutants G12V (constitutively active form of the protein) (Seeburg *et al*., 1984) and S17N (dominant negative form of the protein) (Stacey *et al*., 1991) on the localization and expression of DNAJC3. Confocal and fluorescence analysis showed that the transfection of the EGFP tagged HRas plasmids in to HEK293T cells was successful

(Figure 6.5). However, the localization and expression of DNAJC3 (Figure 6.6) were not altered in cells transfected with any of the HRas plasmids. Literature reports that, the expression of HRas G12V activates UPR, leading in the upregulation of ER chaperones such as Grp94 (Denoyelle *et al*., 2006). ER stress due to UPR has been shown to cause an upregulation in DNAJC3 expression (van Huizen *et al*., 2003), suggesting that an increase in DNAJC3 protein levels should have been observed in HRas G12V transfected cells.

Several of the Ras downstream kinases have been shown to either regulate or be regulated by DNAJC3 (Figure 6.9). In Coxsackle virus B3 (CVB3) infected cells, phosphorylation of the kinase AKT was found to be reduced by the silencing of DNAJC3 but not that of ERK p42/44 (Zhang *et al*., 2010b). In influenza virus infected cells, the activation of the p38 resulted in the activation of downstream kinases MK2 and MK3 which recruit a complex consisting of DNAJC3 and its repressor $p88^{rIPK}$, which activated DNAJC3 inhibitory activity against PRK/PERK, allowing proteins synthesis to occur (Luig *et al*., 2010). The same process has been suggested in highly mitogenic tumor cells, where the constitutive activation of ERK p42/44 by Ras or Raf recruits the same complex of DNAJC3 and its inhibitors and prevents protein synthesis attenuation by PKR/PERK (Luig *et al*., 2010). However, it is unclear whether the activation of DNAJC3 by ERKp42/44 and p38 alters expression levels of the protein. If so, levels of DNAJC3 should be altered in cells transfected with HRas G12V plasmids since its expression results in the production of the constitutively active form of the protein, which is known to lead to activation of ERK p42/44.

For this study, the expression levels of the kinases p38, JNK and ERK was also analyzed in HRas and HRas mutant transfected cells. The levels of phosphorylated ERK p-42/44 were not altered in HRas transfected cells compared to untransfected cells. Similar results were observed in phosphorylated p38 and JNK, although a slight decrease in these two kinases was observed in HRasS17N transfected cells. These observations are in contrast to reports in literature, which showed that transfecting MCF10A cell with the HRas plasmid activated ERK and p38 but not JNK compared to untransfected cells (Kim *et al*., 2003). HRasG12V also activated (phosphorylated) p38, ERK p42/44 and JNK in melanocytes (Denoyelle *et al*., 2006) and HRas S17N did not activate ERK p42/44 in COS-7 cells (Lorenz *et al*., 2012). However, all the kinases were constitutively activated (phosphorylated) form and therefore this may be the reason why no differences in the expression levels were observed upon transfection with HRas or HRas G12V and S17N.

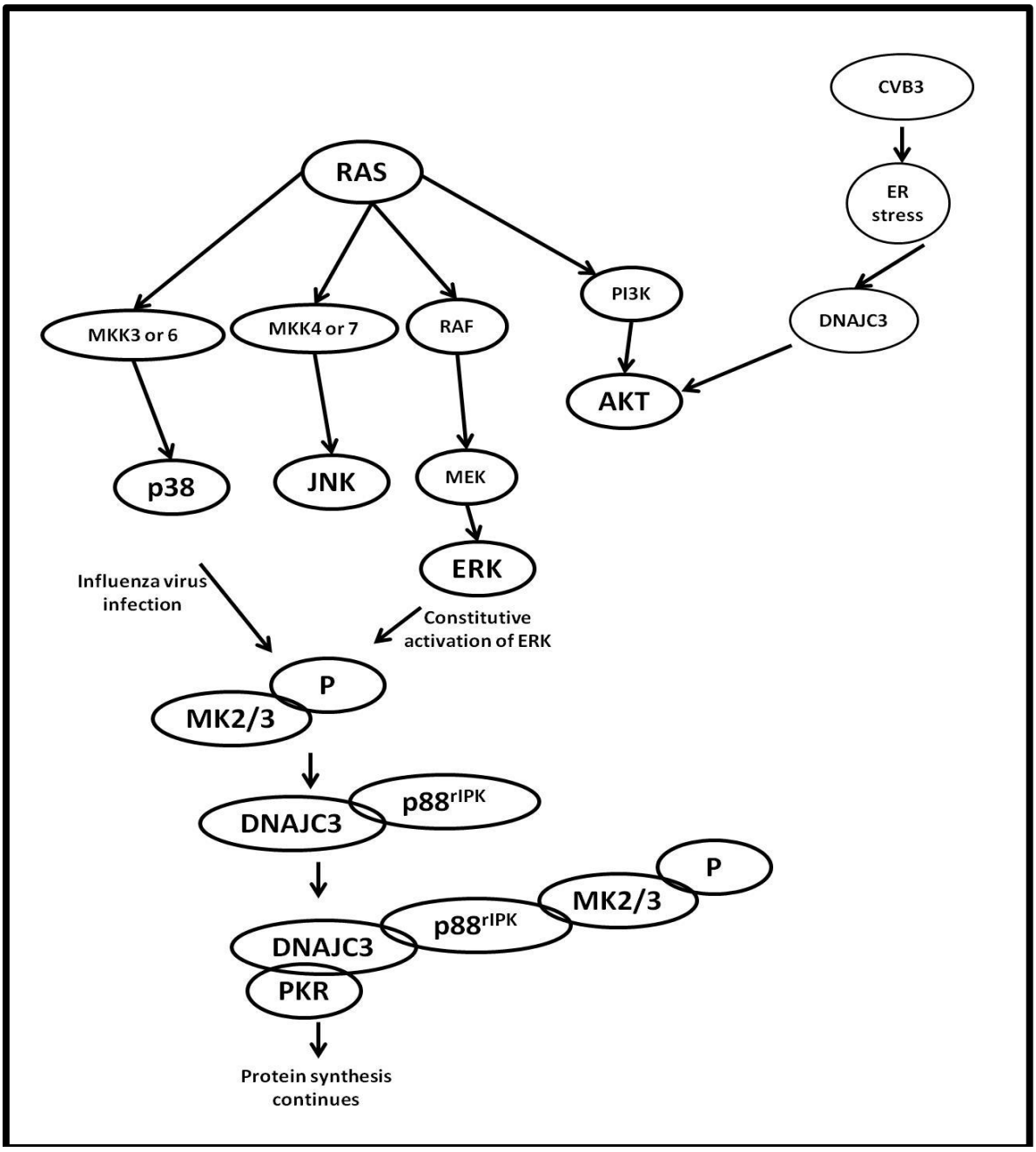

Figure 6.9: Schematic presentation of the Ras signalling transduction pathway and the interaction of DNAJC3 with various downstream kinases in the pathway. During influenza virus infection PKR inhibition is initiated by activation of MK2/3 by phosphorylated p38, which recruits $p88^{rIPK}$ bound to DNAJC3, DNAJC3 in turn binds to PKR forming a complex comprised of MK2/3, $p88^{rIPK}$, DNAJC3 and PKR. The constitutive activation of ERK in cancer has also been shown to inhibit PKR activity via a similar pathway as in influenza virus infected cells (Luig *et al*., 2010). In Coxsackle virus B3 (CVB3) infected cells, the depletion of DNAJC3 has been shown to affect the activation of AKT and not ERK, negatively (Zhang *et al*., 2010b).

From the analyses of the confocal images (Figure 6.6), the ratio of HRas transfected cells to untransfected cells is also very low, suggesting that the effects of the HRas proteins could be

masked by the large proportion of untransfected cells. Hence the anticipated changes in DNAJC3 and kinases were not observed in transfected cells compared to the untransfected control cells. To resolve this problem in the future, transfected cells could enriched by FACS *(*Fluorescence Activated Cell Sorting*)*, ensuring an equal number of transfected cells (vector and HRas) are analyzed and the effects of the HRas plasmid are not masked by the presence of untransfected cells.

DNAJC3 knockdown experiments were conducted to determine the effects of silencing DNAJC3 would have on the expression of the chaperones, Grp78 and Grp94 and the co-chaperone HOP. Transfection of MCF-7 carcinoma cells with DNAJC3 siRNA, resulted in the expression levels of DNAJC3 being reduced by 40 % compared to the untransfected control (Figure 6.7). However, no changes were observed in the expression levels of either Grp78 or Grp94, suggesting that the reduction of its DNAJC3 had no effect on Grp78. DNAJC3 is one of seven ER DNAJ proteins known to co-chaperone Grp78 activity, suggesting that one of the other six DNAJ proteins could have compensated for the loss of DNAJC3 (Feldheim *et al*., 1992, Brightman *et al*., 1995, Shen *et al*., 2002, Hosoda *et al*., 2003, Shen and Hendershot, 2005).

Interestingly, the levels of the Hsp90/Hsp70 TPR-containing co-chaperone, HOP, were dramatically reduced in DNAJC3 depleted cells (Figure 6.7). In the reciprocal experiment, when HOP was knocked down in HEK293T cells, the protein levels of DNAJC3 were found to increase (Figure 6.8). HOP is mostly cytosolic and migrates to the nucleus during stress using its nuclear localization signal (NLS) (Daniels *et al*., 2008). Recently, HOP has been found in a complex with Hsp90 in the ER, facilitating the transportation of the rice chitin receptor, OsCERK1, from the ER to the plasma membrane (Chen *et al*., 2010). However, although DNAJC3 and HOP both TPR-containing co-chaperones, the TPR domains in HOP and DNAJC3 seem to have different functions. The carboxylate clamp residues found in the HOP TPR domains that enable the protein to interact with Hsp90 and Hsp70 are missing in DNAJC3 TPR domains (Figure 3.4) (Odunuga *et al*., 2003, Tao *et al*., 2010). On the other hand, the EEVD motif crucial for Hsp70 and Hsp90 interaction with HOP TPR domains is missing in the ER homologues, Grp78 and Grp94 (Figure 3.7) (Argon and Simen,1999, Fewell *et al*., 2004, Tastan Bishop *et al*., 2013). This strongly suggested that HOP and DNAJC3 are not interchangeable when it comes to their interaction with the cytosolic Hsp90 and Hsp70 and ER Grp78 and Grp94. However, several studies have analyzed the changes in Hsp90 and or Hsp70 expression after knockdown of co-chaperones such as Cdc37

(Smith *et al*., 2013), p23 (Nguyen *et al*., 2012, Song *et al*., 2013), Aha1 (Holmes *et al*., 2008) and HOP (Willmer *et. al.*, 2013), the effects observed differed depending on the depleted co-chaperone. To the best of our knowledge, no published study has determined the changes in the protein levels of other co-chaperones, although the knockdown of HOP has been shown to increase the levels of Cdc37 and Aha1, but not p23 (Tarryn Willmer, MSc thesis 2012). The results from these knockdown studies need to be extended to examine the changes in protein levels for the cytosolic Hsp90 and Hsp70 and the ER Grp94 and Grp78 as well as determining the underlying mechanism behind the increased expression of Hop detected.

Chapter 7: Summary, Conclusions and Future Work

DNAJC3 is a member of the DNAJ family that contains TPR domains as well as the canonical J domain. DNAJC3 has been functionally identified as a DNAJ co-chaperone to both cytosolic Hsp70 and the ER Hsp70, Grp78, as well as an inhibitor of PKR and PERK kinase activity (Oyadomari *et al*., 2006, Rutkowski *et al*., Petrova *et al*., 2008, Tao *et al*., 2010, Svärd *et al*., 2011). TPR domains are known to mediate protein-protein interaction, and TPR domains of co-chaperones such as HOP are known to interact with Hsp90 and/or Hsp70. In this study we extended the characterization of the DNAJC3 TPR domains using a combination of *in silico*, *in vitro* and *ex vivo* techniques. Despite showing structural similarity to a number of TPR containing proteins, *in silico* analysis suggested that DNAJC3 TPR domains would be unlikely to interact with either Hsp90 or Hsp70. The lack of direct interaction was subsequently demonstrated experimentally using isolated proteins in pull down assays. This was despite the identification of a putative binding site in the Hsp90 chaperones that shared limited structural similarity with a region of $p88^{rIPK}$ known to interact with DNAJC3 (Gale *et al*., 1998). It might be interesting as part of a future study to engineer the carboxylate clamp residues into DNAJC3 to determine whether this is sufficient to allow interaction of the TPR domains with Hsp90/Hsp70. The similarity between DNAJC3 and DNAJC7 suggest that introduction of the necessary residues would support an interaction. Our study demonstrated however that the TPR domains of DNAJC3 can bind to multiple model substrates when these substrates are in either native or denatured forms, thereby extending the previous substrate binding analysis (Tao *et al*., 2010). Murine DNAJC3 TPR domains are known to bind preferably to denatured substrate than native; this study found that human DNAJC3 TPR domains bound indiscriminately to both native and denatured substrates. In addition, the observation that DNAJC3 TPR domain bound to the substrate β-galactosidase with greater affinity to MDH might suggest substrate specificity for the DNAJC3 TPR domains. Although DNAJC3 could bind substrate proteins *in vitro*, we were not able to observe a complex of Grp78 or Grp94 with DNAJC3 and a model denatured substrate. The DNAJC3 TPR domains were able to isolate a complex containing Hsp90 and Grp94 from mammalian cell lysates, although this interaction was deemed likely to be indirect based on the direct binding assay. Taken together with the results of the pull down assays, we predict that the putative complex in mammalian cells includes an as

yet unidentified protein or proteins that are responsible for mediating the interactions between the chaperones and the DNAJC3 TPR domains. We predict that this may be a specialised substrate protein, particularly since Grp94 is known to be highly selective with respect to substrate binding (Randow and Seed, 2001, Yang *et al*., 2007, Morales *et al*., 2009). Indeed, it is possible that there are multiple independent complexes that involved the DNAJC3 TPR domains. For example, DNAJC3 may interact via one protein with Hsp90 in the cytosol and via another protein in the ER with Grp94. *In silico* analysis suggested that DNAJC3 TPR domains could not interact with Hsp90 and Hsp70, hence could not function as a co-chaperone through this domain. Identification and analysis of structural homologues of DNAJC3 TPR domains illustrated that DNJC3 TPR domains were highly similar to TPR-containing proteins with functions independent of both Hsp90 and Hsp70. The pull down assay should be repeated and the complexes analyzed by mass spectrometry in order to identify proteins that interact with DNAJC3 via the TPR domains (Link *et al*., 1999, Corthals *et al*., 2000). Any putative interactions identified could subsequently be analysed for direct binding. These data would indicate potentially novel functions of the protein, or could be used to understand existing functions.

Preliminary *ex vivo* analysis of DNAJC3 suggested that the protein was not stress inducible nor was its localization altered by general stress conditions. The expression of HRas and HRas mutant oncoproteins did not substantially alter DNAJC3 expression or subcellular localisation, suggesting that the role of DNAJC3 in kinase activity did not involve the Ras pathway. We demonstrated that the levels of the DNAJC3 protein were however, dramatically reduced by high concentrations of the C-terminal Hsp90 inhibitor NOVO, but not the N-terminal inhibitor, GA. This observation suggested that the interaction observed between DNAJC3 and Hsp90 or Grp94 might be disrupted by NOVO and not GA, although the lysate pull down assay conducted with DNAJC3 TPR will need to be repeated in the presence of a range of concentrations of both inhibitors, to verify that NOVO is disrupting the interaction. Knockdown of DNAJC3 reduced the protein levels of HOP, while levels of DNAJC3 protein were increased in a reciprocal experiment where expression of HOP was silenced. HOP is required for transfer of protein substrates from Hsp70 to Hsp90 and therefore controls entry of client proteins into the Hsp90 cycle. Therefore, the depletion of Hop levels might perturb the functions of a cohort of Hsp90 client proteins or indeed change the expression of certain proteins. It is possible that these changes might culminate in ER stress, which

might explain the increase in the levels of DNAJC3 (van Huizen *et a*l., 2003, Oyadomari *et al*., 2006, Rutkowski *et al*., 2007).

This study is the first to demonstrate experimentally that DNAJC3 TPR domains do not bind directly to either Hsp90 or Grp94, although the TPR domains could bind substrate and DNAJC3 was able to be isolated in a complex containing Hsp90 and Grp94 from a mammalian cell lysate. At the start of the project, we hypothesised that DNAJC3 would be involved in non-canonical interactions with Hsp70 and Hsp90 chaperones via its TPR motifs. Based on our observations, we have technically disproved this hypothesis by demonstrating experimentally a lack of direct interaction between the TPR domains from DNAJC3 and these Hsp90 chaperones. However, we did demonstrate that the TPR domains can bind model substrates, which might suggest that the DNAJC3 TPR domains are equivalent to the substrate binding domain of the DNAJ, which together with the J domain result in a functional ER resident Hsp70 co-chaperone, possibly with independent chaperone activity. Further work will be required in order to identify the physiological interacting partners for the DNAJC3 TPR domains. However, our data currently do not support a role for DNAJC3 as a co-chaperone for either Hsp90 or the ER Grp94. Therefore, the existence of ER equivalents of established cytosolic co-chaperones of Hsp90 remains to be definitively proven.

Chapter 8: References

Abe, Y, T Shodai, T Muto, K Mihara, H Torii, S Nishikawa, T Endo, and D Kohda. 2000. "[Structural Basis of Presequence Recognition by the Mitochondrial Protein Import Receptor Tom20]." *Cell* 92 (7) (July): 266–71.

Agarraberes, F, and FJ Dice. 2001. "Protein Translocation across Membranes." *Biochimica et Biophysica Acta (BBA) - Biomembranes* 1513 (1) (July 2): 1–24.

Aguirre-Ghiso, J a, D Liu, a Mignatti, K Kovalski, and L Ossowski. 2001. "Urokinase Receptor and Fibronectin Regulate the ERK(MAPK) to p38(MAPK) Activity Ratios That Determine Carcinoma Cell Proliferation or Dormancy in Vivo." *Molecular Biology of the Cell* 12 (4) (April): 863–79.

Aguirre-Ghiso, Julio A, Yeriel Estrada, David Liu, and Liliana Ossowski. 2003. "ERKMAPK Activity as a Determinant of Tumor Growth and Dormancy; Regulation by p38SAPK ." *Cancer Research* 63 (7) (April 1): 1684–1695.

Alarcon, Cristina, Barton Wicksteed, Marc Prentki, Barbara E Corkey, and Christopher J Rhodes. 2002. "Succinate Is a Preferential Metabolic Stimulus-Coupling Signal for Glucose-Induced Proinsulin Biosynthesis Translation." *Diabetes* 51 (8) (August 1): 2496–2504.

Ali, Maruf M U, S Mark Roe, Cara K Vaughan, Phillipe Meyer, Barry Panaretou, Peter W Piper, Chrisostomos Prodromou, and Laurence H Pearl. 2006. "Crystal Structure of an Hsp90–nucleotide–p23/Sba1 Closed Chaperone Complex." *Nature* 440 (7087) (April 20): 1013–1017.

Allan, Rudi Kenneth, and Thomas Ratajczak. 2011. "Versatile TPR Domains Accommodate Different Modes of Target Protein Recognition and Function." *Cell Stress & Chaperones* 16 (4) (July): 353–67.

Altmeyer A, Maki RG, Feldweg AM, Heike M, Protopopov VP, Masur SK, and Srivastava PK. 1996. "Tumor-Specific Cell Surface Expression of the-KDEL Containing, Endoplasmic Reticular Heat Shock Protein gp96." *The International Journal of Cancer* 69 (4): 340–349.

Altschul, S F, W Gish, W Miller, E W Myers, and D J Lipman. 1990. "Basic Local Alignment Search Tool." *Journal of Molecular Biology* 215 (3) (October 5): 403–10.

Altschul, S F, T L Madden, a a Schäffer, J Zhang, Z Zhang, W Miller, and D J Lipman. 1997. "Gapped BLAST and PSI-BLAST: A New Generation of Protein Database Search Programs." *Nucleic Acids Research* 25 (17) (September 1): 3389–402.

Anfinsen, C B. 1973. "Principles That Govern the Folding of Protein Chains." *Science (New York, N.Y.)* 181: 223–230.

Argon, Yair, and Birgitte B. Simen. 1999. "GRP94, an ER Chaperone with Protein and Peptide Binding Properties." *Seminars in Cell & Developmental Biology* 10 (5): 495–505.

Arrigo, André-Patrick. 2005. "In Search of the Molecular Mechanism by Which Small Stress Proteins Counteract Apoptosis during Cellular Differentiation." *Journal of Cellular Biochemistry* 94 (2) (February 1): 241–6.

Bagatell, Rochelle, and Luke Whitesell. 2004. "Altered Hsp90 Function in Cancer: A Unique Therapeutic Opportunity." *Molecular Cancer Therapeutics* 3: 1021–1030.

Bailey, Timothy L, Mikael Boden, Fabian a Buske, Martin Frith, Charles E Grant, Luca Clementi, Jingyuan Ren, Wilfred W Li, and William S Noble. 2009. "MEME SUITE: Tools for Motif Discovery and Searching." *Nucleic Acids Research* 37 (Web Server issue) (July): W202–8.

Baker, Michael J, Ann E Frazier, Jacqueline M Gulbis, and Michael T Ryan. 2007. "Mitochondrial Protein-Import Machinery: Correlating Structure with Function." *Trends in Cell Biology* 17 (9) (September): 456–64.

Ballinger, C a, P Connell, Y Wu, Z Hu, L J Thompson, L Y Yin, and C Patterson. 1999. "Identification of CHIP, a Novel Tetratricopeptide Repeat-Containing Protein That Interacts with Heat Shock Proteins and Negatively Regulates Chaperone Functions." *Molecular and Cellular Biology* 19 (6) (June): 4535–45.

Bambang, I Fon, Songci Xu, Jianbiao Zhou, Manuel Salto-Tellez, Sunil K Sethi, and Daohai Zhang. 2009. "Overexpression of Endoplasmic Reticulum Protein 29 Regulates Mesenchymal-Epithelial Transition and Suppresses Xenograft Tumor Growth of Invasive Breast Cancer Cells." *Lab Invest* 89 (11) (September 21): 1229–1242.

Banecki, Bogdan, Krzysztof Liberek, Daniel Wall, Alicja Wawrzynów, Costa Georgopoulos, Enrico Bertoli, Fabio Tanfani, and Maciej Zylicz. 1996. "Structure-Function Analysis of the Zinc Finger Region of the DnaJ Molecular Chaperone." *Journal of Biological Chemistry* 271 (25) (June 21): 14840–14848.

Bankston, John R, Stacey S Camp, Frank DiMaio, Alan S Lewis, Dane M Chetkovich, and William N Zagotta. 2012. "Structure and Stoichiometry of an Accessory Subunit TRIP8b Interaction with Hyperpolarization-Activated Cyclic Nucleotide-Gated Channels." *Proceedings of the National Academy of Sciences of the United States of America* 109 (20) (May 15): 7899–904.

Barber, G N, S Thompson, T G Lee, T Strom, R Jagus, a Darveau, and M G Katze. 1994. "The 58-Kilodalton Inhibitor of the Interferon-Induced Double-Stranded RNA-Activated Protein Kinase Is a Tetratricopeptide Repeat Protein with Oncogenic Properties." *Proceedings of the National Academy of Sciences of the United States of America* 91 (10) (May 10): 4278–82.

Barford, David. 1996. "Molecular Mechanisms of Theprotein Serine/threonine Phosphatases." *Trends in Biochemical Sciences* 21 (11) (November): 407–412.

Berman, H M, J Westbrook, Z Feng, G Gilliland, T N Bhat, H Weissig, I N Shindyalov, and P E Bourne. 2000. "The Protein Data Bank." *Nucleic Acids Research* 28 (1) (January 1): 235–42.

Berwin, Brent, Justin P Hart, Stuart Rice, Cecilia Gass, Salvatore V Pizzo, Steven R Post, and Christopher V Nicchitta. 2003. "Scavenger Receptor-A Mediates gp96/GRP94 and Calreticulin Internalization by Antigen-Presenting Cells." *The EMBO Journal* 22 (22) (November 17): 6127–36.

Bhairi, SM, and C Mohan. 2007. "Calbiochem Detergents: A Guide to the Properties and Uses of Detergents in Biology and Biochemistry". Diego, CA: EMD Biosciences.

Bienz, M, and H R Pelham. 1986. "Heat Shock Regulatory Elements Function as an Inducible Enhancer in the Xenopus hsp70 Gene and When Linked to a Heterologous Promoter." *Cell* 45: 753–760.

Bilgin, Damla D, Yule Liu, Michael Schiff, and S.P Dinesh-Kumar. 2003. "P58IPK, a Plant Ortholog of Double-Stranded RNA-Dependent Protein Kinase PKR Inhibitor, Functions in Viral Pathogenesis." *Developmental Cell* 4 (5) (May): 651–661.

Biswas, Chhanda, Uma Sriram, Bogoljub Ciric, Olga Ostrovsky, Stefania Gallucci, and Yair Argon. 2006. "The N-Terminal Fragment of GRP94 Is Sufficient for Peptide Presentation via Professional Antigen-Presenting Cells." *International Immunology* 18 (7) (July): 1147–57.

Blatch, Gregory L, and Michael Lässle. 1999. "The Tetratricopeptide Repeat: A Structural Motif Mediating Protein-Protein Interactions." *BioEssays* 21 (11) (November 1): 932–939.

Bork, Peer, and Marius Sudol. 1994. "The WW Domain: A Signalling Site in Dystrophin?" *Trends in Biochemical Sciences* 19 (12) (December): 531–533.

Borkovich, K a, F W Farrelly, D B Finkelstein, J Taulien, and S Lindquist. 1989. "Hsp82 Is an Essential Protein That Is Required in Higher Concentrations for Growth of Cells At Higher Temperatures." *Molecular and Cellular Biology* 9 (9) (September): 3919–30.

Botha, M, E-R Pesce, and G L Blatch. 2007. "The Hsp40 Proteins of Plasmodium Falciparum and Other Apicomplexa: Regulating Chaperone Power in the Parasite and the Host." *The International Journal of Biochemistry & Cell Biology* 39 (10) (January): 1781–803.

Brightman, Shannon E., Gregory L. Blatch, and Bruce R. Zetter. 1995. "Isolation of a Mouse cDNA Encoding MTJ1, a New Murine Member of the DnaJ Family of Proteins." *Gene* 153 (2) (February): 249–254.

Brocard, Cécile, and Andreas Hartig. 2006. "Peroxisome Targeting Signal 1: Is It Really a Simple Tripeptide?" *Biochimica et Biophysica Acta* 1763 (12) (December): 1565–73.

Bröms, Jeanette E, Petra J Edqvist, Katrin E Carlsson, Åke Forsberg, and Matthew S Francis. 2005. "Mapping of a YscY Binding Domain within the LcrH Chaperone That Is Required for Regulation of Yersinia Type III Secretion." *Journal of Bacteriology* 187 (22): 7738–7752.

Bröms, Jeanette E, Anna-Lena Forslund, Åke Forsberg, and Matthew S Francis. 2003. "PcrH of Pseudomonas Aeruginosa Is Essential for Secretion and Assembly of the Type III Translocon." *Journal of Infectious Diseases* 188 (12) (December 15): 1909–1921.

Bruneau, N, D Lombardo, and M Bendayan. 1998. "Participation of GRP94-Related Protein in Secretion of Pancreatic Bile Salt-Dependent Lipase and in Its Internalization by the Intestinal Epithelium." *Journal of Cell Science* 111 (Pt 1 (September): 2665–79.

Brychzy, Alexander, Theo Rein, Konstanze F Winklhofer, F Ulrich Hartl, Jason C Young, and Wolfgang M J Obermann. 2003. "Cofactor Tpr2 Combines Two TPR Domains and a J Domain to Regulate the Hsp70/Hsp90 Chaperone System." *The EMBO Journal* 22 (14) (July 15): 3613–23.

Buchberger, A, H Schröder, M Büttner, A Valencia, and B Bukau. 1994. "A Conserved Loop in the ATPase Domain of the DnaK Chaperone Is Essential for Stable Binding of GrpE." *Nature Structural & Molecular Biology* 1 (2): 95–101.

Buchner, Johannes. 1999. "Hsp90 & Co. – a Holding for Folding." *Trends in Biochemical Sciences* 24 (4) (April): 136–141.

Bukau, Bernd, and Arthur L Horwich. 1998. "The Hsp70 and Hsp60 Chaperone Machines." *Cell* 92 (3) (February): 351–366.

Büttner, Carina R, Isabel Sorg, Guy R Cornelis, Dirk W Heinz, and Hartmut H Niemann. 2008. “Structure of the Yersinia Enterocolitica Type III Secretion Translocator Chaperone SycD.” *Journal of Molecular Biology* 375 (4) (January 25): 997–1012.

Cadepond, F, N Binart, N Jibard, G Schweizer-Groyer, I Segard-Maurel, and EE Baulieu. 1993. “Interaction of Glucocorticosteroid Receptor and Wild-Type or Mutated 90-kDa Heat Shock Protein Coexpressed in Baculovirus-Infected Sf9 Cells.” *Proceedings of the National Academy of Sciences of the United States of America* 90: 10434–10438.

Calfon, Marcella, Huiqing Zeng, Fumihiko Urano, Jeffery H Till, Stevan R Hubbard, Heather P Harding, Scott G Clark, and David Ron. 2002. “IRE1 Couples Endoplasmic Reticulum Load to Secretory Capacity by Processing the XBP-1 mRNA.” *Nature* 415 (6867) (January 3): 92–96.

Callahan, Margaret K, Delphine Chaillot, Claire Jacquin, Paul R Clark, and Antoine Ménoret. 2002. “Differential Acquisition of Antigenic Peptides by Hsp70 and Hsc70 under Oxidative Conditions.” *Journal of Biological Chemistry* 277 (37) (September 13): 33604–33609.

Caplan, Avrom J. 2003. “What Is a Co-Chaperone?” *Cell Stress & Chaperones* 8 (2): 105.

Carrello, Amerigo, Rudi K Allan, Sarah L Morgan, Barbara a L Owen, Danny Mok, Bryan K Ward, Rodney F Minchin, David O Toft, and Thomas Ratajczak. 2004. “Interaction of the Hsp90 Cochaperone Cyclophilin 40 with Hsc70.” *Cell Stress & Chaperones* 9 (2) (January): 167–81.

Carugo, Oliviero, and Sándor Pongor. 2001. “A Normalized Root-Mean-Spuare Distance for Comparing Protein Three-Dimensional Structures.” *Protein Science* 10 (7) (July 1): 1470–1473.

Chadli, a, I Bouhouche, W Sullivan, B Stensgard, N McMahon, M G Catelli, and D O Toft. 2000. “Dimerization and N-Terminal Domain Proximity Underlie the Function of the Molecular Chaperone Heat Shock Protein 90.” *Proceedings of the National Academy of Sciences of the United States of America* 97 (23) (November 7): 12524–9.

Chang, S C, a E Erwin, and a S Lee. 1989. “Glucose-Regulated Protein (GRP94 and GRP78) Genes Share Common Regulatory Domains and Are Coordinately Regulated by Common Trans-Acting Factors.” *Molecular and Cellular Biology* 9 (5) (May): 2153–62.

Chartron, Justin W, Grecia M Gonzalez, and William M Clemons. 2011. “A Structural Model of the Sgt2 Protein and Its Interactions with Chaperones and the Get4/Get5 Complex.” *Journal of Biological Chemistry* 286 (39) (September 30): 34325–34334.

Chau, DavidH.W., Ji Yuan, Huifang Zhang, Paul Cheung, Travis Lim, Zhen Liu, Alhousseynou Sall, and Decheng Yang. 2007. “Coxsackievirus B3 Proteases 2A and 3C Induce Apoptotic Cell Death through Mitochondrial Injury and Cleavage of eIF4GI but Not DAP5/p97/NAT1.” *Apoptosis* 12 (3): 513–524.

Chavany, Christine, Edward Mimnaugh, Penny Miller, Roberto Bitton, Phongmai Nguyen, Jane Trepel, Luke Whitesell, Rodney Schnur, James D Moyer, and Len Neckers. 1996. “p185 Binds to GRP94 in Vivo: DISSOCIATION OF THE p185/GRP94 HETEROCOMPLEX BY BENZOQUINONE ANSAMYCINS PRECEDES DEPLETION OF p185 .” *Journal of Biological Chemistry* 271 (9) (March 1): 4974–4977.

Cheetham, Micheal E, and Avrom J Caplan. 1998. “Structure, Function and Evolution of DNAj: Conservation and Adaptation of Chaperone Function.” *Cell Stress & Chaperone* 3 (1): 28–36.

Chen, Bin, William H Piel, Liming Gui, Elspeth Bruford, and Antónia Monteiro. 2005. “The HSP90 Family of Genes in the Human Genome: Insights into Their Divergence and Evolution.” *Genomics* 86 (6) (December): 627–37.

Chen, C F, Y Chen, K Dai, P L Chen, D J Riley, and W H Lee. 1996. “A New Member of the hsp90 Family of Molecular Chaperones Interacts with the Retinoblastoma Protein during Mitosis and after Heat Shock.” *Molecular and Cellular Biology* 16 (9) (September): 4691–9.

Chen, Letian, Satoshi Hamada, Masayuki Fujiwara, Tingheng Zhu, Nguyen Phuong Thao, Hann Ling Wong, Priti Krishna, et al. 2010. “The Hop/Sti1-Hsp90 Chaperone Complex Facilitates the Maturation and Transport of a PAMP Receptor in Rice Innate Immunity.” *Cell Host & Microbe* 7 (3) (March 18): 185–96.

Cheng, Ming Y, F.-Ulrich Hartl, and Arthur L Norwich. 1990. “The Mitochondrial Chaperonin hsp60 Is Required for Its Own Assembly.” *Nature* 348 (6300) (November 29): 455–458.

Chiosis, Gabriela, Maria Vilenchik, Joungnam Kim, and David Solit. 2004. “Hsp90: The Vulnerable Chaperone.” *Drug Discovery Today* 9 (20) (October 15): 881–8.

Chromy, Laura R, James M Pipas, and Robert L Garcea. 2003. “Chaperone-Mediated in Vitro Assembly of Polyomavirus Capsids.” *Proceedings of the National Academy of Sciences* 100 (18) (September 2): 10477–10482.

Chu, Y, and X Yang. 2011. “SUMO E3 Ligase Activity of TRIM Proteins.” *Oncogene* 30 (9) (March 3): 1108–1116.

Connell, Patrice, Carol A Ballinger, Jihong Jiang, Yaxu Wu, Larry J Thompson, Jorg Hohfeld, and Cam Patterson. 2001. "The Co-Chaperone CHIP Regulates Protein Triage Decisions Mediated by Heat-Shock Proteins." *Nat Cell Biol* 3 (1) (January): 93–96.

Cornejo, VíctorHugo, and Claudio Hetz. 2013. "The Unfolded Protein Response in Alzheimer's Disease." *Seminars in Immunopathology* 35 (3): 277–292.

Cortajarena, Aitziber L. 2006. "Ligand Binding by TPR Domains." *Protein Science* 15: 1193–1198.

Cortajarena, Aitziber L, Fang Yi, and Lynne Regan. 2008. "Designed TPR Modules as Novel Anticancer Agents." *ACS Chemical Biology* 3 (3) (March 1): 161–166.

Corthals, G L, S P Gygi, R Aebersold, and S D Patterson. 2000. "Identification of Proteins by Mass Spectrometry." In *Proteome Research: Two-Dimensional Gel Electrophoresis and Identification Methods SE - 10*, edited by Thierry Rabilloud, 197–231. Springer Berlin Heidelberg.

Cox, MarcB., and JillL. Johnson. 2011. "The Role of p23, Hop, Immunophilins, and Other Co-Chaperones in Regulating Hsp90 Function." In *Molecular Chaperones SE - 4*, edited by Stuart K Calderwood and Thomas L Prince, 787:45–66. Humana Press.

Cry, Douglas M. 1995. "Cooperation of the Molecular Chaperone Ydj1 with Specific Hsp70 Homologs to Suppress Protein Aggregation." *FEBS Letters* 359 (2-3) (February): 129–132.

Csermely, P. 1999. "Chaperone-Percolator Model: A Possible Molecular Mechanism of Anfinsen-Cage-Type Chaperones." *BioEssays : News and Reviews in Molecular, Cellular and Developmental Biology* 21: 959–965.

Csermely, Péter, Tamás Schnaider, Csaba Sőti, Zoltán Prohászka, and Gábor Nardai. 1998. "Chaperone-Percolator Model: A Possible Molecular Mechanism of Anfinsen-Cage-Type Chaperones." *Pharmacology & Therapeutics* 79 (2) (August): 129–168.

Cyr, Douglas M, Jörg Höhfeld, and Cam Patterson. 2002. "Protein Quality Control: U-Box-Containing E3 Ubiquitin Ligases Join the Fold." *Trends in Biochemical Sciences* 27 (7) (July): 368–375.

Cziepluch, C, E Kordes, R Poirey, a Grewenig, J Rommelaere, and J C Jauniaux. 1998. "Identification of a Novel Cellular TPR-Containing Protein, SGT, That Interacts with the Nonstructural Protein NS1 of Parvovirus H-1." *Journal of Virology* 72 (5) (May): 4149–56.

D'Andrea, Luca D, and Lynne Regan. 2003. "TPR Proteins: The Versatile Helix." *Trends in Biochemical Sciences* 28 (12) (December): 655–62.

Daniel, Sheril, Graeme Bradley, Victoria M Longshaw, Csaba Söti, Peter Csermely, and Gregory L Blatch. 2008. "Nuclear Translocation of the Phosphoprotein Hop (Hsp70/Hsp90 Organizing Protein) Occurs under Heat Shock, and Its Proposed Nuclear Localization Signal Is Involved in Hsp90 Binding." *Biochimica et Biophysica Acta* 1783 (6) (June): 1003–14.

Das, a K, P W Cohen, and D Barford. 1998. "The Structure of the Tetratricopeptide Repeats of Protein Phosphatase 5: Implications for TPR-Mediated Protein-Protein Interactions." *The EMBO Journal* 17 (5) (March 2): 1192–9.

Dauber, Bianca, and Thorsten Wolff. 2009. "Activation of the Antiviral Kinase PKR and Viral Countermeasures." *Viruses* 1 (3) (December): 523–44.

Daugaard, Mads, Mikkel Rohde, and Marja Jäättelä. 2007. "The Heat Shock Protein 70 Family: Highly Homologous Proteins with Overlapping and Distinct Functions." *FEBS Letters* 581 (19) (July 31): 3702–10.

Davies, Todd H, and Edwin R Sánchez. 2005. "FKBP52." *The International Journal of Biochemistry & Cell Biology* 37 (1) (January): 42–7.

DeLano, WL, and JW Lam. 2005. "PyMOL: A Communications Tool for Computational Models." *Abstracts of Papers of the American Chemical Society* 230: U1371–U1372.

Denoyelle, Christophe, George Abou-Rjaily, Vladimir Bezrookove, Monique Verhaegen, Timothy M Johnson, Douglas R Fullen, Jenny N Pointer, et al. 2006. "Anti-Oncogenic Role of the Endoplasmic Reticulum Differentially Activated by Mutations in the MAPK Pathway." *Nat Cell Biol* 8 (10) (October): 1053–1063.

Deuerling, Elke, and Bernd Bukau. 2004. "Chaperone-Assisted Folding of Newly Synthesized Proteins in the Cytosol." *Critical Reviews in Biochemistry and Molecular Biology* 39 (5-6): 261–77.

Didenko, Tatiana, Afonso M S Duarte, G Elif Karagöz, and Stefan G D Rüdiger. 2012. "Hsp90 Structure and Function Studied by NMR Spectroscopy." *Biochimica et Biophysica Acta* 1823 (3) (March): 636–47.

Dinkel, Holger, Sushama Michael, Robert J Weatheritt, Norman E Davey, Kim Van Roey, Brigitte Altenberg, Grischa Toedt, et al. 2012. "ELM—the Database of Eukaryotic Linear Motifs." *Nucleic Acids Research* 40 (D1) (January 1): D242–D251.

Dittmar, Kurt D, Damon R Demady, Louis F Stancato, Priti Krishna, and William B Pratt. 1997. "Folding of the Glucocorticoid Receptor by the Heat Shock Protein (hsp) 90-Based Chaperone Machinery: the role of p23 is to stabilize receptor·hsp90 heterocomplexes formed by hsp90·p60·hsp70 ." *Journal of Biological Chemistry* 272 (34) (August 22): 21213–21220.

Dollins, D E, J J Warren, R M Immormino, and D T Gewirth. 2007. “Structures of GRP94-Nucleotide Complexes Reveal Mechanistic Differences between the hsp90 Chaperones.” *Molecular Cell* 28 (1) (October): 41–56.

Domanico, S Z, D C DeNagel, J N Dahlseid, J M Green, and S K Pierce. 1993. “Cloning of the Gene Encoding Peptide-Binding Protein 74 Shows That It Is a New Member of the Heat Shock Protein 70 Family.” *Molecular and Cellular Biology* 13 (6) (June): 3598–610.

Donnelly, Alison, and Brian S J Blagg. 2009. “Novobiocin and Additional Inhibitors of the Hsp90 C-Terminal Nucleotide-Binding Pocket.” *Current Medicinal Chemistry* 15 (26): 2702–2717.

Duina, AA, HM Kalton, and RF Gaber. 1998. “Requirement for Hsp90 and a CyP-40-Type Cyclophilin in Negative Regulation of the Heat Shock Response.” *Journal of Biological Chemistry* 273: 18974–18978.

Dutta, Rinku, and Masayori Inouye. 2000. “GHKL , an Emergent ATPase / Kinase Superfamily.” *Trends in Biochemical Sciences* 25: 24–28.

Eisenberg, David, Roland Lüthy, and James U. Bowie. 1997. “VERIFY3D: Assessment of Protein Models with Three-Dimensional Profiles.” *Methods in Enzymology* 277: 396–404.

Elleto, D, D Dersh, and Y Argon. 2010. “GRP94 in ER Quality Control and Stress Responses.” *Seminars in Cell & Developmental Biology* 21 (5): 479–485.

Ellis, John. 1987. “Proteins as Molecular Chaperones.” *Nature* 328 (6129) (July 30): 378–379.

Ellis, R J, and S M Van Der Vies. 1988. “The Rubisco Subunit Binding Protein.” *Photosynthesis Research* 16 (1-2) (April): 101–15.

Ellis, R J, S M Van Der Vies, and SM Hemmingsen. 1987. “He Rubisco Large Subunit Binding Protein -- a Molecular Chaperone?” In *In: Von Wettstein D and Chuva N-H (eds) Proceedings of the NATO Advanced Study Institute Plant Molecular Biology*, 33–40. New York: Plenum Publishing Co.

Fan, Chun-Yang, Soojin Lee, and Douglas M Cyr. 2003. “Mechanisms for Regulation of Hsp70 Function by Hsp40.” *Cell Stress & Chaperones* 8 (4) (October 1): 309–316.

Feldheim, D, J Rothblatt, and R Schekman. 1992. “Topology and Functional Domains of Sec63p, an Endoplasmic Reticulum Membrane Protein Required for Secretory Protein Translocation.” *Molecular and Cellular Biology* 12 (7) (July 1): 3288–3296. doi:10.1128/MCB.12.7.3288.

Feldman, D E, and J Frydman. 2000. “Protein Folding in Vivo: The Importance of Molecular Chaperones.” *Current Opinion in Structural Biology* 10: 26–33.

Ferri, Karine F, and Guido Kroemer. 2001. “Organelle-Specific Initiation of Cell Death Pathways.” *Nat Cell Biol* 3 (11) (November): E255–E263.

Fink, A L. 1999. “Chaperone-Mediated Protein Folding.” *Physiological Reviews* 79 (2): 425–449.

Fischer, Gunter, Brigitte Wittmann-Liebold, Kurt Lang, Thomas Kiefhaber, and Franz X Schmid. 1989. “Cyclophilin and Peptidyl-Prolyl Cis-Trans Isomerase Are Probably Identical Proteins.” *Nature* 337 (6206) (February 2): 476–478.

Flaherty, Kevin M, Camilla DeLuca-Flaherty, and David B McKay. 1990. “Three-Dimensional Structure of the ATPase Fragment of a 70K Heat-Shock Cognate Protein.” *Nature* 346 (6285) (August 16): 623–628.

Fliss, Albert E, Jie Rao, Mark W Melville, Michael E Cheetham, and Avrom J Caplan. 1999. “Domain Requirements of DnaJ-like (Hsp40) Molecular Chaperones in the Activation of a Steroid Hormone Receptor.” *Journal of Biological Chemistry* 274 (48) (November 26): 34045–34052.

Fohlman, J, D Eaker, E Karlsoon, and S Thesleff. 1976. “Taipoxin, an Extremely Potent Presynaptic Neurotoxin from the Venom of the Australian Snake Taipan (Oxyuranus S. Scutellatus). Isolation, Characterization, Quaternary Structure and Pharmacological Properties.” *European Journal of Biochemistry / FEBS* 68: 457–469.

Fortugno, Paola, Elena Beltrami, Janet Plescia, Jason Fontana, Deepti Pradhan, Pier Carlo Marchisio, William C Sessa, and Dario C Altieri. 2003. “Regulation of Survivin Function by Hsp90.” *Proceedings of the National Academy of Sciences of the United States of America* 100 (24) (November 25): 13791–6.

Fox, JeffreyD., and DavidS. Waugh. 2003. “Maltose-Binding Protein as a Solubility Enhancer.” In *E. coliGene Expression Protocols*, edited by PeterE. Vaillancourt, 205:99–117. Humana Press.

Frasson, Martina, Maurizio Vitadello, Anna Maria Brunati, Nicoletta La Rocca, Elena Tibaldi, Lorenzo a Pinna, Luisa Gorza, and Arianna Donella-Deana. 2009. “Grp94 Is Tyr-Phosphorylated by Fyn in the Lumen of the Endoplasmic Reticulum and Translocates to Golgi in Differentiating Myoblasts.” *Biochimica et Biophysica Acta* 1793 (2) (February): 239–52.

Freeman, B C, and R I Morimoto. 1996. “The Human Cytosolic Molecular Chaperones hsp90, hsp70 (hsc70) and Hdj-1 Have Distinct Roles in Recognition of a Non-Native Protein and Protein Refolding.” *The EMBO Journal* 15 (12) (June 17): 2969–79.

Freeman, B C, M P Myers, R Schumacher, and R I Morimoto. 1995. “Identification of a Regulatory Motif in Hsp70 That Affects ATPase Activity, Substrate Binding and Interaction with HDJ-1.” *The EMBO Journal* 14 (10) (May 15): 2281–92.

Frey, Stephan, Adriane Leskovar, Jochen Reinstein, and Johannes Buchner. 2007. “The ATPase Cycle of the Endoplasmic Chaperone Grp94.” *Journal of Biological Chemistry* 282 (49) (December 7): 35612–35620.

Frydman, J. 2001. “Folding of Newly Translated Proteins in Vivo: The Role of Molecular Chaperones.” *Annual Review of Biochemistry* 70: 603–647.

Galam, Lakshmi, M Kyle Hadden, Zeqiang Ma, Qi-Zhuang Ye, Bo-Geon Yun, Brian S J Blagg, and Robert L Matts. 2007. “High-Throughput Assay for the Identification of Hsp90 Inhibitors Based on Hsp90-Dependent Refolding of Firefly Luciferase.” *Bioorganic & Medicinal Chemistry* 15 (5) (March 1): 1939–46.

Gale Michael, Collin M Blakely, André Darveau, Patrick R Romano, Marcus J Korth, and Michael G Katze. 2002. “P52rIPK Regulates the Molecular Cochaperone P58IPK To Mediate Control of the RNA-Dependent Protein Kinase in Response to Cytoplasmic Stress†.” *Biochemistry* 41 (39) (August 20): 11878–11887.

Gale, M, C M Blakely, D a Hopkins, M W Melville, M Wambach, P R Romano, and M G Katze. 1998. “Regulation of Interferon-Induced Protein Kinase PKR: Modulation of P58IPK Inhibitory Function by a Novel Protein, P52rIPK.” *Molecular and Cellular Biology* 18 (2) (February): 859–71.

Gale, M, S L Tan, M Wambach, and M G Katze. 1996. “Interaction of the Interferon-Induced PKR Protein Kinase with Inhibitory Proteins P58IPK and Vaccinia Virus K3L Is Mediated by Unique Domains: Implications for Kinase Regulation.” *Molecular and Cellular Biology* 16 (8) (August 1): 4172–4181.

Gale, Michael, and Michael G Katze. 1998. “Molecular Mechanisms of Interferon Resistance Mediated by Viral-Directed Inhibition of PKR, the Interferon-Induced Protein Kinase.” *Pharmacology & Therapeutics* 78 (1) (April): 29–46.

Gao, Danmei, I Fon Bambang, Thomas C Putti, Yuan Kun Lee, Des R Richardson, and Daohai Zhang. 2012. “ERp29 Induces Breast Cancer Cell Growth Arrest and Survival through Modulation of Activation of p38 and Upregulation of ER Stress Protein p58IPK.” *Lab Invest* 92 (2) (February): 200–213.

Gatsos, Xenia, Andrew J Perry, Khatira Anwari, Pavel Dolezal, P Peter Wolynec, Vladimir A Likić, Anthony W Purcell, Susan K Buchanan, and Trevor Lithgow. 2008. “Protein Secretion and Outer Membrane Assembly in Alphaproteobacteria.” *FEMS Microbiology Reviews* 32 (6) (November 1): 995–1009.

Gatto, Gregory J, Brian V Geisbrecht, Stephen J Gould, and Jeremy M Berg. 2000. “A Proposed Model for the PEX5-Peroxisomal Targeting Signal-1 Recognition Complex.” *Proteins: Structure, Function, and Bioinformatics* 38 (3) (February 15): 241–246.

Ghosh, Dipanjana, Han Yu, Xing Fei Tan, Teck Kwang Lim, Ramdzan M Zubaidah, Hwee Tong Tan, Maxey C M Chung, and Qingsong Lin. 2011. “Identification of Key Players for Colorectal Cancer Metastasis by iTRAQ Quantitative Proteomics Profiling of Isogenic SW480 and SW620 Cell Lines.” *Journal of Proteome Research* 10 (10) (August 22): 4373–4387.

Goebl, Mark, and Mitsuhiro Yanagida. 1991. “The TPR Snap Helix: A Novel Protein Repeat Motif from Mitosis to Transcription.” *Trends in Biochemical Sciences* 16 (January): 173–177.

Golovanov, Alexander P, Guillaume M Hautbergue, Stuart a Wilson, and Lu-Yun Lian. 2004. “A Simple Method for Improving Protein Solubility and Long-Term Stability.” *Journal of the American Chemical Society* 126 (29) (July 28): 8933–9.

Goodman, Alan G, Jamie L Fornek, Guruprasad R Medigeshi, Lucy a Perrone, Xinxia Peng, Matthew D Dyer, Sean C Proll, et al. 2009. “P58(IPK): A Novel ‘CIHD’ Member of the Host Innate Defense Response against Pathogenic Virus Infection.” *PLoS Pathogens* 5 (5) (May): e1000438.

Goodman, Alan G, Jennifer a Smith, Siddharth Balachandran, Olivia Perwitasari, Sean C Proll, Matthew J Thomas, Marcus J Korth, Glen N Barber, Leslie a Schiff, and Michael G Katze. 2007. “The Cellular Protein P58IPK Regulates Influenza Virus mRNA Translation and Replication through a PKR-Mediated Mechanism.” *Journal of Virology* 81 (5) (March): 2221–30.

Goodman, Alan G, Bertrand C W Tanner, Stewart T Chang, Mariano Esteban, and Michael G Katze. 2011. “Virus Infection Rapidly Activates the P58(IPK) Pathway, Delaying Peak Kinase Activation to Enhance Viral Replication.” *Virology* 417 (1) (August 15): 27–36.

Grad, Iwona, Christopher R Cederroth, Joël Walicki, Corinne Grey, Sofia Barluenga, Nicolas Winssinger, Bernard De Massy, Serge Nef, and Didier Picard. 2010. “The Molecular Chaperone Hsp90α Is Required for Meiotic Progression of Spermatocytes beyond Pachytene in the Mouse.” *PloS One* 5 (12) (January): e15770.

Grammatikakis, N, J H Lin, a Grammatikakis, P N Tsichlis, and B H Cochran. 1999. “p50(cdc37) Acting in Concert with Hsp90 Is Required for Raf-1 Function.” *Molecular and Cellular Biology* 19 (3) (March): 1661–72.

Grammatikakis, Nicholas, Adina Vultur, Chilakamarti V Ramana, Aliki Siganou, Clifford W Schweinfest, Dennis K Watson, and Leda Raptis. 2002. “The Role of Hsp90N, a New Member of the Hsp90 Family, in Signal Transduction and Neoplastic Transformation.” *Journal of Biological Chemistry* 277 (10) (March 8): 8312–8320.

Gray, Phillip J, Thomas Prince, Jinrong Cheng, Mary Ann Stevenson, and Stuart K Calderwood. 2008. “Targeting the Oncogene and Kinome Chaperone CDC37.” *Nat Rev Cancer* 8 (7) (July): 491–495.

Greene, M K, K Maskos, and S J Landry. 1998. “Role of the J-Domain in the Cooperation of Hsp40 with Hsp70.” *Proceedings of the National Academy of Sciences of the United States of America* 95 (11) (May 26): 6108–13.

Grenert, James P, William P Sullivan, Patrick Fadden, Timothy A J Haystead, Jenny Clark, Edward Mimnaugh, Henry Krutzsch, et al. 1997. “The Amino-Terminal Domain of Heat Shock Protein 90 (hsp90) That Binds Geldanamycin Is an ATP/ADP Switch Domain That Regulates hsp90 Conformation.” *Journal of Biological Chemistry* 272 (38) (September 19): 23843–23850.

Guan, Jikui, and Li Yuan. 2008. “A Heat-Shock Protein 40, DNAJB13, Is an Axoneme-Associated Component in Mouse Spermatozoa.” *Molecular Reproduction and Development* 75 (9) (September 1): 1379–1386.

Guan, KunLiang, and Jack E. Dixon. 1991. “Eukaryotic Proteins Expressed in Escherichia Coli: An Improved Thrombin Cleavage and Purification Procedure of Fusion Proteins with Glutathione S-Transferase.” *Analytical Biochemistry* 192 (2) (February): 262–267.

Guan, Zhenhong, Di Liu, Shuofu Mi, Jie Zhang, Qinong Ye, Ming Wang, George F Gao, and Jinghua Yan. 2010. “Interaction of Hsp40 with Influenza Virus M2 Protein: Implications for PKR Signaling Pathway.” *Protein & Cell* 1 (10) (October): 944–55.

Guex, Nicolas, and Manuel C Peitsch. 1997. “SWISS-MODEL and the Swiss-Pdb Viewer: An Environment for Comparative Protein Modeling.” *ELECTROPHORESIS* 18 (15) (January 1): 2714–2723.

Gupta, Radhey S. 1995. “Phylogenetic Analysis of the 90 kD Heat Shock Family of Protein Sequences Amd an Examination of the Relationship among Animals, Plants, and Fungi Species.” *Molecular Biology and Evolution* 12 (6): 1063–1073.

Hainzl, Otmar, Maria Claribel Lapina, Johannes Buchner, and Klaus Richter. 2009. “The Charged Linker Region Is an Important Regulator of Hsp90 Function.” *Journal of Biological Chemistry* 284 (34) (August 21): 22559–22567.

Hall, T. 1999. “BioEdit: A User-Friendly Biological Sequence Alingment Editor and Analysis Program for Windows 95/98/NT.” *Nucleic Acids Symposium Series* 41: 95–98.

Harding, H P, Y Zhang, a Bertolotti, H Zeng, and D Ron. 2000. “Perk Is Essential for Translational Regulation and Cell Survival during the Unfolded Protein Response.” *Molecular Cell* 5 (5) (May): 897–904.

Harding, Heather P, Marcella Calfon, Fumihiko Urano, Isabel Novoa, and David Ron. 2002. “transcriptional and translational control in the mammalian unfolded protein response.” *Annual Review of Cell and Developmental Biology* 18 (1) (November 1): 575–599.

Harding, Heather P, Isabel Novoa, Yuhong Zhang, Huiqing Zeng, Ron Wek, Matthieu Schapira, and David Ron. 2000. “Regulated Translation Initiation Controls Stress-Induced Gene Expression in Mammalian Cells.” *Molecular Cell* 6 (5) (November): 1099–1108.

Harding, Heather P, Yuhong Zhang, and David Ron. 1999. “Protein Translation and Folding Are Coupled by an Endoplasmic-Reticulum-Resident Kinase.” *Nature* 397 (6716) (January 21): 271–274.

Harding, Heather P., Huiqing Zeng, Yuhong Zhang, Rivka Jungries, Peter Chung, Heidi Plesken, David D. Sabatini, and David Ron. 2001. “Diabetes Mellitus and Exocrine Pancreatic Dysfunction in Perk−/− Mice Reveals a Role for Translational Control in Secretory Cell Survival.” *Molecular Cell* 7 (6) (June): 1153–1163.

Hartl, F U. 1995. “Principles of Chaperone-Mediated Protein Folding.” *Philosophical Transactions of the Royal Society of London. Series B, Biological Sciences* 348: 107–112.

Hartl, F Ulrich, and Manajit Hayer-Hartl. 2002. “Molecular Chaperones in the Cytosol: From Nascent Chain to Folded Protein.” *Science* 295 (5561) (March 8): 1852–1858.

Haslbeck, Martin, Titus Franzmann, Daniel Weinfurtner, and Johannes Buchner. 2005. “Some like It Hot: The Structure and Function of Small Heat-Shock Proteins.” *Nature Structural & Molecular Biology* 12 (10): 842–846.

Haze, Kyosuke, Hiderou Yoshida, Hideki Yanagi, Takashi Yura, and Kazutoshi Mori. 1999. “Mammalian Transcription Factor ATF6 Is Synthesized as a Transmembrane Protein and Activated by Proteolysis in Response to Endoplasmic Reticulum Stress.” *Molecular Biology of the Cell* 10 (11) (November 1): 3787–3799.

Hendershot, LM. 2004. “The ER Function BiP Is a Master Regulator of ER Function.” *Mount Sinai Journal of Medicine* 71: 289–297.

Hetz, Claudio, Eric Chevet, and Heather P Harding. 2013. “Targeting the Unfolded Protein Response in Disease.” *Nat Rev Drug Discov* 12 (9) (September): 703–719.

Hirano, Tatsuya, Noriyuki Kinoshita, Kosuke Morikawa, and Mitsuhiro Yanagida. 1990. “Snap Helix with Knob and Hole: Essential Repeats in S. Pombe Nuclear Protein nuc2 +.” *Cell* 60 (2) (January): 319–328.

Höhfeld, J, D M Cyr, and C Patterson. 2001. “From the Cradle to the Grave: Molecular Chaperones That May Choose between Folding and Degradation.” *EMBO Reports* 2 (10) (October): 885–90.

Höhfeld, J, Y Minami, and F U Hartl. 1995. “Hip, a Novel Cochaperone Involved in the Eukaryotic Hsc70/Hsp40 Reaction Cycle.” *Cell* 83 (4) (November 17): 589–98.

Holmes, Joanna L, Swee Y Sharp, Steve Hobbs, and Paul Workman. 2008. “Silencing of HSP90 Cochaperone AHA1 Expression Decreases Client Protein Activation and Increases Cellular Sensitivity to the HSP90 Inhibitor 17-Allylamino-17-Demethoxygeldanamycin.” *Cancer Research* 68 (4) (February 15): 1188–1197.

Horne, B Erin, Tingfeng Li, Pierre Genevaux, Costa Georgopoulos, and Samuel J Landry. 2010. “The Hsp40 J-Domain Stimulates Hsp70 When Tethered by the Client to the ATPase Domain.” *Journal of Biological Chemistry* 285 (28) (July 9): 21679–21688.

Hosoda, Akira, Yukio Kimata, Akio Tsuru, and Kenji Kohno. 2003. “JPDI, a Novel Endoplasmic Reticulum-Resident Protein Containing Both a BiP-Interacting J-Domain and Thioredoxin-like Motifs.” *Journal of Biological Chemistry* 278 (4) (January 24): 2669–2676.

HOVANESSIAN, Ara G, and Julien GALABRU. 1987. “The Double-Stranded RNA-Dependent Protein Kinase Is Also Activated by Heparin.” *European Journal of Biochemistry* 167 (3) (September 1): 467–473.

Huber, Anne-Laure, Justine Lebeau, Patricia Guillaumot, Virginie Pétrilli, Mouhannad Malek, Julien Chilloux, Frédérique Fauvet, et al. 2013. “p58(IPK)-Mediated Attenuation of the Proapoptotic PERK-CHOP Pathway Allows Malignant Progression upon Low Glucose.” *Molecular Cell* 49 (6) (March 28): 1049–59.

Jackson, SophieE. 2013. “Hsp90: Structure and Function.” Edited by Sophie Jackson. *Topics in Current Chemistry* 328: 155–240.

Jansen, Gregor, Pekka Määttänen, Alexey Y Denisov, Leslie Scarffe, Babette Schade, Haouaria Balghi, Kurt Dejgaard, et al. 2012. “An Interaction Map of Endoplasmic Reticulum Chaperones and Foldases.” *Molecular & Cellular Proteomics* 11 (9) (September 1): 710–723.

Job, Viviana, Pierre-Jean Matteï, David Lemaire, Ina Attree, and Andréa Dessen. 2010. “Structural Basis of Chaperone Recognition of Type III Secretion System Minor Translocator Proteins.” *Journal of Biological Chemistry* 285 (30) (July 23): 23224–23232.

Jones, David T, William R Taylor, and Janet M Thornton. 1992. “The Rapid Generation of Mutation Data Matrices from Protein Sequences.” *Computer Applications in the Biosciences : CABIOS* 8 (3) (June 1): 275–282.

Kajander, Tommi, Jonathan N Sachs, Adrian Goldman, and Lynne Regan. 2009. “Electrostatic Interactions of Hsp-Organizing Protein Tetratricopeptide Domains with Hsp70 and Hsp90: computational analysis and protein engineering.” *Journal of Biological Chemistry* 284 (37) (September 11): 25364–25374.

Kalia, Lorraine V, Suneil K Kalia, Hien Chau, Andres M Lozano, Bradley T Hyman, and Pamela J McLean. 2011. “Ubiquitinylation of A-Synuclein by Carboxyl Terminus Hsp70-Interacting Protein (CHIP) Is Regulated by Bcl-2-Associated Athanogene 5 (BAG5).” *PloS One* 6 (2) (January): e14695.

Kampinga, Harm H, and Elizabeth A Craig. 2010. “The HSP70 Chaperone Machinery: J Proteins as Drivers of Functional Specificity.” *Nat Rev Mol Cell Biol* 11 (10) (October): 750.

Kassube, Susanne A, Tobias Stuwe, Daniel H Lin, C Danielle Antonuk, Johanna Napetschnig, Günter Blobel, and André Hoelz. 2012. “Crystal Structure of the N-Terminal Domain of Nup358/RanBP2.” *Journal of Molecular Biology* 423 (5) (November 9): 752–65.

Katoh, Kazutaka, Kazuharu Misawa, Kei-ichi Kuma, and Takashi Miyata. 2002. “MAFFT: A Novel Method for Rapid Multiple Sequence Alignment Based on Fast Fourier Transform.” *Nucleic Acids Research* 30 (14) (July 15): 3059–66.

Katze, M G, J Tomita, T Black, R M Krug, B Safer, and a Hovanessian. 1988. “Influenza Virus Regulates Protein Synthesis during Infection by Repressing Autophosphorylation and Activity of the Cellular 68,000-Mr Protein Kinase.” *Journal of Virology* 62 (10) (October): 3710–7.

Katze, Michael G. 1995. “Regulation of the Interferon-Induced PKR: Can Viruses Cope?” *Trends in Microbiology* 3 (2) (February): 75–78.

Kaufman, Randal J. 1999. “Stress Signaling from the Lumen of the Endoplasmic Reticulum: Coordination of Gene Transcriptional and Translational Controls.” *Genes & Development* 13 (10) (May 15): 1211–1233.

Kim, Mi-Sung, Eun-Jung Lee, Hyeong-Reh Choi Kim, and Aree Moon. 2003. “p38 Kinase Is a Key Signaling Molecule for H-Ras-Induced Cell Motility and Invasive Phenotype in Human Breast Epithelial Cells.” *Cancer Research* 63 (17) (September 1): 5454–5461.

Kim, Yujin E, Mark S Hipp, Andreas Bracher, Manajit Hayer-Hartl, and F Ulrich Hartl. 2013. “Molecular Chaperone Functions in Protein Folding and Proteostasis.” *Annual Review of Biochemistry* 82 (January): 323–55.

Kobayashi, Hiroshi, Takeshi Yoshida, and Masayori Inouye. 2009. “Significant Enhanced Expression and Solubility of Human Proteins in Escherichia Coli by Fusion with Protein S from Myxococcus Xanthus.” *Applied and Environmental Microbiology* 75 (16) (August): 5356–62.

Koo, Bon-Hun, and Suneel S Apte. 2010. “Cell-Surface Processing of the Metalloprotease Pro-ADAMTS9 Is Influenced by the Chaperone GRP94/gp96.” *Journal of Biological Chemistry* 285 (1) (January 1): 197–205.

Korth, Marcus J., Christopher N. Lyons, Marlene Wambach, and Michael G. Katze. 1996. “Cloning, Expression, and Cellular Localization of the Oncogenic 58-kDa Inhibitor of the RNA-Activated Human and Mouse Protein Kinase.” *Gene* 170 (2) (May): 181–188.

Kosano, Hiroshi, Bridget Stensgard, M Cristine Charlesworth, Nancy McMahon, and David Toft. 1998. “The Assembly of Progesterone Receptor-hsp90 Complexes Using Purified Proteins.” *Journal of Biological Chemistry* 273 (49) (December 4): 32973–32979.

Krachler, Anne Marie, Amit Sharma, and Colin Kleanthous. 2010. “Self-Association of TPR Domains: Lessons Learned from a Designed, Consensus-Based TPR Oligomer.” *Proteins* 78 (9) (July): 2131–43.

Krüger, E, U Völker, and M Hecker. 1994. “Stress Induction of clpC in Bacillus Subtilis and Its Involvement in Stress Tolerance.” *Journal of Bacteriology* 176 (11) (June): 3360–7.

Kumar, A, C Roach, I S Hirsh, S Turley, S deWalque, P A Michels, and W G Hol. 2001. “An Unexpected Extended Conformation for the Third TPR Motif of the Peroxin PEX5 from Trypanosoma Brucei.” *Journal of Molecular Biology* 307 (1) (March 16): 271–82.

Kyte, Jack, and Russell F. Doolittle. 1982. “A Simple Method for Displaying the Hydropathic Character of a Protein.” *Journal of Molecular Biology* 157 (1) (May): 105–132.

Ladiges, Warren C, Sue E Knoblaugh, John F Morton, Marcus J Korth, Bryce L Sopher, Carole R Baskin, Alasdair MacAuley, Alan G Goodman, Renee C LeBoeuf, and Michael G Katze. 2005. “Pancreatic B-Cell Failure and Diabetes in Mice With a Deletion Mutation of the Endoplasmic Reticulum Molecular Chaperone Gene P58IPK.” *Diabetes* 54 (4) (April 1): 1074–1081.

Lai, B T, N W Chin, A E Stanek, W Keh, and K W Lanks. 1984. “Quantitation and Intracellular Localization of the 85K Heat Shock Protein by Using Monoclonal and Polyclonal Antibodies.” *Molecular and Cellular Biology* 4 (12) (December 1): 2802–2810.

Lamb, John R, Stuart Tugendreich, and Phil Hieter. 1995. “Tetratrico Peptide Repeat Interactions: To TPR or Not to TPR?” *Trends in Biochemical Sciences* 20 (7) (July): 257–259.

Langer, Thomas, Chi Lu, Harrison Echols, John Flanagan, Manajit K Hayer, and F Ulrich Hartl. 1992. “Successive Action of DnaK, DnaJ and GroEL along the Pathway of Chaperone-Mediated Protein Folding.” *Nature* 356 (6371) (April 23): 683–689.

Langland, J O, S Jin, B L Jacobs, and D a Roth. 1995. “Identification of a Plant-Encoded Analog of PKR, the Mammalian Double-Stranded RNA-Dependent Protein Kinase.” *Plant Physiology* 108 (3) (July): 1259–67.

Langland, Jeffrey, and L Jacobs. 1992. “Cytosolic Double-Stranded RNA-Dependent Protein Kinase Is Likely a Dimer of Partially Phosphorylated Mr=66,000 Subunits.” *Journal of Biological Chemistry* 267 (15): 10729–10736.

Laskey, R A, B M Honda, A D Mills, and J T Finch. 1978. “Nucleosomes Are Assembled by an Acidic Protein Which Binds Histones and Transfers Them to DNA.” *Nature* 275: 416–420.

Lässle, Michael, Gregory L Blatch, Vikas Kundra, Toshiro Takatori, and Bruce R Zetter. 1997. “Stress-Inducible, Murine Protein mSTI1: characterization of binding domains for heat shock proteins and in vitro phosphorylation by different kinases .” *Journal of Biological Chemistry* 272 (3) (January 17): 1876–1884.

Lee, Chung-Tien, Christian Graf, Franz J Mayer, Sebastian M Richter, and Matthias P Mayer. 2012. “Dynamics of the Regulation of Hsp90 by the Co-Chaperone Sti1.” *The EMBO Journal* 31 (6) (March 21): 1518–28..

Lee, Jaemin, and Umut Ozcan. 2014. “Unfolded Protein Response Signaling and Metabolic Diseases.” *The Journal of Biological Chemistry* 289 (3) (January 17): 1203–11.

Lee, Soojin, Chun Yang Fan, J Michael Younger, Hongyu Ren, and Douglas M Cyr. 2002. “Identification of Essential Residues in the Type II Hsp40 Sis1 That Function in Polypeptide Binding.” *Journal of Biological Chemistry* 277 (24) (June 14): 21675–21682.

Lee, T G, N Tang, S Thompson, J Miller, and M G Katze. 1994. “The 58,000-Dalton Cellular Inhibitor of the Interferon-Induced Double-Stranded RNA-Activated Protein Kinase (PKR) Is a Member of the Tetratricopeptide Repeat Family of Proteins.” *Molecular and Cellular Biology* 14 (4) (April 1): 2331–2342.

Lee, T G, J Tomita, A G Hovanessian, and M G Katze. 1990. “Purification and Partial Characterization of a Cellular Inhibitor of the Interferon-Induced Protein Kinase of Mr 68,000 from Influenza Virus-Infected Cells.” *Proceedings of the National Academy of Sciences* 87 (16) (August 1): 6208–6212.

Lee, T G, J Tomita, A G Hovanessian, and M G Katze. 1992. “Characterization and Regulation of the 58,000-Dalton Cellular Inhibitor of the Interferon-Induced, dsRNA-Activated Protein Kinase.” *Journal of Biological Chemistry* 267 (20) (July 15): 14238–14243.

Lee, Ung, Chris Wie, Mindy Escobar, Ben Williams, Suk-whan Hong, and Elizabeth Vierling. 2005. “Genetic Analysis Reveals Domain Interactions of Arabidopsis Hsp100 / ClpB and Cooperation with the Small Heat Shock Protein Chaperone System.” *The Plant Cell* 17: 559–571. Letunic, Ivica, Tobias Doerks, and Peer Bork. 2012. “SMART 7: Recent Updates to the Protein Domain Annotation Resource.” *Nucleic Acids Research* 40 (Database issue) (January): D302–5.

Lewis, M J, and H R Pelham. 1985. “Involvement of ATP in the Nuclear and Nucleolar Functions of the 70 Kd Heat Shock Protein.” *The EMBO Journal* 4: 3137–3143.

Li, Jianze, Brenda Lee, and Amy S Lee. 2006. “Endoplasmic Reticulum Stress-Induced Apoptosis: multiple pathways and activation of p53-up-regulated modulator of apoptosis (PUMA) and NOXA by p53 .” *Journal of Biological Chemistry* 281 (11) (March 17): 7260–7270.

Li, Jing, and Johannes Buchner. 2013. “Structure, Function and Regulation of the Hsp90 Machinery.” *Biomedical Journal* 36 (3) (May 1): 106–117.

Lindquist, S, and E A Craig. 1988. “The Heat-Shock Proteins.” *Annual Review of Genetics* 22 (1) (December 1): 631–677.

Lindquisttt, Susan. 1993. “Heat-Shock Protein hsp9O Governs the Activity of pp6Ov-Src Kinase.” *Proceedings of the National Academy of Sciences of the United States of America* 90: 7074–7078.

Link, Andrew J, Jimmy Eng, David M Schieltz, Edwin Carmack, Gregory J Mize, David R Morris, Barbara M Garvik, and John R Yates. 1999. “Direct Analysis of Protein Complexes Using Mass Spectrometry.” *Nat Biotech* 17 (7) (July): 676–682.

Lipson, Kathryn L, Sonya G Fonseca, Shinsuke Ishigaki, Linh X Nguyen, Elizabeth Foss, Rita Bortell, Aldo A Rossini, and Fumihiko Urano. 2006. “Regulation of Insulin Biosynthesis in Pancreatic Beta Cells by an Endoplasmic Reticulum-Resident Protein Kinase IRE1.” *Cell Metabolism* 4 (3) (September): 245–54.

Lithgow, T, T Junne, K Suda, S Gratzer, and G Schatz. 1994. “The Mitochondrial Outer Membrane Protein Mas22p Is Essential for Protein Import and Viability of Yeast.” *Proceedings of the National Academy of Sciences* 91 (25) (December 6): 11973–11977.

Louvion, J F, T Abbas-Terki, and D Picard. 1998. “Hsp90 Is Required for Pheromone Signaling in Yeast.” *Molecular Biology of the Cell* 9 (11) (November): 3071–83.

Louvion, J F, R Warth, and D Picard. 1996. “Two Eukaryote-Specific Regions of Hsp82 Are Dispensable for Its Viability and Signal Transduction Functions in Yeast.” *Proceedings of the National Academy of Sciences of the United States of America* 93 (24) (November 26): 13937–42.

Lu, Zhen, and Douglas M Cyr. 1998a. “The Conserved Carboxyl Terminus and Zinc Finger-like Domain of the Co-Chaperone Ydj1 Assist Hsp70 in Protein Folding.” *Journal of Biological Chemistry* 273 (10) (March 6): 5970–5978.

Lu, Zhen, and Douglas M Cyr. 1998b. “Protein Folding Activity of Hsp70 Is Modified Differentially by the Hsp40 Co-Chaperones Sis1 and Ydj1.” *Journal of Biological Chemistry* 273 (43) (October 23): 27824–27830.

Luig, Christina, Katharina Köther, Sabine Eva Dudek, Matthias Gaestel, John Hiscott, Viktor Wixler, and Stephan Ludwig. 2010. “MAP Kinase-Activated Protein Kinases 2 and 3 Are Required for Influenza A Virus Propagation and Act via Inhibition of PKR.” *FASEB Journal : Official Publication of the Federation of American Societies for Experimental Biology* 24 (10) (October): 4068–77.

Mahalingam, D, R Swords, J S Carew, S T Nawrocki, K Bhalla, and F J Giles. 2009. “Targeting HSP90 for Cancer Therapy.” *Br J Cancer* 100 (10) (April 28): 1523–1529.

Mandal, Atin K, Paul Lee, Jennifer A Chen, Nadinath Nillegoda, Alana Heller, Handy Oen, Jacob Victor, Devi M Nair, Jeffrey L Brodsky, and AvromJ. Caplan. 2007. “Cdc37 Has Distinct Roles in Protein Kinase Quality Control That Protect Nascent Chains from Degradation and Promote Posttranslational Maturation.” *Journal of Cell Biology* 176 (3): 319–328.

Marciniak, Stefan J, Chi Y Yun, Seiichi Oyadomari, Isabel Novoa, Yuhong Zhang, Rivka Jungreis, Kazuhiro Nagata, Heather P Harding, and David Ron. 2004. “CHOP Induces Death by Promoting Protein Synthesis and Oxidation in the Stressed Endoplasmic Reticulum.” *Genes & Development* 18: 3066–3077.

Marcu, Monica G, Ahmed Chadli, Ilham Bouhouche, Maria Catelli, and Leonard M Neckers. 2000. “The Heat Shock Protein 90 Antagonist Novobiocin Interacts with a Previously Unrecognized ATP-Binding Domain in the Carboxyl Terminus of the Chaperone.” *Journal of Biological Chemistry* 275 (47) (November 24): 37181–37186.

Marcu, Monica G, Theodore W Schulte, and Leonard Neckers. 2000. “Novobiocin and Related Coumarins and Depletion of Heat Shock Protein 90-Dependent Signaling Proteins.” *Journal of the National Cancer Institute* 92 (3) (February 2): 242–248.

Marzec, M, D Elleto, and Yair Argon. 2012. “GRP94: An HSP90-like Protein Specialized for Protein Folding and Quality Control in the Endoplasmic Reticulum.” *Biochimica et Biophysica Acta* 1823 (3): 774–787.

Matts, RL, A Dixit, LB Peterson, L Sun, S Voruganti, P Kalyanaraman, SD Hartson, GM Verkhivker, and Brian S J Blagg. 2011. “Elucidation of the Hsp90 C-Terminal Inhibitor Binding Site.” *ACS Chemical Biology* 6 (8): 800–807.

Matts, Robert, and AvromJ. Caplan. 2007. “Cdc37 and Protein Kinase Folding.” In *Heat Shock Proteins in Cancer*, edited by StuartK. Calderwood, MichaelY. Sherman, and DanielR. Ciocca, 2:331–350. Springer Netherlands.

Mayer, M P, and B Bukau. 1998. “Hsp70 Chaperone Systems: Diversity of Cellular Functions and Mechanism of Action.” *Biological Chemistry* 379 (3): 261–268.

Mayer, M P, and B Bukau. 2005. “Hsp70 Chaperones: Cellular Functions and Molecular Mechanism.” *Cellular and Molecular Life Sciences : CMLS* 62 (6) (March): 670–84.

Mayer, Matthias P, Rainer Nikolay, and Bernd Bukau. 2002. “Aha, Another Regulator for Hsp90 Chaperones.” *Molecular Cell* 10 (6) (December): 1255–1256.

McLaughlin, Stephen H, Frank Sobott, Zhong-ping Yao, Wei Zhang, Peter R Nielsen, J Günter Grossmann, Ernest D Laue, Carol V Robinson, and Sophie E Jackson. 2006. “The Co-Chaperone p23 Arrests the Hsp90 ATPase Cycle to Trap Client Proteins.” *Journal of Molecular Biology* 356 (3) (February 24): 746–58.

Meacham, G C, Z Lu, S King, E Sorscher, a Tousson, and D M Cyr. 1999. “The Hdj-2/Hsc70 Chaperone Pair Facilitates Early Steps in CFTR Biogenesis.” *The EMBO Journal* 18 (6) (March 15): 1492–505.

Meacham, G C, C Patterson, W Zhang, J M Younger, and D M Cyr. 2001. “The Hsc70 Co-Chaperone CHIP Targets Immature CFTR for Proteasomal Degradation.” *Nature Cell Biology* 3 (1) (January): 100–5.

Melnick, Jeffrey, Jeanne L Dul, and Yair Argon. 1994. “Sequential Interaction of the Chaperones BiP and GRP94 with Immunoglobulin Chains in the Endoplasmic Reticulum.” *Nature* 370 (6488) (August 4): 373–375.

Melville, M W, W J Hansen, B C Freeman, W J Welch, and M G Katze. 1997. “The Molecular Chaperone hsp40 Regulates the Activity of P58IPK, the Cellular Inhibitor of PKR.” *Proceedings of the National Academy of Sciences of the United States of America* 94 (1) (January 7): 97–102.

Melville, M W, M G Katze, and S.-L. Tan. 2000. “P58IPK, a Novel Cochaperone Containing Tetratricopeptide Repeats and a J-Domain with Oncogenic Potential.” *Cellular and Molecular Life Sciences CMLS* 57 (2): 311–322.

Melville, M W, S L Tan, M Wambach, J Song, R I Morimoto, and M G Katze. 1999. “The Cellular Inhibitor of the PKR Protein Kinase, P58(IPK), Is an Influenza Virus-Activated Co-Chaperone That Modulates Heat Shock Protein 70 Activity.” *The Journal of Biological Chemistry* 274 (6) (February 5): 3797–803.

Meng, X, J Devin, W P Sullivan, D Toft, E E Baulieu, and M G Catelli. 1996. “Mutational Analysis of Hsp90 Alpha Dimerization and Subcellular Localization: Dimer Disruption Does Not Impede “in Vivo’ Interaction with Estrogen Receptor.” *Journal of Cell Science* 109 (7) (July 1): 1677–1687.

Merrick, William C. 1992. “Mechanism and Regulation of Eukaryotic Protein Synthesis.” *Microbiological Review* 56 (2): 291–315.

Meunier, Laurent, Young-kwang Usherwood, Kyung Tae Chung, and Linda M Hendershot. 2002. “A Subset of Chaperones and Folding Enzymes Form Multiprotein Complexes in Endoplasmic Reticulum to Bind Nascent Proteins.” *Molecular Biology of the Cell* 13: 4456–4469.

Meyer, Philippe, Chrisostomos Prodromou, Bin Hu, Cara Vaughan, S. Mark Roe, Barry Panaretou, Peter W. Piper, and Laurence H. Pearl. 2003. “Structural and Functional Analysis of the Middle Segment of Hsp90: Implications for ATP Hydrolysis and Client Protein and Cochaperone Interactions.” *Molecular Cell* 11 (3) (March): 647–658.

Meyer, Philippe, Chrisostomos Prodromou, Chunyan Liao, Bin Hu, S Mark Roe, Cara K Vaughan, Ignacija Vlasic, Barry Panaretou, Peter W Piper, and Laurence H Pearl. 2004. “Structural Basis for Recruitment of the ATPase Activator Aha1 to the Hsp90 Chaperone Machinery.” *The EMBO Journal* 23 (3) (February 11): 511–9.

Minami, Y, Y Kimura, H Kawasaki, K Suzuki, and I Yahara. 1994. “The Carboxy-Terminal Region of Mammalian HSP90 Is Required for Its Dimerization and Function in Vivo.” *Molecular and Cellular Biology* 14 (2) (February): 1459–64.

Minet, E, D Mottet, G Michel, I Roland, M Raes, J Remacle, and C Michiels. 1999. “Hypoxia-Induced Activation of HIF-1: Role of HIF-1alpha-Hsp90 Interaction.” *FEBS Letters* 460 (2) (October 29): 251–6.

Ming-Zhi, Shen, Zhai Ya-li Zhao, Zhao Meng, Ding Ming-ge, and Wang Xiaoming. 2010. “e0140 Endoplasmic Reticulum Stress Induced-Apoptotic Model by Tunicamycin in Cultured Neonatal Rat Cardiomyocytes.” *Heart* 96 (Suppl 3) (October 1): A45–A45.

Miot, Marika, Michael Reidy, Shannon M Doyle, Joel R Hoskins, Danielle M Johnston, Olivier Genest, Maria-Carmen Vitery, Daniel C Masison, and Sue Wickner. 2011. “Species-Specific Collaboration of Heat Shock Proteins (Hsp) 70 and 100 in Thermotolerance and Protein Disaggregation.” *Proceedings of the National Academy of Sciences of the United States of America* 108 (17) (April 26): 6915–20.

Mirus, Oliver, Tihana Bionda, Arndt Haeseler, and Enrico Schleiff. 2009. “Evolutionarily Evolved Discriminators in the 3-TPR Domain of the Toc64 Family Involved in Protein Translocation at the Outer Membrane of Chloroplasts and Mitochondria.” *Journal of Molecular Modeling* 15 (8): 971–982.

Mitra, Aparna, LalitaA. Shevde, and RajeevS. Samant. 2009. “Multi-Faceted Role of HSP40 in Cancer.” *Clinical & Experimental Metastasis* 26 (6): 559–567.

Miyata, Yoshihiko, and Ichiro Yahara. 1995. “Interaction between Casein Kinase II and the 90-kDa Stress Protein, HSP90.” *Biochemistry* 34 (25) (June 1): 8123–8129.

Moffatt, Nela S Cintrón, Elizabeth Bruinsma, Cindy Uhl, Wolfgang M J Obermann, and David Toft. 2008. “Role of the Cochaperone Tpr2 in Hsp90 Chaperoning†.” *Biochemistry* 47 (31) (July 12): 8203–8213.

Mollapour, Mehdi, and Len Neckers. 2012. “Post-Translational Modifications of Hsp90 and Their Contributions to Chaperone Regulation.” *Biochimica et Biophysica Acta* 1823 (3) (March): 648–55.

Moore, S K, C Kozak, E A Robinson, S J Ullrich, and E Appella. 1989. “Murine 86- and 84-kDa Heat Shock Proteins, cDNA Sequences, Chromosome Assignments, and Evolutionary Origins.” *Journal of Biological Chemistry* 264 (10) (April 5): 5343–5351.

Morales, Crystal, Shuang Wu, Yi Yang, Bing Hao, and Zihai Li. 2009. “Drosophila Glycoprotein 93 Is an Ortholog of Mammalian Heat Shock Protein gp96 (grp94, HSP90b1, HSPC4) and Retains Disulfide Bond-Independent Chaperone Function for TLRs and Integrins.” *The Journal of Immunology* 183 (8) (October 15): 5121–5128.

Munro, S, and H R Pelham. 1986. “An Hsp70-like Protein in the ER: Identity with the 78 Kd Glucose-Regulated Protein and Immunoglobulin Heavy Chain Binding Protein.” *Cell* 46: 291–300.

Munro, Sean, and Hugh R.B. Pelham. 1987. “A C-Terminal Signal Prevents Secretion of Luminal ER Proteins.” *Cell* 48 (5) (March): 899–907.

Murthy, AE, A Bernards, D Church, J Wasmuth, and J F Gusella. 1996. “Identification and Characterization of Two Novel Tetratricopeptide Repeat-Containing Genes.” *DNA and Cell Biology* 15 (9) (September): 727–35.

Nemoto, Takayuki, Tomonori Matsusaka, Minoru Ota, Takashi Takagi, David B Collinge, and Haidee Walther-Larsen. 1996. “Dimerization Characteristics of the 94-kDa Glucose-Regulated Protein.” *Journal of Biochemistry* 120 (2) (August 1): 249–256.

Neyt, C, and G R Cornelis. 1999. “Role of SycD, the Chaperone of the Yersinia Yop Translocators YopB and YopD.” *Molecular Microbiology* 31 (1) (January): 143–56.

Nguyen, Phuong Minh, Depeng Wang, Yu Wang, Yanjie Li, James A Uchizono, and William K Chan. 2012. “p23 Co-Chaperone Protects the Aryl Hydrocarbon Receptor from Degradation in Mouse and Human Cell Lines.” *Biochemical Pharmacology* 84 (6) (September 15): 838–50.

Nollen, Ellen A A, Alexander E Kabakov, Jeanette F Brunsting, Bart Kanon, Jörg Höhfeld, and Harm H Kampinga. 2001. “Modulation of in Vivo HSP70 Chaperone Activity by Hip and Bag-1 .” *Journal of Biological Chemistry* 276 (7) (February 16): 4677–4682.

Notredame, C, D G Higgins, and J Heringa. 2000. “T-Coffee: A Novel Method for Fast and Accurate Multiple Sequence Alignment.” *Journal of Molecular Biology* 302 (1) (September 8): 205–17.

Nyarko, Afua, Khédidja Mosbahi, Arthur J Rowe, Andrew Leech, Marta Boter, Ken Shirasu, and Colin Kleanthous. 2007. “TPR-Mediated Self-Association of Plant SGT1†.” *Biochemistry* 46 (40) (September 18): 11331–11341.

Odunuga, Odutayo O, Judith A Hornby, Christiane Bies, Richard Zimmermann, David J Pugh, and Gregory L Blatch. 2003. “Tetratricopeptide Repeat Motif-Mediated Hsc70-mSTI1 Interaction: molecular characterization of the critical contacts for successful binding and specificity.” *Journal of Biological Chemistry* 278 (9) (February 28): 6896–6904.

Ostrovsky, Olga, Noreen T Ahmed, and Yair Argon. 2009. “The Chaperone Activity of GRP94 Toward Insulin-like Growth Factor II Is Necessary for the Stress Response to Serum Deprivation.” *Molecular Biology of the Cell* 20 (6) (March 15): 1855–1864.

Ostrovsky, Olga, Davide Eletto, Catherine Makarewich, Elisabeth R Barton, and Yair Argon. 2010. “Glucose Regulated Protein 94 Is Required for Muscle Differentiation through Its Control of the Autocrine Production of Insulin-like Growth Factors.” *Biochimica et Biophysica Acta* 1803 (2) (February): 333–41.

Oyadomari, S, E Araki, and M Mori. 2002. “Endoplasmic Reticulum Stress-Mediated Apoptosis in Pancreatic B-Cells.” *Apoptosis* 7 (4): 335–345.

Oyadomari, Seiichi, Akio Koizumi, Kiyoshi Takeda, Tomomi Gotoh, Shizuo Akira, Eiichi Araki, and Masataka Mori. 2002. “Targeted Disruption of the Chop Gene Delays Endoplasmic Reticulum Stress – Mediated Diabetes.” *Journal of Cilical Investigations* 109 (4): 443–445.

Oyadomari, Seiichi, Chi Yun, Edward A Fisher, Nicola Kreglinger, Gert Kreibich, Miho Oyadomari, Heather P Harding, et al. 2006. “Cotranslocational Degradation Protects the Stressed Endoplasmic Reticulum from Protein Overload.” *Cell* 126 (4) (August 25): 727–39.

Page, Anne-Laure, and Claude Parsot. 2002. “Chaperones of the Type III Secretion Pathway: Jacks of All Trades.” *Molecular Microbiology* 46 (1) (October 1): 1–11.

Parsot, C. 2003. “The Various and Varying Roles of Specific Chaperones in Type III Secretion Systems.” *Current Opinion in Microbiology* 6 (1) (February): 7–14.

Patil, Chris, and Peter Walter. 2001. “Intracellular Signaling from the Endoplasmic Reticulum to the Nucleus: The Unfolded Protein Response in Yeast and Mammals.” *Current Opinion in Cell Biology* 13 (3) (June): 349–355.

Pawlowski, Marcin, MichalJ Gajda, Ryszard Matlak, and JanuszM Bujnicki. 2008. “MetaMQAP: A Meta-Server for the Quality Assessment of Protein Models.” *BMC Bioinformatics* 9 (1): 1–20.

Pearl, Laurence H, and Chrisostomos Prodromou. 2006. “Structure and Mechanism of the Hsp90 Molecular Chaperone Machinery.” *Annual Review of Biochemistry* 75 (1) (June 1): 271–294.

Pei, Jimin, Bong-Hyun Kim, and Nick V Grishin. 2008. “PROMALS3D: A Tool for Multiple Protein Sequence and Structure Alignments.” *Nucleic Acids Research* 36 (7) (April): 2295–300.

Pelham, H R. 1984. “Hsp70 Accelerates the Recovery of Nucleolar Morphology after Heat Shock.” *The EMBO Journal* 3: 3095–3100.

Perry, Andrew J, Joanne M Hulett, Vladimir A Likić, Trevor Lithgow, and Paul R Gooley. 2006. “Convergent Evolution of Receptors for Protein Import into Mitochondria.” *Current Biology : CB* 16 (3) (February 7): 221–9.

Petrova, Kseniya, Seiichi Oyadomari, Linda M Hendershot, and David Ron. 2008. “Regulated Association of Misfolded Endoplasmic Reticulum Lumenal Proteins with P58/DNAJc3.” *The EMBO Journal* 27 (21) (November 5): 2862–72.

Picard, D. 2002. “Heat-Shock Protein 90 , a Chaperone for Folding and Regulation.” *Cellular and Molecular Life Sciences* 59: 1640–1648.

Picard, Didier, Bushra Khursheed, Michael J Garabedian, Marc G Fortin, Susan Lindquist, and Keith R Yamamoto. 1990. “Reduced Levels of hsp90 Compromise Steroid Receptor Action in Vivo.” *Nature* 348 (6297) (November 8): 166–168.

Polyak, Stephen J, Norina Tang, Glen N Barber, G Michael, J Biol Chem, Marlene Wambach, and Michael G Katze. 1996. “Enzymology : The P58 Cellular Inhibitor Complexes with Regulate Its Autophosphorylation and Activity The P58 Cellular Inhibitor Complexes with the Interferon-Induced , Double-Stranded RNA-Dependent Protein Kinase , PKR , to Regulate Its Autophosphorylatio.” *Enzymology* 271: 1702–1707.

Pratt, William B, and David O Toft. 2003. “Regulation of Signaling Protein Function and Trafficking by the hsp90/hsp70-Based Chaperone Machinery.” *Experimental Biology and Medicine* 228 (2) (February 1): 111–133.

Prodromou, C, B Panaretou, S Chohan, G Siligardi, R O’Brien, J E Ladbury, S M Roe, P W Piper, and L H Pearl. 2000. “The ATPase Cycle of Hsp90 Drives a Molecular ‘Clamp’ via Transient Dimerization of the N-Terminal Domains.” *The EMBO Journal* 19 (16) (August 15): 4383–92.

Prodromou, C, S M Roe, R O’Brien, J E Ladbury, P W Piper, and L H Pearl. 1997. “Identification and Structural Characterization of the ATP/ADP-Binding Site in the Hsp90 Molecular Chaperone.” *Cell* 90 (1) (July 11): 65–75.

Prodromou, Chrisostomos, S Mark Roe, Peter W Piper, and Laurence H Pearl. 1997. “A Molecular Clamp in the Crystal Structure of the N-Terminal Domain of the Yeast Hsp90 Chaperone.” *Nat Struct Mol Biol* 4 (6) (June): 477–482.

Qiu, X, Y. -M. Shao, S. Miao, and L. Wang. 2006. “The Diversity of the DnaJ/Hsp40 Family, the Crucial Partners for Hsp70 Chaperones.” *Cellular and Molecular Life Sciences* 63 (22) (September 4): 2560–2570.

Rampelt, Heike, Janine Kirstein-Miles, Nadinath B Nillegoda, Kang Chi, Sebastian R Scholz, Richard I Morimoto, and Bernd Bukau. 2012. “Metazoan Hsp70 Machines Use Hsp110 to Power Protein Disaggregation.” *The EMBO Journal* 31 (21) (November 5): 4221–35.

Randow, Felix, and Brian Seed. 2001. “Endoplasmic Reticulum Chaperone gp96 Is Required for Innate Immunity but Not Cell Viability.” *Nat Cell Biol* 3 (10) (October): 891–896.

Ratzke, C, M Mickler, B Hellenkamp, J Buchner, and T Hugel. 2010. “Dynamics of Heat Shock Protein 90 C-Terminal Dimerization Is an Important Part of Its Conformational Cycle.” *Proceedings of the National Academy of Sciences* 107 (37) (August 24): 16101–16106.

Reece, Richard J, Anthony Maxwell, and James C Wang. 1991. “DNA Gyrase: Structure and Function.” *Critical Reviews in Biochemistry and Molecular Biology* 26 (3-4) (January 1): 335–375.

Ren, Jian, Longping Wen, Xinjiao Gao, Changjiang Jin, Yu Xue, and Xuebiao Yao. 2009. “DOG 1.0: Illustrator of Protein Domain Structures.” *Cell Research* 19 (2) (February): 271–3.

Retzlaff, Marco, Franz Hagn, Lars Mitschke, Martin Hessling, Frederik Gugel, Horst Kessler, Klaus Richter, and Johannes Buchner. 2010. “Asymmetric Activation of the hsp90 Dimer by Its Cochaperone aha1.” *Molecular Cell* 37 (3) (February 12): 344–54.

Ritossa, F. 1962. “A New Puffing Pattern Induced by Temperature Shock and DNP in Drosophila.” *Experientia*.

Roe, S Mark, Chrisostomos Prodromou, Ronan O’Brien, John E Ladbury, Peter W Piper, and Laurence H Pearl. 1999. “Structural Basis for Inhibition of the Hsp90 Molecular Chaperone by the Antitumor Antibiotics Radicicol and Geldanamycin.” *Journal of Medicinal Chemistry* 42 (2) (January 1): 260–266.

Rohner, Nicolas, Dan F Jarosz, Johanna E Kowalko, Masato Yoshizawa, William R Jeffery, Richard L Borowsky, Susan Lindquist, and Clifford J Tabin. 2013. “Cryptic Variation in Morphological Evolution: HSP90 as a Capacitor for Loss of Eyes in Cavefish.” *Science* 342 (6164) (December 13): 1372–1375.

Roller, Corinna, and Danilo Maddalo. 2013. “The Molecular Chaperone GRP78/BiP in the Development of Chemoresistance: Mechanism and Possible Treatment.” *Frontiers in Pharmacology* 4 (February) (January): 10.

Ron, David, and Peter Walter. 2007. “Signal Integration in the Endoplasmic Reticulum Unfolded Protein Response.” *Nat Rev Mol Cell Biol* 8 (7) (July): 519–529.

Rosser, M F, and C V Nicchitta. 2000. “Ligand Interactions in the Adenosine Nucleotide-Binding Domain of the Hsp90 Chaperone, GRP94. I. Evidence for Allosteric Regulation of Ligand Binding.” *The Journal of Biological Chemistry* 275 (30) (July 28): 22798–805.

Rosser, Meredith F N, and Douglas M Cyr. 2007. “Do Hsp40s Act as Chaperones or Co-Chaperones.” In *Networking of Chaperones by Co-Chaperones*, edited by Gregory L Blatch, 38–51. Austin: Landes Bioscience; New York: Springer Science+Business Media.

Rutherford, S L, and S Lindquist. 1998. “Hsp90 as a Capacitor for Morphological Evolution.” *Nature* 396 (6709) (November 26): 336–42.

Rutherford, Suzanne L. 2003. “Between Genotype and Phenotype: Protein Chaperones and Evolvability.” *Nature Reviews. Genetics* 4 (4) (April): 263–74.

Rutkowski, D Thomas, Sang-Wook Kang, Alan G Goodman, Jennifer L Garrison, Jack Taunton, Michael G Katze, Randal J Kaufman, and Ramanujan S Hegde. 2007. “The Role of p58IPK in Protecting the Stressed Endoplasmic Reticulum.” *Molecular Biology of the Cell* 18 (9) (September 1): 3681–3691.

Rutkowski, D.Thomas, and Randal J. Kaufman. 2004. “A Trip to the ER: Coping with Stress.” *Trends in Cell Biology* 14 (1) (January): 20–28.

Ryan, MT, and N Pfanner. 2001. “Hsp70 Proteins in Protein Translocation.” *Advances in Protein Chemistry* 59: 223–242.

Samuel, Charles E. 1993. “The eIF-2α Protein Kinases, Regulators of Translation in Eukaryotes from Yeasts to Humans.” *The Journal of Biological Chemistry* 268 (11): 7603–7606.

Sanchez, Yolanda, John Taulien, Katherine A Borkovich, and Susan Lindquist. 1992. “Hsp 104 Is Required for Tolerance to Many Forms of Stress.” *The EMBO Journal* 1 (6): 2357–2364.

Sandee, Duanpen, Sumalee Tungpradabkul, Yoichi Kurokawa, Kiichi Fukui, and Masahiro Takagi. 2005. “Combination of Dsb Coexpression and an Addition of Sorbitol Markedly Enhanced Soluble Expression of Single-Chain Fv in Escherichia Coli.” *Biotechnology and Bioengineering* 91 (4) (August 20): 418–24.

Sangster, Todd A, Neeraj Salathia, Soledad Undurraga, Ron Milo, Kurt Schellenberg, Susan Lindquist, and Christine Queitsch. 2008. “HSP90 Affects the Expression of Genetic Variation and Developmental Stability in Quantitative Traits.” *Proceedings of the National Academy of Sciences* 105 (8) (February 26): 2963–2968.

San-Miguel, Teresa, Pedro Pérez-Bermúdez, and Isabel Gavidia. 2013. “Production of Soluble Eukaryotic Recombinant Proteins in E. Coli Is Favoured in Early Log-Phase Cultures Induced at Low Temperature.” *SpringerPlus* 2 (1) (December): 89.

Santoro, Bina, Lei Hu, Haiying Liu, Andrea Saponaro, Phillip Pian, Rebecca a Piskorowski, Anna Moroni, and Steven a Siegelbaum. 2011. “TRIP8b Regulates HCN1 Channel Trafficking and Gating through Two Distinct C-Terminal Interaction Sites.” *The Journal of Neuroscience : The Official Journal of the Society for Neuroscience* 31 (11) (March 16): 4074–86.

Sato, S, N Fujita, and T Tsuruo. 2000. “Modulation of Akt Kinase Activity by Binding to Hsp90.” *Proceedings of the National Academy of Sciences of the United States of America* 97 (20) (September 26): 10832–7.

Scheufler, C, A Brinker, G Bourenkov, S Pegoraro, L Moroder, H Bartunik, F U Hartl, and I Moarefi. 2000. “Structure of TPR Domain-Peptide Complexes: Critical Elements in the Assembly of the Hsp70-Hsp90 Multichaperone Machine.” *Cell* 101 (2) (April 14): 199–210.

Schlager, Benjamin, Anna Straessle, and Ernst Hafen. 2012. “Use of Anionic Denaturing Detergents to Purify Insoluble Proteins after Overexpression.” *BMC Biotechnology* 12 (1) (January): 95.

Schliebs, Wolfgang, Jürgen Saidowsky, Bogos Agianian, Gabriele Dodt, Friedrich W Herberg, and Wolf-H. Kunau. 1999. “Recombinant Human Peroxisomal Targeting Signal Receptor PEX5: structural basis for interaction of PEX5 with PEX14 .” *Journal of Biological Chemistry* 274 (9) (February 26): 5666–5673.

Schmid, Andreas B, Stephan Lagleder, Melissa Ann Gräwert, Alina Röhl, Franz Hagn, Sebastian K Wandinger, Marc B Cox, et al. 2012. “The Architecture of Functional Modules in the Hsp90 Co-Chaperone Sti1/Hop.” *The EMBO Journal* 31 (6) (March 21): 1506–17..

Schreiner, Madeleine, and HartmutH Niemann. 2012. “Crystal Structure of the Yersinia Enterocolitica Type III Secretion Chaperone SycD in Complex with a Peptide of the Minor Translocator YopD.” *BMC Structural Biology* 12 (1): 1–9..

Schröder, Martin, and Randal J Kaufman. 2005. “The Mammalian Unfolded Protein Response.” *Annual Review of Biochemistry* 74 (1) (June 1): 739–789.

Schulte, Theodor W, Shiro Akinaga, T Murakata, Tsutomu Agatsuma, Seiji Sugimoto, Hirofumi Nakano, Yong S Lee, et al. 1999. “Interaction of Radicicol with Members of the Heat Shock Protein 90 Family of Molecular Chaperones.” *Molecular Endocrinology* 13 (9) (September 1): 1435–1448.

Schulte, Theodor W, Shiro Akinaga, Shiro Soga, William Sullivan, Bridget Stensgard, David O Toft, and Leonard M Neckers. 1998. “Antibiotic Radicicol Binds to the N-Terminal Domain of Hsp90 and Shares Important Biologic Activities with Geldanamycin.” *Cell Stress & Chaperone* 3 (2): 100–108.

Schulte, Theodor W, Mikhail V Blagosklonny, Christian Ingui, and Len Neckers. 1995. “Disruption of the Raf-1-Hsp90 Molecular Complex Results in Destabilization of Raf-1 and Loss of Raf-1-Ras Association.” *Journal of Biological Chemistry* 270 (41) (October 13): 24585–24588.

Schultz, Jörg, Frank Milpetz, Peer Bork, and Chris P Ponting. 1998. “SMART, a Simple Modular Architecture Research Tool: Identification of Signaling Domains.” *Proceedings of the National Academy of Sciences* 95 (11) (May 26): 5857–5864.

Schwarz, Daniel, Volker Dötsch, and Frank Bernhard. 2008. “Production of Membrane Proteins Using Cell-Free Expression Systems.” *Proteomics* 8 (19) (October): 3933–46.

Seeburg, Peter H, Wendy W Colby, Daniel J Capon, David V Goeddel, and Arthur D Levinson. 1984. “Biological Properties of Human c-Ha-ras1 Genes Mutated at Codon 12.” *Nature* 312 (5989) (November 1): 71–75.

Sha, B, S Lee, and D M Cyr. 2000. “The Crystal Structure of the Peptide-Binding Fragment from the Yeast Hsp40 Protein Sis1.” *Structure (London, England : 1993)* 8 (8) (August 15): 799–807.

Shan, Y. 2003. “Hsp10 and Hsp60 Modulate Bcl-2 Family and Mitochondria Apoptosis Signaling Induced by Doxorubicin in Cardiac Muscle Cells.” *Journal of Molecular and Cellular Cardiology* 35 (9) (September): 1135–1143.

Sharma, Kulbhushan, Shashank Tripathi, Priya Ranjan, Purnima Kumar, Rebecca Garten, Varough Deyde, Jacqueline M Katz, et al. 2011. “Influenza A Virus Nucleoprotein Exploits Hsp40 to Inhibit PKR Activation.” *PloS One* 6 (6) (January): e20215.

Shen, Jingshi, Xi Chen, Linda Hendershot, and Ron Prywes. 2002. “ER Stress Regulation of ATF6 Localization by Dissociation of BiP/GRP78 Binding and Unmasking of Golgi Localization Signals.” *Developmental Cell* 3 (1) (July): 99–111.

Shen, Ying, and Linda M Hendershot. 2005. “ERdj3 , a Stress-Inducible Endoplasmic Reticulum DnaJ Homologue , Serves as a CoFactor for BiP ’ S Interactions with Unfolded Substrates.” *Molecular Biology of the Cell* 16: 40–50.

Shi, Y, K M Vattem, R Sood, J An, J Liang, L Stramm, and R C Wek. 1998. “Identification and Characterization of Pancreatic Eukaryotic Initiation Factor 2 Alpha-Subunit Kinase, PEK, Involved in Translational Control.” *Molecular and Cellular Biology* 18 (12) (December): 7499–509.

Sigrist, Christian J a, Lorenzo Cerutti, Nicolas Hulo, Alexandre Gattiker, Laurent Falquet, Marco Pagni, Amos Bairoch, and Philipp Bucher. 2002. “PROSITE: A Documented Database Using Patterns and Profiles as Motif Descriptors.” *Briefings in Bioinformatics* 3 (3) (September): 265–74.

Sikorski, Robert S., Mark S. Boguski, Mark Goebl, and Philip Hieter. 1990. “A Repeating Amino Acid Motif in CDC23 Defines a Family of Proteins and a New Relationship among Genes Required for Mitosis and RNA Synthesis.” *Cell* 60 (2) (January): 307–317.

Smith, David F. 2004. “Tetratricopeptide Repeat Cochaperones in Steroid Receptor Complexes.” *Cell Stress & Chaperones* 9 (2) (January): 109–21.

Smith, Donald B., and Kevin S. Johnson. 1988. “Single-Step Purification of Polypeptides Expressed in Escherichia Coli as Fusions with Glutathione S-Transferase.” *Gene* 67 (1) (July): 31–40.

Smith, J R, E de Billy, S Hobbs, M Powers, C Prodromou, L Pearl, P A Clarke, and P Workman. 2013. “Restricting Direct Interaction of CDC37 with HSP90 Does Not Compromise Chaperoning of Client Proteins.” *Oncogene* (December 2).

Snapp, Erik L, Ajay Sharma, Jennifer Lippincott-Schwartz, and Ramanujan S Hegde. 2006. “Monitoring Chaperone Engagement of Substrates in the Endoplasmic Reticulum of Live Cells.” *Proceedings of the National Academy of Sciences* 103 (17) (April 25): 6536–6541.

Söding, Johannes, Andreas Biegert, and Andrei N Lupas. 2005. “The HHpred Interactive Server for Protein Homology Detection and Structure Prediction.” *Nucleic Acids Research* 33 (suppl 2) (July 1): W244–W248.

Soldano, Karen L, Arif Jivan, Christopher V Nicchitta, and Daniel T Gewirth. 2003. “Structure of the N-Terminal Domain of GRP94: Basis For Ligand Specificity And Regulation .” *Journal of Biological Chemistry* 278 (48) (November 28): 48330–48338.

Song, Daisheng, Lin-Sheng Li, Katherine J Heaton-Johnson, Patrick R Arsenault, Stephen R Master, and Frank S Lee. 2013. “Prolyl Hydroxylase Domain Protein 2 (PHD2) Binds a Pro-Xaa-Leu-Glu Motif, Linking It to the Heat Shock Protein 90 Pathway.” *Journal of Biological Chemistry* 288 (14) (April 5): 9662–9674.

Song, Ho Yeong, James D Dunbar, Yuan Xin Zhang, Danqun Guo, and David B Donner. 1995. “Identification of a Protein with Homology to hsp90 That Binds the Type 1 Tumor Necrosis Factor Receptor.” *Journal of Biological Chemistry* 270 (8) (February 24): 3574–3581.

Song, Zhimin, S Krishna, D Thanos, JL Strominger, and SJ Ono. 1994. “A Novel Cysteine-Rich Sequence-Specific DNA-Binding Protein Interacts with the Conserved X-Box Motif of the Human Major Histocompatibility Complex Class II Genes Via a Repeated Cys-His Domain and Functions as a Transcriptional Repressor.” *Journal of Experimental Medicine* 180: 1763–1774.

Sørensen, Hans Peter, and Kim Kusk Mortensen. 2005. “Soluble Expression of Recombinant Proteins in the Cytoplasm of Escherichia Coli.” *Microbial Cell Factories* 4 (1) (January 4): 1.

Söti, Csaba, Attila Rácz, and Péter Csermely. 2002. “A Nucleotide-Dependent Molecular Switch Controls ATP Binding at the C-Terminal Domain of Hsp90: N-Terminal Nucleotide Binding Unmasks A C-Terminal Binding Pocket .” *Journal of Biological Chemistry* 277 (9) (March 1): 7066–7075.

Southworth, Daniel R, and David a Agard. 2011. “Client-Loading Conformation of the Hsp90 Molecular Chaperone Revealed in the Cryo-EM Structure of the Human Hsp90:Hop Complex.” *Molecular Cell* 42 (6) (June 24): 771–81.

Sreedhar, Amere Subbarao, Éva Kalmár, Péter Csermely, and Yu-Fei Shen. 2004. “Hsp90 Isoforms: Functions, Expression and Clinical Importance.” *FEBS Letters* 562 (March): 11–15.

Sreedhar, Amere Subbarao, Csaba Soti, and Péter Csermely. 2004. “Inhibition of Hsp90: A New Strategy for Inhibiting Protein Kinases.” *Biochimica et Biophysica Acta* 1697 (1-2) (March 11): 233–42.

Stacey, DW, M Roudebush, R Day, SD Mosser, JB Gibbs, and LA Feig. 1991. “Dominant Inhibitory Ras Mutants Demonstrate the Requirement for Ras Activity in the Action of Tyrosine Kinase Oncogenes.” *Oncogene* 6 (12): 2297–2304.

Staron, Matthew, Shuang Wu, Feng Hong, Aleksandra Stojanovic, Xiaoping Du, Robert Bona, Bei Liu, and Zihai Li. 2011. “Heat-Shock Protein gp96/grp94 Is an Essential Chaperone for the Platelet Glycoprotein Ib-IX-V Complex.” *Blood* 117 (26) (June 30): 7136–44.

Stebbins, C E, a a Russo, C Schneider, N Rosen, F U Hartl, and N P Pavletich. 1997. “Crystal Structure of an Hsp90-Geldanamycin Complex: Targeting of a Protein Chaperone by an Antitumor Agent.” *Cell* 89 (2) (April 18): 239–50.

Sterrenberg, Jason N, Gregory L Blatch, and Adrienne L Edkins. 2011. “Human DNAJ in Cancer and Stem Cells.” *Cancer Letters* 312 (2) (December 22): 129–42.

Sullivan, William P, Barbara A L Owen, and David O Toft. 2002. “The Influence of ATP and p23 on the Conformation of hsp90.” *Journal of Biological Chemistry* 277 (48) (November 29): 45942–45948.

Svärd, M, Ekaterina I Biterova, Jean-marie Bourhis, and Jodie E Guy. 2011. “The Crystal Structure of the Human Co-Chaperone P58 IPK.” *PloS One* 6 (7).

Szabo, a, R Korszun, F U Hartl, and J Flanagan. 1996. “A Zinc Finger-like Domain of the Molecular Chaperone DnaJ Is Involved in Binding to Denatured Protein Substrates.” *The EMBO Journal* 15 (2) (January 15): 408–17.

Szegezdi, Eva, Susan E Logue, Adrienne M Gorman, and Afshin Samali. 2006. “Mediators of Endoplasmic Reticulum Stress-Induced Apoptosis.” *EMBO Reports* 7 (9) (September): 880–5.

Takemoto, Hiroto, Tamotsu Yoshimori, Akitsugu Yamamoto, Yoshihiko Miyata, Ichiro Yahara, Kyoichi Inoue, and Yutaka Tashiro. 1992. “Heavy Chain Binding Protein (BiP/GRP78) and Endoplasmin Are Exported from the Endoplasmic Reticulum in Rat Exocrine Pancreatic Cells, Similar to Protein Disulfide-Isomerase.” *Archives of Biochemistry and Biophysics* 296 (1) (July): 129–136.

Tamura, Koichiro, Daniel Peterson, Nicholas Peterson, Glen Stecher, Masatoshi Nei, and Sudhir Kumar. 2011. “MEGA5: Molecular Evolutionary Genetics Analysis Using Maximum Likelihood, Evolutionary Distance, and Maximum Parsimony Methods.” *Molecular Biology and Evolution* (May 4).

Tan, S L, M J Gale, and M G Katze. 1998. “Double-Stranded RNA-Independent Dimerization of Interferon-Induced Protein Kinase PKR and Inhibition of Dimerization by the Cellular P58IPK Inhibitor.” *Molecular and Cellular Biology* 18 (5) (May): 2431–43.

Tan, S L, and M G Katze. 1999. “The Emerging Role of the Interferon-Induced PKR Protein Kinase as an Apoptotic Effector: A New Face of Death?” *Journal of Interferon & Cytokine Research : The Official Journal of the International Society for Interferon and Cytokine Research* 19 (6) (June): 543–54.

Tang, N, CY Ho, and Michael G. Katze. 1996. “The 58-kDa Cellular Inhibitor of the Double Stranded RNA-Dependent Protein Kinase Requires the Tetratricopeptide Repeat 6 and DnaJ Motifs to Stimulate Protein Synthesis in Vivo.” *Journal of Biological Chemistry* 271 (45): 28660–28666.

Tang, Norina M, Marcus J Korth, Michael Gale, Marlene Wambach, Sandy D Der, Sudip K Bandyopadhyay, Bryan R G Williams, and Michael G Katze. 1999. “Inhibition of Double-Stranded RNA- and Tumor Necrosis Factor Alpha-Mediated Apoptosis by Tetratricopeptide Repeat Protein and Cochaperone P58IPK .” *Molecular and Cellular Biology* 19 (7) (July 1): 4757–4765.

Tao, J, K Petrova, D Ron, and B Sha. 2010. “Crystal Structure of P58(IPK) TPR Fragment Reveals the Mechanism for Its Molecular Chaperone Activity in UPR.” *Journal of Molecular Biology* 397 (5): 1307–1315.

Tastan Bishop, Özlem, Adrienne Lesley Edkins, and Gregory Lloyd Blatch. 2013. “Sequence and Domain Conservation of the Coelacanth Hsp40 and Hsp90 Chaperones Suggests Conservation of Function.” *Journal of Experimental Zoology Part B: Molecular and Developmental Evolution* (September 1): n/a–n/a.

Taylor, P, J Dornan, a Carrello, R F Minchin, T Ratajczak, and M D Walkinshaw. 2001. “Two Structures of Cyclophilin 40: Folding and Fidelity in the TPR Domains.” *Structure (London, England : 1993)* 9 (5) (May 9): 431–8.

Terpe, K. 2003. “Overview of Tag Protein Fusions: From Molecular and Biochemical Fundamentals to Commercial Systems.” *Applied Microbiology and Biotechnology* 60 (5) (January): 523–33.

Thomis, D C, and C E Samuel. 1993. “Mechanism of Interferon Action: Evidence for Intermolecular Autophosphorylation and Autoactivation of the Interferon-Induced, RNA-Dependent Protein Kinase PKR.” *Journal of Virology* 67 (12) (December): 7695–700.

Thompson, J D, D G Higgins, and T J Gibson. 1994. “CLUSTAL W: Improving the Sensitivity of Progressive Multiple Sequence Alignment through Sequence Weighting, Position-Specific Gap Penalties and Weight Matrix Choice.” *Nucleic Acids Research* 22 (22) (November 11): 4673–80.

Ting, J, and A Lee. 1988. “Human Gene Encoding the 78,000-Dalton Glucose-Regulated Protein and Its Pseudogene: Structure, Conservation, and Regulation.” *DNA* 7 (4): 275–286.

Tissières, A, H K Mitchell, and U M Tracy. 1974. “Protein Synthesis in Salivary Glands of Drosophila Melanogaster: Relation to Chromosome Puffs.” *Journal of Molecular Biology* 84: 389–398.

Tkáčavá, Jana, and Mária Angelovičova. 2012. “Heat Shock Proteins (HSPs): A Review.” *Scientific Papers: Animal Science and Biotechnologies* 45 (1): 349–353.

Tsai, Joyce, and Michael G Douglas. 1996. “A Conserved HPD Sequence of the J-Domain Is Necessary for YDJ1 Stimulation of Hsp70 ATPase Activity at a Site Distinct from Substrate Binding.” *Journal of Biological Chemistry* 271 (16) (April 19): 9347–9354.

Tutar, Lütfi, and Yusuf Tutar. 2010. “Heat Shock Proteins; an Overview.” *Current Pharmaceutical Biotechnology* 11: 216–222.

Van Huizen, Rika, Jennifer L Martindale, Myriam Gorospe, and Nikki J Holbrook. 2003. “P58IPK, a Novel Endoplasmic Reticulum Stress-Inducible Protein and Potential Negative Regulator of eIF2α Signaling .” *Journal of Biological Chemistry* 278 (18) (May 2): 15558–15564.

Vasina, J A, and F Baneyx. 1997. “Expression of Aggregation-Prone Recombinant Proteins at Low Temperatures: A Comparative Study of the Escherichia Coli cspA and Tac Promoter Systems.” *Protein Expression and Purification* 9 (2) (March): 211–8.

Vaughan, Cara K, Mehdi Mollapour, Jennifer R Smith, Andrew Truman, Bin Hu, Valerie M Good, Barry Panaretou, et al. 2008. “Hsp90-Dependent Activation of Protein Kinases Is Regulated by Chaperone-Targeted Dephosphorylation of Cdc37.” *Molecular Cell* 31 (6) (September 26): 886–95.

Vogen, Shawn, Tali Gidalevitz, Chhanda Biswas, Birgitte B Simen, Eytan Stein, Funda Gulmen, and Yair Argon. 2002. “Radicicol-Sensitive Peptide Binding to the N-Terminal Portion of GRP94.” *Journal of Biological Chemistry* 277 (43) (October 25): 40742–40750.

Vos, Michel J, Jurre Hageman, Serena Carra, and Harm H Kampinga. 2008. “Structural and Functional Diversities between Members of the Human HSPB, HSPH, HSPA, and DNAJ Chaperone Families†.” *Biochemistry* 47 (27) (June 17): 7001–7011.

Voss, A K, T Thomas, and P Gruss. 2000. “Mice Lacking HSP90beta Fail to Develop a Placental Labyrinth.” *Development* 127 (1) (January 1): 1–11.

Voulgaridou, Georgia-Persephoni, Theodora Mantso, Katerina Chlichlia, Mihalis I Panayiotidis, and Aglaia Pappa. 2013. “Efficient E. Coli Expression Strategies for Production of Soluble Human Crystallin ALDH3A1.” *PloS One* 8 (2) (January): e56582.

Wadhwa, Renu, Kazunari Taira, and Sunil C Kaul. 2002. “An Hsp70 Family Chaperone, mortalin/mthsp70/PBP74/Grp75: What, When, and Where?” *Cell Stress & Chaperones* 7 (3) (July): 309–16.

Wall, Daniel, Maciej Zyliczll, and Costa Georgopoulosss. 1994. “The NH2-Terminal 108 Amino Acids of the Escherichia coZi DnaJ Protein Stimulate the ATPase Activity of DnaK and Are Sufficient for A Replication.” *Journal of Biological Chemistry* 269 (7): 5446–5451.

Walsh, Peter, Dejan Bursać, Yin Chern Law, Douglas Cyr, and Trevor Lithgow. 2004. “The J-Protein Family: Modulating Protein Assembly, Disassembly and Translocation.” *EMBO Reports* 5 (6) (June): 567–71.

Walter, Peter, and David Ron. 2011. “The Unfolded Protein Response: From Stress Pathway to Homeostatic Regulation.” *Science* 334 (6059) (November 25): 1081–1086.

Wang, Shiyu, and Randal J Kaufman. 2012. “The Impact of the Unfolded Protein Response on Human Disease.” *The Journal of Cell Biology* 197 (7) (June 25): 857–867.

Wearsch, P A, and C V Nicchitta. 1996. “Purification and Partial Molecular Characterization of GRP94, an ER Resident Chaperone.” *Protein Expression and Purification* 7 (1) (February): 114–21.

Wearsch, Pamela A, and Christopher V Nicchitta. 1997. “Interaction of Endoplasmic Reticulum Chaperone GRP94 with Peptide Substrates Is Adenine Nucleotide-Independent.” *Journal of Biological Chemistry* 272 (8) (February 21): 5152–5156.

Wen, JG, H Song, Y Sun, Y Gao, ZK Xu, LF Bo, and Zhang DL. 2011. “Cloning, Prokaryotic Expression of Novel Swine Gene P58IPK and Its Polyclonal Antibody Preparation.” *Xi Bao Yu Fen Zi Mian Yi Xue Za Zhi* 27: 637–640.

Whitesell, L, E G Mimnaugh, B De Costa, C E Myers, and L M Neckers. 1994. “Inhibition of Heat Shock Protein HSP90-pp60v-Src Heteroprotein Complex Formation by Benzoquinone Ansamycins: Essential Role for Stress Proteins in Oncogenic Transformation.” *Proceedings of the National Academy of Sciences of the United States of America* 91 (18) (August 30): 8324–8.

Whitesell, Luke, and Susan L Lindquist. 2005. “HSP90 and the Chaperoning of Cancer.” *Nature Reviews. Cancer* 5 (10) (October): 761–772.

Willmer, Tarryn, Lara Contu, Gregory L Blatch, and Adrienne L Edkins. 2013. “Knockdown of Hop Downregulates RhoC Expression, and Decreases Pseudopodia Formation and Migration in Cancer Cell Lines.” *Cancer Letters* 328 (2) (January 28): 252–60.

Winograd, E, MA Pulido, and M Wasserman. 1993. “Production of DNA-Recombinant Polypeptides by Tac-Inducible Vectors Using Micromolar Concentrations of IPTG.” *Biotechniques* 14 (6): 886–890.

Wiseman, R Luke, Yuhong Zhang, Kenneth P K Lee, Heather P Harding, Cole M Haynes, Joshua Price, Frank Sicheri, and David Ron. 2010. “Flavonol Activation Defines an Unanticipated Ligand-Binding Site in the Kinase-RNase Domain of IRE1.” *Molecular Cell* 38 (2) (April 23): 291–304.

Wittung-Stafshede, Pernilla, Jesse Guidry, B Erin Horne, and Samuel J Landry. 2003. “The J-Domain of Hsp40 Couples ATP Hydrolysis to Substrate Capture in Hsp70†.” *Biochemistry* 42 (17) (April 11): 4937–4944.

Woestyn, Sophie, Marie-Paule Sory, Anne Boland, Olivier Lequenne, and Guy R Cornelis. 1996. “The Cytosolic SycE and SycH Chaperones of Yersinia Protect the Region of YopE and YopH Involved in Translocation across Eukaryotic Cell Membranes.” *Molecular Microbiology* 20 (6) (June 1): 1261–1271.

Wu, Yunkun, and Bingdong Sha. 2006. “Crystal Structure of Yeast Mitochondrial Outer Membrane Translocon Member Tom70p.” *Nat Struct Mol Biol* 13 (7) (July): 589–593.

Yan, Wei, Christopher L Frank, Marcus J Korth, Bryce L Sopher, Isabel Novoa, David Ron, and Michael G Katze. 2002. “Control of PERK eIF2 ⎵ Kinase Activity by the Endoplasmic Reticulum Stress-Induced Molecular Chaperone P58 IPK.” *Proceedings of the National Academy of Sciences* 99 (25): 2–7.

Yang, Chun, Heather A Owen, and Pinfen Yang. 2008. “Dimeric Heat Shock Protein 40 Binds Radial Spokes for Generating Coupled Power Strokes and Recovery Strokes of 9 + 2 Flagella.” *The Journal of Cell Biology* 180 (2) (January 28): 403–415.

Yang, Yi, Bei Liu, Jie Dai, Pramod K Srivastava, David J Zammit, Leo Lefrançois, and Zihai Li. 2007. “Heat Shock Protein gp96 Is a Master Chaperone for Toll-like Receptors and Is Important in the Innate Function of Macrophages.” *Immunity* 26 (2) (February): 215–26.

YanLong, C, D Zhuang, G ZhenHong, M MaoLin Zhang, and D Ming. 2009. “Expression, Purification and Identification of Recombinant GST-P58IPK Fusion Protein.” *Chinese Journal of Veterinary Science* 29 (8): 1023–1027.

Ye, Jin, Robert B Rawson, Ryutaro Komuro, Xi Chen, Utpal P Dave, Ron Prywes, Michael S Brown, and Joseph L Goldstein. 2000. “ER Stress Induced Clevage of Membrane-Bound ATF6 by the Same Proteases That Process SREBPs.” *Molecular Cell* 6: 1355–1364.

Yoshida, H, T Matsui, a Yamamoto, T Okada, and K Mori. 2001. “XBP1 mRNA Is Induced by ATF6 and Spliced by IRE1 in Response to ER Stress to Produce a Highly Active Transcription Factor.” *Cell* 107 (7) (December 28): 881–91.

Young, J C, and F U Hartl. 2000. “Polypeptide Release by Hsp90 Involves ATP Hydrolysis and Is Enhanced by the Co-Chaperone p23.” *The EMBO Journal* 19 (21) (November 1): 5930–40.

Young, J. C. 2001. “Hsp90: A Specialized but Essential Protein-Folding Tool.” *The Journal of Cell Biology* 154 (2) (July 23): 267–274.

Young, Jason C, Vishwas R Agashe, Katja Siegers, and F Ulrich Hartl. 2004. “Pathways of Chaperone-Mediated Protein Folding in the Cytosol.” *Nature Reviews. Molecular Cell Biology* 5: 781–791.

Young, Jason C, José M Barral, and F Ulrich Hartl. 2003. “More than Folding: Localized Functions of Cytosolic Chaperones.” *Trends in Biochemical Sciences* 28 (10) (October): 541–7.

Yun, Bo-Geon, Wenjun Huang, Natalie Leach, Steven D Hartson, and Robert L Matts. 2004. “Novobiocin Induces a Distinct Conformation of Hsp90 and Alters Hsp90−Cochaperone−Client Interactions†.” *Biochemistry* 43 (25) (June 1): 8217–8229.

Zeytuni, Natalie, Ertan Ozyamak, Kfir Ben-Harush, Geula Davidov, Maxim Levin, Yair Gat, Tal Moyal, Ashraf Brik, Arash Komeili, and Raz Zarivach. 2011. “Self-Recognition Mechanism of MamA, a Magnetosome-Associated TPR-Containing Protein, Promotes Complex Assembly.” *Proceedings of the National Academy of Sciences* 108 (33) (August 16): E480–E487.

Zeytuni, Natalie, and Raz Zarivach. 2012. “Structural and Functional Discussion of the Tetra-Trico-Peptide Repeat, a Protein Interaction Module.” *Structure (London, England : 1993)* 20 (3) (March 7): 397–405.

Zhang, Huifang M, Xin Ye, Yue Su, Ji Yuan, Zhen Liu, David a Stein, and Decheng Yang. 2010. “Coxsackievirus B3 Infection Activates the Unfolded Protein Response and Induces Apoptosis through Downregulation of p58IPK and Activation of CHOP and SREBP1.” *Journal of Virology* 84 (17) (September): 8446–59.

Zhang, K, and R J Kaufman. 2006. “Protein Folding in the Endoplasmic Reticulum and the Unfolded Protein Response.” In *Molecular Chaperones in Health and Disease SE - 3*, edited by K Starke and Matthias Gaestel, 172:69–91. Springer Berlin Heidelberg.

Zhang, Minghao, Mark Windheim, S Mark Roe, Mark Peggie, Philip Cohen, Chrisostomos Prodromou, and Laurence H Pearl. 2005. “Chaperoned Ubiquitylation--Crystal Structures of the CHIP U Box E3 Ubiquitin Ligase and a CHIP-Ubc13-Uev1a Complex.” *Molecular Cell* 20 (4) (November 23): 525–38.

Zhang, Wei, Daorong Feng, Yulin Li, Kaori Iida, Barbara McGrath, and Douglas R Cavener. 2006. “PERK EIF2AK3 Control of Pancreatic Beta Cell Differentiation and Proliferation Is Required for Postnatal Glucose Homeostasis.” *Cell Metabolism* 4 (6) (December): 491–7.

Zhang, Yi, Ren Liu, Min Ni, Parkash Gill, and Amy S Lee. 2010. “Cell Surface Relocalization of the Endoplasmic Reticulum Chaperone and Unfolded Protein Response Regulator GRP78/BiP.” *The Journal of Biological Chemistry* 285 (20) (May 14): 15065–75.

Zhao, C. 2004. “Heat Shock Protein 90 Suppresses Tumor Necrosis Factor Alpha Induced Apoptosis by Preventing the Cleavage of Bid in NIH3T3 Fibroblasts.” *Cellular Signalling* 16 (3) (March): 313–321.

Zhu, Xiaotian, Xun Zhao, William F Burkholder, Alexander Gragerov, Craig M Ogata, Max E Gottesman, and Wayne A Hendrickson. 1996. “Structural Analysis of Substrate Binding by the Molecular Chaperone DnaK.” *Science* 272 (5268) (June 14): 1606–1614.

Zinchuk, Vadim, Yong Wu, Olga Grossenbacher-Zinchuk, and Enrico Stefani. 2011. “Quantifying Spatial Correlations of Fluorescent Markers Using Enhanced Background Reduction with Protein Proximity Index and Correlation Coefficient Estimations.” *Nat. Protocols* 6 (10) (September): 1554–1567.

Zinszner, Helene, Masahiko Kuroda, XiaoZhong Wang, Nikoleta Batchvarova, Richard T Lightfoot, Helen Remotti, James L Stevens, and David Ron. 1998. “CHOP Is Implicated in Programmed Cell Death in Response to Impaired Function of the Endoplasmic Reticulum.” *Genes & Development* 12 (7) (April 1): 982–995.

Zurawska, Anna, Jakub Urbanski, and Pawel Bieganowski. 2008. “Hsp90n - An Accidental Product of a Fortuitous Chromosomal Translocation rather than a Regular Hsp90 Family Member of Human Proteome.” *Biochimica et Biophysica Acta* 1784 (11) (November): 1844–6.